Higher order corrections and soft gluon resummation in perturbative QCD

By

PRASANNA KUMAR DHANI

PHYS10201205007

The Institute of Mathematical Sciences, Chennai

A thesis submitted to the

Board of Studies in Physical Sciences

In partial fulfilment of requirements

For the Degree of

DOCTOR OF PHILOSOPHY

of

HOMI BHABHA NATIONAL INSTITUTE

August, 2018

Homi Bhabha National Institute

Recommendations of the Viva Voce Board

As members of the Viva Voce Board, we certify that we have read the dissertation prepared by Mr. Prasanna Kumar Dhani entitled "Higher order corrections and soft gluon resummation in perturbative QCD" and recommend that it maybe accepted as fulfilling the dissertation requirement for the Degree of Doctor of Philosophy.

____ Date:

Chair - Prof. Rahul Sinha

____ Date:

Guide/Convener - Prof. V. Ravindran

____ Date:

Member 1 - Prof. D. Indumathi

____ Date:

Member 2 - Prof. Shrihari Gopalakrishna

____ Date:

Member 3 - Prof. Sibasish Ghosh

____ Date:

External Examiner - Prof. Sukanta Dutta

Final approval and acceptance of this dissertation is contingent upon the candidate's submission of the final copies of the dissertation to HBNI.

I hereby certify that I have read this dissertation prepared under my direction and recommend that it may be accepted as fulfilling the dissertation requirement.

Date:

Place: IMSc, Chennai Guide - Prof. V. Ravindran

STATEMENT BY AUTHOR

Prasanna Kumar Dhani

DECLARATION

I, hereby declare that the investigation presented in the thesis has been carried out by me. The work is original and has not been submitted earlier as a whole or in part for a degree / diploma at this or any other Institution / University.

Prasanna Kumar Dhani

List of Publications arising from this thesis

- **Journal**

1. **Threshold resummation of the rapidity distribution for Higgs production at NNLO+NNLL**

   Pulak Banerjee, Goutam Das, Prasanna K. Dhani and V. Ravindran

   Phys. Rev. D 97, 054024 (2018)

2. **Two loop QCD corrections for the process Pseudo-scalar Higgs $\rightarrow$ 3 partons**

   Pulak Banerjee, Prasanna K. Dhani and V. Ravindran

   JHEP 1710, 067 (2017)

3. **Finite remainders of the Konishi at two loops in $\mathcal{N} = 4$ SYM**

   Pulak Banerjee, Prasanna K. Dhani, Maguni Mahakhud, V. Ravindran and Satyajit Seth

   JHEP 1705, 085 (2017)

4. **Konishi form factor at three loops in $\mathcal{N} = 4$ supersymmetric Yang-Mills theory**

   Taushif Ahmed, Pulak Banerjee, Prasanna K. Dhani, Narayan Rana, V. Ravindran and Satyajit Seth

   Phys. Rev. D 95, 085019 (2017)

List of other Publications, Not included in this thesis

- **Journal**

1. **Threshold resummation of the rapidity distribution for Drell-Yan production at NNLO+NNLL**

   Pulak Banerjee, Goutam Das, Prasanna K. Dhani and V. Ravindran

   Phys. Rev. D 98, 054018 (2018)

2. **NNLO QCD corrections to production of a spin-2 particle with nonuniversal couplings in the Drell-Yan process**

   Pulak Banerjee, Prasanna K. Dhani, M.C. Kumar, Prakash Mathews and V. Ravindran

   Phys. Rev. D 97, 094028 (2018)

3. **Three loop form factors of a massive spin-2 particle with nonuniversal coupling**

   Taushif Ahmed, Pulak Banerjee, Prasanna K. Dhani, Prakash Mathews, Narayan Rana and V. Ravindran

   Phys. Rev. D 95, 034035 (2017)

4. **NNLO QCD corrections to the Drell-Yan cross section in models of TeV-scale gravity**

   Taushif Ahmed, Pulak Banerjee, Prasanna K. Dhani, M.C. Kumar, Prakash Mathews, Narayan Rana and V. Ravindran

   Eur. Phys. J. C (2017) 77:22

- **Preprint**

1. **Two-loop massless QCD corrections to the $g + g \rightarrow H + H$ four-point amplitude**

   Pulak Banerjee, Sophia Borowka, Prasanna K. Dhani, Thomas Gehrmann and V. Ravindran

   arXiv:1809.05388 [hep-ph]

2. **Resummed transverse momentum distribution of pseudo-scalar Higgs boson at NNLO$_A$+NNLL**

   Neelima Agarwal, Pulak Banerjee, Goutam Das, Prasanna K. Dhani, Ayan Mukhopadhyay, V. Ravindran and Anurag Tripathi

   arXiv:1805.12553 [hep-ph]

3. **The gluon jet function at three loops in QCD**

Pulak Banerjee, Prasanna K. Dhani and V. Ravindran

arXiv:1805.02637 [hep-ph]

Prasanna Kumar Dhani

Conference and School Attended

1. 27 - 30 January 2018 : ***Workshop on Top Quark Physics at Present and Future Colliders***, Department of Physical Sciences, IISER Kolkata, Kolkata, India.
2. 04 - 13 December 2017 : ***GIAN School on The Infrared Structure of Perturbative Gauge Theories***, IIT Hyderabad, Hyderabad, India.
3. 27 - 31 March 2017 : ***Collider Physics: Events, Analysis and QCD***, Department of Physics, IIT Guwahati, Guwahati, India.
4. 09 - 28 January 2017 : ***SERC Main School in Theoretical High Energy Physics***, University of Kalyani, Kolkata, India.
5. 02 - 09 November 2016 : ***GIAN School on Introduction to Quantum Chromodynamics***, University of Mumbai, Mumbai, India.
6. 23 - 27 February 2016 : ***Saha Theory Workshop: Multi-loop and Multi-leg processes for precision physics at the LHC***, Saha Institute of Nuclear Physics, Kolkata, India.
7. 15 - 19 February 2016 : ***Sangam@HRI: Instructional Workshop in Particle Physics***, Harish-Chandra Research Institute, Allahabad, India.

Seminars Presented

1. January 2018 ***Threshold resummation of the rapidity distribution for Higgs production at NNLO+NNLL***, IISER Kolkata, India.
2. November 2017 ***Threshold resummation of the rapidity distribution for Higgs production at NNLO+NNLL***, Johannes Gutenberg Universitat, Mainz, Germany.
3. October 2017 ***Threshold resummation of the rapidity distribution for Higgs production at NNLO+NNLL***, Centre for Cosmology, Particle Physics and Phenomenology (CP3), Louvain-la-Neuve, Belgium.

4. October 2017 ***Threshold resummation of the rapidity distribution for Higgs production at NNLO+NNLL***, Max-Planck-Institute for Physics, Munich, Germany.

5. October 2017 ***Threshold resummation of the rapidity distribution for Higgs production at NNLO+NNLL***, RWTH Aachen University, Aachen, Germany.

6. October 2017 ***Threshold resummation of the rapidity distribution for Higgs production at NNLO+NNLL***, INFN, Genova, Italy.

7. January 2015 ***Two-loop QCD Corrections for the process pseudoscalar Higgs → 3 partons***, The Institute of Mathematical Sciences, Chennai, India.

Prasanna Kumar Dhani

To My Family and Friends

ACKNOWLEDGEMENTS

I am about to write the most difficult part of the thesis because there is always a chance of forgetting someone. So, at the beginning, I would like to thank all the people I have come across during this stage of my life.

First of all I would like to express my deepest gratitude to my supervisor Prof. V. Ravindran, for being such an inspiration to me. Thank you for providing unending support, collegiality behaviour and amazing mentorship which helped me to complete this beautiful and daring journey of my life. Thank you for sharing your ideas and understanding of physics and helping me to understand them, improving my way of thinking in both professional as well as personal level. Not only that, you are truly symbolises the say, ‘A Teacher is a Friend, a Philosopher and a Guide’. It has been a privilege being your student.

I would like to extend my gratitude to all those people I had the opportunity to work with. To my close friend and colleague Pulak Banerjee for being a magnificent collaborator. Working with you has made many things possible over a short span of time. Thank you for bearing my casualness during work and for always providing helping hands both in work and outside. To Taushif Ahmed, Goutam Das, Maguni Mahakhud and Narayan Rana for fantastic collaborations, valuable discussions and many helps for academic as well as non-academic purposes. Thank you all for being my best seniors. To Prof. Prakash Mathews who has been like a second supervisor to me. Thank you for your guidance, collaboration and support throughout my PhD life. To Prof. Thomas Gehrmann for collaboration and several helps about the master integrals. To Dr. M.C. Kumar and Dr. Satyajit Seth for fruitful collaborations, discussions. To three new youths in our group, Ajjath A.H., Amlan Chakraborty and Pooja Mukherjee for wonderful collaborations and many valuable discussions. Thank you for being my juniors-cum-friends. To all the professors of IMSc for some good courses during my PhD course work.

I would not have reached anywhere near where I am now if it had not been for my teachers. My journey through academia has provided me the opportunity to learn from many good teachers whose influence have strengthened my passion for research. I take this opportunity to convey my sincere thanks to all of them.

Special thanks to my office mates, in particular Sumit Giri, Anirban Karan, Abinash K. Nayak, Sohan Lal Saini and Priyamvad Srivastav for all those amazing moments we shared starting from my PhD. You guys are really awesome and I always feel special in the office if you people are around. I am thankful to Rusa Mandal for being such a special senior to me. I convey my heartiest thanks to my wonderful friends, in particular Subodha, Anil, Ranjit, Nirakar, Prashanta, Prasanta, Dillip and Soumya for all those wonderful moments we shared. You guys were the very first inspiration for choosing research as my career! Our outstanding discussions, academic as well as non-academic, starting from the BSc really have helped us to explore and understand many things in a different way. My gratitude goes out to all of my friends, specifically, Satyabrat, Sankha, Ajay, Narottam, Arabinda, Arpita, Monalisha, Dipanjan, Arindam, Sanjoy, Sagnik, Arnab, Madhusudhan, Balakrishnan, Pratik, Anand, Dheeraj, Prafulla, Rathul, Jilmy, Anvy, Ankita, Swaroop, Minati, Prosenjit, Atanu and Shilpa.

Several members of the non-academic staff at IMSc, have been very helpful to me. I would like to thank them all.

I would like to extend my special thanks to my beloved friend and my fiancee Saswati for her trust, love and constant encouragement. Thank you for accepting me as what I am!

Finally, I am thankful to my beloved parents, younger brother Pradipta, elder brother Pradyumna, Sister-in-law Sonali and whole family for their unconditional love, supports and sacrifices, without those it would have been impossible to achieve my PhD.

Contents

Synopsis

Thanks to thousands of physicists, for whom today we have a remarkable insight into the fundamental structure of matter: everything in the universe is made from a few basic building blocks called fundamental particles, governed by four fundamental forces. Our best understanding of how these particles and three of the forces are related to each other is encapsulated in the Standard Model (SM) of particle physics which got its finishing touch on July 2012 through the discovery of the long-awaited particle, "the Higgs boson", at the biggest underground particle research laboratory, the Large Hadron Collider (LHC) [1,2]. It would take a while to make the conclusive remarks about the true identity of the newly-discovered particle. However, after the discovery of the SM Higgs boson, the high energy physics is standing on the verge of a crucial era where the new physics may show up as tiny deviations from the predictions of the SM. To exploit this possibility, it is absolutely necessary to have precise theoretical predictions along with measurements to a very good accuracy within the SM and beyond (BSM).

The most successful methodology to perform the theoretical computations within the SM and BSM is based on the perturbation theory, due to our inability to solve the theory exactly. Under the prescriptions of perturbation theory, all the observables are expanded in powers of the coupling constants present in the Lagrangian. The result obtained from the first non-zero term in the expansion is called the leading order (LO), the next one is called next-to-leading order (NLO) and so on. Often the LO results fail miserably to deliver a reliable theoretical prediction of the associated observables, one must go beyond the wall of LO result to achieve a higher accuracy.

Due to presence of three fundamental forces within the SM, any observable can be expanded in powers of coupling constants associated with the corresponding forces, namely, electromagnetic ($\alpha_{\rm EM}$), weak ($\alpha_{\rm EW}$) and strong (α_s) ones and consequently, perturbative calculations can be performed with respect to each of these constants. However, at typical energy scales, at which the hadron colliders operate, the contributions arising from the α_s expansion dominate over the others due to comparatively large value of α_s. Hence, to capture the dominant contributions to any observables, we must concentrate on the α_s expansion and evaluate the terms beyond LO. The underlying theory to describe the strong interaction dynamics is called Quantum Chromodynamics (QCD). Perturbative predictions of QCD (pQCD) depend on two unphysical scales, the renormalisation (μ_R) and factorisation (μ_F) scales. The μ_R arises from the ultraviolet (UV) renormalisation, whereas the mass factorisation (which removes initial state collinear singularities) introduces the μ_F. Any fixed order result does depend on these unphysical scales which happens due to the truncation of the perturbative expansion. As we include the contributions from higher and higher orders, the dependence of a physical observable on these unphysical scales gradually goes down. Hence, to make a reliable theoretical prediction, it is absolutely necessary to take into account the contributions arising from the higher order QCD corrections to any observable at the hadron colliders. Moreover higher order results provide deeper insight on the structure of UV and infrared (IR) divergences of the scattering amplitudes and helps to find connections between amplitudes in SM and BSM. For example amplitudes in QCD are related to amplitudes in a simpler theory called $\mathcal{N} = 4$ Supersymmetric Yang-Mills (SYM) theory when the number of colours for the former case become infinite.

Although the higher order computations provide reliable theoretical predictions however the task of computing them often becomes highly non-trivial beyond NNLO. Hence, it is natural to try alternative approaches to capture the dominant contributions from the missing higher order. The very first approach towards this direction is to compute the observables under soft-virtual (SV) approximation which often captures the dominant contributions and provide better results. However, this may give rise to large logarithms for certain observables in some kinematic regions which can spoil the convergence of the perturbation theory and hence those must be resummed to all orders to get more reliable predictions. This has been accomplished through soft-gluon resummation techniques.

This thesis arises exactly in the above mentioned contexts and comprises of two parts: the first part deals with the QCD radiative corrections to few important field theory quantities in BSM and the second part discusses soft gluon resummation to one of the very important observables called rapidity distribution associated with the Higgs boson production. In the subsequent discussions, we will concentrate only on these processes.

0.1 pQCD corrections to multiloop and multileg processes

Multiloop and multileg computations play a crucial role to achieve the task of making precise theoretical predictions. However, complexity of these computations grows very rapidly with the increase of number of loops and/or external particles. Nevertheless, it has become feasible due to several remarkable developments in due course of time.

0.1.1 2-loop virtual corrections to pseudoscalar plus a jet

One of the most popular extensions of the SM, namely, the minimal supersymmetric SM (MSSM) and two Higgs doublet model have richer Higgs sector containing more than one Higgs boson and there have been intense search strategies to observe them at the LHC. In particular, production of CP odd Higgs boson/pseudoscalar in BSM at the LHC has been studied in detail, taking into account higher order radiative corrections, due to similarities with its CP even counter part. Very recently, NNLO corrections to the inclusive production cross section of the CP-even Higgs boson in association with a jet is computed. So, it is very natural to extend the theoretical accuracy for the CP-odd Higgs boson to the same order of NNLO. First step to achieve this goal is to compute pure virtual corrections to the production of a pseudoscalar Higgs boson in association with a jet. *This section is devoted to demonstrate the computation of 2-loop pure virtual contributions to the production of pseudoscalar Higgs boson plus a jet.*

The coupling of a pseudoscalar Higgs boson to gluons is mediated through a heavy quark loop. In the limit of large quark mass, it is described by an effective Lagrangian that only admits light degrees of freedom. The evaluation of 2-loop virtual corrections to this process is truly a non-trivial task not only because of the involvement of a large number of Feynman diagrams but also due to the presence of the axial vector coupling. We work in dimensional regularisation and use the 't Hooft-Veltman prescription for the axial vector current. The state-of-the-art techniques including integration-by-parts (IBP) and Lorentz invariant (LI) identities have been employed to accomplish this task. The UV renormalisation is quite involved since the two operators, present in the Lagrangian, mix under renormalization due to the axial anomaly and additionally, a finite renormalisation constant needs to be introduced in order to fulfill the chiral Ward identities. *Our findings [3] are consistent with the universal structure of the infrared poles predicted by Catani [4]. We have also studied connection of this amplitude with $\mathcal{N} = 4$ SYM amplitudes in the context of leading transcendentality principle.*

0.1.2 Konishi form factor at N^{3}LO in $\mathcal{N} = 4$ SYM

The ability to accomplish the challenging job of calculating quantities is of fundamental importance in any potential mathematical theory. In quantum field theory (QFT), this manifests itself in the quest for computing the multiloop and multileg scattering amplitudes under the framework of perturbation theory. Calculation of these scattering amplitudes are often highly non-trivial beyond certain power in strong coupling constant in a real theory such as QCD. There are several approaches to avoid the complex QCD calculation adopting certain approximations: for instance $\mathcal{N} = 4$ SYM provides a very good platform which resembles QCD in large N limit. Recently, there has been surge of interest to study the form factors (FFs) as they connect fully on-shell amplitudes and correlation functions. The FFs are a set of quantities which are constructed out of the scattering amplitudes involving on-shell states consisting of elementary fields and an off-shell state described through a composite operator.

Composite operators which are often studied in $\mathcal{N} = 4$ SYM theory are called the half-BPS and the Konishi. The half-BPS operator is protected under supersymmetry i.e. it does not exhibit UV divergences up to all orders in perturbation theory. However, the Konishi operator which depends on space time dimension is not protected under supersymmetry and develops UV divergences beyond leading order. Note that both the half-BPS and the Konishi operators demonstrate divergences coming from IR region starting from NLO in perturbation theory. Bearing in mind recent developments to the FF of both the operators, *we have worked out for the first time the complete third order corrections to the on-shell FF of the Konishi operator employing state-of-the-art techniques*. This section is devoted to demonstrate calculation of 3-loop FF contribution to the Konishi operator.

One of the main issues in computing higher order corrections in $\mathcal{N} = 4$ SYM is related to the necessity of preserving the supersymmetry throughout the computation. In order to achieve that, one generally follows either of the two regularisation scheme: modified dimensional reduction ($\overline{DR}$) and four dimensional helicity scheme (FDH). Through performing the computation explicitly in both the schemes, we have shown that the FF in $\overline{DR}$ automatically provides the correct results, where as, the results obtained in the FDH needs to be suitably modified, the modification is operator dependent and non-trivial. Hence, performing a computation in $\overline{DR}$ is much more preferable for unprotected operators like the Konishi. We have also discussed superiority of the Feynman diagrammatic approach over unitarity method in the context of the Konishi type composite operators. *Moreover computation performed by us [5] is the most advanced one in the context of Konishi FF.*

0.1.3 Finite remainders of the Konishi operator at NNLO

Scattering amplitudes are the building blocks of many important observables in high energy physics and they exhibit remarkable structures of the underlying QFT. Those computed in the electroweak theory and QCD play important role in the phenomenology of collider physics. With the increase in number of loops and legs, amplitudes are not only difficult to calculate but also one obtains very large expressions. Enormous simplification can be achieved if the underlying QFT has some symmetries which leads to conserved currents. One such theory is $\mathcal{N} = 4$ SYM theory which resembles QCD in large N limit. Like QCD, $\mathcal{N} = 4$ SYM theory is a renormalizable gauge theory in four dimensional Minkowski space. Apart from having all the symmetries of QCD there are two extra features of $\mathcal{N} = 4$ SYM, namely supersymmetry and conformal symmetry that makes this theory interesting to study. The on-shell amplitudes evaluated in $\mathcal{N} = 4$ SYM have a simpler analytical structure in comparison to QCD amplitudes. *In this work we have computed 3-point FFs and hence finite remainders (FR) using Feynman diagrammatic approach at 2-loop level for both the half-BPS and the Konishi operator for two sets of on-shell final states consisting of $g\phi\phi$ and $\phi\lambda\lambda$, where ϕ, λ, g are scalar, Majorana fermion and gauge fields respectively*. This section is devoted to demonstrate computation of these quantities.

It is well known that the IR divergences of MHV amplitudes have an exponential structure (BDS ansatz [6]). Such a behaviour is reminiscent of the factorisation properties of gauge theory amplitudes. However we can also see this kind of exponentiation in FFs. By exponentiating the one loop IR singularities following BDS like exponentiation, we compute FR at two loops. Our result on the half-BPS for the final on-shell state $g\phi\phi$ presented in terms of harmonic polylogarithms (HPLs) numerically agrees with the earlier calculation [7] presented in terms of classical polylogarithms which was computed using unitarity based method. We find that the leading transcendental terms of the remainder function for the Konishi operator computed between $g\phi\phi$ external state coincide with the corresponding one of the half-BPS. However, for the $\phi\lambda\lambda$ external state we find that the expressions for the Konishi and the half-BPS operators do not have anything common. *In this way our calculation [8] not only gives new results on the 2-loop FRs for the both the operators but also reveals many important properties.*.

0.2 Soft gluon resummation in the Higgs rapidity

While inclusive rates are important for any phenomenological study, the differential cross sections often carry more informations on the nature of interaction, quantum number of particles produced in the hard collisions. Rapidity distributions of Drell-Yan pair, Z boson and charge asymmetries of leptons in $W^{\pm}$ boson decays are already used to measure parton distribution functions (PDFs). Possible excess events in these directions can hint to BSM physics, namely R-parity violating supersymmetric models, models with Z' or with contact interactions and large extra dimension models. Like in Drell-Yan, measurements of transverse momentum and rapidity distributions of the Higgs boson will be very useful to study the properties of the Higgs boson and its couplings. In this section, *we include the dominant effect of the uncalculated higher order terms, by exploiting the resummation of soft gluon emission in the rapidity distributions of the Higgs boson up to next-to-next-to-leading-logarithmic (NNLO+NNLL) accuracy*.

The possibility of performing such an improvement relies upon the observation that an accurate use of the soft gluon approximation provides the bulk of the NLO term and a reliable estimate of the NNLO effects. So, it makes sense to add the higher order terms that can be obtained in the soft gluon approximation, in order to give precise prediction.

We present a formalism that resums threshold enhanced logarithms in double Mellin space to all orders in pQCD for the rapidity distribution of any colourless particle produced in hadron colliders. We achieve this by exploiting the factorisation properties and K+G equations satisfied by the soft and virtual parts of the cross section. We compute for the first time compact and most general expressions for the resummed coefficients up to NNLO+NNLL accuracy. We find that the resummed result not only changes the fixed order predictions but also remarkably improves the perturbative convergence. *This is the most accurate result [9] for the rapidity distribution of the Higgs boson which exists in the literature till date and it is expected to play an important role in coming days at the LHC.*

List of Figures

List of Tables

1 Introduction

Our World consists of elementary particles communicating with each other via electromagnetic force, the weak and the strong nuclear forces and gravity. The main aim of particle physics is to persistently search for increasingly accurate theories describing all the above mentioned fundamental forces in a single framework which we believe underly all physical phenomena, ranging from an understanding of the structure of the nucleus and spanning to the dynamics of the universe as a whole. While the classical descriptions of these forces were clearly insufficient, the success of quantum physics and special theory of relativity led to the modern view of each fundamental interaction in term of fields. Such a field theoretical description of three out of four fundamental interactions is given by the Standard Model (SM) of particle physics where electromagnetic, weak and strong forces are unified in an eccentric way. Gravity is still a puzzle at small scales, but since it is much weaker than the other forces, it plays a minor role at the energies we are probing with particle physics experiments and usually ignored. Over the duration of many decades, the theoretical predictions of the SM were verified one after another with a spectacular accuracy and it got the ultimate credence on July 2012 through the discovery of the long-awaited particle, “the Higgs boson”, at the biggest underground particle research laboratory, the Large Hadron Collider (LHC).

In mathematical terms, the SM is a non-Abelian gauge theory based on the symmetry group $\mathrm{SU(3)} \times \mathrm{SU(2)_L} \times \mathrm{U(1)_Y}$ described through a Lagrangian which controls the dynamics and kinematics of the theory. The construction of the SM proceeds through the modern methodology of constructing a quantum field theory (QFT). It happens through postulating a set of symmetries of the system and writing down the most general renormalizable Lagrangian from its field content. As a gauge theory, the SM is based on the fundamental concept of gauge symmetries. Unlike global symmetries, gauge symmetries are not new symmetries of nature, in the sense that they don't imply the existence of new conserved charges. However, their existence is of a much deeper significance, since they determine in a unique way how the fields (particles) interact. In the SM, each gauge symmetry group manifestly gives rise to a fundamental interaction: the electromagnetic interactions are characterised by U(1), the weak interactions by SU(2) and the strong interactions by SU(3) symmetry group.

In the current formulation of the SM, there are two different families of elementary particles. Particles belonging to first family are called fermions which arises from the quantisation of the fermionic fields and constitute the matter content of the theory. Second family includes the quanta of bosonic fields, are the force carriers i.e. the mediators of the strong, weak and electromagnetic interactions. In addition to these families of elementary particles, there is a boson, namely, the Higgs boson resulting from the quantum excitation of the Higgs field. This is the only known scalar particle whose existence was postulated long ago and observed very recently at the LHC [1,2]. The presence of this field explains the mechanism of acquiring mass of some of the fundamental particles when, based on the underlying gauge symmetries controlling their interactions, they should be massless. This mechanism which believed to be one of the most revolutionary ideas of the last century, is known as Higgs mechanism [10–14].

Out of four known fundamental forces, electromagnetic and weak forces which appear to be very different at low energies, are unified to so called electroweak force in high energy regime. The structure of this unified picture is visualised under the gauge group $\mathrm{SU(2)_L \times U(1)_Y}$. The corresponding gauge bosons are the three W bosons of weak isospin from SU(2) and the B boson of weak hyper-charge from U(1), all of which are massless.

Upon spontaneous symmetry breaking from $\mathrm{SU(2)_L \times U(1)_Y}$ to $\mathrm{U(1)_{EM}}$, caused by the Higgs mechanism, the three mediators of the electroweak force, the $W^{\pm}, Z$ bosons acquire mass, leaving the mediator of the electromagnetic force, the photon, as massless. Finally, the theory of strong interactions, Quantum Chromodynamics (QCD) is governed by the unbroken gauge group SU(3), whose force carriers, the gluons remain massless.

Although the SM is believed to be theoretically self consistent with remarkable accuracy and has demonstrated huge and continued successes in proving experimental predictions, it indeed does leave some phenomena unexplained and falls short of being a complete theory of nature. Firstly, a proper field theoretical description of gravitational force still remains missing. The model does not contain any viable dark matter candidate that possesses all the required properties deduced from observational cosmology. Another shortcoming of the SM is mass of the neutrinos. Neutrinos are massless in the model, whereas experimental observation like neutrino oscillation demands them to be massive. Also the model fails to account for the baryon asymmetry of the universe.

Currently, the high energy physics community is standing on the verge of a crucial era where the new physics may show up as tiny deviations from the predictions of the SM. To exploit this possibility, it is absolutely necessary to have precise theoretical predictions along with measurements to a very good accuracy within the SM and beyond (BSM). The context of this thesis is to acquire results, as precise as possible, for few important field theoretical quantities and one of the very important observables called rapidity distribution associated with the SM Higgs boson production.

The quantity which is of great importance in accomplishing the task of making any prediction based on QFT is undoubtedly the scattering amplitude. These scattering amplitudes are the building blocks of many important observables in high energy physics. For example one can get cross section for any process of interest out of these scattering amplitudes by squaring and integrating it over the phase space of the final state particles. These scattering amplitudes also exhibit remarkable structures of the underlying QFT. In the upcoming section, we will elaborate on the idea of scattering amplitude which will be followed by a brief description of QCD.

1.1 Scattering Amplitudes in QFT

The object which encodes all the underlying symmetries of the theory in any QFT is called the action. This is constructed by integrating the Lagrangian density over all space time points:

$$S = \int d^4x \, \mathcal{L}\left[\phi_i(x)\right] \,. \tag{1.1}$$

In the above equation, $\phi_i(x)$ denotes all the dynamical fields in the theory. By construction the QFT is a probabilistic theory and all the observables calculated based on this theory always carry a probabilistic interpretation. For example, cross section measures the probability of an event to happen in colliders. The computation of any observables in QFT requires the evaluation of scattering matrix (S-matrix) elements which describe the evolution of the system from asymptotic initial to final states due to presence of the interaction. The S-matrix elements are defined as

$$\langle f|S|i\rangle = \delta_{fi} + i(2\pi)^4\delta^{(4)}\left(p_f - p_i\right)\mathcal{M}_{i\to f} \tag{1.2}$$

where, the δ_{fi} represents the unscattered forward scattering states, while the other part $\mathcal{M}_{i\to f}$ encapsulates the "actual" interaction (for simplicity, we will call $\mathcal{M}_{i\to f}$ as scattering matrix element). So, the calculation of all those observables essentially boils down to the computation of the corresponding scattering matrix elements. However, the exact computation of this quantity is impossible in any general field theory. The only viable methodology is provided under the framework of perturbation theory where the matrix elements as well as the observables are expanded in powers of coupling constants, c, present in the theory:

$$\mathcal{M}_{i\to f} = \sum_{n=0}^{\infty} c^n \mathcal{M}^{(n)}_{i\to f} \,. \tag{1.3}$$

If the coupling constant is small enough, computation of only the first term of the perturbation series often turns out to be a very good approximation and it provides a reliable prediction to any observable. However, it is a well-known fact that the coupling constants are truly not 'constants', their strength depends on the energy scale at which the interaction takes place. In case of Quantum Electrodynamics (QED), quantum field theory of electromagnetism, the magnitude of the coupling constant, $c = \alpha_{\rm EM}$, increases with the increase of momentum transfer:

$$\alpha_{\rm EM}(Q^2 \approx 0) \approx \frac{1}{137}\,, \qquad \text{and} \qquad \alpha_{\rm EM}(Q^2 \approx m_W^2) \approx \frac{1}{128} \tag{1.4}$$

where, $m_W \approx 80$ GeV is the invariant mass of the W boson. The smallness of $\alpha_{\rm EM}$ at all typical energy scales guarantees fast convergence of the perturbation series to what we expect to be real non-perturbative result. However, this picture no longer holds true in case of QCD where the coupling constant, $c = \alpha_s$, may become quite large at certain energy scales:

$$\alpha_s(m_p^2) \approx 0.55, \qquad \text{and} \qquad \alpha_s(m_Z^2) \approx 0.1 \tag{1.5}$$

where, $m_p \approx 938 MeV$ and $m_Z \approx 90 GeV$ are the masses of the proton and Z boson. Clearly the magnitude 0.55 is far from being small! Hence, computation of only the leading term in the perturbation series often turns out to be a very crude approximation and fails miserably to deliver a reliable theoretical prediction of the associated observable. Hence, we must take into account the contributions arising beyond leading term.

The most acceptable and well known prescription to compute the terms in a perturbative series is given by R. P. Feynman through Feynman diagrams. Every term of the series is represented through a set of Feynman diagrams and each diagram corresponds to a mathematical expression. Hence, evaluation of a term in the series boils down to the computation of all the corresponding Feynman diagrams. Given the action of a QFT, one first necessitates to derive a set of rules, called Feynman rules, which essentially establish the connection between the Feynman diagrams and mathematical expressions. With the rules in hand, we just need to draw all possible Feynman diagrams contributing to the order in coupling constant of our interest and eventually evaluate those using the rules. Needless to say, as the power in coupling constant increases, the number of Feynman diagrams contributing to that order grows so rapidly that after certain power it becomes almost prohibitively large to draw the diagrams.

In this thesis, we will concentrate only on the aspects of perturbative QCD (pQCD). We will start our discussion of QCD by introducing the basic aspects of this QFT which will be followed by the writing down the Lagrangian and corresponding Feynman rules. Then we will briefly study a relatively simpler theory called $\mathcal{N} = 4$ supersymmetric Yang-Mills (SYM) theory and work out corresponding Feynman rules. Using these tools in hand, we will discuss how to compute amplitudes beyond leading order (LO) in QCD and eventually get reliable numerical predictions at hadron colliders for the process of interest.

1.2 Basic aspects of QCD

1.2.1 The quark model

QCD is the gauge theory which describes one of the four fundamental forces of nature, namely, strong interactions and hadrons are the particles which undergo strong interactions. These hadrons are observed either in fermionic (baryons) or bosonic (mesons) states. Observation of hadrons in large number was an indication that they were not elementary entities but composite objects of other elementary constituents. According to the quark model, the baryons are the bound states of three quarks (qqq) while the mesons are bound states of a quark and an anti-quark ($q\bar{q}$). There have been observed six types (flavours) of quarks: up (u), down (d), strange (s), charm (c), bottom (b) and top (t), all carrying spin 1/2. The electric charge of u, c and t is +2/3 while the charge of d, s and b is -1/3.

Problems with the spin statistics of baryon bound states, suggested that quarks must be allowed an additional degree of freedom to the electric charge and flavour, which is named colour charge. To distinguish between three otherwise identical quarks making for example the Δ^{++}(uuu) baryon state, one has to introduce at least three different colour indices (e.g red, blue, green). But, of course, these colour charges have nothing to do with optical colours. Rather, they have properties analogous to electric charges in QED. In particular, colour charges are conserved in a strong interaction process. Another experimental fact is that all the observed hadrons are confined to colourless states (red+blue+green, red+anti-red, etc). No single quark or bound colourful states of two quarks qq, etc have ever been observed. Confinement, is an additional theoretical hypothesis but it is believed that it may be a consequence of the dynamical properties of the quarks.

The dynamics of the elementary particles in hadrons is described by QCD. Quarks are considered to be point-like entities, as demonstrated from the scaling behaviour observed in deep inelastic experiments, carrying colour charge. In analogy with QED where charged particles interact via the mediation of the photon, in QCD the carriers of the strong interaction are bosons called gluons. Unlike photons, gluons themselves carry colour charges. As a consequence, gluons participate in the strong interactions in addition to mediating it, making QCD substantially harder to analyse than QED.

The theory postulates invariance under the local gauge group SU(3). The quarks transform according to the fundamental representation and the anti-quarks according to the complex conjugate representation. The gluons transform in the adjoint representation. As a consequence, the basic colour singlet states $q_i\bar{q}^i$ and the totally antisymmetric $\epsilon^{ijk}q_iq_jq_k$ correspond to the observed meson and baryon states.

In addition to confinement, QCD shows another interesting property, the asymptotic freedom, causes bonds between quarks/gluons become asymptotically weaker as energy increases or distance decreases which allows us to perform the calculation using the technique of perturbation theory. In perturbative QCD, the basic building blocks of performing any calculation are the Feynman rules, which will be discussed in next subsection.

1.2.2 QCD Lagrangian and Feynman Rules

The first step in performing perturbative calculations in a QFT is to work out the Feynman rules from the Lagrangian density describing the theory. Classical Lagrangian density for the QCD is given by

$$\mathcal{L}_{classical} = -\frac{1}{4}G^a_{\mu\nu}G^{a,\mu\nu} + \sum_{f=1}^{n_f} \overline{\psi}^{(f)}_{\alpha,i}\left(i\not{D}_{\alpha\beta,ij} - m_f\delta_{\alpha\beta}\delta_{ij}\right)\psi^{(f)}_{\beta,j}\,. \tag{1.6}$$

$\mathcal{L}_{classical}$ describes the dynamics of the quarks as relativistic spin-1/2 particles, carrying colour charge. Invariance under local SU(N) transformations, with $N = 3$ colour degrees freedom, demands the existence of $N^2 - 1$ vector boson gluons mediating the interactions between quarks. In the above expression,

$$\begin{aligned} G^a_{\mu\nu} &= \partial_\mu A^a_\nu - \partial_\nu A^a_\mu + g_s f^{abc}A^b_\mu A^c_\nu\,, \\ \not{D}_{\alpha\beta,ij} &\equiv \gamma^\mu_{\alpha\beta}D_{\mu,ij} = \gamma^\mu\left(\delta_{ij}\partial_\mu - ig_sT^a_{ij}A^a_\mu\right) \end{aligned} \tag{1.7}$$

In QCD, gluons carry colour charge themselves and due to the last term in $G^a_{\mu\nu}$, we can have gluon self interactions. In QED this non-Abelian term is missing and we do not observe interactions between the neutral photons. The Dirac gamma matrices satisfy the

Clifford algebra

$$\{\gamma^\mu, \gamma^\nu\} \equiv \gamma^\mu\gamma^\nu + \gamma^\nu\gamma^\mu = 2g^{\mu\nu}. \tag{1.8}$$

A_μ^a and $\psi_{\alpha,i}^{(f)}$ are the gauge and quark fields, respectively. The indices represent the following things:

$$\begin{aligned}
&a, b, \cdots : \quad \text{colour indices in the adjoint representation} \Rightarrow [1, N^2 - 1]\,, \\
&i, j, \cdots : \quad \text{color indices in the fundamental representation} \Rightarrow [1, N]\,, \\
&\alpha, \beta, \cdots : \quad \text{Dirac spinor indices} \Rightarrow [1, 4]\,, \\
&\mu, \nu, \cdots : \quad \text{Lorentz indices} \Rightarrow [1, d]\,.
\end{aligned} \tag{1.9}$$

Numbers within the '[]' signifies the range of the corresponding indices. d is the space-time dimensions. f is the quark flavour index which runs from 1 to n_f. m_f and g_s are the mass of the quark corresponding to $\psi^{(f)}$ and strong coupling constant, respectively. f^{abc} are the structure constants of SU(N) group. These are related to the Gell-Mann matrices T^a, generators of SU(N), through

$$\left[T^a, T^b\right]_- = i f^{abc} T^c\,. \tag{1.10}$$

The T^a are traceless, Hermitian matrices and these are normalised with

$$Tr\left(T^a T^b\right) = T_F \delta^{ab} \tag{1.11}$$

where, $T_F = \frac{1}{2}$. They satisfy the following completeness relation

$$\sum_a T^a_{ij} T^a_{kl} = \frac{1}{2}\left(\delta_{il}\delta_{kj} - \frac{1}{N}\delta_{ij}\delta_{kl}\right)\,. \tag{1.12}$$

In addition to the above three parent identities expressed through the Eqs. (1.10, 1.11, 1.12), we can have some auxiliary ones which are often useful in simplifying colour algebra:

$$\sum_a (T^a T^a)_{ij} = C_F \delta_{ij} \,,$$
$$f^{acd} f^{bcd} = C_A \delta^{ab} \,. \tag{1.13}$$

The $C_A = N$ and $C_F = \frac{N^2-1}{2N}$ are the quadratic Casimir of the SU(N) group in the adjoint and fundamental representations, respectively. The quantisation of the non-Abelian gauge theory or the Yang-Mills theory faces an immediate problem, arising from the freedom of the gluon fields to change by a total derivative and leave the Lagrangian invariant under the gauge transformation. In the canonical quantization method this problem appears as a vanishing conjugate momentum for the time-like components of the gluon field, thereby invalidating the canonical commutation relations. In the path integral approach, the contribution of each gluon field to the path integral over the exponential of the action is overestimated by an infinite amount since one can perform an infinite number of gauge transformations to the field without changing the action. It is necessary to perform the gauge fixing in order to get rid of this problem. The gauge fixing in a covariant way, when done through the path integral formalism, generates new particles called Faddeev-Popov ghosts having spin-0 but obeying fermionic statistics. The absolute necessity of introducing the ghosts in the process of quantising the Yang-Mills theory is a consequence of the Lagrangian formulation of QFT. There is no observable consequence of these particles, we just need them in order to describe an interacting theory of a massless spin-1 particle using a local manifestly Lorentz invariant Lagrangian. These particles never appear as physical external states but must be included in internal lines to cancel the unphysical degrees of freedom of the gauge fields. Some alternative formulations of non-Abelian gauge theory (such as the lattice) also do not require ghosts. Perturbative gauge theories in certain non-covariant gauges, such as light-cone or axial gauges, are also ghost free. However, to maintain manifest Lorentz invariance in a perturbative gauge theory, it seems ghosts are unavoidable and in this thesis we will be remained within the regime of covariant gauge and consequently will include ghost fields consistently into our computations.

Upon applying this technique to quantise the Yang-Mills theory, we end up with getting the following full quantum Lagrangian density:

$$\mathcal{L}_{YM} = \mathcal{L}_{classical} + \mathcal{L}_{gauge-fix} + \mathcal{L}_{ghost} \tag{1.14}$$

where, the second and third terms on the right hand side correspond to the gauge fixing and FP contributions, respectively. These are obtained as

$$\begin{aligned}\mathcal{L}_{gauge-fix} &= -\frac{1}{2\xi}\left(\partial^\mu A^a_\mu\right)^2 , \\ \mathcal{L}_{ghost} &= (\partial^\mu \bar{\eta}^a)\, D_{\mu,ab}\, \eta^b\end{aligned} \tag{1.15}$$

with

$$D_{\mu,ab} \equiv \delta_{ab}\partial_\mu - g_s f_{abc} A^c_\mu . \tag{1.16}$$

The gauge parameter ξ is arbitrary and it is introduced in order to specify the gauge in a covariant way. The total Lagrangian is no longer gauge invariant, but the physical predictions stemming from it should be gauge invariant and independent of ξ. This prescription of fixing gauge in a covariant way is known as R_ξ gauge. A typical choice which is often used is $\xi = 1$, known as Feynman gauge. We will be working in this Feynman gauge throughout this thesis, unless otherwise mentioned specifically. However, we emphasize that the physical results are independent of the choice of the gauges. The field η^a and η^{a*} are ghost and anti-ghost fields, respectively.

All the Feynman rules can be read off from the quantized Lagrangian $\mathcal{L}_{YM}$ in Eq. (1.14). We will denote the quarks through straight lines, gluons through curly and ghosts through dashed lines. We provide the rules in R_ξ gauge.

- The propagators for quarks, gluons and ghosts are obtained as respectively:

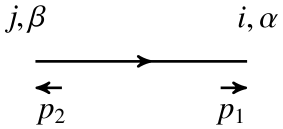

$$i\,(2\pi)^4\,\delta^{(4)}\,(p_1+p_2)\,\delta_{ij}\left(\frac{1}{\not{p}_1 - m_f + i\varepsilon}\right)_{\alpha\beta}$$

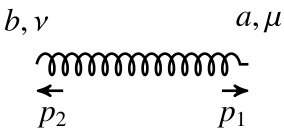

$$i\,(2\pi)^4\,\delta^{(4)}\,(p_1+p_2)\,\frac{\delta_{ab}}{p_1^2+i\varepsilon}\left[-g_{\mu\nu}+(1-\xi)\frac{p_{1\mu}p_{1\nu}}{p_1^2}\right]$$

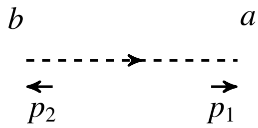

$$i\,(2\pi)^4\,\delta^{(4)}\,(p_1+p_2)\,\frac{\delta_{ab}}{p_1^2+i\varepsilon}$$

- The interacting vertices are given by:

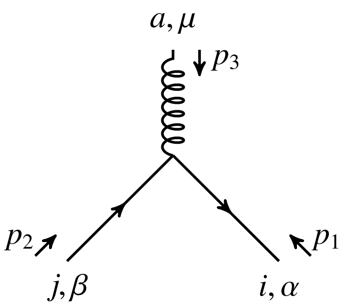

$$ig_s\,(2\pi)^4\,\delta^{(4)}\,(p_1+p_2+p_3)\,T^a_{ij}\,(\gamma^\mu)_{\alpha\beta}$$

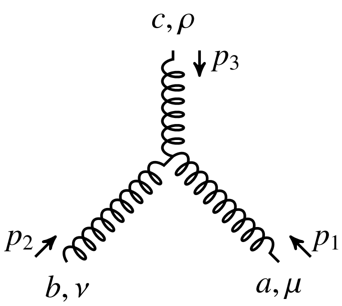

$$\frac{g_s}{3!}\,(2\pi)^4\,\delta^{(4)}\,(p_1+p_2+p_3)\,f^{abc}$$
$$\times\left[g^{\mu\nu}(p_1-p_2)^\rho + g^{\nu\rho}(p_2-p_3)^\mu + g^{\rho\mu}(p_3-p_1)^\nu\right]$$

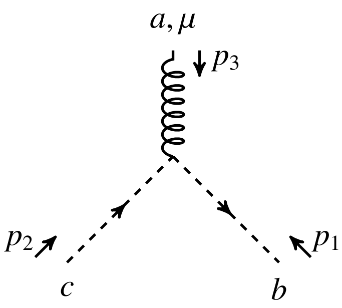

$$-g_s\,(2\pi)^4\,\delta^{(4)}\,(p_1+p_2+p_3)\,f^{abc}p_1^\mu$$

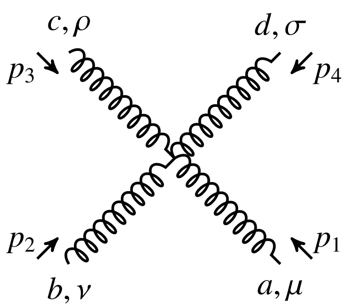

$$-\frac{g_s^2}{4!}(2\pi)^4\,\delta^{(4)}\,(p_1+p_2+p_3+p_4)$$
$$\times\left\{\left(f^{ac,bd}-f^{ad,cb}\right)g^{\mu\nu}g^{\rho\sigma}+\left(f^{ab,cd}-f^{ad,bc}\right)g^{\mu\rho}g^{\nu\sigma}\right.$$
$$\left.+\left(f^{ac,db}-f^{ab,cd}\right)g^{\mu\sigma}g^{\nu\rho}\right\}$$

with

$$f^{ab,cd}\equiv f^{abx}f^{cdx}$$

1.3 $\mathcal{N} = 4$ SYM Theory

Scattering amplitudes in gauge theories are known to have a significantly simpler structure than that which is implied by the manifestly local construction in Feynman diagrams. One theory which has received much attention in recent years and where these simplifications are particularly striking is the planar $\mathcal{N} = 4$ SYM theory. Like QCD, the $\mathcal{N} = 4$ SYM theory is a renormalizable gauge theory in four dimensional Minkowski space. Apart from having all the symmetries of QCD there are two extra features of $\mathcal{N} = 4$ SYM, namely supersymmetry and conformal symmetry that make this theory interesting to study. Due to the presence of these extra symmetries, the on-shell amplitudes evaluated in this theory have a simpler analytical structure in comparison to QCD amplitudes.

1.3.1 Lagrangian and Feynman Rules

In this sub-section we briefly describe the Lagrangian density and its associated fields. The massless Lagrangian density for $\mathcal{N} = 4$ SYM theory in four dimensional Minkowski space reads as [15–18],

$$\begin{aligned}\mathcal{L}_{\mathcal{N}4\mathrm{SYM}} = &-\frac{1}{4}G^a_{\mu\nu}G^{\mu\nu a}-\frac{1}{2\xi}(\partial^\mu A^a_\mu)^2+\partial_\mu\bar{\eta}^a D^\mu\eta_a+\frac{i}{2}\bar{\lambda}^a_m \not{D}\lambda^a_m+\frac{1}{2}(D_\mu\phi^a_r)^2\\ &+\frac{1}{2}(D_\mu\chi^a_r)^2-\frac{g_s}{2}f^{abc}\bar{\lambda}^a_m[\alpha^r_{m,n}\phi^b_r+\gamma_5\beta^r_{m,n}\chi^b_r]\lambda^c_n-\frac{g^2_{\mathrm{YM}}}{4}\Big[(f^{abc}\phi^b_r\phi^c_t)^2\end{aligned}$$

$$+ (f^{abc}\chi_r^b\chi_t^c)^2 + 2(f^{abc}\phi_r^b\chi_t^c)^2\Big]. \tag{1.17}$$

In the above Lagrangian all the fields transform in adjoint representation and hence carry SU(N) colour indices a, b, c. A_μ^a, η^a represent the gauge and ghost fields respectively while ξ is the gauge fixing parameter. The Majorana fields are denoted by λ_m^a, with $m = 1, ..., 4$ denoting their generation type. The scalar and pseudo-scalar fields ϕ_r^a and χ_r^a, which help to maintain fermionic and bosonic degrees of freedom same, interact identically with the gauge fields. Here the indices r, t represent different types of scalars and pseudo-scalars in the theory. In four dimensions, $r, t = 1, 2, 3$.

The six antisymmetric matrices α and β satisfy the following commutation and anti-commutation relations

$$[\alpha^r, \alpha^t]_+ = [\beta^r, \beta^t]_+ = -2\delta^{rt}\mathbb{I}, \quad [\alpha^r, \beta^t]_- = 0. \tag{1.18}$$

The traces of the above mentioned matrices are given by

$$\mathrm{tr}(\alpha^r) = \mathrm{tr}(\beta^r) = \mathrm{tr}(\alpha^r\beta^t) = 0, \quad \mathrm{tr}(\alpha^r\alpha^t) = \mathrm{tr}(\beta^r\beta^t) = -4\delta^{rt}. \tag{1.19}$$

Feynman rules for the first three terms of the Lagrangian in Eq. (1.17) are given in the previous section and the remaining ones are furnished below. We denote Majorana fermions through straight lines, scalar through dotted lines and pseudo-scalars through dash dot lines.

- The propagators for Majorana fermions, scalars and pseudo-scalars are given by:

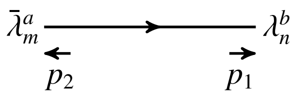

$$i\,(2\pi)^4\,\delta^{(4)}\,(p_1 + p_2)\,\frac{\not{p}_1}{p_1^2 + i\varepsilon}\delta^{ab}\delta_{mn}$$

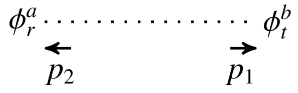

$$i\,(2\pi)^4\,\delta^{(4)}\,(p_1 + p_2)\,\frac{1}{p_1^2 + i\varepsilon}\delta^{ab}\delta_{rt}$$

$$i\,(2\pi)^4\,\delta^{(4)}\,(p_1 + p_2)\,\frac{1}{p_1^2 + i\varepsilon}\delta^{ab}\delta_{rt}$$

- The interacting vertices are given by:

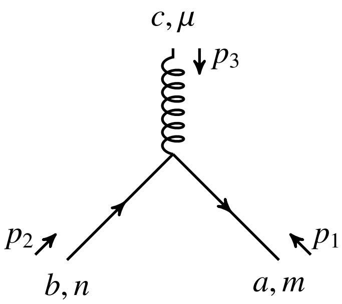

$$g_{\mathrm{YM}}\gamma^\mu\,(2\pi)^4\,\delta^{(4)}\,(p_1 + p_2 + p_3)\,f^{abc}\,\delta_{mn}$$

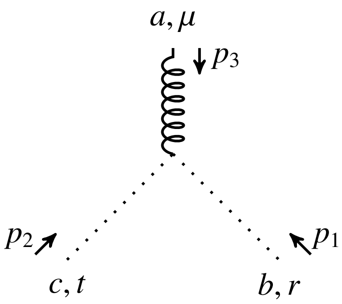

$$-g_{\mathrm{YM}}\,(2\pi)^4\,\delta^{(4)}\,(p_1 + p_2 + p_3)\,(p_1 - p_2)^\mu f^{abc}\delta_{rt}$$

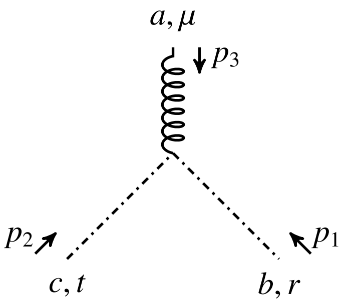

$$-g_{\mathrm{YM}}\,(2\pi)^4\,\delta^{(4)}\,(p_1 + p_2 + p_3)\,(p_1 - p_2)^\mu f^{abc}\delta_{rt}$$

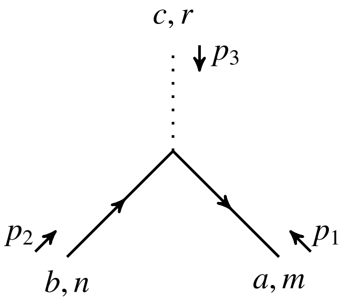

$$i g_{\rm YM} (2\pi)^4 \, \delta^{(4)} (p_1 + p_2 + p_3) \, \alpha^r_{mn} f^{abc}$$

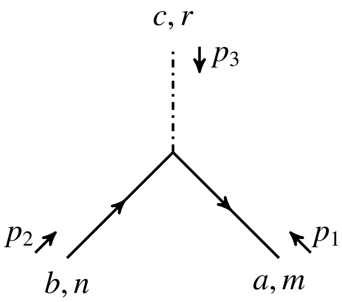

$$-g_{\rm YM} \gamma_5 \, (2\pi)^4 \, \delta^{(4)} (p_1 + p_2 + p_3) \, \beta^r_{mn} f^{abc}$$

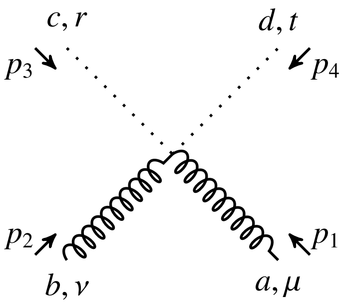

$$\begin{aligned} & i g^2_{\rm YM} (2\pi)^4 \, \delta^{(4)} (p_1 + p_2 + p_3 + p_4) \\ & \times \left(f^{ad,bc} + f^{ac,bd} \right) g^{\mu\nu} \delta_{rt} \end{aligned}$$

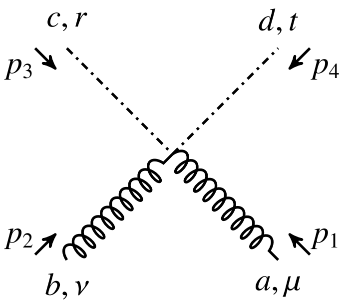

$$\begin{aligned} & i g^2_{\rm YM} (2\pi)^4 \, \delta^{(4)} (p_1 + p_2 + p_3 + p_4) \\ & \times \left(f^{ad,bc} + f^{ac,bd} \right) g^{\mu\nu} \delta_{rt} \end{aligned}$$

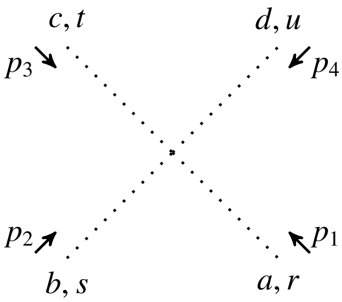

$$\begin{aligned} & i g^2_{\rm YM} (2\pi)^4 \, \delta^{(4)} (p_1 + p_2 + p_3 + p_4) \\ & \times \Big\{ (\delta_{ru}\delta_{st} - \delta_{rt}\delta_{su}) \, f^{ab,cd} + (\delta_{ru}\delta_{st} - \delta_{rs}\delta_{tu}) \, f^{ac,bd} \\ & + (\delta_{rt}\delta_{su} - \delta_{rs}\delta_{tu}) \, f^{ad,bc} \Big\} \end{aligned}$$

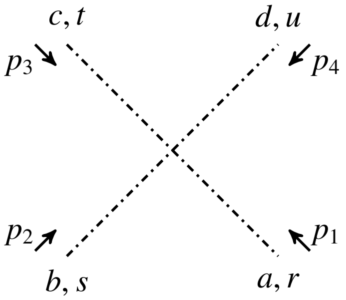

$$
\begin{aligned}
& i g_{\mathrm{YM}}^2 \, (2\pi)^4 \, \delta^{(4)} \, (p_1 + p_2 + p_3 + p_4) \\
& \times \Big\{ (\delta_{ru}\delta_{st} - \delta_{rt}\delta_{su}) \, f^{ab,cd} + (\delta_{ru}\delta_{st} - \delta_{rs}\delta_{tu}) \, f^{ac,bd} \\
& + (\delta_{rt}\delta_{su} - \delta_{rs}\delta_{tu}) \, f^{ad,bc} \Big\}
\end{aligned}
$$

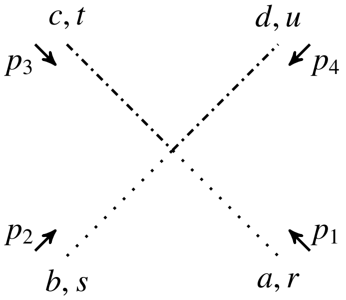

$$
\begin{aligned}
& - i g_{\mathrm{YM}}^2 \, (2\pi)^4 \, \delta^{(4)} \, (p_1 + p_2 + p_3 + p_4) \\
& \times \left(f^{ad,bc} + f^{ac,bd} \right) \delta_{rs}\delta_{tu}
\end{aligned}
$$

In addition to these rules, we have to keep in mind the following points:

- For any Feynman diagram, the symmetry factor needs to be multiplied appropriately. The symmetry factor is defined as the number of ways one can obtain the topological configuration of the Feynman diagram under consideration.
- For each loop momenta, the integration over the loop momenta, k, needs to be performed with the integration measure $d^d k/(2\pi)^d$ in d-dimensions (in dimensional regularisation).
- For each quark/Majorana fermion/ghost loop, one has to multiply a factor of (-1).

1.4 Perturbative Calculations in QCD

Thanks to the property of asymptotic freedom which allows us to perform the calculations in high energy regime using the techniques of pQCD. In pQCD, theoretical predictions are made through the computations of S-matrix elements. The S-matrix elements are directly related to the scattering amplitude which is expanded in powers of coupling constants within the framework of perturbation theory. This expansion is represented through the set of Feynman diagrams and the Feynman rules encapsulate the connection between these two. Hence, the theoretical predictions boil down to evaluate the set of Feynman diagrams. Using the Feynman rules presented in Sec. 1.2.2 and Sec. 1.3.1, we can evaluate all the Feynman diagrams order by order in the perturbation theory.

Achieving precise theoretical predictions demand to go beyond the wall of LO which consists of evaluating the virtual/loop as well as real emission diagrams. However, the contribution arising from the individual one is not finite i.e. they are divergent. These divergences are of three types: ultraviolet (UV), soft and collinear divergences. For simplicity, we call both soft and collinear as infrared (IR) divergences.

The UV divergences arise from the region of large momentum or very high energy of the Feynman integrals, or, equivalently, because of the physical phenomena at very short distances and through UV renormalisation we can get rid of these divergences. Note that unlike QCD, $\mathcal{N} = 4$ SYM theory is a UV complete theory i.e. there are no divergences which has UV origin. Before performing the UV renormalisation, we need to regulate the Feynman integrals which is essentially required to identify the true nature of divergences. There are several ways to regulate the integrals. The most consistent and beautiful way is the framework of dimensional regularisation [19–21]. Within the framework, we need to perform the integrals in general d-dimensions which is taken as $4 + \epsilon$ in this thesis. Upon performing the integrals, all the UV singularities appear as poles in ϵ. The UV renormalisation, which is performed through redefining all the quantities present in the Lagrangian, absorbs these poles and gives rise to a UV finite result. The UV renormalisation is done at an energy scale, known as renormalisation scale, μ_R. On the other hand, the soft divergences arise from the low momentum limit (approaching zero) of the loop integrals and the collinear ones arise when any loop momentum becomes collinear to any of the external massless particles. The collinear divergence is a property of theories with massless particles. Hence, even after performing the UV renormalisation, the resulting expressions obtained through the evaluation the loop integrals are not finite, they contain poles arising from soft and collinear regions of the loop integrals. To remove the residual IR divergences, we need to add the contributions arising from the real emission diagrams. The latter contains soft as well as collinear divergences which have the same form as that of loop integrals. Once we add the virtual and real emission diagrams and evaluate the phase space integrals, the resulting expressions are guaranteed to be freed from UV, soft and final state collinear singularities, thanks to the Kinoshita-Lee-Nauenberg (KLN) theorem [22, 23]. An analogous result for QED alone is known as Bloch-Nordsieck cancellation [24]. However, the collinear singularities arising from the collinear configurations involving initial state particles remain. Those are removed at the hadronic level through the techniques, known as mass factorisation, where the residual singularities are absorbed into the bare parton distribution functions (PDFs). So, the observables at the hadronic level are finite which are compared with the experimental outcomes at the hadron colliders. Just like UV renormalisation, mass factorisation is done at some energy scale, called mass factorisation scale, μ_F. The μ_R as well as μ_F are unphysical scales. The dependence of the fixed order results on these scale is an artifact of the truncation of the perturbative series to a finite order. If we can capture the results to all order, then the dependence goes away.

The core part of this thesis deals with the higher order QCD corrections employing the methodology of perturbation theory to few important field theory quantities in BSM and soft gluon/threshold resummation to one of the very important observables called rapidity distribution associated with the SM Higgs boson production. More specifically, the thesis contains

- two-loop virtual corrections to the production of a pseudo-scalar Higgs boson (A) associated with a jet [3],
- form factor (FF) contributions to the Konishi operator at next-to-next-to-next-to-leading order (N^{3}LO) in $\mathcal{N} = 4$ SYM theory [5],

- two-loop finite remainders (FR) of the Konishi operator in $\mathcal{N} = 4$ SYM theory [8],
- threshold resummation to the rapidity distribution of the SM Higgs boson production at next-to-next-to-leading order (NNLO) + next-to-next-to-leading logarithmic (NNLL) accuracy [9].

1.4.1 2-loop virtual corrections to pseudo-scalar plus a jet

Although the SM is remarkably successful in explaining most of the observed phenomena at the subatomic level, it has many shortfalls. For example, it does not have dark matter candidate to explain relic abundance in the early universe, similarly the observed baryon asymmetry and the phenomena of neutrino oscillations. There exist several BSM scenarios that address these issues and provide plausible explanations. One of the most popular extensions of the SM, namely, the minimal supersymmetric SM (MSSM) and two Higgs doublet model [25–32] have richer Higgs sector containing more than one Higgs boson and there have been intense search strategies to observe them at the LHC. In particular, production of CP odd Higgs boson, A in BSM at the LHC has been studied in detail due to similarities with its CP even counter part i.e. the SM Higgs boson. While, the searches for A have been underway at the LHC, predictions for observables involving A, in the theoretical side, are already available. In [33–36] the next-to-leading order (NLO) perturbative QCD corrections to inclusive production of A were computed and the corrections were found to be as large as 67% compared to LO. The results on NNLO production cross section for A in effective field theory can be found in [37–39].

In order to probe the nature of A and its coupling to other SM particles, one also needs to study exclusive observables namely the differential cross sections. In addition, observables involving A recoiled against one or two hard jets can help to efficiently reject the background from other sources. It was noted in [40, 41] that observables with jet vetos enhance the significance of the signal considerably allowing one to study the properties of the Higgs boson and its coupling to other SM particles. Recently, in [42], a complete NNLO prediction for Higgs-plus-jet final states and for the transverse momentum distribution of the Higgs boson taking into account the experimental definition of the fiducial cross sections has been achieved. For Higgs-plus-jet production at NNLO, see [43–47]. The relevant two loop amplitudes can be found in [48–54]. A being produced dominantly in gluon initiated processes shares a lot with its counter part, namely the scalar Higgs boson. In particular one finds that the theoretical uncertainties and the perturbative corrections are significantly large. For the A, the results for differential distributions are available only up to NLO level, for example, see [55, 56]. Hence it is desirable to have predictions up to NNLO level for observables like A + 1jet, transverse momentum and rapidity distributions of A, taking into account various experimental cuts. As a first step, *in the published work [3], we demonstrate the computation of virtual contributions up to NNLO in effective theory to the production of A in association with a jet.*

The coupling of A to gluons is mediated through a heavy quark loop. In the limit of large quark mass, it is described by an effective Lagrangian that only admits light degrees of freedom. The evaluation of 2-loop virtual corrections to this process is truly a non-trivial task not only because of the involvement of a large number of Feynman diagrams but also due to the presence of the axial vector coupling. We work in dimensional regularisation [19–21] and use the 't Hooft-Veltman prescription [19] for the axial vector current. The state-of-the-art techniques including integration-by-parts (IBP) [57, 58] and Lorentz invariant (LI) [59] identities have been employed to accomplish this task. The UV renormalisation is quite involved since the two operators, present in the Lagrangian, mix under renormalization due to the axial anomaly and additionally, a finite renormalisation constant [60, 61] needs to be introduced in order to fulfil the chiral Ward identities. *Our findings in [3] are consistent with the universal structure of the infrared poles predicted by Catani [4]. We have also studied connection of this amplitude with $\mathcal{N} = 4$ SYM amplitudes in the context of leading transcendentality principle.*

1.4.2 Konishi form factor at N^{3}LO in $\mathcal{N}=4$ SYM Theory

The ability to accomplish the challenging job of calculating quantities is of fundamental importance in any potential mathematical theory. In QFT, this manifests itself in the quest for computing the multi-loop and multi-leg scattering amplitudes under the framework of perturbation theory. Calculation of these scattering amplitudes are often highly non-trivial beyond certain power in strong coupling constant in a real theory such as QCD. There are several approaches to avoid the complex QCD calculation adopting certain approximations: for instance $\mathcal{N}=4$ SYM theory provides a very good platform which resembles QCD in large N limit. Recently, there has been surge of interest to study the FFs as they connect fully on-shell amplitudes and correlation functions. The FFs are a set of quantities which are constructed out of the scattering amplitudes involving on-shell states consisting of elementary fields and an off-shell state described through a composite operator.

Composite operators which are often studied in $\mathcal{N}=4$ SYM theory are called the half-BPS and the Konishi. The half-BPS operator is protected under supersymmetry i.e. it does not exhibit UV divergences up to all orders in perturbation theory. However, the Konishi operator which depends on space-time dimensions is not protected under supersymmetry and develops UV divergences beyond LO. Note that both the half-BPS and the Konishi operators demonstrate divergences coming from IR region starting from NLO in perturbation theory. The FFs for the half-BPS operator up to 2-loop order was investigated by van Neerven [62] almost three decades back. Very recently, this was extended to 3-loops in [63]. But for the Konishi operator it is known up to two loop level [64] employing on-shell unitarity method. *In [5], we demonstrate the analytic evaluation of complete third order corrections to the on-shell FFs of the Konishi operator using conventional Feynman diagrammatic approach.*

One of the main issues in computing higher order corrections in $\mathcal{N}=4$ SYM is related to the necessity of preserving the supersymmetry throughout the computation. In order to achieve that, one generally follows either of the two regularisation scheme: modified dimensional reduction ($\overline{DR}$) [65, 66] and four dimensional helicity scheme (FDH) [67, 68]. Through performing the computation explicitly in both the schemes, we have shown that the FF in $\overline{DR}$ automatically provides the correct results, where as, the results obtained in the FDH needs to be suitably modified, the modification is operator dependent and non-trivial. Hence, performing a computation in $\overline{DR}$ is much more preferable for unprotected operators like the Konishi. We have also discussed superiority of the Feynman diagrammatic approach over unitarity method in the context of the Konishi type operators. *Moreover our result [5] is the most advanced one in the context of Konishi FFs.*

1.4.3 Finite remainders of the Konishi operator at NNLO

Scattering amplitudes are the building blocks of many important observables in high energy physics and they exhibit remarkable structures of the underlying QFT. Those computed in the electroweak theory and QCD play important role in the phenomenology of collider physics. With the increase in number of loops and legs, amplitudes are not only difficult to calculate but also one obtains very large expressions. Enormous simplification can be achieved if the underlying QFT has some symmetries which leads to conserved currents. One such theory is $\mathcal{N} = 4$ SYM theory which resembles QCD in large N limit. Like QCD, $\mathcal{N} = 4$ SYM theory is a renormalizable gauge theory in four dimensional Minkowski space. Apart from having all the symmetries of QCD there are two extra features of $\mathcal{N} = 4$ SYM, namely supersymmetry and conformal symmetry that makes this theory interesting to study. The on-shell amplitudes evaluated in $\mathcal{N} = 4$ SYM theory have a simpler analytical structure in comparison to QCD amplitudes.

Over the last few years, there are several results [69–72] on n-point FFs for the Konishi operator in the weak coupling limit of $\mathcal{N} = 4$ SYM. Through them we can, not only confirm the results on the known anomalous dimension but also study the perturbative infrared structure of the off-shell amplitudes in general. In addition, they provide testing grounds for various modern techniques that were developed to compute on-shell amplitudes, namely the on-shell unitarity based methods that use unitarity [73, 74] and various recursion relations [75, 76]. The results for the one-loop two-point, two-loop two-point and one-loop three-point FFs were presented in [64]. In our earlier work [5], we have computed the three-loop two-point FF for the Konishi operator and also predicted up to $1/\epsilon$ pole at four-loop order. *In the published work [8], we demonstrate the analytic computation of 3-point FFs and hence FRs using Feynman diagrammatic approach at 2-loop level for both the half-BPS and the Konishi operator for two sets of on-shell final states consisting of* $g\phi\phi$ *and* $\phi\lambda\lambda$.

It is well known that the IR divergences of maximally helicity violating (MHV) amplitudes have an exponential structure (BDS ansatz [6]). Such a behaviour is reminiscent of the factorisation properties of gauge theory amplitudes. However we can also see this kind of exponentiation in FFs. By exponentiating the one loop IR singularities following BDS like exponentiation, we compute FR at two loops. Our result on the half-BPS for the final on-shell state $g\phi\phi$ presented in terms of harmonic polylogarithms (HPLs) numerically agrees with the earlier calculation [7] presented in terms of classical polylogarithms which was computed using unitarity based method. We find that the leading transcendental terms of the remainder function for the Konishi operator computed between $g\phi\phi$ external state coincide with the corresponding one of the half-BPS. However, for the $\phi\lambda\lambda$ external state we find that the expressions for the Konishi and the half-BPS operators do not have anything common. *In this way our calculation [8] not only gives new results on the 2-loop FRs for the both the operators but also reveals many important properties.*

1.5 Threshold resummation

Although the higher order computations provide reliable theoretical predictions however the task of computing them often becomes highly non-trivial beyond NNLO. Hence, it is natural to try alternative approaches to capture the dominant contributions from the missing higher order. The very first approach towards this direction is to compute the observables under soft-virtual (SV) approximation which often captures the dominant contributions and provide better results. However, this may give rise to large logarithms for certain observables in some kinematic regions which can spoil the convergence of the perturbation theory and hence those must be resummed to all orders to get more reliable predictions. This has been accomplished through threshold resummation techniques.

1.5.1 Threshold resummation in the Higgs rapidity distribution

While inclusive rates are important for any phenomenological study, the differential cross sections often carry more informations on the nature of interaction, quantum number of particles produced in the hard collisions. Rapidity distributions of Drell-Yan pair [77], Z boson [78] and charge asymmetries of leptons in $W^{\pm}$ boson decays [79] are already used to measure PDFs. Possible excess events in these directions can hint to BSM physics, namely R-parity violating supersymmetric models [80], models with Z' or with contact interactions and large extra dimension models [81, 82]. Like in Drell-Yan, measurements of transverse momentum and rapidity distributions of the Higgs boson will be very useful to study the properties of the Higgs boson and its couplings. *In the published work [9], we include the dominant effect of the uncalculated higher order terms, by exploiting the resummation of soft gluon emission in the rapidity distributions of the SM Higgs boson up to NNLO+NNLL accuracy.*

The possibility of performing such an improvement relies upon the observation that an accurate use of the soft gluon approximation provides the bulk of the NLO term and a reliable estimate of the NNLO effects. So, it makes sense to add the higher order terms that can be obtained in the soft gluon approximation, in order to give precise prediction.

We present a formalism that resums threshold-enhanced logarithms in double Mellin space to all orders in pQCD for the rapidity distribution of any colourless particle produced in hadron colliders. We achieve this by exploiting factorisation properties and K+G equations satisfied by the soft and virtual parts of the cross section. We compute for the first time compact and most general expressions for the resummed coefficients up to NNLO+NNLL accuracy. We find that the resummed result not only changes the fixed order predictions but also improves the perturbative convergence. *This is the most accurate result [9] for the rapidity distribution of the Higgs boson which exists in the literature till date and it is expected to play an important role in coming days at the LHC.*

2 Two loop QCD corrections for the process Pseudo-scalar Higgs $\to$ 3 partons

The materials presented in this chapter are the result of an original research done in collaboration with Pulak Banerjee and V. Ravindran, and these are based on the published article [3].

2.1 Prologue

After the landmark discovery of a scalar particle in 2012 at the LHC [1, 2], the detailed study on the nature of this particle and its couplings to other SM particles is underway. There are already several compelling evidences from both theoretical and experimental side, pointing to the fact that the discovered boson is none other than the Higgs boson of the SM. Although the SM is remarkably successful in explaining most of the observed phenomena at the subatomic level, it has many shortfalls. For example it does not have dark matter candidate to explain relic abundance in the early universe, similarly the observed baryon asymmetry and the phenomena of neutrino oscillations. In addition, a proper field theoretical description of gravitational force still remains missing. There exist several BSM scenarios that address these issues and provide plausible explanations.

Often these BSM models have larger symmetry and contain more particles than the SM, providing the scope for rich phenomenology at the LHC. The precise measurements of the coupling of the Higgs boson with other SM particles as well as the dedicated direct searches of new scalars at the LHC can constrain the parameters of the scalar sectors in the BSM models. For example, the MSSM which addresses some of the shortfalls of the SM contains in addition to other fields, two isospin doublets of Higgs field [25–32]. These two doublets preserve the analyticity of the scalar potential, maintain the anomaly cancellation and responsible for masses of up and down type fermions. After spontaneous symmetry breaking, scalar sector contains three neutral (h, H, A) and two charged $(H^{\pm})$ Higgs bosons, where h and H are CP-even scalars while A is CP-odd pseudo-scalar. The upper bound on the mass of the light scalar Higgs h can be predicted within the theory as the self couplings of the Higgs fields are fixed in terms of the gauge couplings.

Since the coupling of A with the fermions is appreciable in the small and moderate $\tan\beta$, the ratio of vacuum expectation values $v_i, i = 1, 2$ of the Higgs doublets, it can be searched at the LHC. Note that large gluon flux at the LHC can also boost the cross section. While, the searches for A have been underway from the experimental side at the LHC, predictions for observables involving A, in the theoretical side, are already available. Like the production of CP scalar Higgs boson, the LO predictions for A severely suffer from theoretical uncertainties resulting from μ_R and μ_F scales as well as large higher order radiative corrections. These scales enter at leading order through the renormalised strong coupling constant $g_s(\mu_R)$ and the PDFs defined at the factorisation scale μ_F. This necessitates to go beyond LO in perturbation theory. In [33–36] the NLO pQCD corrections to inclusive production of A were computed. It was found that the scale dependence reduced from 48% to 35% and the corrections were found to be as large as 67% compared to LO. The effective field theory approach where the top quark degrees of freedom are integrated out has provided opportunity to go beyond NLO level to further improve the predictions. The results on NNLO production cross section for A can be found in [37–39] which further improves the reliability of the predictions.

There have been continued efforts to go beyond NNLO as the results on the FFs and soft gluon contributions at third order level have become available. For this purpose, in [83], one of the authors computed FFs of the effective composite operators between quark and gluon states at three loop level in QCD along with the lower order. Using the formalism developed in [84, 85] and the third order results on the FFs of the A [83], operator renormalisation constant [83, 86, 87], the universal soft-collinear distribution [88] and the mass factorisation kernels [89, 90], the first results on the threshold N^{3}LO corrections for the inclusive production of A were reported in [91]. In addition, the third order corrections to both the N-independent part of the resummed cross section [92, 93] and the matching coefficients in soft-collinear effective theory (SCET) were also computed in [83]. In [94], one of the authors obtained the approximate N^{3}LO contribution using the full N^{3}LO results available for the scalar Higgs boson. This along with the threshold effects at next-to-next-to-next-to-leading logarithmic (N^{3}LL) accuracy using both conventional [92, 93] and SCET [95–101] set ups provide the accurate prediction [94] for the inclusive production of A at the LHC.

In order to probe the nature of A and its coupling to other SM particles, one also needs to study exclusive observables namely the differential cross sections. The distributions of transverse momentum and rapidity of the produced A are often very useful for characterising its properties. In addition, observables involving A recoiled against one or two hard jets can help to efficiently reject the background from other sources. There are already several studies in the case of scalar Higgs boson in the literature. For example, the differential cross sections for scalar Higgs boson via gluon fusion are available including its decay to two photons or two weak gauge bosons, see [102–104]. It was noted in [40, 41] that observables with jet vetos enhance the significance of the signal considerably allowing one to study the properties of the Higgs boson and its coupling to other SM particles. Recently, in [42], a complete NNLO prediction for Higgs-plus-jet final states and for the transverse momentum distribution of the Higgs boson taking into account the experimental definition of the fiducial cross sections has been achieved. For Higgs-plus-jet production at NNLO, see [43–47]. The relevant two-loop amplitudes can be found in [48–54]. A being produced dominantly in gluon initiated processes shares a lot with its counter part, namely the scalar Higgs boson. In particular one finds that the theoretical uncertainties and the perturbative corrections are significantly large. For the A, the results for differential distributions are available only up to NLO level, for example, see [55, 56]. Hence it is desirable to have predictions up to NNLO level for observables like $A + 1$jet, transverse momentum and rapidity distributions of A, taking into account various experimental cuts. At NNLO, one encounters three different production channels that contribute to these observables: pure virtual, virtual-real emissions, pure real emissions. In this thesis, we present all the relevant contributions resulting from pure virtual amplitudes. In particular, we consider the processes $A \to ggg$ and $A \to q\bar{q}g$ up to two-loop level in effective theory where top quark has been integrated out. These amplitudes can be used to predict the production of A associated with a jet in hadron collider up to two-loop level in QCD after performing straightforward crossing of kinematic variables. In the effective theory for A, one is left with two effective operators with same quantum numbers and mass dimensions, hence they mix under renormalisation. We will present the results in the $\overline{MS}$ scheme.

This chapter is organised as follows. In Section 2.2.1, the effective Lagrangian for the coupling of A with partons along with the relevant Wilson coefficients are presented. After introducing the notation in Section 2.2.2, we elaborate on how to deal with γ_5 and Levi-Civita tensor in dimensional regularisation and subtleties involved in operator mixing and finite renormalisation in Section 2.2.3. In Section 2.2.4, we describe the method of our computation of relevant matrix elements up to two-loop level in QCD and Section 2.2.5 contains the study of IR structure of the results obtained in the context of Catani's predictions. In Section 2.3, we discuss our results on one and two loops QCD amplitudes in the light of maximum transcendentality principle in $\mathcal{N} = 4$ SYM theory. Finally we summarize in Section 2.4.

2.2 Theoretical Framework

2.2.1 Effective Lagrangian

In the generic BSM scenarios, A couples to heavy quarks through Yukawa interaction. If we restrict ourselves to the dominant contribution coming from top Yukawa coupling, then the interaction Lagrangian is given by

$$\mathcal{L}_{At\bar{t}} = -ig_t \frac{A}{v} m_t \bar{t}\gamma_5 t \tag{2.1}$$

where the model dependent constant g_t in MSSM is $\cos\beta$ where $\tan\beta$ is ratio of vacuum expectation values of the two Higgs fields, m_t is the top quark mass, v the SM vacuum expectation value.

In the limit of infinite top quark mass, the interaction between a pseudo-scalar A and the fields of the remaining SM is encapsulated by an effective Lagrangian [105] which reads as

$$\mathcal{L}^A_{\text{eff}} = \Phi^A(x)\Big[-\frac{1}{8} C_G O_G(x) - \frac{1}{2} C_J O_J(x) \Big] \tag{2.2}$$

where the operators are defined as

$$O_G(x) = G^{\mu\nu}_a \tilde{G}_{a,\mu\nu} \equiv \epsilon_{\mu\nu\rho\sigma} G^{\mu\nu}_a G^{\rho\sigma}_a \,, \qquad O_J(x) = \partial_\mu \left(\bar{\psi}\gamma^\mu\gamma_5\psi\right) \,. \tag{2.3}$$

The Wilson coefficients C_G and C_J are obtained by integrating out the loops resulting from top quark. The coefficient C_G does not receive any QCD corrections beyond one loop in the perturbation series expanded in strong coupling constant $a_s \equiv g_s^2/(16\pi^2) = \alpha_s/(4\pi)$ due to the Adler-Bardeen theorem [60] and C_J starts at second order. Their expressions are given below

$$
\begin{aligned}
C_G &= -a_s 2^{\frac{5}{4}} G_F^{\frac{1}{2}} \cot\beta \\
C_J &= -\left[a_s C_F \left(\frac{3}{2} - 3 \ln \frac{\mu_R^2}{m_t^2} \right) + a_s^2 C_J^{(2)} + \cdots \right] C_G \,.
\end{aligned}
\tag{2.4}
$$

In the above expressions, $G_a^{\mu\nu}$ and ψ represent gluonic field strength tensor and light quark fields, respectively and G_F is the Fermi constant. Here, $a_s \equiv a_s\left(\mu_R^2\right)$ is the renormalised strong coupling constant at the scale μ_R which is related to the unrenormalised one, $\hat{a}_s \equiv \hat{g}_s^2/(16\pi^2)$ through

$$
\hat{a}_s S_\epsilon = \left(\frac{\mu^2}{\mu_R^2} \right)^{\epsilon/2} Z_{a_s} a_s \tag{2.5}
$$

with $S_\epsilon = \exp\left[(\gamma_E - \ln 4\pi)\epsilon/2\right]$ and μ is the scale introduced to keep the strong coupling constant dimensionless in $d = 4 + \epsilon$ space-time dimensions. The renormalisation constant Z_{a_s} [106] up to order $O(a_s^2)$ is given by

$$
Z_{a_s} = 1 + a_s \left[\frac{2}{\epsilon} \beta_0 \right] + a_s^2 \left[\frac{4}{\epsilon^2} \beta_0^2 + \frac{1}{\epsilon} \beta_1 \right] \tag{2.6}
$$

β_i are the coefficients of the QCD β-functions [106], given by

$$
\begin{aligned}
\beta_0 &= \frac{11}{3} C_A - \frac{4}{3} n_f T_F \,, \\
\beta_1 &= \frac{34}{3} C_A^2 - 4 n_f C_F T_F - \frac{20}{3} n_f T_F C_A \,,
\end{aligned}
\tag{2.7}
$$

with the SU(N) QCD color factors

$$
C_A = N, \qquad C_F = \frac{N^2 - 1}{2N} \quad \text{and} \quad T_F = \frac{1}{2} \,. \tag{2.8}
$$

n_f is the number of active light quark flavours.

2.2.2 Notation

Since the amplitudes for the production of a pseudo-scalar in association with a jet from gluon gluon or quark anti-quark initiated channels are related to the decay of the same to three gluons or quark anti-quark gluon by crossing symmetry, in the rest of the chapter we consider the decay of A to both ggg and $q\bar{q}g$ which can be expressed as

$$
\begin{aligned}
A(q) &\rightarrow g(p_1) + g(p_2) + g(p_3) \\
A(q) &\rightarrow q(p_1) + \bar{q}(p_2) + g(p_3)
\end{aligned}
\tag{2.9}
$$

The associated Mandelstam variables are defined as

$$
s \equiv (p_1 + p_2)^2 > 0, \qquad t \equiv (p_2 + p_3)^2 > 0, \qquad u \equiv (p_1 + p_3)^2 > 0, \tag{2.10}
$$

which satisfy the relation

$$
s + t + u = M_A^2 \equiv q^2 = Q^2 > 0, \tag{2.11}
$$

where M_A is the mass of A. We also define following dimensionless invariants, which we use to describe our results in terms of HPLs [107] and 2d-HPLs [108, 109] as

$$
x \equiv \frac{s}{Q^2}, \qquad y \equiv \frac{u}{Q^2}, \qquad z \equiv \frac{t}{Q^2}, \tag{2.12}
$$

where (x, y, z) lie between 0 and 1 and satisfy the condition

$$
x + y + z = 1\,. \tag{2.13}
$$

2.2.3 Operator mixing and UV renormalisation

In the following, we describe the computation of one and two loop matrix elements that are needed to perform NNLO QCD corrections to the decay of A to three jets. The composite operators present in the effective Lagrangian Eq. (2.2), develop UV divergences that require additional renormalisation. Also these operators mix under renormalisation due to same quantum numbers.

In higher order computations involving chiral quantities, the inherently four dimensional objects like γ_5 and $\varepsilon^{\mu\nu\rho\sigma}$, the Levi-Civita tensor, in $d \neq 4$ dimensions pose problems. In this article, we have followed self-consistent and the most practical definition of γ_5 introduced for multi-loop calculations in dimensional regularization by 't Hooft and Veltman through [19]

$$\gamma_5 = i\frac{1}{4!}\varepsilon_{\nu_1\nu_2\nu_3\nu_4}\gamma^{\nu_1}\gamma^{\nu_2}\gamma^{\nu_3}\gamma^{\nu_4}\,. \tag{2.14}$$

Here, $\varepsilon^{\mu\nu\rho\sigma}$ is contracted according to the rule

$$\varepsilon_{\mu_1\nu_1\rho_1\sigma_1}\,\varepsilon^{\mu_2\nu_2\rho_2\sigma_2} = \begin{vmatrix} \delta^{\mu_2}_{\mu_1} & \delta^{\nu_2}_{\mu_1} & \delta^{\rho_2}_{\mu_1} & \delta^{\sigma_2}_{\mu_1} \\ \delta^{\mu_2}_{\nu_1} & \delta^{\nu_2}_{\nu_1} & \delta^{\rho_2}_{\nu_1} & \delta^{\sigma_2}_{\nu_1} \\ \delta^{\mu_2}_{\rho_1} & \delta^{\nu_2}_{\rho_1} & \delta^{\rho_2}_{\rho_1} & \delta^{\sigma_2}_{\rho_1} \\ \delta^{\mu_2}_{\sigma_1} & \delta^{\nu_2}_{\sigma_1} & \delta^{\rho_2}_{\sigma_1} & \delta^{\sigma_2}_{\sigma_1} \end{vmatrix} \tag{2.15}$$

where all the Lorentz indices are considered to be d-dimensional [86]. The prescription used here fails to preserve the anti-commutativity of γ_5 with γ^μ in arbitrary d-dimensions. In addition, the Ward identities, which are valid in a 4-dimensional regularization scheme like the one of Pauli-Villars where γ_5 does not pose any problem, are violated as well. Due to this, it is not possible to restore the correct renormalisation of axial current, which is defined as [86, 110]. A finite renormalisation of the axial vector current is required to preserve chiral Ward identities and the Adler-Bardeen theorem. The axial current is defined as

$$J_5^\mu \equiv \bar{\psi}\gamma^\mu\gamma_5\psi = i\frac{1}{3!}\varepsilon^{\mu\nu_1\nu_2\nu_3}\bar{\psi}\gamma_{\nu_1}\gamma_{\nu_2}\gamma_{\nu_3}\psi \tag{2.16}$$

in dimensional regularization. The chiral Ward identities can be fixed by introducing a finite renormalisation constant Z_5^s [60, 61] in addition to the standard overall UV renormalisation constant $Z^s_{\overline{MS}}$ within the $\overline{MS}$-scheme:

$$\left[J_5^\mu\right]_R = Z_5^s Z^s_{\overline{MS}} \left[J_5^\mu\right]_B \,. \tag{2.17}$$

While the evaluation of the appropriate Feynman diagrams explicitly fixes the constants $Z^s_{\overline{MS}}$, the finite renormalisation constant can not be fixed without using the anomaly equation. In other words, Z_5^s can be determined by demanding the conservation of the one loop character [111] of the operator relation of the axial anomaly in dimensional regularization:

$$\begin{aligned} \left[\partial_\mu J_5^\mu\right]_R &= a_s\frac{n_f}{2}\left[G\tilde{G}\right]_R \\ \text{i.e.} \quad [O_J]_R &= a_s\frac{n_f}{2}\left[O_G\right]_R \,. \end{aligned} \tag{2.18}$$

The bare operator $[O_J]_B$ is renormalised multiplicatively as the axial current J_5^μ through

$$[O_J]_R = Z_5^s Z^s_{\overline{MS}} \left[O_J\right]_B \,, \tag{2.19}$$

but the other bare operator $[O_G]_B$ mixes under the renormalisation through

$$[O_G]_R = Z_{GG}\left[O_G\right]_B + Z_{GJ}\left[O_J\right]_B \tag{2.20}$$

through renormalisation constants Z_{GG} and Z_{GJ}. The above two equations can be written as

$$[O_\Sigma]_R = Z_{\Sigma\Lambda}\, [O_\Lambda]_B \tag{2.21}$$

with

$$\begin{aligned}
&\Sigma, \Lambda = \{G, J\}\,,\\
&O \equiv \begin{bmatrix} O_G \\ O_J \end{bmatrix} \qquad \text{and} \qquad Z \equiv \begin{bmatrix} Z_{GG} & Z_{GJ} \\ Z_{JG} & Z_{JJ} \end{bmatrix},
\end{aligned}\tag{2.22}$$

where

$$\begin{aligned}
Z_{JG} &= 0 \qquad \text{to all orders in perturbation theory}\,,\\
Z_{JJ} &\equiv Z_5^s Z^s_{\overline{MS}}\,.
\end{aligned}\tag{2.23}$$

The expressions for the above mentioned renormalisation constants $Z^s_{\overline{MS}}, Z_{GG}, Z_{GJ}$ up to $O\left(a_s^3\right)$ are given in [86, 87] using operator product expansion. In [83] one of the author in the current article has calculated the same quantities in a completely different way and found exact agreement with the original calculation. In the latter article, authors have used universality of the IR poles of the FF to determine the UV renormalisation constants and also computed Z_5^s up to $O(a_s^2)$ by demanding the operator relation of the axial anomaly Eq. (2.18). These renormalisation constants up to sufficient order in the perturbation theory appropriate for our calculation are given below:

$$\begin{aligned}
Z_{GG} &= 1 + a_s\left[\frac{22}{3\epsilon}C_A - \frac{4}{3\epsilon}n_f\right] + a_s^2\left[\frac{1}{\epsilon^2}\left\{\frac{484}{9}C_A^2 - \frac{176}{9}C_A n_f + \frac{16}{9}n_f^2\right\}\right.\\
&\quad\left. + \frac{1}{\epsilon}\left\{\frac{34}{3}C_A^2 - \frac{10}{3}C_A n_f - 2C_F n_f\right\}\right],\\
Z_{GJ} &= a_s\left[-\frac{24}{\epsilon}C_F\right] + a_s^2\left[\frac{1}{\epsilon^2}\left\{-176 C_A C_F + 32 C_F n_f\right\}\right.
\end{aligned}$$

$$
\begin{aligned}
&+\frac{1}{\epsilon}\left\{-\frac{284}{3}C_AC_F+84C_F^2+\frac{8}{3}C_Fn_f\right\}\Bigg],\\
Z_{JJ} &= 1+a_s\left[-4C_F\right]+a_s^2\left[-\frac{44}{3\epsilon}C_AC_F-\frac{10}{3\epsilon}C_Fn_f+22C_F^2-\frac{107}{9}C_AC_F+\frac{31}{18}C_Fn_f\right].
\end{aligned}
\tag{2.24}
$$

Using these operator renormalisation constants along with strong coupling constant renormalisation through Z_{a_s}, we obtain UV finite amplitudes.

2.2.4 Matrix elements

Our next step is to compute all the relevant matrix elements resulting from virtual amplitudes for the decay of A to three gluons and also to quark antiquark gluon. They are obtained from the amplitudes $|\mathcal{A}_f\rangle$, where $f = ggg, q\bar{q}g$ up to two loop level, contain two sub-amplitudes namely $|\mathcal{M}_f^\Lambda\rangle$ computed using O_G ($\Lambda = G$) and O_J ($\Lambda = J$) operators multiplied by the appropriate Wilson coefficients C_Λ:

$$
|\mathcal{A}_f\rangle = \sum_{\Lambda=G,J} C_\Lambda(a_s)|\mathcal{M}_f^\Lambda\rangle \tag{2.25}
$$

The above UV finite sub-amplitudes $|\mathcal{M}_f^\Lambda\rangle$ can be expressed in terms unrenormalised sub-amplitudes $|\hat{\mathcal{M}}_f^{\Lambda,(n)}\rangle$ as follows:

$$
|\mathcal{M}_f^\Lambda\rangle = (16\pi^2 a_s)^{\frac{1}{2}} \sum_{\Sigma=G,J} Z_{\Lambda\Sigma}\left(|\mathcal{M}_f^{\Sigma,(0)}\rangle + a_s|\mathcal{M}_f^{\Sigma,(1)}\rangle + a_s^2|\mathcal{M}_f^{\Sigma,(2)}\rangle + O(a_s^3)\right), \tag{2.26}
$$

where

$$
\begin{aligned}
|\mathcal{M}_f^{\Sigma,(0)}\rangle &= \left(\frac{1}{\mu_R^\epsilon}\right)^{\frac{1}{2}} |\hat{\mathcal{M}}_f^{\Sigma,(0)}\rangle,\\
|\mathcal{M}_f^{\Sigma,(1)}\rangle &= \left(\frac{1}{\mu_R^\epsilon}\right)^{\frac{3}{2}} \left[|\hat{\mathcal{M}}_f^{\Sigma,(1)}\rangle + \mu_R^\epsilon\frac{r_1}{2}|\hat{\mathcal{M}}_f^{\Sigma,(0)}\rangle\right],\\
|\mathcal{M}_f^{\Sigma,(2)}\rangle &= \left(\frac{1}{\mu_R^\epsilon}\right)^{\frac{5}{2}} \left[|\hat{\mathcal{M}}_f^{\Sigma,(2)}\rangle + \mu_R^\epsilon\frac{3r_1}{2}|\hat{\mathcal{M}}_f^{\Sigma,(1)}\rangle + \mu_R^{2\epsilon}\left(\frac{r_2}{2}-\frac{r_1^2}{8}\right)|\hat{\mathcal{M}}_f^{\Sigma,(0)}\rangle\right]
\end{aligned}
\tag{2.27}
$$

with

$$r_1 = \frac{2\beta_0}{\epsilon}, \qquad r_2 = \left(\frac{4\beta_0^2}{\epsilon^2} + \frac{\beta_1}{\epsilon}\right). \tag{2.28}$$

In the above equations, the unrenormalised sub-amplitudes $|\hat{\mathcal{M}}_f^{\Sigma}\rangle$ are computed in powers of bare coupling constant $\hat{a}_s$. Using these UV finite sub-amplitudes $|\mathcal{M}_f^{\Sigma}\rangle$, we then obtain relevant matrix element squares to observables to desired order in a_s. For $A \rightarrow ggg$, we find

$$\begin{aligned}\mathcal{S}_{ggg} &= \langle \mathcal{A}_{ggg} | \mathcal{A}_{ggg} \rangle \\ &= a_s^3 \left(C_G^{(1)}\right)^2 \left[S_g^{G,(0)} + a_s S_g^{G,(1)} + a_s^2 \left(S_g^{G,(2)} + 2C_J^{(1)} S_g^{GJ,(1)}\right)\right]\end{aligned} \tag{2.29}$$

where

$$\begin{aligned}S_g^{G,(0)} &= \langle \mathcal{M}_{ggg}^{G,(0)} | \mathcal{M}_{ggg}^{G,(0)} \rangle\,, \\ S_g^{G,(1)} &= 2\langle \mathcal{M}_{ggg}^{G,(0)} | \mathcal{M}_{ggg}^{G,(1)} \rangle\,, \\ S_g^{GJ,(1)} &= \langle \mathcal{M}_{ggg}^{G,(0)} | \mathcal{M}_{ggg}^{J,(1)} \rangle\,, \\ S_g^{G,(2)} &= \langle \mathcal{M}_{ggg}^{G,(1)} | \mathcal{M}_{ggg}^{G,(1)} \rangle + 2\langle \mathcal{M}_{ggg}^{G,(0)} | \mathcal{M}_{ggg}^{G,(2)} \rangle\end{aligned} \tag{2.30}$$

and similarly for $A \rightarrow q\bar{q}g$, we find

$$\begin{aligned}\mathcal{S}_{q\bar{q}g} &= \langle \mathcal{A}_{q\bar{q}g} | \mathcal{A}_{q\bar{q}g} \rangle \\ &= a_s^3 \left(C_G^{(1)}\right)^2 \Bigg[S_q^{G,(0)} + a_s \left(2S_q^{G,(1)} + 2C_J^{(1)} S_q^{JG,(0)}\right) \\ &\quad + a_s^2 \left(S_q^{G,(2)} + C_J^{(1)} S_q^{JG,(1)} + \left(C_J^{(1)}\right)^2 S_q^{J,(0)} + 2C_J^{(2)} S_q^{JG,(0)}\right)\Bigg]\end{aligned} \tag{2.31}$$

where

$$\begin{aligned}S_q^{G,(0)} &= \langle \mathcal{M}_{q\bar{q}g}^{G,(0)} | \mathcal{M}_{q\bar{q}g}^{G,(0)} \rangle\,, \\ S_q^{J,(0)} &= \langle \mathcal{M}_{q\bar{q}g}^{J,(0)} | \mathcal{M}_{q\bar{q}g}^{J,(0)} \rangle\,, \\ S_q^{G,(1)} &= \langle \mathcal{M}_{q\bar{q}g}^{G,(0)} | \mathcal{M}_{q\bar{q}g}^{G,(1)} \rangle\,,\end{aligned}$$

$$
\begin{aligned}
S_q^{JG,(0)} &= \langle \mathcal{M}_{q\bar{q}g}^{J,(0)} | \mathcal{M}_{q\bar{q}g}^{G,(0)} \rangle \,, \\
S_q^{G,(2)} &= \langle \mathcal{M}_{q\bar{q}g}^{G,(1)} | \mathcal{M}_{q\bar{q}g}^{G,(1)} \rangle + 2\langle \mathcal{M}_{q\bar{q}g}^{G,(0)} | \mathcal{M}_{q\bar{q}g}^{G,(2)} \rangle \,, \\
S_q^{JG,(1)} &= 2\langle \mathcal{M}_{q\bar{q}g}^{J,(1)} | \mathcal{M}_{q\bar{q}g}^{G,(0)} \rangle + 2\langle \mathcal{M}_{q\bar{q}g}^{J,(0)} | \mathcal{M}_{q\bar{q}g}^{G,(1)} \rangle \,,
\end{aligned}
\tag{2.32}
$$

and

$$
C_G^{(1)} = -2^{\frac{5}{4}} G_F^{\frac{1}{2}} \cot\beta \,, \qquad C_J^{(1)} = -C_F \left(\frac{3}{2} - 3 \ln \frac{\mu_R^2}{m_t^2} \right). \tag{2.33}
$$

The computation of $S_a^{\Lambda,(i)}$ for $a = g, q; \Lambda = G, J, GJ, JG, i = 0, 1, 2$ closely follows the steps used in [112–119]. We briefly describe the main steps involved. The relevant tree, one and two-loop Feynman diagrams are generated using the package QGRAF [120]. While there are only few diagrams at tree and one loop level, at two loops we encounter large number of diagrams. We find that the number of two loop diagrams is 1306 for $|\hat{\mathcal{M}}_{ggg}^{G,(2)}\rangle$, 264 for $|\hat{\mathcal{M}}_{ggg}^{J,(2)}\rangle$, 328 for $|\hat{\mathcal{M}}_{q\bar{q}g}^{G,(2)}\rangle$ and 229 for $|\hat{\mathcal{M}}_{q\bar{q}g}^{J,(2)}\rangle$. We set all the external particles on-shell, in other words, the quarks, anti-quarks, gluons are kept massless and the pseudo-scalar has non-zero mass M_A. The raw QGRAF output is converted to a format that can be further used to perform the substitution of Feynman rules, contraction of color and Lorentz indices and simplification of Dirac and Gell-Mann matrices using a set of in-house routines written in the symbolic manipulating program FORM [121]. We have included ghost loops in the Feynman gauge. For the external on-shell gluons, we have kept only transversely polarization states in d-dimensions. The next step is to organise all the d-dimensional one and two loop integrals such that they can be reduced to a minimum set of scalar integrals, called master integrals (MIs). To do this, we first use Reduze2 [122, 123] to shift loop momenta to get suitable integral classes. Each integral belonging to specific class can be expressed in terms of MIs using a set of IBP [57, 58] and LI [59] identities. The LI identities are not linearly independent from the IBP identities [124], however they help to increase the speed to solve the large number of linear equations resulting from IBP. The method of IBP to reduce certain class of integrals to a set of MIs is achieved using

Laporta algorithm, [125]. This has been implemented in various symbolic manipulation packages such as AIR [126], FIRE [127], Reduze2 [122,123] and LiteRed [128,129]. We have used LiteRed [128,129] to perform the reductions of all the integrals to MIs. For one and two loop, we find the number of MIs are 7 and 89 respectively. The next task is to express all the MIs in terms of those computed analytically in [108,109]. Using these MIs in the appropriate kinematic regions, we obtain analytical results for $\mathcal{S}_f$ for $f = ggg, q\bar{q}g$. While these amplitude squares are UV finite, they are sensitive to IR divergences. Thanks to universality of these divergences, our results can be verified up to finite terms.

2.2.5 Universal Structure of IR divergences

Beyond leading order in perturbation theory, the UV renormalised amplitudes in gauge theories suffer from IR divergences due to the presence of massless particles. These IR divergences are of two types, namely soft and collinear. Soft divergences arise when momentum of a massless particle in the loop goes to zero and the collinear ones result when a massless particle in the loop becomes parallel to one of the external particles. Note that the amplitudes are not observables, instead the cross sections or decay rates made out of these amplitudes are the observables. Thanks to KLN theorem [22, 23], the finiteness of the observables can be guaranteed by summing over the degenerate final states and performing mass factorisation for the initial states. While these divergences go away in the physical observables, the amplitudes demonstrate very rich universal structure in the IR region at every order in perturbation theory. The IR structure of amplitudes in QCD is well understood and in particular, the universal structure of IR poles was predicted in a seminal paper [4] by Catani for n-point two loop amplitudes. The iterative structure of singular part of the UV renormalised amplitudes in QCD was exploited in [4] to predict the subtraction operators that capture the universal IR divergences. Later on Sterman and Tejeda-Yeomans related the predictions by Catani to the factorisation and resummation properties of QCD amplitudes [130]. The generalization of Catani's proposal for arbitrary number of loops and legs for SU(N) gauge theory using SCET was given by Becher and Neubert [131]. A similar result was also presented by Gardi and Magnea [132] by analyzing Wilson lines for hard partons.

We follow here Catani's proposal and express the UV renormalised amplitudes $|\mathcal{M}_f^{\Sigma,(n)}\rangle$ for the three point function up to two loop order in terms of universal subtraction operators $\mathbf{I}_f^{(n)}(\epsilon)$,

$$
\begin{aligned}
|\mathcal{M}_f^{\Sigma,(1)}\rangle &= 2\mathbf{I}_f^{(1)}(\epsilon)|\mathcal{M}_f^{\Sigma,(0)}\rangle + |\mathcal{M}_f^{\Sigma,(1)fin}\rangle \\
|\mathcal{M}_f^{\Sigma,(2)}\rangle &= 4\mathbf{I}_f^{(2)}(\epsilon)|\mathcal{M}_f^{\Sigma,(0)}\rangle + 2\mathbf{I}_f^{(1)}(\epsilon)|\mathcal{M}_f^{\Sigma,(1)}\rangle + |\mathcal{M}_f^{\Sigma,(2)fin}\rangle\,, \qquad (2.34)
\end{aligned}
$$

where

$$
\begin{aligned}
\mathbf{I}_{ggg}^{(1)}(\epsilon) &= -\frac{1}{2}\frac{e^{-\frac{\epsilon}{2}\gamma_E}}{\Gamma(1+\frac{\epsilon}{2})}\left(C_A\frac{4}{\epsilon^2} - \frac{\beta_0}{\epsilon}\right)\left[\left(-\frac{s}{\mu_R^2}\right)^{\frac{\epsilon}{2}} + \left(-\frac{t}{\mu_R^2}\right)^{\frac{\epsilon}{2}} + \left(-\frac{u}{\mu_R^2}\right)^{\frac{\epsilon}{2}}\right], \\
\mathbf{I}_{q\bar{q}g}^{(1)}(\epsilon) &= -\frac{1}{2}\frac{e^{-\frac{\epsilon}{2}\gamma_E}}{\Gamma(1+\frac{\epsilon}{2})}\left\{\left(\frac{4}{\epsilon^2} - \frac{3}{\epsilon}\right)(C_A - 2C_F)\left[\left(-\frac{s}{\mu_R^2}\right)^{\frac{\epsilon}{2}}\right]\right. \\
&\quad \left. + \left(-\frac{4C_A}{\epsilon^2} + \frac{3C_A}{2\epsilon} + \frac{\beta_0}{2\epsilon}\right)\left[\left(-\frac{t}{\mu_R^2}\right)^{\frac{\epsilon}{2}} + \left(-\frac{u}{\mu_R^2}\right)^{\frac{\epsilon}{2}}\right]\right\}, \\
\mathbf{I}_f^{(2)}(\epsilon) &= -\frac{1}{2}\mathbf{I}_f^{(1)}(\epsilon)\left[\mathbf{I}_f^{(1)}(\epsilon) - \frac{2\beta_0}{\epsilon}\right] + \frac{e^{\frac{\epsilon}{2}\gamma_E}\Gamma(1+\epsilon)}{\Gamma(1+\frac{\epsilon}{2})}\left[-\frac{\beta_0}{\epsilon} + K\right]\mathbf{I}_f^{(1)}(2\epsilon) + \mathbf{H}_f^{(2)}(\epsilon) \qquad (2.35)
\end{aligned}
$$

with

$$
\begin{aligned}
K &= \left(\frac{67}{18} - \zeta_2\right)C_A - \frac{10}{9}T_F n_f, \\
\mathbf{H}_{ggg}^{(2)}(\epsilon) &= \frac{3}{\epsilon}\left\{C_A^2\left(-\frac{5}{24} - \frac{11}{48}\zeta_2 - \frac{1}{4}\zeta_3\right) + C_A n_f\left(\frac{29}{54} + \frac{1}{24}\zeta_2\right) - \frac{1}{4}C_F n_f - \frac{5}{54}n_f^2\right\}, \\
\mathbf{H}_{q\bar{q}g}^{(2)}(\epsilon) &= \frac{1}{\epsilon}\left\{C_A^2\left(-\frac{5}{24} - \frac{11}{48}\zeta_2 - \frac{1}{4}\zeta_3\right) + C_A n_f\left(\frac{29}{54} + \frac{1}{24}\zeta_2\right) + C_F n_f\left(-\frac{1}{54} - \frac{1}{4}\zeta_2\right)\right. \\
&\quad \left. + C_A C_F\left(-\frac{245}{216} + \frac{23}{8}\zeta_2 - \frac{13}{2}\zeta_3\right) + C_F^2\left(\frac{3}{8} - 3\zeta_2 + 6\zeta_3\right) - \frac{5}{54}n_f^2\right\}. \qquad (2.36)
\end{aligned}
$$

The IR singular part of $\mathcal{S}_f$ ($\langle\mathcal{A}_f|\mathcal{A}_f\rangle$) computed up to a_s^5 agrees perfectly with the predictions based on Catani's proposal. Hence, we present only the finite part of $\mathcal{S}_f$ for

$f = ggg, q\bar{q}g$, namely $\mathcal{S}_{ggg,fin}$ and $\mathcal{S}_{q\bar{q}g,fin}$ in the Appendix B.

2.3 Universality of leading transcendental terms

Kotikov and Lipatov [133–135] (see also [136, 137]) conjectured maximum transcendentality principle which relates transcendental terms in the anomalous dimensions of leading twist two operators in $\mathcal{N} = 4$ SYM theory with those in the corresponding QCD results [89, 90]. In the perturbative calculations, one associates transcendentality weight n to the constants $\zeta(n)$, ϵ^{-n} and the functions namely HPLs of weight n. In $\mathcal{N} = 4$ SYM, the FFs of the half-BPS type operators show uniform transcendentality. On the other hand QCD results contain terms of all transcendental weights in addition to rational terms (zero transcendentality). From various higher order results that are available in QCD and $\mathcal{N} = 4$ SYM theories, one finds similar connection. In particular, the leading transcendental (LT) terms of anomalous dimensions of twist two operators, two and three point FFs in QCD when $C_A = C_F = N$ and $T_f n_f = N/2$ coincide with the corresponding ones of the half-BPS operators in $\mathcal{N} = 4$ SYM theory. The leading transcendental terms of the QCD amplitude for the Higgs boson decaying to three on-shell gluons [54, 138] are also related to the two-loop three-point MHV FFs of the half-BPS operators [7] in $\mathcal{N} = 4$ SYM. Similar relations are found for two point FFs of quark current, scalar and pseudo-scalar operators constructed out of gluon field strengths, energy momentum tensor of the QCD up to three loops see [5, 83, 139, 140]. Recently, in [8] which will be discussed in Chapter 4 of this thesis, we studied several three point FFs of the half-BPS as well as the Konishi operators in $\mathcal{N} = 4$ SYM theory at two loops level in ‘t Hooft coupling. We evaluated them between on-shell final states $g\phi\phi$ and $\phi\lambda\lambda$ where ϕ, λ, g are scalar, Majorana fermion and gluon states. Unlike the half-BPS, the Konishi operator is not protected by supersymmetry and hence we find non-trivial structure at higher orders. The explicit computation shows that the FF of the Konishi operator does not show uniform transcendentality [5, 8, 64]. Interestingly, the LT terms of the Konishi for the states $g\phi\phi$ agree with those of the half-BPS operator [8]. On the other hand, for $\phi\lambda\lambda$ states, we did not find any such relation to the corresponding ones for the half-BPS. In the present context, it is tempting to relate our results for FFs to the Konishi operator, rather than the half-BPS owing to the fact that both are not protected. We find that the amplitude $A \to ggg$ agrees with the FF of the Konishi operator between $g\phi\phi$ states at the leading transcendental level while $A \to q\bar{q}g$ for O_G does not have any relation with that of the Konishi operator computed between $\phi\lambda\lambda$ states. Surprisingly, we find that the leading transcendental terms of the amplitude $A \to q\bar{q}g$ multiplied by its born and normalised by its born square contribution agrees with the half-BPS. In summary both the amplitudes namely $A \to ggg$ and $A \to q\bar{q}g$ computed using O_G operator multiplied by respective born amplitudes and normalised by their born squares have leading transcendental terms identical to those of the half-BPS. Our results with pseudo-scalar operator computed between different on shell states shed more light on the universal structure of higher order terms in gauge theories.

2.4 Summary

The motivation to compute two-loop virtual corrections to decay of a pseudo-scalar to three gluons or quark, anti-quark, gluon is two fold. Firstly, with larger data set that are available at the LHC, constraining BSM scalar sector has become feasible and hence precise theoretical predictions for production of A and its subsequent decays to jets need to be achieved. Secondly, such a computation of NNLO level for the differential rates is technically challenging due to non-trivial tensorial interaction encountered here. We have successfully computed UV renormalised virtual contributions to $A \to ggg$ and $A \to q\bar{q}g$ up to two level in QCD perturbation series using dimensional regularisation. We confirm the correctness of our results up to finite terms using Catani's infrared factorisation formula which predict all the poles resulting from soft and collinear configurations up to two loops. Expressing our results using Catani's subtraction operators, the remaining infrared finite terms of the amplitudes are presented in the appendix B. With appropriate analytical continuation, our results can be readily used for the study of production of A in association with a jet at two loop level at the hadron colliders.

3 Konishi Form Factor at Three Loops in $\mathcal{N} = 4$ SYM Theory

The materials presented in this chapter are the result of an original research done in collaboration with Taushif Ahmed, Pulak Banerjee, Narayan Rana, V. Ravindran and Satyajit Seth, and these are based on the published article [5].

3.1 Prologue

The ability to accomplish the challenging job of calculating quantities is of great importance in any potential mathematical theory. In QFT, this manifests itself in the quest for computing the multi-loop and multi-leg scattering amplitudes under the framework perturbation theory. The fundamental quantities to be calculated in any gauge theory are the scattering amplitudes or the correlation functions. Recently, there have been surge of interest to study FFs as they connect fully on-shell amplitudes and correlation functions. The FFs are a set of quantities which are constructed out of the scattering amplitudes involving on-shell states consisting of elementary fields and an off-shell state described through a composite operator. These are operator matrix elements of the form $\langle p_1^{\sigma_1}, \cdots, p_l^{\sigma_l}|O|0\rangle$ where, O represents a gauge invariant composite operator which generates a multi-particle on-shell state $|p_1^{\sigma_1}, \cdots, p_l^{\sigma_l}\rangle$ upon operating on the vacuum of the theory. p_i are the momenta and σ_i encapsulate all the other quantum numbers of the particles. More precisely, FFs are the amplitudes of the processes where classical current or field, coupled through gauge invariant composite operator O, produces some quantum state. Studying these quantities not only help to understand the underlying UV and IR structures of the theory, but also enable us to calculate the anomalous dimensions of the associated composite operator.

The Sudakov FFs ($l = 2$) in $\mathcal{N} = 4$ SYM theory [15, 16] were initially considered by van Neerven in [62], almost three decades back, where a half-BPS operator belonging to the stress energy supermultiplet, that contains the conserved currents of $\mathcal{N} = 4$ SYM theory, was investigated up to 2-loop order:

$$O^{\rm BPS}_{rt} = \phi^a_r \phi^a_t - \frac{1}{3}\delta_{rt}\phi^a_s\phi^a_s\,. \tag{3.1}$$

Very recently, this was extended to 3-loop in [63]. We will represent scalar and pseudo-scalar fields by ϕ^a_r and χ^a_r, respectively. The symbol $a \in [1, N^2 - 1]$ denotes the SU(N) adjoint color index, whereas r, t stand for the generation indices which run from $[1, n_g]$. In $d = 4$ space-time dimensions, we have $n_g = 3$. One of the most salient features of this operator is that, it is protected by the supersymmetry i.e. the FFs exhibit no UV divergences but IR ones to all orders in perturbation theory. In this thesis, our goal is to investigate the Sudakov FFs of another very important operator in the context of $\mathcal{N} = 4$ SYM theory, called the Konishi operator, which is not protected by the supersymmetry and consequently, exhibits UV divergences beyond LO:

$$O^{\mathcal{K}} = \phi^a_r\phi^a_r + \chi^a_r\chi^a_r\,. \tag{3.2}$$

The existence of UV divergences is captured through the presence of non-zero anomalous dimensions. This operator is one of the members of the Konishi supermultiplet and all the members of the multiplet give rise to same anomalous dimensions. The one and two loop Sudakov FFs of Konishi operator were computed in [64] employing the on-shell unitarity method. In addition, the IR poles at 3-loop were also predicted in the same article using the universal behaviour of those, though the finite part was not computed. In this thesis, we calculate the full 3-loop Sudakov FFs using Feynman diagrammatic approach. In the same spirit of the FFs in QCD, we examine the results in the context of K+G equation [141–144]. Quite remarkably, it has been found that the logarithms of the FFs satisfy the universal decomposition in terms of the cusp, collinear, soft and UV anomalous dimensions, exactly similar to those of QCD [145, 146]! Except UV, which is a property of the associated operator, all the remaining universal anomalous dimensions match exactly with the leading transcendental terms of the corresponding ones in QCD upon putting $C_F = n_f = C_A$.

We begin this chapter by presenting computational framework in the Sec. 3.2. In Sec. 3.3, we differentiates between the prescriptions that has been used in calculating quantities in $\mathcal{N} = 4$ SYM theory. After setting up the required ingredients, we achieve our goal in Sec. 3.4 and present the results of 3-loop FFs in Sec. 3.5. Then in Sec. 3.6, we elaborate on the overall operator renormalisation which a composite operator requires during UV renormalisation and present some interesting features of FFs using renormalisation group equation (RGE) in Sec. 3.7. Finally in Sec. 3.8 we predict all the poles at four loops using RGE that FF satisfies before summarising in Sec. 3.9.

3.2 Framework of the Calculation

The interacting Lagrangian encapsulating the interaction between off-shell state (J) described by $\mathcal{O}^{\rm BPS}$ or $\mathcal{O}^{\mathcal{K}}$ and the fields in $\mathcal{N} = 4$ SYM are given by

$$\mathcal{L}_{int}^{\rm BPS} = J_{rt}^{\rm BPS} \mathcal{O}_{rt}^{\rm BPS} \,, \quad \mathcal{L}_{int}^{\mathcal{K}} = J^{\mathcal{K}} \mathcal{O}^{\mathcal{K}} \,. \tag{3.3}$$

We define the form factors at $O(\hat{a}^n)$ as

$$\mathcal{F}_f^{\rho,(n)} \equiv \frac{\langle \mathcal{M}_f^{\rho,(0)} | \mathcal{M}_f^{\rho,(n)} \rangle}{\langle \mathcal{M}_f^{\rho,(0)} | \mathcal{M}_f^{\rho,(0)} \rangle} \tag{3.4}$$

where, $n = 0, 1, 2, \cdots$ and $\hat{a}$ is the bare 't Hooft coupling [6]:

$$\hat{a} \equiv \frac{\hat{g}_{\rm YM}^2 C_A}{(4\pi)^2} \left(4\pi e^{-\gamma_E}\right)^{-\frac{\epsilon}{2}} \, , \tag{3.5}$$

that depends on the Yang-Mills coupling constant $g_{\rm YM}$, the loop counting parameter and C_A. The quantity $|\mathcal{M}_f^{\rho,(n)}\rangle$ is the transition matrix element of $O(a^n)$ for the production of a pair of on-shell particles $f\bar{f}$ from the off-shell state represented through ρ. For the case under consideration, we take $f = \phi_r^a = \bar{f}$, $\rho = \mathcal{K}$ and BPS for $J^{\mathcal{K}}$ and $J_{rt}^{\rm BPS}$, respectively. The full form factor in terms of the components Eq. (3.4) reads as

$$\mathcal{F}_f^{\rho} = 1 + \sum_{n=1}^{\infty} \left[\hat{a}^n \left(\frac{Q^2}{\mu^2} \right)^{n\frac{\epsilon}{2}} \mathcal{F}_f^{\rho,(n)} \right] . \tag{3.6}$$

The transition matrix element also follows same expansion. The quantity $Q^2 = -2p_1.p_2$ and μ is introduced to keep the coupling constant $\hat{a}$ dimensionless in $d = 4+\epsilon$ dimensions.

3.3 Regularization Prescriptions

The calculation of the FFs in $\mathcal{N} = 4$ SYM theory involves a subtlety originating from the dependence of the composite operators on space-time dimensions d. Unlike the half-BPS operator $\mathcal{O}_{rt}^{\rm BPS}$, the Konishi operator $\mathcal{O}^{\mathcal{K}}$ involves a sum over generation of the scalar and pseudo-scalar fields and consequently, it does depend on d. The problem arises while making the choice of regularization scheme [64], which is necessary in order to regulate the theory. Though the FFs of the protected operators are free from UV divergences in 4-dimensions, these do involve IR divergences arising from the soft and collinear configurations of the loop momenta.

For performing the regularization, there exists several schemes, the FDH [67, 68] formalism is the most popular one where everything is treated in 4-dimensions, except the loop integrals that are evaluated in d-dimensions. In spite of its spectacular applicability, this prescription fails to produce the correct result for the operators involving space-time dimensions [64], such as Konishi! However, this can be rectified and the rectification scenarios differ from one operator to another. According to the prescription prescribed in the article [64], in order to obtain the correct result for the Konishi operator, one requires to multiply a factor of $\Delta_{\mathcal{K}}^{\rm BPS}$ which is $\Delta_{\mathcal{K}}^{\rm BPS} = n_{g,\epsilon}/2n_g$ with the difference between the FFs of the Konishi and those of BPS i.e.

$$\mathcal{F}_f^{\mathcal{K}} = \mathcal{F}_f^{\rm BPS} + \delta\mathcal{F}_f^{\mathcal{K}}, \tag{3.7}$$

where, $\delta\mathcal{F}_f^{\mathcal{K}} = \Delta_{\mathcal{K}}^{\rm BPS}(\mathcal{F}_f^{\mathcal{K}} - \mathcal{F}_f^{\rm BPS})$. The second subscript of $n_{g,\epsilon}$ represents the dependence of the number of generations of the scalar and pseudo-scalar fields on the space-time dimensions: $n_{g,\epsilon} = (2n_g - \epsilon)$. The prescription is validated through the production of the correct anomalous dimensions up to 2-loop. In this thesis, for the first time, this formalism is applied to the case of 3-loop FFs and is observed to produce the correct anomalous dimensions for the Konishi.

On the other hand, there exists another very elegant formalism, called $\overline{\rm DR}$ [65, 66], which is very much similar to the 't Hooft and Veltman prescription of the dimensional regularization and quite remarkably, it is universally applicable to all kinds of operators including the ones dependent on the space-time dimensions. In this prescription, in addition to treating everything in $d = 4 + \epsilon$ dimensions, the number of generations of the scalar and pseudo-scalar fields is considered as $n_{g,\epsilon}/2$ instead of n_g in order to preserve the supersymmetry throughout. The dependence on ϵ preserves supersymmetry in a sense that the total number of gauge, scalar (n_g) and pseudo-scalar (n_g) degrees of freedom continues to remain 8. Within this framework, we have calculated the Konishi FFs up to 3-loop level and the results come out to be exactly same as the ones obtained in Eq. (3.7). This, in turn, provides a direct check on the earlier prescription. In the next section, we will discuss the methodology of computing the FFs.

3.4 Calculation of the FFs

The calculation of the FFs follows closely the steps used in the derivation of the 3-loop spin-2 and pseudoscalar FFs in QCD [83,117]. The relevant Feynman diagrams are generated using QGRAF [120]. Indeed, very special care is taken to incorporate the Majorana fermions present in the $\mathcal{N} = 4$ SYM theory appropriately. For the Konishi as well as half-BPS operator, 1631 number of Feynman diagrams appear at 3-loop order which include the scalar, pseudo-scalar, gauge boson as well as Majorana fermions in the loops. The ghost loops are also taken into account ensuring the inclusion of only the physical degrees of freedom of the gauge bosons. The raw output of the QGRAF is converted to a suitable format for further calculation. Employing a set of in-house routines based on Python and the symbolic manipulating program FORM [121], the simplification of the matrix elements involving the Lorentz, colour, Dirac and generation indices is performed. In the FDH regularization scheme, except the loop integrals all the remaining algebra is performed in $d = 4$, whereas in $\overline{\text{DR}}$, everything is executed in $d = 4 + \epsilon$ dimensions. While calculating within the framework of $\overline{\text{DR}}$, the factor of $1/3$ in the second part of $\mathcal{O}_{rt}^{\text{BPS}}$, Eq. (3.1), should be replaced by $2/n_{g,\epsilon}$ to maintain its traceless property in d-dimensions.

The expressions involve thousands of apparently different 3-loop Feynman scalar integrals. However, they are expressible in terms of a much smaller set, called MIs, by employing the IBP [57,58] and LI [59] identities. Though, the LI are not linearly independent of the IBP [124], their inclusion however accelerates the procedure of obtaining the solutions. All the scalar integrals are reduced to the set of MIs using a Mathematica based package LiteRed [128, 129]. In the literature, there exists similar packages to perform the reduction: AIR [126], FIRE [127], Reduze2 [122, 123]. As a result, all the thousands of scalar integrals can be expressed in terms of 22 topologically different MIs which were computed analytically as Laurent series in ϵ in the articles [147–153] and are collected in the appendix of [140]. Using those, we obtain the final expressions for the 3-loop FFs of the O_{rt}^{BPS} and $O^{\mathcal{K}}$.

3.5 Results of the FFs

Employing the Feynman diagrammatic approach described in the previous section, we have first confirmed the form factor results for the O_{rt}^{BPS} up to 3-loop level presented in [62, 63] and for $O^{\mathcal{K}}$ up to 2-loop [64]. In this thesis, we present only the ϵ expanded results for the $\mathcal{F}_{\phi}^{\mathcal{K},(i)}$, $i = 1, 2, 3$ (see Eq. (3.6)). The exact results in terms of d and MIs are too long to present here and can be obtained from the authors. In order to demonstrate the subtleties involved in the choice of regularization scheme, we have expressed them in terms of δ_R which is unity in $\overline{DR}$ scheme and zero in FDH scheme.

$$
\begin{aligned}
\mathcal{F}_{\phi}^{\mathcal{K},(1)} &= \frac{1}{\epsilon^2}\Big\{-8\Big\} + \frac{1}{\epsilon}\Big\{12\Big\} - 12 + \zeta_2 + \epsilon\Big\{12 - \frac{7}{3}\zeta_3 - \frac{3}{2}\zeta_2\Big\} + \epsilon^2\Big\{-12 + \frac{7}{2}\zeta_3 + \frac{3}{2}\zeta_2 \\
&+ \frac{47}{80}\zeta_2^2\Big\} + \epsilon^3\Big\{12 - \frac{31}{20}\zeta_5 - \frac{7}{2}\zeta_3 - \frac{3}{2}\zeta_2 + \frac{7}{24}\zeta_2\zeta_3 - \frac{141}{160}\zeta_2^2\Big\} + \epsilon^4\Big\{-12 + \frac{93}{40}\zeta_5 \\
&+ \frac{7}{2}\zeta_3 - \frac{49}{144}\zeta_3^2 + \frac{3}{2}\zeta_2 - \frac{7}{16}\zeta_2\zeta_3 + \frac{141}{160}\zeta_2^2 + \frac{949}{4480}\zeta_2^3\Big\} + \epsilon^5\Big\{12 - \frac{127}{112}\zeta_7 - \frac{93}{40}\zeta_5 \\
&- \frac{7}{2}\zeta_3 + \frac{49}{96}\zeta_3^2 - \frac{3}{2}\zeta_2 + \frac{31}{160}\zeta_2\zeta_5 + \frac{7}{16}\zeta_2\zeta_3 - \frac{141}{160}\zeta_2^2 + \frac{329}{1920}\zeta_2^2\zeta_3 - \frac{2847}{8960}\zeta_2^3\Big\} \\
&+ \delta_R\Big[-2 + 2\epsilon + \epsilon^2\Big\{-2 + \frac{1}{4}\zeta_2\Big\} + \epsilon^3\Big\{2 - \frac{7}{12}\zeta_3 - \frac{1}{4}\zeta_2\Big\} + \epsilon^4\Big\{-2 + \frac{7}{12}\zeta_3 \\
&+ \frac{1}{4}\zeta_2 + \frac{47}{320}\zeta_2^2\Big\} + \epsilon^5\Big\{2 - \frac{31}{80}\zeta_5 - \frac{7}{12}\zeta_3 - \frac{1}{4}\zeta_2 + \frac{7}{96}\zeta_2\zeta_3 - \frac{47}{320}\zeta_2^2\Big\}\Big], \\
\mathcal{F}_{\phi}^{\mathcal{K},(2)} &= \frac{1}{\epsilon^4}\Big\{32\Big\} + \frac{1}{\epsilon^3}\Big\{-96\Big\} + \frac{1}{\epsilon^2}\Big\{168 - 4\zeta_2\Big\} + \frac{1}{\epsilon}\Big\{-276 + \frac{50}{3}\zeta_3 + 24\zeta_2\Big\} + 438 \\
&- 56\zeta_3 - 66\zeta_2 - \frac{21}{5}\zeta_2^2 + \epsilon\Big\{-681 - \frac{71}{10}\zeta_5 + 128\zeta_3 + 141\zeta_2 - \frac{23}{6}\zeta_2\zeta_3 + 15\zeta_2^2\Big\}
\end{aligned}
$$

$$
+\epsilon^2\Big\{\frac{2091}{2}+\frac{84}{5}\zeta_5-314\zeta_3+\frac{901}{36}\zeta_3^2-\frac{519}{2}\zeta_2+26\zeta_2\zeta_3-\frac{741}{20}\zeta_2^2+\frac{2313}{280}\zeta_2^3\Big\}
+\epsilon^3\Big\{-\frac{6369}{4}-\frac{3169}{28}\zeta_7-\frac{12}{5}\zeta_5+722\zeta_3-\frac{247}{3}\zeta_3^2+\frac{1761}{4}\zeta_2+\frac{313}{40}\zeta_2\zeta_5-82\zeta_2\zeta_3
+\frac{3813}{40}\zeta_2^2-\frac{1291}{80}\zeta_2^2\zeta_3-\frac{3891}{140}\zeta_2^3\Big\}+\epsilon^4\Big\{\frac{19299}{8}+\frac{18825}{56}\zeta_7-\frac{1227}{10}\zeta_5-\frac{33}{2}\zeta_5 3
-\frac{3085}{2}\zeta_3+\frac{845}{24}\zeta_3\zeta_5+\frac{577}{3}\zeta_3^2-\frac{5703}{8}\zeta_2-\frac{21}{5}\zeta_2\zeta_5+\frac{409}{2}\zeta_2\zeta_3-\frac{1547}{144}\zeta_2\zeta_3^2
-\frac{17931}{80}\zeta_2^2+\frac{1063}{20}\zeta_2^2\zeta_3+\frac{31401}{560}\zeta_2^3+\frac{50419}{1600}\zeta_2^4\Big\}+\delta_R\Big[\frac{1}{\epsilon^2}\Big\{16\Big\}+\frac{1}{\epsilon}\Big\{-28\Big\}+46
-4\zeta_2+\epsilon\Big\{-73+\frac{28}{3}\zeta_3+11\zeta_2\Big\}+\epsilon^2\Big\{\frac{227}{2}-\frac{64}{3}\zeta_3-\frac{47}{2}\zeta_2-\frac{5}{2}\zeta_2^2\Big\}+\epsilon^3\Big\{-\frac{697}{4}
-\frac{14}{5}\zeta_5+\frac{157}{3}\zeta_3+\frac{173}{4}\zeta_2-\frac{13}{3}\zeta_2\zeta_3+\frac{247}{40}\zeta_2^2\Big\}+\epsilon^4\Big\{+\frac{2123}{8}+\frac{2}{5}\zeta_5-\frac{361}{3}\zeta_3
+\frac{247}{18}\zeta_3^2-\frac{587}{8}\zeta_2+\frac{41}{3}\zeta_2\zeta_3-\frac{1271}{80}\zeta_2^2+\frac{1297}{280}\zeta_2^3\Big\}\Big],
$$

$$
\mathcal{F}_\phi^{\mathcal{K},(3)}=\frac{1}{\epsilon^6}\Big\{-\frac{256}{3}\Big\}+\frac{1}{\epsilon^5}\Big\{384\Big\}+\frac{1}{\epsilon^4}\Big\{-960\Big\}+\frac{1}{\epsilon^3}\Big\{2112-\frac{176}{3}\zeta_3-96\zeta_2\Big\}
+\frac{1}{\epsilon^2}\Big\{-4368+312\zeta_3+504\zeta_2+\frac{494}{45}\zeta_2^2\Big\}+\frac{1}{\epsilon}\Big\{8760+\frac{1756}{15}\zeta_5-1056\zeta_3-1608\zeta_2
+\frac{170}{9}\zeta_2\zeta_3-\frac{459}{5}\zeta_2^2\Big\}-17316-\frac{1014}{5}\zeta_5+3192\zeta_3-\frac{1766}{9}\zeta_3^2+4158\zeta_2-195\zeta_2\zeta_3
+\frac{3789}{10}\zeta_2^2-\frac{22523}{270}\zeta_2^3+\delta_R\Big[\frac{1}{\epsilon^4}\Big\{-64\Big\}+\frac{1}{\epsilon^3}\Big\{160\Big\}+\frac{1}{\epsilon^2}\Big\{-352+16\zeta_2\Big\}
+\frac{1}{\epsilon}\Big\{728-52\zeta_3-84\zeta_2\Big\}-1460+176\zeta_3+268\zeta_2+\frac{153}{10}\zeta_2^2\Big], \tag{3.8}
$$

where $\zeta_2=\pi^2/6, \zeta_3\approx 1.2020569, \zeta_5\approx 1.0369277, \zeta_7\approx 1.0083492$. The presence of the non-zero coefficients of δ_R signifies the shortcoming of the FDH scheme in case of Konishi operator. We observe that our results for $\delta\mathcal{F}_\phi^{\mathcal{K},(i)}, i=1,2,3$ expressed in terms of d and MIs contain an overall factor $(6-\delta_R\epsilon)/6$ explaining the necessity of correcting the results computed in FDH scheme by this factor advocated in [64].

3.6 Operator Renormalization

Though the $\mathcal{N} = 4$ SYM theory is UV finite i.e. neither coupling constant nor wave function renormalization is required, nevertheless the FFs of the composite unprotected operators, like Konishi, do involve divergences of the UV source which are captured by the presence of non-zero UV anomalous dimensions, γ^ρ. As a consequence, to get rid of the UV divergences, the FFs are required to undergo UV renormalization which is performed through the multiplication of an overall operator renormalization, $Z^\rho\,(a(\mu_R), \epsilon)$:

$$\frac{d}{d\ln\mu_R^2}\ln Z^\rho = \gamma^\rho = \sum_{i=1}^{\infty} a^i \gamma_i^\rho\,, \tag{3.9}$$

where $a = \hat{a}\,(\mu_R/\mu)^\epsilon$. The solution to the above equation takes the simple form:

$$Z^\rho = \exp\Big(\sum_{n=1}^{\infty} a^n \frac{2\gamma_n^\rho}{n\epsilon}\Big). \tag{3.10}$$

The UV finite Konishi FFs is obtained as $\left[\mathcal{F}_f^{\mathcal{K}}\right]_R = Z^{\mathcal{K}}\mathcal{F}_f^{\mathcal{K}}$, whereas $\left[\mathcal{F}_f^{\rm BPS}\right]_R = \mathcal{F}_f^{\rm BPS}$. Since, this is a property of the associated composite operator, the γ^ρ and so Z^ρ are independent of the type as well as number of the external on-shell states. In the next section, we will discuss the methodology to obtain the γ^ρ for the Konishi type of operators in addition to discussing the IR singularities of the FFs.

3.7 Universality of the Pole Structures

The FFs in $\mathcal{N} = 4$ SYM theory contain divergences arising from the IR region which show up as poles in ϵ. The associated pole structures can be revealed and studied in an elegant way through the K+G equation [141–144] which is obeyed by the FFs as a consequence of factorization, gauge and renormalization group invariances:

$$\frac{d}{d\ln Q^2}\ln\mathcal{F}^{\rho}_{f} = \frac{1}{2}\left[K^{\rho}_{f} + G^{\rho}_{f}\right]. \tag{3.11}$$

The Q^2 independent $K^{\rho}_{f}(a,\epsilon)$ contains all the poles in ϵ, whereas $G^{\rho}_{f}\left(a, Q^2/\mu_R^2, \epsilon\right)$ involves only the finite terms in $\epsilon \to 0$. Inspired from QCD [6, 84, 85], we propose the general solution to be

$$\ln\mathcal{F}^{\rho}_{f}(a, Q^2, \mu_R^2, \epsilon) = \sum_{j=1}^{\infty} a^j \left(\frac{Q^2}{\mu_R^2}\right)^{j\frac{\epsilon}{2}} \mathcal{L}^{\rho}_{f,j}(\epsilon) \tag{3.12}$$

with

$$\mathcal{L}^{\rho}_{f,j}(\epsilon) = \frac{1}{\epsilon^2}\left\{-\frac{2}{j^2}A_j\right\} + \frac{1}{\epsilon}\left\{\frac{1}{j}G^{\rho}_{f,j}(\epsilon)\right\} \tag{3.13}$$

where, $A = \sum_{j=1}^{\infty} a^j A_j$ are the cusp anomalous dimensions in $\mathcal{N} = 4$ SYM. The absence of the superscript ρ and subscript f signifies the independence of these quantities on the nature of composite operators as well as external particles. These are determined by looking at the highest poles of the $\ln\mathcal{F}^{\rho}_{f}$ which are found to be

$$A_1 = 4\,, A_2 = -8\zeta_2\,, A_3 = \frac{176}{5}\zeta_2^2 \tag{3.14}$$

up to 3-loops which are consistent with the results presented in [154, 155]. These are basically the highest transcendental parts of those of QCD [89, 90, 146, 156]. The other quantities in Eq. (3.13), $G^{\rho}_{f,j}$ are postulated, like QCD [145, 146], to satisfy

$$G^{\rho}_{f,j}(\epsilon) = 2\left(B_j - \gamma^{\rho}_j\right) + f_j + \sum_{k=1}^{\infty} \epsilon^k g^{\rho,k}_{f,j} \tag{3.15}$$

where, $B = \sum_{j=1}^{\infty} a^j B_j$ and $f = \sum_{j=1}^{\infty} a^j f_j$ are the collinear and soft anomalous dimensions in $\mathcal{N} = 4$ SYM which are independent of the operators as well as external legs. For the

O_{rt}^{BPS} and $O^{\mathcal{K}}$, we obtain

$$\gamma_j^{\mathrm{BPS}} = 0\,,$$
$$\gamma_1^{\mathcal{K}} = -6\,,\gamma_2^{\mathcal{K}} = 24\,,\gamma_3^{\mathcal{K}} = -168 \tag{3.16}$$

up to 3-loop. For the Konishi operator, the results up to 2-loop are in agreement with the existing ones [157–159] and the 3-loop result also matches with previous computations [135,160] . By subtracting out the γ_j, we can only calculate the combination of $(2B_j + f_j)$. However, by looking at the similarities between A_j of QCD and $\mathcal{N} = 4$ SYM theory, we propose

$$B_1 = 0\,, B_2 = 12\zeta_3\,, B_3 = 16\,(-\zeta_2\zeta_3 - 5\zeta_5)\ ,$$
$$f_1 = 0\,, f_2 = -28\zeta_3\,, f_3 = \left(\frac{176}{3}\zeta_2\zeta_3 + 192\zeta_5\right) \tag{3.17}$$

which are essentially the highest transcendental parts of those of QCD [89, 145, 146]. The other process dependent constants, that are relevant up to 3-loop, in Eq. (3.15) are obtained as

$$g_{\phi,1}^{\mathrm{BPS},1} = \zeta_2\,, g_{\phi,1}^{\mathrm{BPS},2} = -\frac{7}{3}\zeta_3\,, g_{\phi,1}^{\mathrm{BPS},3} = \frac{47}{80}\,\zeta_2^2\,, g_{\phi,1}^{\mathrm{BPS},4} = \frac{7}{24}\zeta_2\zeta_3 - \frac{31}{20}\zeta_5\,,$$
$$g_{\phi,1}^{\mathrm{BPS},5} = \frac{949}{4480}\zeta_2^3 - \frac{49}{144}\zeta_3^2\,, g_{\phi,2}^{\mathrm{BPS},1} = 0\,, g_{\phi,2}^{\mathrm{BPS},2} = \frac{5}{3}\zeta_2\zeta_3 - 39\zeta_5\,, g_{\phi,2}^{\mathrm{BPS},3} = \frac{2623}{140}\zeta_2^3$$
$$+ \frac{235}{6}\zeta_3^2\,, g_{\phi,3}^{\mathrm{BPS},1} = -\frac{12352}{315}\zeta_2^3 - \frac{104}{3}\zeta_3^2 \tag{3.18}$$

for O_{rt}^{BPS}. Similarly for the $O^{\mathcal{K}}$, we get

$$g_{\phi,1}^{\mathcal{K},1} = g_{\phi,1}^{\mathrm{BPS},1} - 14\,, g_{\phi,1}^{\mathcal{K},2} = g_{\phi,1}^{\mathrm{BPS},2} + 14 - \frac{3}{2}\zeta_2\,, g_{\phi,1}^{\mathcal{K},3} = g_{\phi,1}^{\mathrm{BPS},3} - 14 + \frac{7}{4}\zeta_2 + \frac{7}{2}\zeta_3\,,$$
$$g_{\phi,1}^{\mathcal{K},4} = g_{\phi,1}^{\mathrm{BPS},4} + 14 - \frac{7}{4}\zeta_2 - \frac{141}{160}\zeta_2^2 - \frac{49}{12}\zeta_3\,, g_{\phi,1}^{\mathcal{K},5} = g_{\phi,1}^{\mathrm{BPS},5} - 14 + \frac{7}{4}\zeta_2 + \frac{329}{320}\zeta_2^2$$
$$+ \frac{49}{12}\zeta_3 - \frac{7}{16}\zeta_2\zeta_3 + \frac{93}{40}\zeta_5\,, g_{\phi,2}^{\mathcal{K},1} = g_{\phi,2}^{\mathrm{BPS},1} + 212 - 48\zeta_2\,, g_{\phi,2}^{\mathcal{K},2} = g_{\phi,2}^{\mathrm{BPS},2} - 556$$
$$+ 164\zeta_2 + \frac{24}{5}\zeta_2^2 + 60\zeta_3\,, g_{\phi,2}^{\mathcal{K},3} = g_{\phi,2}^{\mathrm{BPS},3} + 1170 - 377\zeta_2 - \frac{154}{5}\zeta_2^2 - 344\zeta_3 + 24\zeta_2\zeta_3$$

$$+ 108\zeta_5 \,, g^{\mathcal{K},1}_{\phi,3} = g^{\mathrm{BPS},1}_{\phi,3} - 2936 + 504\zeta_2 + \frac{1224}{5}\zeta_2^2 - 648\zeta_3 + 720\zeta_5 \,. \tag{3.19}$$

In a clear contrast to that of QCD, due to absence of the non-zero β-functions in $\mathcal{N} = 4$ SYM, all the higher poles vanish in Eq. (3.13). We observe that the LT terms in the operator dependent parts of the FFs of $O^{\mathcal{K}}$ and O^{BPS}_{rt}, namely $g^{\rho,k}_{\phi,j}$, coincide. This is indeed the case with QCD form factors when the colour factors are chosen suitably.

3.8 Form Factors Beyond Three Loop

The K+G equation given by Eq. (3.11) enables us to predict all the poles but constant term of the FFs at 4-loop. Expanding the results of the FFs of previous orders sufficiently high, using the A_4 [6, 161–164], $(2B_4 + f_4)$ [164–166] denoted by α from [167] and $\gamma^{\mathcal{K}}_4$ from [168–171] we obtain $\mathcal{F}^{\mathcal{K},(4)}_{\phi}|_{\mathrm{poles}}$:

$$\begin{aligned}
\mathcal{F}^{\mathcal{K},(4)}_{\phi}|_{\mathrm{poles}} = {} & \frac{1}{\epsilon^8}\left\{\frac{512}{3}\right\} + \frac{1}{\epsilon^7}\left\{-1024\right\} + \frac{1}{\epsilon^6}\left\{\frac{10496}{3} + \frac{128}{3}\zeta_2\right\} + \frac{1}{\epsilon^5}\left\{-\frac{28928}{3} + \frac{1216}{9}\zeta_3\right. \\
& \left. + 128\zeta_2\right\} + \frac{1}{\epsilon^4}\left\{\frac{72992}{3} - \frac{3008}{3}\zeta_3 - \frac{5344}{3}\zeta_2 + \frac{40}{9}\zeta_2^2\right\} + \frac{1}{\epsilon^3}\left\{-\frac{176192}{3}\right. \\
& \left. - \frac{8656}{15}\zeta_5 + \frac{42064}{9}\zeta_3 + \frac{25024}{3}\zeta_2 - \frac{184}{3}\zeta_2\zeta_3 + \frac{4256}{15}\zeta_2^2\right\} + \frac{1}{\epsilon^2}\left\{\frac{416096}{3}\right. \\
& + \frac{5072}{5}\zeta_5 - \frac{151648}{9}\zeta_3 + \frac{21706}{27}\zeta_3^2 - \frac{85408}{3}\zeta_2 + 736\zeta_2\zeta_3 - \frac{18488}{9}\zeta_2^2 \\
& \left. + \frac{381908}{945}\zeta_2^3\right\} + \frac{1}{\epsilon}\left\{-\frac{973136}{3} - 4\alpha - \frac{536894}{63}\zeta_7 + \frac{160412}{15}\zeta_5 + \frac{409192}{9}\zeta_3\right. \\
& - \frac{18680}{9}\zeta_3^2 + \frac{254536}{3}\zeta_2 + \frac{33938}{45}\zeta_2\zeta_5 - \frac{14336}{3}\zeta_2\zeta_3 + \frac{67664}{9}\zeta_2^2 - \frac{14590}{27}\zeta_2^2\zeta_3 \\
& \left. - \frac{333712}{315}\zeta_2^3\right\},
\end{aligned} \tag{3.20}$$

where $\alpha = -(77.56 \pm 0.02)$. Explicit computation is required to get the constant terms. The exact matching of the highest transcendental terms of $O^{\mathcal{K}}$ and O^{BPS}_{rt} at 4-loop holds true, similar to the previous orders.

3.9 Summary

To summarize, we have presented for the first time the complete third order and partial fourth order corrections to the on-shell form factor of the Konishi operator employing state-of-the-art techniques. One of the main issues in computing the higher order corrections in $\mathcal{N} = 4$ SYM is related to the necessity of preserving the supersymmetry throughout the computation. In order to achieve that, one generally follows either of the two regularization schemes: $\overline{DR}$ and FDH. Through performing the computation explicitly in both the schemes, we have shown that the form factor in $\overline{DR}$ automatically provides the correct results, whereas, the results obtained in the FDH needs to be suitably modified. In addition, the modification in FDH is operator dependent and non-trivial. Hence, performing a computation in $\overline{DR}$ is much more preferable for unprotected operators like Konishi.

Moreover, using an independent methodology, we have computed the UV anomalous dimensions of the Konishi operator by exploiting the universal infrared structure of the scattering amplitudes through K+G equation. This prescription is much more general and it can be applied to any other operator to extract the anomalous dimensions. In the end, the principle of leading transcendentality in the context of non-BPS operator at three loops level is studied for the first time. This has the potential to unravel the underlying deeper connections between the amplitudes in $\mathcal{N} = 4$ SYM theory and those of QCD.

4 Finite remainders of the Konishi at two loops in $\mathcal{N} = 4$ SYM Theory

The materials presented in this chapter are the result of an original research done in collaboration with Pulak Banerjee, Maguni Mahakhud, V. Ravindran and Satyajit Seth, and these are based on the published article [8].

4.1 Prologue

Scattering amplitudes computed in QCD as well as in electroweak theory play an important role in the phenomenology of collider physics. For example, scattering of gluons giving rise to multi jets is important to understand physics at very high energies. With increase in number of loops and legs, amplitudes are not only difficult to calculate but also one obtains very large expressions. Enormous simplifications can be achieved if one uses on-shell helicity amplitude methods. The formalism developed by Parke and Taylor [172] generated a lot of interest in the study of scattering amplitudes with a large number of external gluons. Subsequent developments [67, 73, 173–181] helped to explore more difficult sets of on-shell amplitudes. The BCW/BCFW recursion relations [74, 182] made tree level computation simpler.

Like QCD, the $\mathcal{N} = 4$ SYM theory is a renormalizable gauge theory in four dimensional Minkowski space. Apart from having all the symmetries of QCD there are two extra features of $\mathcal{N} = 4$ SYM theory, namely supersymmetry and conformal symmetry [1] that make this theory interesting to study. The on-shell amplitudes evaluated in $\mathcal{N} = 4$ SYM theory have a simpler analytical structure in comparison to QCD amplitudes. The tree level on-shell amplitudes vanish in $\mathcal{N} = 4$ SYM theory when all the external legs have identical helicities. This is a consequence of supersymmetric Ward identities [186]. In [73, 75], one loop supersymmetric on-shell amplitudes having all external particles as gluons were computed and found to be constructible from the tree level amplitudes.

There is another interesting feature of on-shell amplitudes in $\mathcal{N} = 4$ SYM theory that deserves some discussion. The Anti-de-Sitter/conformal field theory (AdS/CFT) conjecture proposed by Maldacena [187] establishes one-to-one correspondence between maximally SYM theory in four dimensions and gravity in five-dimensional anti-de Sitter space. Due to this conjecture certain quantities in the strong coupling limit of $\mathcal{N} = 4$ SYM theory can be related to those in the weakly coupled gravity. As a consequence of this duality, quantities computed in a perturbative expansion should add up to some simple expression. For such quantities, it may be quite likely that the terms in the perturbative expansion are related to one another in some simple way. An important step towards this direction was taken in [158, 188–190]. In [188], the planar two-loop four-point on-shell amplitudes of $\mathcal{N} = 4$ SYM theory was shown to be related to that of one-loop counterpart. Such a relation for infrared divergent parts of the amplitude can be understood based on the factorisation properties of gauge theory amplitudes. Demanding that this property goes through for finite terms as well, an ansatz by Bern, Dixon and Smirnov was put forward for n-point m-loop amplitudes, known as BDS conjecture in the article [6]. Later on, in [191], the BDS ansatz was shown to be a consequence of the anomalous Ward identity. The ansatz was confirmed for the four-point amplitudes at three loops [6, 188] and for the five-point amplitudes up to two-loop order [192, 193] in perturbative expansion. In the seminal paper [194] Alday and Maldacena provided a connection between on-shell scattering ampli-

[1] In the past, conformal symmetry has been used to understand connections between various perturbative results in gauge theories, see [183–185]

tudes in the strong coupling and Wilson loops defined in dual coordinate space with light like segments. Drummond, Korchemsky, and Sokatchev [195] demonstrated the equality of results of Wilson loop with four light-like segments and the one-loop four-point MHV amplitude and in [196], the equality was established between n-sided polygon and one-loop n-point MHV amplitude. Later Alday and Maldacena showed that their Wilson loop calculation does not agree with BDS ansatz when the number of legs is large [197–199]. It is now well known from evidences that the BDS ansatz requires modifications starting from two-loop six-leg MHV amplitudes [167, 200].

In QFT, the other quantity that has been studied in great detail is the FF of composite operators. The FFs, like on-shell amplitudes, contribute to scattering cross sections when one or few of the external particles become off-shell. In QCD, the study of FFs in perturbation theory provided vital informations on the infrared structure of gauge theories in general. In recent times there are several studies [7, 63, 201–204] on the FFs in the context of $\mathcal{N} = 4$ SYM theory which may provide more evidences for the AdS/CFT correspondence. The most widely studied composite operator in $\mathcal{N} = 4$ SYM theory is the half-BPS operator. This operator is often referred as protected because using supersymmetry algebra [205–209], their anomalous dimension can be shown to vanish to all orders in perturbation theory. Hence the FFs of these composite operators look relatively simple. While the study of FFs in $\mathcal{N} = 4$ SYM theory has gained momentum over past few years, the first study along this direction was made long ago by van Neerven [62] where he had computed the two-loop contributions to two-point FF of a half-BPS operator belonging to the stress energy supermultiplet. The corresponding three-loop result was reported in [63]. The authors of [63] have shown a remarkable connection between their results and those in non-supersymmetric SU(N) gauge theory with n_f fermions when the colour factors satisfy the condition $C_A = C_F = n_f$.

The other type of composite operators that are of interest belongs to non-BPS operators. One such representative is the Konishi operator. The Konishi operator [210] is the primary operator of the Konishi supermultiplet. It is the simplest gauge invariant Wilson operator in $\mathcal{N} = 4$ SYM theory that receives anomalous dimension to all orders in perturbation theory. The Konishi supermultiplet has interesting connections with string theory. In an $AdS_5 \times S^5$ background having type IIB superstring excitations, the first string level of the spectrum corresponds to the Konishi supermultiplet [211]. All the operators of the Konishi supermultiplet have same anomalous dimension. The few terms of the anomalous dimension in the strong coupling region using semiclassical quantisation of short strings in $AdS_5 \times S^5$ background are available . Similarly, when the coupling is weak, the results are available to fifth order in perturbation theory. The results up to two loop were reported in [157–159], third order result was obtained in [135, 160]. At four and five loops, they were predicted in [212, 213] using integrable string sigma model. The four-loop result was later confirmed using $\mathcal{N} = 1$ Feynman super-graphs method in [168, 169] and also by Feynman diagrammatic approach in [170]. Confirmation of anomalous dimension at fifth order was obtained in [214].

Over the last few years, there are several results [69–72] on n-point FFs for the Konishi operator. Through them we can, not only confirm the results on the known anomalous dimension but also study the perturbative infrared structure of off-shell amplitudes in general. In addition, they provide testing grounds for various modern techniques that were developed to compute on-shell amplitudes, namely the on-shell unitarity based methods that use unitarity [73, 74] and various recursion relations [75, 76]. The results for the one-loop two-point, two-loop two-point and one-loop three-point FFs were presented in [64]. In the work [5] discussed in Chapter 3, we have computed the three-loop two-point FF for the Konishi operator and also predicted up to $1/\epsilon$ pole at four loops order in d dimensions.

In QFT, on-shell amplitudes beyond LO are plagued with UV and IR divergences. The FFs of composite operators in addition acquire UV divergences due to the compositeness of the operator. By properly multiplying an overall operator renormalization factor, we can eliminate these divergences. The study on the IR structure of on-shell amplitudes and

FFs is not only wide but also rich. In QCD, the IR structure of the two point FFs using gauge invariance, factorization and renormalization group invariances were demonstrated through the K+G equation [141–144]. Through his pioneering contribution, Catani [4] predicted the universal IR divergences for n-point QCD amplitudes up to two loops. Later on Catani's proposal of prediction of these divergences was successfully related to factorization and resummation properties of QCD amplitudes in [130]. The generalisation of the results in [4] and [130] for all loop in SU(N) gauge theory having n_f light flavours in terms of cusp, collinear and soft anomalous dimensions was formulated by Becher and Neubert [131] and independently by Gardi and Magnea [132]. These results are not only useful to understand the perturbative structure of multi-loop multi-leg processes in QCD but also provide deep insight into the structure gauge theories in general. In addition, iterative structure observed among the IR sensitive quantities in the perturbative expansion of QCD amplitudes lead to a very successful program to achieve resummed observables that have played an important role in understanding the physics at high energies. In many respects, $\mathcal{N} = 4$ SYM and SU(N) gauge theory with massless fermions show several similarities. The fact that there is no coupling constant renormalization in $\mathcal{N} = 4$ SYM theory makes it more tractable than SU(N) gauge theory. Many of the perturbative results in $\mathcal{N} = 4$ SYM theory can be easily understood using the well known frameworks in SU(N) gauge theory that deal with organising UV and IR divergences in perturbation theory. For example, in [6, 188], the IR structure of SU(N) gauge theory along with the explicit results in $\mathcal{N} = 4$ SYM theory was readily used to conjecture an all order resummation of finite terms of planar amplitudes. For FFs of both the BPS and non-BPS operators in $\mathcal{N} = 4$ SYM theory, one can readily use the K+G equation to unravel the IR structure of these form factors in terms of IR anomalous dimensions as is done for FFs in SU(N) gauge theory. In other words, it opens up a rich avenue for investigation of universal structures of FFs in $\mathcal{N} = 4$ SYM and gives hints for studying resummation methods. The FFs of the half-BPS and the Konishi operators are expressible in terms of cusp, soft and collinear anomalous dimensions. In the work [5] discussed in Chapter 3 we have studied third order corrections to two point FFs for both the half-BPS and the Konishi operator. The FFs were shown to obey the K+G equation. The universality of IR structure of FF was confirmed as the cusp, soft and collinear divergences obtained to third order were found to be same for both of the operators.

In this chapter of the thesis we will extend our study to three point FFs of the half-BPS and the Konishi operators. We will present for the first time the full analytical results for the FFs as well as FR functions of the Konishi operator up to two loops for both choices of external states $f = g\phi\phi, \phi\lambda\lambda$. In order to show the universality of IR divergences we will use Catani's prediction for SU(N) after suitably modifying it to the case of $\mathcal{N} = 4$ SYM theory and demonstrate that Catani's subtraction operators in $\mathcal{N} = 4$ SYM theory removes all the IR singularities. This will be a clear demonstration of exponentiation of IR singularities of FFs in $\mathcal{N} = 4$ SYM theory, a phenomenon that is well known to occur in QCD [4, 130–132]. Following BDS type of analysis, the exponentiation of IR singularities in FFs guarantee to yield a finite result so called FR function. A similar study for the amplitudes in $\mathcal{N} = 4$ SYM theory can be found in [6]. After subtracting the IR divergent parts, we present the finite part of the FFs for both the half-BPS and the Konishi operators computed using the external states $f = g\phi\phi, \phi\lambda\lambda$. In addition, we will present their corresponding FR functions. It is worth mentioning here the work of Brandhuber, Travaglini, and Yang [7] who used the generalised unitarity method to build the two-loop three-point FFs for the half-BPS operator between the states $f = g\phi\phi$. Their result for the FR expressed in terms of loop integrals was then compared numerically against the one obtained using the method of symbols that uses the concept of coproduct [215]. We will reproduce their results for the half-BPS operator at two loops for two sets of external states. Our results are expressed fully in terms of HPLs. After quiet a bit of simplifications, we have shown that HPLs that appear in our expression are of transcendentality four. This is expected as half-BPS operators contain only the highest transcendental terms. We will discuss the relation between the highest transcendental terms of finite terms of FFs of the Konishi operator computed using Catani's as well as

BDS approaches and the corresponding ones of the half-BPS operator. We will report the method as well as the important findings for the three point FFs of the half-BPS and the Konishi operators up to two-loop level in the subsequent sections of this paper.

This chapter is organised as follows. In section 4.2.1 we briefly discuss the definition of form factors of both the half-BPS and the Konishi operators. In section 4.2.2, we present the method that we follow to perform the computation of the FFs up to two loop level in perturbation theory. Various methods of regularisations, a discussion on UV and IR structures of the three point FFs and the results for their finite parts are presented in section 4.3. The finite remainder functions are presented in section 4.4 after exponentiating the FFs and following BDS approach. We have devoted section 4.5 to the discussion of the maximum transcendentality principle in the context of both the half-BPS and the Konishi FFs. Finally we summarize in section 4.6.

4.2 Theoretical framework

4.2.1 Form Factors

Composite operators provide valuable information about the underlying QFT through their correlation functions and FFs. Those in the $\mathcal{N} = 4$ SYM theory are special in the context of AdS/CFT correspondence. As we have discussed in the introduction, the BPS and non-BPS composite operators have attracted the attention for a long time. In the following, we will study structure of the three point form factors of each operator, namely one half-BPS and the Konishi belonging to non-BPS type up to two-loop level in perturbation theory. Thanks to supersymmetry the half-BPS one is protected, hence it is UV finite. In other words, it does not require any overall UV renormalisation constant to all orders in perturbation theory. On the other hand, the Konishi operator develops UV divergences which can be renormalised away by over all renormalisation constant. Consequently, unlike the half-BPS, the Konishi operator develops anomalous dimension that can be computable in powers of the coupling constant $g_{\rm YM}$. Let us denote these operators by $\mathcal{O}^\rho$ with $\rho = BPS, \mathcal{K}$ respectively. The half-BPS operator that we will study is given by [62, 216]

$$\mathcal{O}^{\rm BPS}_{rt} = \phi^a_r \phi^a_t - \frac{1}{3}\delta_{rt}\phi^a_s\phi^a_s, \tag{4.1}$$

where the symbol $a \in [1, N^2 - 1]$ represents the SU(N) adjoint colour index, while ϕ_r are the scalar fields. The factor 1/3 has been used to maintain tracelessness property in 4 dimension. The Konishi operator ($\rho = \mathcal{K}$) which is the primary operator of the Konishi supermultiplet is given by

$$\mathcal{O}^{\mathcal{K}} = \phi^a_r \phi^a_r + \chi^a_r \chi^a_r. \tag{4.2}$$

The fields ϕ and χ represent the scalar and pseudoscalar types respectively, with $r \in [1, 3]$. It is one of the non-BPS operators that has been studied extensively. An interesting feature of this operator could be noted in context of operator product expansion. During loop calculations the leading asymptotic behaviour of the four point correlation function at short distances was found to be regulated by the Konishi operator.

The interaction parts of the Lagrangian that describe the couplings of external currents J ($J^{\rm BPS}_{rt}$, $J^{\mathcal{K}}$) to the operators in Eqs. (4.1, 4.2) are given in

$$\mathcal{L}^{\rm BPS}_{\rm int} = J^{\rm BPS}_{rt}\mathcal{O}^{\rm BPS}_{rt}, \quad \mathcal{L}^{\mathcal{K}}_{\rm int} = J^{\mathcal{K}}\mathcal{O}^{\mathcal{K}}. \tag{4.3}$$

We are interested to study three point FFs of the above two operators for two specific final states, $f = g\phi\phi$ and $f = \phi\lambda\lambda$. We define the renormalized FF of composite operators $\mathcal{O}^\rho$ between the set of states, f by

$$\mathcal{F}^{\rho,(n)}_f \equiv \frac{\langle \mathcal{M}^{\rho,(0)}_f | \mathcal{M}^{\rho,(n)}_f \rangle}{\langle \mathcal{M}^{\rho,(0)}_f | \mathcal{M}^{\rho,(0)}_f \rangle} \tag{4.4}$$

where $n = 0, 1, 2, ...$ and $\rho =$ BPS or $\mathcal{K}$. In the above expression $|\mathcal{M}^{\rho,(n)}_f\rangle$ is the $\mathcal{O}(a^n)$

contribution to the transition amplitude for an off-shell state created by $\mathcal{O}^\rho$ to the three on-shell states denoted by $f = g\phi\phi, \phi\lambda\lambda$. Since we work in momentum space, these amplitudes are dependent on momentum q of the off-shell state and momenta $p_i, i = 1, 2, 3$ of the on-shell final states. The corresponding Mandelstam variables are given by

$$s \equiv (p_1 + p_2)^2, \quad t \equiv (p_2 + p_3)^2, \quad u \equiv (p_1 + p_3)^2 \tag{4.5}$$

which obey the relation

$$s + t + u = q^2 = Q^2. \tag{4.6}$$

We also define the following dimensionless invariants, which we will use to describe our results in terms of HPL [107] and 2dHPL [108, 109] as

$$x \equiv \frac{s}{Q^2}, \quad y \equiv \frac{u}{Q^2}, \quad z \equiv \frac{t}{Q^2}, \tag{4.7}$$

where (x, y, z) lie between 0 and 1 and satisfy the condition

$$x + y + z = 1. \tag{4.8}$$

In the following, we will describe how we have performed our computation of the FFs of these two operators between various sets of states f at two loop level.

4.2.2 Methodology of calculation

In this section we describe the methodology to compute the FFs, as defined in Eq. (4.4), for the three external on-shell states up to second order in perturbative expansion. There has been a vast amount of developments over last two decades to compute scattering amplitudes, form factors etc to very high orders in perturbative QCD. In the present context, it is worth mentioning earlier works on the two-loop three-point FF computations for the scattering cross section $e^+ e^- \to 3\,\text{jets}$ [217], Higgs decays $H \to g+g+g$ and $H \to g+q+\bar{q}$

in [54, 116]. Decays of a massive spin-2 resonance to 3-gluons as well as fermion anti-fermion and a gluon can be found in [115, 119] and some other works [118, 139]. Computation of the production of massive spin-1 bosons at two loops level in QCD can be found in the literature [218]. Similar calculation can be found in [219]. These computations often use modern helicity methods to compute the amplitudes first and then the resulting large number of two loop integrals are reduced to fewer master integrals using an elegant integral reduction technique, called IBP, pioneered by Tkachov and Chetyrkin in [57, 58] supplemented by identities that are obtained using Lorentz invariance [59]. Dedicated efforts were made in order to compute these two-loop master integrals thanks to the method of differential equations that these master integrals satisfy. Thanks to various modern techniques that followed, such as the 'on-shell' techniques, where one uses recursion relations [74, 182] and unitarity [73, 75] relations, the loop computations with many legs become tractable. In the context of $\mathcal{N} = 4$ SYM, the loop induced contributions to n-point FF for the half-BPS operator were presented in [201, 220], also in [203, 204]. For the half-BPS operator made up of k scalar fields, the results for FFs can be found in [220–222]. The n-point MHV as well as next to MHV FFs, up to first order in perturbative expansion are presented in [201, 203, 204, 223–225]. At strong coupling limit, FFs have also been studied via AdS/CFT correspondence in [197]. We will follow the standard Feynman diagrammatic approach to compute three point FFs at two loops level. We perform the computation in $d = 4 + \epsilon$ dimensions so that divergences appearing in the intermediate stages can be regularised. We will discuss details of the reguralization schemes and the nature of various singularities that appear in the computation.

We have used QGRAF [120] to generate Feynman diagrams for the computation of $|\mathcal{M}_f^{\rho,(n)}\rangle$ where $\rho = \mathrm{BPS}, \mathcal{K}$, f is one of the sets $f = \phi\lambda\lambda$ and $f = g\phi\phi$. For the BPS operator at two loop, there are 1024 diagrams when $f = g\phi\phi$ and 616 diagrams for $f = \phi\lambda\lambda$. At same order in perturbative expansion, for the Konishi operator with $f = g\phi\phi$, we have 1220 diagrams while for $f = \phi\lambda\lambda$, we get 825 diagrams. While dealing with the Majorana fermions care must be taken to ensure its self conjugacy property. Being its own antiparticle, we have to modify QGRAF output in such a way that the fermion flows remain intact. We use in-house PYTHON code to deal with the issue. The raw output from QGRAF is converted to a suitable format for further computations. The simplification of matrix elements involving the Lorentz, Dirac, colour and generation indices is done by employing a set of in-house routines based on the symbolic manipulating program FORM [121]. For external on-shell gluon legs the sum over polarizations is carried out using

$$\sum_s \epsilon^\mu(p_1;s)\epsilon^{*\nu}(p_1;s) = -g^{\mu\nu} + \frac{p_1^\mu q^\nu + p_1^\nu q^\mu}{p_1.q} \tag{4.9}$$

where q^μ is an arbitrary light-like four vector. These matrix elements comprises of huge number of one and two loop scalar Feynman integrals. We have classified them so that they belong to a few integral sets. Using Reduze [122], the loop momenta in various integrals can be shifted suitably in order to belong to these sets. All the one loop diagrams are reduced to three sets expressed in a condensed way as follows:

$$\{\mathcal{P}, \mathcal{P}_i, \mathcal{P}_{i,i+1}, \mathcal{P}_{i,i+1,i+2}\}. \tag{4.10}$$

Here for each set, i takes any one value from $\{1,2,3\}$ whose elements are arranged cyclically. $\mathcal{P}$'s are

$$\mathcal{P} = k_1^2, \mathcal{P}_i = (k_1 - p_i)^2, \mathcal{P}_{i,j} = (k_1 - p_i - p_j)^2, \mathcal{P}_{i,j,k} = (k_1 - p_i - p_j - p_k)^2. \tag{4.11}$$

This becomes more complicated at two loops. At two loops, we have nine independent Lorentz invariants constructed out of two loop momentas k_1 and k_2, namely $\{k_\delta.k_\gamma, k_\delta.p_j\}$, $\delta,\gamma = 1,2; j = 1,2,3$. After shifting of loop momenta we can fit all the Feynman integrals into six sets. The first three can be written in a condensed notation as:

$$\{\mathcal{P}_0, \mathcal{P}_1, \mathcal{P}_2, \mathcal{P}_{1:i}, \mathcal{P}_{2:i}, \mathcal{P}_{1:i,i+1}, \mathcal{P}_{2:i,i+1}, \mathcal{P}_{1:i,i+1,i+2}, \mathcal{P}_{2:i,i+1,i+2}\}, \tag{4.12}$$

and the three remaining sets can be expressed as follows:

$$\{\mathcal{P}_0, \mathcal{P}_1, \mathcal{P}_2, \mathcal{P}_{1:i}, \mathcal{P}_{2:i}, \mathcal{P}_{0:i+2}, \mathcal{P}_{1:i,i+1}, \mathcal{P}_{2:i,i+1}, \mathcal{P}_{1:i,i+1,i+2}\}, \tag{4.13}$$

where for each set, i takes any one value from $\{1,2,3\}$ whose elements are arranged cyclically. The elements of the six sets are

$$\begin{aligned} \mathcal{P}_0 &= (k_1 - k_2)^2, & \mathcal{P}_\beta &= k_\beta^2, \\ \mathcal{P}_{\beta:i} &= (k_\beta - p_i)^2, & \mathcal{P}_{\beta:i,j} &= (k_\beta - p_i - p_j)^2, \\ \mathcal{P}_{0:i} &= (k_1 - k_2 - p_i)^2, & \mathcal{P}_{\beta:i,j,k} &= (k_\beta - p_i - p_j - p_k)^2. \end{aligned} \tag{4.14}$$

Although the number of scalar integrals are huge in number, most of them are however, related to one another. Using IBP [57, 58] and LI identities [59] they can be reduced to a smaller set of topologically different integrals, popularly known as MIs. We have used a Mathematica based package LiteRed [124, 129] to uncover the set of MIs. For one and two loop the number of MIs are 7 and 89 respectively. These MIs were computed by Gehrmann and Remiddi analytically as expansion in Laurent series in ϵ in the references [108, 109].

4.3 Regularization of singularities

$\mathcal{N} = 4$ SYM theory is an UV finite theory in four space-time dimensions, guarantee the UV finiteness of quantities like on shell amplitudes, FFs of protected operators and correlation functions of elementary fields etc whereas unprotected operators develop UV divergences. But due to the presence of massless fields in the theory, on shell amplitudes and FFs of both protected as well as unprotected operator are sensitive to IR divergences order by order in perturbation theory.

In QFT, the method of dimensional regularization has been quite successful in regulating both UV as well as IR singularities. However, different variants or schemes of dimensional regularization exist in the literature. In the scheme proposed by 't Hooft and Veltman [226], called dimensional regularization scheme, the unphysical gauge bosons are treated in $4+\epsilon$ dimensions with $2+\epsilon$ helicity states but the physical ones in 4 dimensions having 2 helicity states. The conventional dimensional regularization scheme proposed by Ellis and Sexton [227] treats both the physical and unphysical gauge fields in $4+\epsilon$ dimensions. The FDH scheme advocated in [67, 68] assumes both the physical and unphysical states in 4 dimension. The common among all these schemes is that the loop integrals are performed in $4+\epsilon$ dimensions. Of course, all these schemes can be related to each other using suitable finite renormalisation constants. FDH scheme has been the most popular one in supersymmetric theories. It was observed in [64] that for certain dimension dependent operators, extra care is needed to get the correct result. One such operator is the Konishi operator. In [64], the authors propose a prescription to correct the result for the Konishi operator computed in FDH scheme. In order to obtain the correct result for its FF, their prescription suggests that one has to take the difference of FFs of the Konishi and the half-BPS operators, multiply the ratio $\Delta_{\mathcal{K}}^{BPS} = n_{g,\epsilon}/2n_g$ and add to the FF of the half-BPS, that is

$$\mathcal{F}_f^{\mathcal{K}} = \mathcal{F}_f^{BPS} + \Delta_{\mathcal{K}}^{BPS}(\mathcal{F}_f^{\mathcal{K}} - \mathcal{F}_f^{BPS}) \tag{4.15}$$

where $n_g = 3$ is the number of scalar or pseudoscalar fields and $n_{g,\epsilon} = 2n_g - \epsilon$. It is shown that this prescription correctly reproduces the anomalous dimension of the Konishi operator up to two loops level. There exists another elegant scheme called $\overline{DR}$ scheme which we will use in our computation. In this scheme, one adjusts the number of generations of scalar and pseudo-scalar fields such that the resulting bosonic degrees of freedom adds to that of fermions in order to preserve supersymmetry. Since the gauge fields have $2+\epsilon$ degrees of freedom, there should be $n_g - \epsilon/2$ scalars and $n_g - \epsilon/2$ pseudo-scalar in the regularised version of the theory so that the total number of bosonic degrees of freedom in $4+\epsilon$ is same as the four dimensional one, namely $2(1+n_g)$. The advantage of this scheme over others is that it can be used even for operators that depend on space-time dimensions. In this scheme, for $\mathcal{N} = 4$ SYM, the number of scalar and pseudo-scalar fields become $6-\epsilon$ as opposed to 6. Here, gluons have $2+\epsilon$ degrees of freedom while fermions degrees of freedom remains 8. This prescription is consistent with $\mathcal{N} = 4$ supersymmetry since the total number of scalar, pseudoscalar and gauge degrees of freedom continues to remain 8. In this scheme, all the traces of α, β and Dirac matrices are done in $4+\epsilon$ dimensions. In [5] three loop FFs of the Konishi was computed in the FDH scheme modified according to [64], as well as in the $\overline{DR}$ scheme up to three loop level in perturbation theory and the results agreed validating the prescription advocated in [64]. In the following we will present the results for the three point FFs of the BPS and the Konishi operators. These results were computed both in the $\overline{DR}$ as well as FDH schemes. For the BPS, both the schemes give same results, but for the Konishi, they agree only when the results computed in the FDH scheme are modified according to the prescription given in [64].

4.3.1 UV divergences

Since, $\mathcal{N} = 4$ SYM theory is UV finite, the coupling constant does not get any renormalisation, i.e., the beta function of the coupling, $\beta(a)$ [17, 18] is identically zero to all orders in perturbation theory. Hence, based on dimensional argument, the coupling constant $\hat{a}$ that appears in the regularised Lagrangian in $4+\epsilon$ dimensions is written in terms of dimensionless coupling a (see Eq. (3.5)) through

$$\hat{a} = a\Big(\frac{\mu^2}{\mu_R^2}\Big)^{\frac{\epsilon}{2}}, \tag{4.16}$$

The UV divergences arising due to short distance effects in the composite operators can by removed by an overall operator renormalization constant $Z^\rho(a, \mu_R, \epsilon)$ and hence the operator's scaling dimension is modified by γ^ρ, the anomalous dimension. The relation between $Z^\rho\,(a,\mu_R,\epsilon)$ and γ^ρ is encapsulated in the following differential equation

$$\frac{d}{d\ln\mu_R^2}\ln Z^\rho = \gamma^\rho = \sum_{i=1}^{\infty} a^i\gamma_i^\rho\,. \tag{4.17}$$

Using Eq. (4.16), the solution to the above equation is:

$$Z^\rho = \exp\Big(\sum_{n=1}^{\infty} a^n\frac{2\gamma_n^\rho}{n\epsilon}\Big). \tag{4.18}$$

In the work [5] discussed in Chapter 3, we extracted the γ^ρ up to three loop order using two-point three-loop FF of the Konishi and found agreement with the known results. The anomalous dimension up to 2-loop are in agreement with the existing ones [157–159]. We used analog of KG that QCD form factors satisfy [6, 84, 85] to determine the anomalous dimension γ^ρ. The values up to two loop are

$$\gamma_j^{\text{BPS}} = 0\,,\quad \gamma_1^{\mathcal{K}} = -6\,,\quad \gamma_2^{\mathcal{K}} = 24\,. \tag{4.19}$$

The operator renormalised transition amplitudes $|\mathcal{M}_f^\rho\rangle$ can be expressed in terms of UV unrenormalized ones $|\hat{\mathcal{M}}_f^{\rho,(n)}\rangle$, expanded in coupling constant a as

$$|\mathcal{M}_f^\rho\rangle = Z^\rho\,(a,\mu_R,\epsilon)\Big(\frac{a}{\mu_R^\epsilon}\Big)^{\frac{1}{2}}\Bigg(|\hat{\mathcal{M}}_f^{\rho,(0)}\rangle + \Big(\frac{a}{\mu_R^\epsilon}\Big)|\hat{\mathcal{M}}_f^{\rho,(1)}\rangle + \Big(\frac{a}{\mu_R^\epsilon}\Big)^2|\hat{\mathcal{M}}_f^{\rho,(2)}\rangle\Bigg). \tag{4.20}$$

For ρ = BPS, $Z^{BPS}\,(a,\mu_R,\epsilon) = 1$. On the other hand, for the Konishi operator, we can express $|\mathcal{M}_f^{\mathcal{K}}\rangle$ in terms of UV finite matrix elements $|\mathcal{M}_f^{\mathcal{K},(j)}\rangle$ as follows

$$|\mathcal{M}_f^{\mathcal{K}}\rangle = a^{1/2}|\mathcal{M}_f^{\mathcal{K},(0)}\rangle + a^{3/2}|\mathcal{M}_f^{\mathcal{K},(1)}\rangle + a^{5/2}|\mathcal{M}_f^{\mathcal{K},(2)}\rangle\,, \tag{4.21}$$

where

$$|\mathcal{M}_f^{\mathcal{K},(0)}\rangle = \Big(\frac{1}{\mu_R^\epsilon}\Big)^{\frac{1}{2}}|\hat{\mathcal{M}}_f^{\mathcal{K},(0)}\rangle,$$

$$
\begin{aligned}
|\mathcal{M}_f^{\mathcal{K},(1)}\rangle &= \Big(\frac{1}{\mu_R^\epsilon}\Big)^{\frac{3}{2}} \Big[\mu_R^\epsilon\, r_1 |\hat{\mathcal{M}}_f^{\mathcal{K},(0)}\rangle + |\hat{\mathcal{M}}_f^{\mathcal{K},(1)}\rangle\Big], \\
|\mathcal{M}_f^{\mathcal{K},(1)}\rangle &= \Big(\frac{1}{\mu_R^\epsilon}\Big)^{\frac{5}{2}} \Big[\mu_R^{2\epsilon}\Big(\frac{r_1^2}{2} + r_2\Big)|\hat{\mathcal{M}}_f^{\mathcal{K},(0)}\rangle + \mu_R^\epsilon\, r_1 |\hat{\mathcal{M}}_f^{\mathcal{K},(1)}\rangle + |\hat{\mathcal{M}}_f^{\mathcal{K},(2)}\rangle\Big],
\end{aligned} \tag{4.22}
$$

with

$$
r_1 = \frac{1}{\epsilon}\, 2\gamma_1^{\mathcal{K}}, \qquad r_2 = \frac{1}{\epsilon}\gamma_2^{\mathcal{K}}. \tag{4.23}
$$

Substituting the above equations in Eq. (4.4) we obtain the renormalised FFs for the half-BPS and the Konishi operator. We will present the results in the following sections after a systematic subtraction of IR divergences.

4.3.2 Universality of IR singularities

In gauge theories, the UV renormalized amplitudes and FFs suffer from IR divergences due to the presence of massless initial and final states. These divergences are of two types, namely soft and collinear. Soft ones arise when the momentum of a massless gauge particle in loop has vanishing components. The collinear divergences emerge when any massless particle in the loop becomes parallel to the external particle. However these amplitudes and FFs are not the observables, instead the cross sections or decay rates made out of these amplitudes and FFs are the observables. Finiteness of the observables has been proved through KLN theorem [22, 23]. The IR structure of amplitudes and FFs in QCD is well understood and in particular, the universal structure of IR divergences was predicted in a seminal paper by Catani [4] for n-point two-loop QCD amplitudes. He exploited the iterative structure of singular part of the renormalised amplitudes in QCD to predict the subtraction operators that capture the universal IR divergences of these amplitudes. Later on Sterman and Tejeda-Yeomans successfully related Catani's predictions to the factorization and resummation properties of QCD amplitudes [130]. Note that iterative structure is the result of factorisation. The generalization of Catani's proposal for arbitrary number of loops and legs for SU(N) gauge theory using SCET was given by Becher and Neubert [131]. A similar result was also presented by Gardi and Magnea [132] by analyzing the Wilson lines for hard partons.

Following Catani's proposal, we can express the UV renormalized amplitudes $|\mathcal{M}_f^{\rho,(n)}\rangle$ for the three point function up to two loop order in terms of universal subtraction operators $\mathbf{I}_f^{(n)}(\epsilon)$ (see similar analysis for MHV amplitudes in [228]),

$$
\begin{aligned}
|\mathcal{M}_f^{\rho,(1)}\rangle &= 2\,\mathbf{I}_f^{(1)}(\epsilon)|\mathcal{M}_f^{\rho,(0)}\rangle + |\mathcal{M}_f^{\rho,(1)\mathrm{fin}}\rangle\,, \\
|\mathcal{M}_f^{\rho,(2)}\rangle &= 2\,\mathbf{I}_f^{(1)}(\epsilon)|\mathcal{M}_f^{\rho,(1)}\rangle + 4\,\mathbf{I}_f^{(2)}(\epsilon)|\mathcal{M}_f^{\rho,(0)}\rangle + |\mathcal{M}_f^{\rho,(2)\mathrm{fin}}\rangle.
\end{aligned}
\tag{4.24}
$$

In context of $\mathcal{N} = 4$ SYM theory where all fields are in adjoint representation and β-function is zero, the universal subtraction operators are found to be

$$
\begin{aligned}
\mathbf{I}_f^{(1)}(\epsilon) &= -\frac{1}{2}\frac{e^{-\frac{\epsilon}{2}\gamma_E}}{\Gamma(1+\frac{\epsilon}{2})}\mathcal{V}^{sing}(\epsilon)\Big\{\Big(-\frac{s}{\mu_R^2}\Big)^{\frac{\epsilon}{2}} + \Big(-\frac{t}{\mu_R^2}\Big)^{\frac{\epsilon}{2}} + \Big(-\frac{u}{\mu_R^2}\Big)^{\frac{\epsilon}{2}}\Big\}\,, \\
\mathbf{I}_f^{(2)}(\epsilon) &= -\frac{1}{2}\Big(\mathbf{I}_f^{(1)}(\epsilon)\Big)^2 + K\frac{e^{\frac{\epsilon}{2}\gamma_E}\Gamma(1+\epsilon)}{\Gamma(1+\frac{\epsilon}{2})}\mathbf{I}_f^{(1)}(2\epsilon) + \mathbf{H}_f^{(2)}(\epsilon),
\end{aligned}
\tag{4.25}
$$

where $\mathcal{V}^{sing}(\epsilon) = \frac{A_1}{\epsilon^2}$ results from the dipole structure of the infrared singularities. The constant A_1 is the first coefficient of the cusp anomalous dimension and found to be 4 in $\mathcal{N} = 4$ SYM. Note that the constant K and $\mathbf{H}_f^{(2)}(\epsilon)$ are unknown at the moment and they can be determined using the explicit results for $|\mathcal{M}_f^{\rho,(i)}\rangle$ computed in this paper demanding the finiteness of $|\mathcal{M}_f^{\rho,(i)\mathrm{fin}}\rangle$ for $i = 1, 2$.

Using these subtraction operators, the UV renormalized FF as defined in Eq. (4.4) for $n = 1, 2$ can be written as

$$
\begin{aligned}
\mathcal{F}_f^{\rho,(1)} &= 2\,\mathbf{I}_f^{(1)}(\epsilon)\mathcal{F}_f^{\rho,(0)} + \mathcal{F}_f^{\rho,(1),\mathrm{fin}}, \\
\mathcal{F}_f^{\rho,(2)} &= 2\,\mathbf{I}_f^{(1)}(\epsilon)\mathcal{F}_f^{\rho,(1)} + 4\,\mathbf{I}_f^{(2)}(\epsilon)\mathcal{F}_f^{\rho,(0)} + \mathcal{F}_f^{\rho,(2),\mathrm{fin}}.
\end{aligned}
\tag{4.26}
$$

Substituting the UV finite $\mathcal{F}_f^{\rho,(i)}$ in Eq. (4.26) and demanding finiteness of $\mathcal{F}_f^{\rho,(i),\mathrm{fin}}$ we can determine K and $\mathbf{H}_f^{(2)}(\epsilon)$. These constants K and $\mathbf{H}_f^{(2)}(\epsilon)$ obtained independently from the results of FFs of the BPS as well as from the Konishi operators, are found to be independent of the type of operator. They are given by

$$K = -\zeta_2, \quad \mathbf{H}_f^{(2)}(\epsilon) = -\frac{3}{4\epsilon}\zeta_3. \tag{4.27}$$

The factor 3 in $\mathbf{H}_f^{(2)}(\epsilon)$ is due to the presence of three massless particles in the final state f all giving same contribution. Like in QCD, we expect that the universality of these constants to hold for two-loop FFs of any composite operator. In the Appendix C, we present remaining finite terms $\mathcal{F}_f^{\rho,(n),\text{fin}}$ for $n = 1, 2$ by setting $\mu_R^2 = -Q^2$ in Eq. (4.26).

In the next section we shall discuss about the finite remainders and examine whether it can be written in terms of some simple structure.

4.4 Finite Remainders

We have seen in the previous section the iterative structure of IR divergences for the FFs in terms of Catani's subtraction operators up to two loops level in perturbation theory. This is a result of factorisation property of the FFs at long distances. This is very similar to on-shell amplitudes in gauge theories. The factorisation and observed universality of these IR divergences can lead to exponentiation of these divergences whose coefficients are controlled by certain universal IR anomalous dimensions. In the case of amplitudes, we have seen in the context of the BDS ansatz [6, 188], both the IR and finite parts can be exponentiated and the exponents are expressed in terms of their one loop counter parts multiplied by a function that depend on the IR anomalous dimensions such as cusp and collinear ones. For amplitudes, the iterative structure of the finite terms breaks down from two-loop six-point amplitudes onwards and the deviation is called the FR function.

In the case of FFs, the IR divergences exponentiate, thanks to their iterative structure but the finite terms. Since, the beta function vanishes to all orders in perturbation theory, the divergent part of the exponent can be normalised in terms of the corresponding one loop FFs by properly adjusting the ϵ at every order. The finite terms of the FFs do not show any iterative structure, hence the corresponding FR functions are always non-zero. For the two-point half-BPS operator, the authors of [201] have obtained the finite reminder function up to two loops. Later it was extended to cases with more than two external states [7, 222]. Following BDS structure, the finite reminder function at two loops is defined by

$$\mathcal{R}_f^{\rho,(2)} = \mathcal{F}_f^{\rho,(2)}(\epsilon) - \frac{1}{2}\Big(\mathcal{F}_f^{\rho,(1)}(\epsilon)\Big)^2 - f^{\rho,(2)}(\epsilon)\mathcal{F}_f^{\rho,(1)}(2\epsilon) - C^{\rho,(2)} + O(\epsilon). \tag{4.28}$$

The form of the function $f^{\rho,(2)}(\epsilon)$ is inspired by the one that appears in BDS ansatz. Expanding $f^{\rho,(2)}(\epsilon)$ (see Eq. (4.28) [7]) as

$$f^{\rho,(2)}(\epsilon) = \sum_{i=0}^{2} \epsilon^i f_i^{\rho,(2)} \tag{4.29}$$

and demanding the finiteness of $\mathcal{R}_f^{\rho,(2)}$, we can uniquely fix $f_0^{\rho,(2)}$ and $f_1^{\rho,(2)}$ but $f_2^{\rho,(2)}$ and $C^{\rho,(2)}$ can not be determined independently. Choosing

$$C^{\rho,(2)} = 4\zeta_4, \tag{4.30}$$

same for $\rho = BPS, \mathcal{K}$, we obtain

$$f^{\rho,(2)}(\epsilon) = -2\zeta_2 + \epsilon\zeta_3 - \frac{1}{2}\epsilon^2\zeta_4. \tag{4.31}$$

Note that the $f^{\rho,(2)}$ as well as $C^{\rho,(2)}$ are independent of the operators as well as the choice of external states. This is a consequence of the universality of IR divergences in $\mathcal{N} = 4$ SYM. The two loop FR function, $\mathcal{R}_f^{\rho,(2)}$, can be expressed in terms of finite parts $\mathcal{F}_f^{\rho,(i),fin}$ in Eq. (4.26) as

$$
\begin{aligned}
\mathcal{R}_f^{\rho,(2)} =& \mathcal{F}_f^{\rho,(2),fin} - \left(\frac{1}{2}\mathcal{F}_f^{\rho,(1),fin} + 2K\right)\mathcal{F}_f^{\rho,(1),fin} + \frac{3}{4}A_1\left(f_2^{\rho,(2)} - \frac{3}{4}K\zeta_2\right) \\
&- C^{\rho,(2)} - \frac{4}{3}\mathbf{H}_f^{\rho,(2)} \log(xyz)\,, \qquad (4.32)
\end{aligned}
$$

where we have set $\mu_R^2 = -Q^2$. We have computed finite remainders for both the half-BPS and the Konishi operators for both the choices of external on shell states f, namely $f = g\phi\phi$ and $f = \phi\lambda\lambda$. The results, after setting $\mu_R^2 = -Q^2$, are listed below. The two loop finite remainder for the half-BPS operator turns out to be same for both choices of f:

$$
\begin{aligned}
\mathcal{R}_f^{\mathrm{BPS},(2)} =& 4\Big(2H(3,3,3,2;y) - H(2,3,2,3;y) + H(2,2,3,2;y) + H(2,2,1,0;y) \\
&+ 2H(1,1,1,0;y) - H(0,1,0,1;y) + H(0,0,3,2;y) + H(0,0,1,0;y)\Big) \\
&+ 8\Big(H(2;y) + H(3;y)\Big)\Big(H(0,0,1;z) - H(1,1,0;z)\Big) + 4\Big(H(2,3,2;y)H(3;y) \\
&- H(2,1,0;y)H(2;y) + H(0,1,0;y)H(1;y) - H(0,3,2;y)H(0;y) \\
&- H(1,0;y)H(3,2;y)\Big) + 4H(0,1;z)\Big(H(2;y) + H(3;y)\Big)^2 + 2H(1;z)\Big[H(3;y) \\
&\times\Big(- H(0;y)^2 + 2H(2;y)H(3;y) + \frac{2}{3}H(3;y)^2 - 2H(1,0;y) - 2H(3,2;y)\Big) \\
&- 2H(2,1,0;y) + 2H(2,2,3;y) + 2H(3,0,0;y)\Big] - 2H(0;z)\Big[H(0;y)\Big(H(2;y)^2 \\
&- 2H(0,2;y)\Big) - 2H(2;y)H(1,0;y) + 2H(0;y)H(3,2;y) + 2H(0,0,2;y) \\
&- 2H(0,2,2;y) - 2H(0,3,2;y) + 2H(2,1,0;y) + H(1;z)\Big(H(2;y)^2 \\
&+ 2H(2,0;y) + 2H(3,0;y) + 2H(3,2;y)\Big)\Big] + 4\zeta_2\Big[2H(0,1;y) - 2H(3,2;y) \\
&+ H(1;y)^2 - 2H(1;z)H(2;y) - H(2;y)^2 - 2H(1;z)H(3;y)\Big]. \qquad (4.33)
\end{aligned}
$$

The finite remainders for the Konishi operator for $f = g\phi\phi$ is given below

$$
\begin{aligned}
\mathcal{R}^{\mathcal{K},(2)}_{g\phi\phi} = \mathcal{R}^{\mathrm{BPS},(2)}_{f} &- \zeta_3 \frac{6y(-1+y+z)}{(1-z)^2} + \zeta_2\Big[\frac{6y(-1+y+z)}{(1-z)^2}\Big(H(0;y)+H(0;z)\Big) \\
&- \frac{3H(1;y)}{z^2}(-1+y)(-1+y+2z) + \frac{3yH(1;z)}{z^2(1-z)^2}\Big(10z^2(-1+z)+y(-1+2z \\
&+ 9z^2)\Big) + \frac{3H(2;y)}{z^2(1-z)^2}\Big((-1+z)^4+y^2(1-2z+3z^2)+y(-2+6z-8z^2+4z^3)\Big)\Big] \\
&- \frac{3H(0;z)^2}{(1-z)}\Big(yH(0;y)+H(2;y)(-1+y+z)\Big) + H(0,1;z)\Big[H(3;y)\Big(\frac{3y^2}{z^2}-3\Big) \\
&- \frac{6yH(0;y)}{(1-z)^2}(-1+y+z) - \frac{3H(2;y)}{z^2(1-z)^2}\Big((-1+z)^4+y^2(1-2z+3z^2)+y(-2 \\
&+ 6z-8z^2+4z^3)\Big)\Big] + \frac{3yH(0;z)H(0,2;y)}{z^2(1-z)^2}\Big(4(-1+z)z^2+y(-1+2z+3z^2)\Big) \\
&+ \frac{3H(1,0;y)}{z^2}\Big[-\frac{H(0;z)}{(1-z)^2}\Big((-1+z)^2(-1+2z)+y^2(-1+2z+3z^2)+2y(1 \\
&- 3z+z^2+z^3)\Big) + H(1;z)(-1+y)(-1+y+2z) + H(2;y)(-1+y)(-1+y \\
&+ 2z)\Big] - \frac{3H(0;z)H(2,0;y)}{z^2(1-z)^2}\Big((-1+z)^4+y^2(1-2z-3z^2)-2y(1-3z+z^2 \\
&+ z^3)\Big) + H(3,2;y)\Big[H(0;y)\Big(3-\frac{3y^2}{z^2}\Big) - \frac{3H(0;z)}{z^2(1-z)^2}\Big(4y(-1+z)z^2+z^2 \\
&\times (-1+z)^2+y^2(-1+2z+3z^2)\Big)\Big] + H(1;z)\Big[\frac{3yH(0;y)H(0;z)}{z^2(1-z)^2}\Big(4(-1+z)z^2 \\
&+ y(-1+2z+3z^2)\Big) - \frac{3H(0;z)H(3;y)}{z^2(1-z)^2}\Big(4y(-1+z)z^2+(1-z)^2z^2+y^2(-1 \\
&+ 2z+3z^2)\Big) - \frac{3H(2;y)H(3;y)}{z^2(1-z)^2}\Big((-1+z)^4+y^2(1-2z+3z^2)+y(-2+6z \\
&- 8z^2+4z^3)\Big) + \frac{3}{2}H(3;y)^2\Big(-1+\frac{y^2}{z^2}\Big) - \frac{6yH(0,3;y)}{(1-z)^2}(-1+y+z) + H(3,0;y) \\
&\times \Big(3-\frac{3y^2}{z^2}\Big) + \frac{3H(3,2;y)}{z^2(1-z)^2}\Big((-1+z)^4+y^2(1-2z+3z^2)+y(-2+6z
\end{aligned}
$$

$$
\begin{aligned}
&- 8z^2 + 4z^3)\Big)\Big] - \frac{6yH(0,0,1;z)}{z^2(1-z)^2}\Big(2z^2(-1+z) + y(-1+2z+2z^2)\Big)\\
&+ \frac{3yH(0,1,0;y)}{z^2(1-z)^2}\Big(2z^2(-1+z) + y(1-2z+3z^2)\Big) + \frac{3yH(0,1,0;z)}{z^2(1-z)^2}\Big(4(-1+z)z^2\\
&+ y(1-2z+3z^2)\Big) - \frac{3H(0,3,2;y)}{z^2(1-z)^2}\Big(2yz^2(-1+z) + z^2(-1+z)^2 + y^2(-1+2z\\
&+ z^2)\Big) - \frac{6yH(1,0,0;z)}{(1-z)} - \frac{3yH(1,0,1;z)}{z^2(1-z)^2}\Big(2z^2(-1+z) + y(1-2z+3z^2)\Big)\\
&- \frac{3H(1,1,0;y)}{z^2}(-1+y)(-1+y+2z) + \frac{6yH(1,1,0;z)}{z^2(1-z)^2}\Big(4(-1+z)z^2\\
&+ y(-1+2z+3z^2)\Big) + \frac{3H(2,1,0;y)}{z^2(1-z)^2}\Big((-1+z)^2(-1+2z) + y^2(-1+2z+z^2)\\
&+ y(2-6z+4z^2)\Big) - \frac{3H(2,3,2;y)}{z^2(1-z)^2}\Big((-1+z)^4 + y^2(1-2z+3z^2) + y(-2\\
&+ 6z - 8z^2 + 4z^3)\Big) + H(3,3,2;y)\Big(-3 + \frac{3y^2}{z^2}\Big) + \frac{1}{(1-z)^4}\Big[\zeta_2\frac{(-1+z)^2}{z}\\
&\times\Big(-52z(-1+z)^2 + 6y^2(-1+5z) + y(9-48z+39z^2)\Big) - 3yH(0;z)^2\Big(6y^3\\
&+ 12y^2(-1+z) + 5y(-1+z)^2 - (-1+z)^3\Big) + \frac{3(-1+z)^3(-1+11z)}{z}H(0;z)\\
&\times\Big(yH(0;y) + (-1+y+z)H(2,y)\Big) - \frac{3(-1+z)^2H(1,z)}{z^2}\Big[H(0;y)y(-1+y+z)\\
&\times(-1+z^2) + H(0;z)yz\Big(1+16z-17z^2-2y(1+3z)\Big) + (-1+z)H(3;y)\\
&\times\Big(-(y^2(1+z)) + y(1-z+2z^2) + z(1-12z+11z^2)\Big)\Big]\\
&- \frac{3yH(0,1;z)}{z^2}(-1+z)^2\Big(-1+y+2yz-7z^2+5yz^2+8z^3\Big)\\
&- \frac{3yH(0,2;y)}{z^2}(-1+z)^3(1+z)(-1+y+z)\\
&- \frac{3H(1,0;y)}{z^2}(-1+z)^3\Big(8z^2(-1+z) - y^2(1+z) + y(1+z-4z^2)\Big)\\
&- \frac{3yH(2,0;y)}{z^2}(-1+z)^3(1+z)(-1+y+z) + \frac{3H(3,2;y)}{z^2}(-1+z)^3\Big(y^2(1+z)
\end{aligned}
$$

$$+ z(-1 + 12z - 11z^2) + y(-1 + z - 2z^2)\Big)\Big] - \frac{12yH(0;z)}{z(1-z)^3}\Big(3y^3 + 6y^2(-1+z)$$

$$+ 5z(-1+z)^2 + y(3 - 11z + 8z^2)\Big) - \frac{2}{z^2(1-z)^2}\Big(9y^4 + 18y^3(-1+z)$$

$$+ 30yz(-1+z)^2 - 53(-1+z)^2z^2 + y^2(9 - 48z + 39z^2)\Big). \tag{4.34}$$

The finite remainders of the Konishi operator for $f = \phi\lambda\lambda$ reads as

$$\mathcal{R}^{\mathcal{K},(2)}_{\phi\lambda\lambda} = \mathcal{R}^{\mathrm{BPS},(2)}_{f} + 3\Big(- 9H(0,0,0,1;z) - 2H(0,0,1,0;y) - 5H(0,0,1,1;z)$$

$$- 3H(0,0,3,2;y) + 3H(0,1,0,1;y) - 4H(0,1,0,1;z) + 2H(0,1,1,0;y)$$

$$+ 2H(0,1,1,0;z) + H(0,2,1,0;y) - H(0,3,2,2;y) + H(0,3,3,2;y)$$

$$- H(1,0,0,1;z) + 2H(1,0,1,0;z) - 2H(1,1,0,0;y) - 2H(1,1,0,1;z)$$

$$- 4H(1,1,1,0;y) + H(2,0,1,0;y) - H(2,1,0,0;y) + H(2,1,1,0;y)$$

$$- 3H(2,2,1,0;y) - 2H(2,2,3,2;y) - H(2,3,0,2;y) - H(2,3,2,0;y)$$

$$+ 3H(2,3,2,3;y) + 2H(2,3,3,2;y) - 2H(3,3,2,2;y) - 4H(3,3,3,2;y)\Big)$$

$$+ 3\zeta_2\Big[\frac{3}{2}\Big(H(1;z) + H(2;y)\Big)^2 - 2H(1;y)^2 + 4H(1;z)H(3;y) - 4H(0,1;y)$$

$$+ 3H(0,1;z) + H(2,1;y) + 4H(3,2;y)\Big] + 3H(0,0,1;z)\Big(2H(0;y) + 2H(0;z)$$

$$- 5H(2;y) - 4H(3;y)\Big) + 3H(0,1,1;z)\Big(5H(0;y) - 4H(3;y)\Big) + 3H(1,0,1;z)$$

$$\times \Big(2H(0;y) - 2H(2;y) - 3H(3;y)\Big) + 6H(1,1,0;z)\Big(H(3;y) - H(0;y)\Big)$$

$$+ 3H(0,1,0;y)\Big(H(1;z) - 3H(1;y) + H(2;y)\Big) + 6H(1,0,0;y)\Big(H(0;z)$$

$$+ 2H(1;z) + 2H(2;y)\Big) + 3H(0,0,2;y)\Big(2H(0;z) + 5H(1;z)\Big) - 3H(2,0,0;y)$$

$$\times\Big(2H(0;z)+5H(1;z)\Big)+6H(2,1,0;y)\Big(H(0;z)+H(1;z)+H(2;y)\Big)$$

$$+3H(2,3,2;y)\Big(2H(0;y)-3H(3;y)\Big)+6H(3,2,2;y)\Big(2H(0;y)-H(0;z)\Big)$$

$$+\frac{3}{4}H(1;z)^2\Big(8H(3,0;y)+6H(0,3;y)-2H(3;y)^2-5H(0;y)^2\Big)$$

$$+3H(1;z)\Big(H(0,3,3;y)-2H(2,2,3;y)-H(2,3,0;y)+2H(2,3,3;y)$$

$$-H(3,0,0;y)-2H(3,3,2;y)\Big)+3H(0;y)\Big[H(0;z)\Big(H(2;y)^2-2H(0,2;y)$$

$$+2H(3,2;y)\Big)+H(1;z)\Big(-5H(0,2;y)+2H(2,3;y)+4H(3,2;y)\Big)$$

$$+2H(0,3,2;y)\Big]+3H(1;z)H(0,3,0;y)-3H(0,3,2;y)\Big(2H(0;z)+H(1;z)\Big)$$

$$+3H(0,1;z)\Big[\frac{1}{2}H(0;y)^2-H(2;y)^2-\Big(4H(2;y)+2H(3;y)\Big)H(3;y)$$

$$+4H(0;y)H(2;y)+H(0,3;y)-H(1,0;y)-H(3,2;y)\Big]+3H(1,0;y)$$

$$\times\Big(H(3,2;y)+H(1;z)H(3;y)-2H(0;z)H(2;y)\Big)-15H(0,0;y)H(2,2;y)$$

$$+\frac{3}{2}H(1;z)\Big[H(0;y)^2\Big(H(3;y)-2H(0;z)\Big)-H(3;y)^2\Big(6H(2;y)+\frac{4}{3}H(3;y)\Big)$$

$$+4H(0;z)H(3,0;y)+6H(3;y)H(3,2;y)\Big]$$

$$+\frac{6z}{1-y}\zeta_3-\frac{3\zeta_2}{1-y}\Big[2z\Big(H(0;y)+H(0;z)\Big)-\frac{H(1;y)}{y(1-y-z)}\Big(1-3z+2z^2$$

$$+y^2(1+7z)+y(-2-4z+6z^2)\Big)+\frac{H(1;z)}{(y+z)(1-y-z)}\Big(y^2(1+3z)$$

$$+z(5-3z-2z^2)+y(-1-8z+z^2)\Big)-\frac{H(2;y)}{y(y+z)}\Big((-1+z)z+y^2(1+3z)$$

$$-y(1+4z+3z^2)\Big)\Big]+\frac{3(y-5z)}{y+z}H(0;y)H(2;y)^2+\frac{3(y-5z)}{y+z}H(1;z)^2\Big(H(0;y)$$

$$-H(3;y)\Big)+\frac{3H(0,1;z)}{y+z}\Big[-\frac{2H(0;y)}{1-y}\Big(3y^2+z(-2+3z)+y(-3+5z)\Big)$$

$$
\begin{aligned}
&+ \frac{H(2;y)}{y(1-y)}\Big(6y^3 - (-1+z)z - y^2(7+3z) + y(1+6z+5z^2)\Big) \\
&- \frac{H(3;y)}{y(1-y-z)}\Big(z(-1+z)(8y+z) + y^2(1+7z)\Big)\Big] + H(0,2;y)\Big[\frac{6H(0;y)}{1-y}(-1 \\
&+ y + 6z) - \frac{3H(0;z)}{(1-y)(y+z)(1-y-z)}\Big(4y^3 + y^2(-7+9z) + z(7-5z-2z^2) \\
&+ y(3-16z+3z^2)\Big) + \frac{6(y-5z)}{y+z}H(1;z)\Big] - \frac{3H(1,0;y)}{y(y+z)(1-y-z)}\Big[H(0;z)\Big(4y^3 \\
&- (-1+z)z + y^2(-5+9z) + y(1-6z+5z^2)\Big) + \Big(H(1;z) + H(2;y)\Big)\Big(4y^3 \\
&- (-1+z)z + y^2(-5+11z) + y(1-8z+7z^2)\Big)\Big] + \frac{3H(2,0;y)}{y+z}\Big[\frac{H(0;z)}{y(1-y)}\Big(4y^3 \\
&- (-1+z)z + y^2(-5+3z) + y(1-8z-3z^2)\Big) + 2(y-5z)H(1;z)\Big] \\
&- \frac{3H(3,2;y)}{y(1-y)(1-y-z)}\Big[H(0;y)\Big(4y^3 + y^2(-7+z) + (-1+z)z - 3y(-1+z^2)\Big) \\
&+ H(0;z)(1-y)\Big(4y^2 - (1-z)(3y-z)\Big)\Big] + H(1;z)\Big[\frac{3H(0;y)^2}{1-y}(-1+y+6z) \\
&+ \frac{3H(0;y)H(0;z)}{(y+z)(1-y-z)}\Big(4y^2 + 5(-1+z)z + y(-3+9z)\Big) \\
&- \frac{6z(1+z)}{(1-y)(y+z)}H(0;z)H(2;y) - \frac{3H(0;z)H(3;y)}{y(1-y-z)}\Big(4y^2 - (1-z)(3y-z)\Big) \\
&+ \frac{3H(2;y)H(3;y)}{y(1-y)(y+z)}\Big(6y^3 - (-1+z)z - y^2(7+3z) + y(1+4z+3z^2)\Big) \\
&- \frac{3H(3;y)^2}{2y(y+z)(1-y-z)}\Big(8y(-1+z)z + (-1+z)z^2 + y^2(1+7z)\Big) \\
&- \frac{6H(0,3;y)}{1-y}(-3+3y+2z) - \frac{3H(3,0;y)}{y(1-y)(1-y-z)}\Big(4y^3 + y^2(-7+z) \\
&+ (-1+z)z - 3y(-1+z^2)\Big) - \frac{3H(3,2;y)}{y(1-y)}\Big(1 + 4y^2 - z + y(-5+3z)\Big)\Big] \\
&- \frac{6H(0,0,1;z)}{(1-y)(y+z)(1-y-z)}\Big(- 3y^2 + y^3 + 2y(1+z) + z(-2+z+z^2)\Big)
\end{aligned}
$$

$$
\begin{aligned}
&-\frac{6H(0,0,2;y)}{1-y}(-1+y+6z)+\frac{3}{(1-y)(y+z)(1-y-z)}\Big[H(0,1,0;y)\Big(6y^3\\
&+y^2(-11+21z)+3z(1-5z+4z^2)+y(5-24z+27z^2)\Big)+H(0,1,0;z)\Big(4y^3\\
&+7y^2(-1+z)+z(1-3z+2z^2)+y(3-8z+5z^2)\Big)\Big]-\frac{6(y-5z)}{y+z}H(0,1,1;z)\\
&+\frac{3H(0,3,2;y)}{y(1-y)(1-y-z)}\Big(10y^3+(-1+z)z+y^2(-19+11z)+y(9-10z+z^2)\Big)\\
&-\frac{6(-1+y+6z)}{1-y}H(1,0,0;y)-\frac{3H(1,0,1;z)}{(1-y)(y+z)(1-y-z)}\Big(6y^3+y^2(-11+5z)\\
&+y(5-2z+z^2)+z(-3+z+2z^2)\Big)+\frac{3H(1,1,0;y)}{y(1-y)(1-y-z)}\Big(1-3z+2z^2\\
&+y^2(1+7z)+y(-2-4z+6z^2)\Big)-\frac{6H(1,1,0;z)}{(1-y)(y+z)(1-y-z)}\Big(y^2(1+z)\\
&-y(1+3z)-z(-2+z+z^2)\Big)+\frac{6(-1+y+6z)}{1-y}H(2,0,0;y)\\
&+\frac{3H(2,1,0;y)}{y(y+z)(1-y-z)}\Big(10y^3-(-1+z)z+y^2(-11+19z)+y(1-10z+9z^2)\Big)\\
&+\frac{3H(2,3,2;y)}{y(1-y)(y+z)}\Big(6y^3-(-1+z)z-y^2(7+3z)+y(1+4z+3z^2)\Big)\\
&-\frac{6(y-5z)}{y+z}H(3,2,2;y)-\frac{3H(3,3,2;y)}{y(y+z)(1-y-z)}\Big(8y(-1+z)z+(-1+z)z^2\\
&+y^2(1+7z)\Big)-\frac{\zeta_2}{1-y}\Big(52(1-y)+12z\Big)-\frac{18z^2}{(1-y)^2}H(0;y)^2\\
&-\frac{18z^2}{(y+z)^2}\Big(H(1;z)+H(2;y)\Big)^2+H(1;z)\Big[\frac{6H(0;y)}{(1-y)(y+z)}\Big(y^2+y(-1+z)\\
&+z(-1+6z)\Big)-24H(0;z)+\frac{6(y-z)}{y+z}H(3;y)\Big]+\frac{6(5y+3z)}{y+z}H(0,1;z)\\
&+\frac{6H(0;y)H(2;y)}{(1-y)(y+z)}\Big(y^2+y(-1+z)+z(-1+6z)\Big)-\frac{6(-1+y+2z)}{1-y}H(1,0;y)\\
&+\frac{6(y-z)}{y+z}H(3,2;y)-\frac{24z}{1-y}H(0;y)+\frac{24z}{y+z}\Big(H(1;z)+H(2;y)\Big)+106.
\end{aligned}
\tag{4.35}
$$

Note that $\mathcal{R}_f^{BPS,(2)}$ for both choices of f contain terms of uniform weight four resulting from HPLs and Riemann zeta function (ζ_ns) with rational coefficients, i.e., no dependence on the scaling variables y, z. This is exactly the case for the finite terms of FFs after subtracting the Catani's subtraction operators and this is not to do with the exponentiation. For the Konishi operator, the results contain HPLs of different weights. Interestingly, HPLs with highest weight in the Konishi when $f = g\phi\phi$ coincide exactly with the result of the half-BPS. This is not the case for $f = \phi\lambda\lambda$. Like the half-BPS, the coefficients of leading HPLs in $\mathcal{R}_f^{\mathcal{K},(2)}$ are rational terms with no y, z dependence for both choices of f. The reason is still unclear. Using the fortran routines of Gehrmann and Remiddi [229] we have compared the finite remainder of the half-BPS operator presented in Eq. (4.33) against the compact result presented in the (Eq. (4.32) of [7]) and found excellent agreement within the numerical accuracy. The numerical comparison for various values of (x, y, z) is presented in the table below.

(x, y, z)	$\mathcal{R}_3^{(2)}$ [7]	$\mathcal{R}_f^{\mathrm{BPS},(2)}$
(1/7, 1/7, 5/7)	-0.08565426912931533	-0.08565426912932168
(7/9, 1/9, 1/9)	-0.06628498978762110	-0.06628498978762294
(4/11, 1/11, 6/11)	-0.09538372586521941	-0.09538372586522141
(20/33, 7/33, 6/33)	-0.11365299782099999	-0.11365299782099962
(10/19, 2/19, 7/19)	-0.10323613406746748	-0.10323613406746739
(8/17, 4/17, 5/17)	-0.13812300982989027	-0.13812300982989134
(75/99, 1/99, 23/99)	-0.01926355459500375	-0.01926355459500363
(67/79, 5/79, 7/79)	-0.04241579611131384	-0.04241579611131386

Table 4.1: Numerical comparison of Eq. (4.32) of [7] against our Eq. (4.33)

4.5 Universality of leading transcendental terms

Based on the supersymmetric extensions of BFKL and DGLAP evoultion equations, Kotikov and Lipatov [133–135] (see also [136, 137]) conjectured maximum transcendentality principle which implies that the anomalous dimensions of leading twist two operators in $\mathcal{N} = 4$ SYM theory contain uniform transcendental terms which are related to those in the corresponding QCD results [89, 90]. The transcendentality weight n is defined by terms such as $\zeta(n)$, ϵ^{-n} and weight of the HPLs that appear in the perturbative calculations. In $\mathcal{N} = 4$ SYM theory, scattering amplitudes of certain type [161, 228], FFs of the BPS type operators [7, 63, 220, 230], light-like Wilson loops [191, 231] and correlation functions [230–233] surprisingly exhibit this property. In [7], the two-loop three-point MHV FFs of the half-BPS operators were shown to have uniform transcendental terms in the FR functions. Using the method of symbology which uses coproducts, the FR function of the half-BPS operator at two loops was expressed in terms of transcendental weight four functions which agreed numerically with their result obtained using the unitarity based approach. Similar results for non-protected operators can be found in [70–72].

Unlike $\mathcal{N} = 4$ SYM, QCD results contain terms of all transcendental weights in addition to rational terms (zero transcendentality). But surprisingly, LT terms of anomalous dimensions of twist two operators, several FFs in QCD when $C_A = C_F = N$ and $T_f n_f = N/2$ coincide with the corresponding ones in $\mathcal{N} = 4$ SYM theory. For example, the LT terms of the amplitude for Higgs boson decaying to three on-shell gluons in QCD [54, 138] are related to the two loop three point MHV FFs of the half-BPS operators [7]. Similarly, the same is true for two point FFs of quark current operator, scalar and pseudo-scalar operators constructed out of gluon field strengths, energy momentum tensor of the QCD up to three loops. In Section 4.3.2, we determined both K and $\mathbf{H}^{(2)}_f$ appearing in Catani's IR subtraction operator by demanding the finiteness of $\mathcal{F}^{\rho,(n),fin}_f$, $n = 1, 2$. In QCD the single pole term in $\mathbf{I}_f^{(2)}$ is denoted by $\mathbf{H}_i^{(2)}$, where $i = q, \bar{q}, g$. This was shown in [84, 145] to be related to the the universal cusp (A_i) [89, 156], collinear (B_i) and soft (f_i) [84, 89] anomalous dimensions in the following way

$$\mathbf{H}_i^{(2)} = \frac{1}{\epsilon}\Big(\frac{1}{8}B_i^{(2)} + \frac{1}{16}f_i^{(2)} - \frac{1}{32C_i}B_i^{(1)}A_i^{(2)} - \frac{3}{16}C_i\beta_0\zeta_2\Big), \tag{4.36}$$

where $C_q = C_F$, $C_g = C_A$ and β_0 is leading coefficient of QCD $\beta-$function. Also the quantity K that appears in $\mathbf{I}_f^{(2)}$ is related to $A_i^{(2)}$. We find $\mathbf{H}_i^{(2)} = -\frac{1}{4\epsilon}N^2\zeta_3$ after setting the QCD colour factors to N and taking the LT terms of A_i, B_i, f_i in Eq. (4.36). In $\mathcal{N} = 4$ SYM for both choices of external states f, $\mathbf{H}_f^{(2)} = \sum_{i=\{f\}} \frac{1}{N^2}\mathbf{H}_i^{(2)}$(see Eq. (4.27)). Here, the factor $1/N^2$ that appears in front of $\mathbf{H}_i^{(2)}$ is due to the definition of 't Hooft coupling constant given in Eq. (3.5). The three point FFs of the half-BPS operator presented up to two loop level for $f = g\phi\phi$ and $f = \phi\lambda\lambda$ contain terms with uniform transcendentality of weight four. On the other hand, the FFs of the Konishi operator for both the choices of $f = g\phi\phi, \phi\lambda\lambda$ do not show this behaviour. But interestingly, the LT terms of it for only $f = g\phi\phi$ agree exactly with the result of the half-BPS operator. For the choice $f = \phi\lambda\lambda$, this is not the case as the type of fields in the operator do not coincide with the external states. In summary, up to two loops, we find

$$\mathcal{F}^{\mathcal{K},(2)}_{g\phi\phi}\Big|_{LT} = \mathcal{F}^{\mathrm{BPS},(2)}_{f}\,, \qquad \mathcal{F}^{\mathcal{K},(2)}_{\phi\lambda\lambda}\Big|_{LT} \neq \mathcal{F}^{\mathrm{BPS},(2)}_{f}\,. \tag{4.37}$$

The above relations hold for finite remainders of FFs of the BPS and the Konishi operator up to two loop level.

$$\mathcal{R}^{\mathrm{BPS},(2)}_{g\phi\phi} = \mathcal{R}^{\mathrm{BPS},(2)}_{\phi\lambda\lambda}\,, \qquad \mathcal{R}^{\mathcal{K},(2)}_{g\phi\phi}|_{LT} = \mathcal{R}^{\mathrm{BPS},(2)}_{f}\,, \qquad \mathcal{R}^{\mathcal{K},(2)}_{\phi\lambda\lambda}|_{LT} \neq \mathcal{R}^{\mathrm{BPS},(2)}_{f}\,. \tag{4.38}$$

The reason for the equality between the LT terms of the Konishi and the half-BPS for $f = g\phi\phi$ could possibly be attributed to the fact that fields in the operator and those in the external states coincide. But one requires to do this exercise with more operators to confirm this reasoning.

4.6 Summary

In this paper we have computed the three-point on-shell FFs for the half-BPS and the Konishi operators up to two-loop order in perturbative expansion by employing the Feynman diagrammatic methods. We have regularized all the divergences using the $\overline{DR}$ scheme. We have also repeated the computation by regularising in the FDH scheme and compared against the one computed in the $\overline{DR}$ after properly modifying the FDH scheme for space-time dependent operators. We find complete agreement between the two approaches. The half-BPS operator is protected by supersymmetry and hence it does not get any quantum corrections to any order in the perturbative expansion. On the other hand, the scaling dimension of the Konishi operator receives corrections at each order in perturbation theory. The UV divergence of the form factor with the Konishi operator insertion are removed by introducing an overall renormalization constant, these constants are function of the coupling constant and the anomalous dimension, where the latter has been computed up to five-loop order in perturbation theory. These matrix elements still suffer from divergences coming from the IR sector which are of universal nature as predicted [4,130–132] in the context of QCD. The subtraction operators which encapsulate these predictions in SU(N) gauge theory are given in terms of the colour factors $C_A, C_F, n_f T_f$. In order to get the corresponding subtraction operators in $\mathcal{N} = 4$ SYM theory(see Eq. (4.25)) we have put $\beta = 0$. The two unknown quantities, K and $\mathbf{H}_f^{(2)}(\epsilon)$, appearing in the subtraction operators have been computed by demanding that the subtraction operators cancel all the IR divergences in the three point FFs. We find out that K and $\mathbf{H}_f^{(2)}(\epsilon)$ are the highest transcendental parts of the corresponding expressions in QCD when proper colour assignments are performed. In this context, we want to mention about some observations that we have made in our earlier work [5] discussed in Chapter 3. The Sudakov FF in $\mathcal{N} =$ 4 SYM theory was shown to satisfy the K+G equation, whose solution can be expressed in terms of collinear, soft and cusp anomalous dimensions. We have observed that these quantities are also the highest transcendental parts of the corresponding expressions in QCD, on assigning proper colour factors. Also the coefficient of the single pole at each order in perturbative expansion coincides with the highest transcendental part of $(2B_i + f_i)$. The UV and IR finite three-point FFs, $\mathcal{F}^{\mathcal{K},(2),\text{fin}}$ show some interesting features. For the half-BPS operator the FF results at one and two loop orders in perturbative expansion for both external states contain only highest transcendental terms (two and four respectively), expressed fully in terms of HPLs and ζ_2 (see Eqs. (C.1, C.2)). The coefficients of these HPLs and ζ's are not functions of any kinematical invariants. It is interesting to note that the Sudakov FF results for the above operator was also found not to depend on the nature of the external legs. In contrast to the half-BPS operator, the three point FF result for the Konishi operator contains both highest as well as lower transcendental terms. When computed between $g\phi\phi$ external state the FF result for the Konishi operator has the same highest transcendental contribution as that of the half-BPS operator. But for the same operator with $\phi\lambda\lambda$ external state, there is no resemblance of LT terms with the half-BPS counterpart.

It is well known that the IR divergences of MHV amplitudes have an exponential structure (BDS ansatz). Such a behavior is reminiscent of the factorisation properties of gauge theory amplitudes. However we can also see this kind of exponentiation in FFs. By exponentiating the one loop IR singularities following BDS like exponentiation, we compute the FR functions $\mathcal{R}_f^{\rho,(2)}$ (see Eq. (4.28)). We have presented the FR functions of the three point FFs for both the operators up to second order in perturbative expansion for both choices of f. The authors in [222] have computed three point function of the half-BPS operator between the states $f = g\phi\phi$ using unitarity based techniques and presented their result in compact form using the method of symbols that uses coproducts. Our result on the half-BPS for $f = g\phi\phi$ presented in terms of HPLs numerically agree with theirs presented in terms of classical polylogarithms for the FR function.

The LT terms of the FR function for the Konishi operator computed between $g\phi\phi$ external state coincide with the corresponding one of the half-BPS. However, for the $\phi\lambda\lambda$ external state we find that the expressions for the Konishi and the half-BPS operators do not have anything common. The reason for the agreement for $g\phi\phi$ state could be due to the fact that both the Konishi operator and the external states have two scalar fields in common. To explore this further, we need more data on other unprotected operators.

5 Threshold resummation of the rapidity distribution for Higgs production at NNLO+NNLL

The materials presented in this chapter are the result of an original research done in collaboration with Pulak Banerjee, Goutam Das and V. Ravindran, and these are based on the published article [9].

5.1 Prologue

With the successful running of the LHC at CERN and precise theoretical predictions from various state-of-the-art computations, we can now test the SM of particle physics with unprecedented accuracy and also severely constrain many physics BSM scenarios. The spectacular discovery [1, 2] of a scalar particle and the most precise prediction on its production cross section [234] improved our understanding of the symmetry breaking mechanism, namely, the Higgs mechanism. The copious production of vector bosons Zs and $W^{\pm}$s and lepton pairs at the LHC through Drell-Yan process [235], which are used to precisely measure the PDFs [236–240] are also very important to study.

While inclusive rates are important for any phenomenological study, the differential cross sections often carry more information on the nature of interaction and quantum number of particles produced in the hard collisions. Rapidity distributions of Drell-Yan pair [77], Z boson [78], and charge asymmetries of leptons in $W^{\pm}$ boson decays [79] are already used to measure PDFs. Possible excess events in these distributions can hint at BSM physics, namely, R-parity violating supersymmetric models [80], models with Z' or with contact interactions, and large extra-dimension models [81, 82]. Like in Drell-Yan, measurements of transverse momentum and rapidity distributions of the Higgs boson will be very useful to study the properties of the Higgs boson and its couplings. Theoretical predictions for inclusive production [36, 39, 241–252] as well as the rapidity distribution [253, 254] of di-leptons in Drell-Yan production and the Higgs bosons in gluon-gluon fusion have been known to NNLO in pQCD for long time. A few years back, a complete N^{3}LO prediction [234] for inclusive Higgs production became available after its SV contributions (N^{3}LO$_{SV}$) were computed in Ref. [255], see also Refs. [84, 85, 256–258] for earlier works and Ref. [259, 260] for Higgs productions in other channels at N^{3}LO$_{SV}$ and Ref. [261] for a renormalization group improved prediction to all orders for $gg \to H$. For Drell-Yan, so far, only N^{3}LO in the SV approximation is known [88], see also Ref. [262, 263].

Both inclusive and differential cross sections are often plagued with large logarithms resulting from certain boundaries of the phase space, spoiling the reliability of the fixed-order predictions. In the inclusive case, this happens when partonic scaling variable $z = Q^2/\hat{s} \to 1$, i.e., threshold limit, resulting from the emission of soft gluons in the DY process ($Q^2 = m^2_{l^+l^-}$) and in Higgs production ($Q^2 = M_H^2$), where $m_{l^+l^-}$, M_H, and $\hat{s}$ are the invariant mass of the dileptons, the mass of the Higgs boson, and centre-of-mass energy squared of the partonic subprocess, respectively. One finds a similar problem when the transverse momentum of the final state becomes small. The resolution to this is to resum these large logarithms to all orders in perturbation theory. To achieve this, several approaches exist in the literature for both inclusive rates (see Refs. [92, 93, 264] for the earliest approach) as well as for transverse momentum distributions [265–273]. Catani and Trentadue, in their seminal work [93], demonstrated the resummation of leading large logarithms for the inclusive rates in Mellin space and extended their approach to a differential x_F distribution using double Mellin moments. In the recent past, there have been several approaches to perform threshold resummation for rapidity distribution. In Ref. [274–277], an appropriate Fourier transformation for the rapidity variable resums certain logarithms for the rapidity distribution, and in Ref. [278–280], the authors have used SCET to identify the potential large logarithms that can be resummed (see also Ref. [281] for resumming timelike logarithms using SCET).

In Refs. [84, 85], one of the authors of the present article developed z-space formalism to obtain a soft distribution function that captures the threshold-enhanced part of the inclusive production of any colourless particle, using factorization properties of cross sections and K+G equations that the form factor as well as soft distribution function satisfy. In Ref. [85], it was shown that the N-th Mellin moment of the finite part of the universal soft distribution function was nothing but the threshold exponent á la Sterman [92] and Catani and Trentadue [93, 264]. The same approach was later extended to obtain rapidity distributions of lepton pairs, Higgs boson [282], and Z and $W^{\pm}$ [283] using two scaling variables z_1 and z_2 in the threshold limit up to N^{3}LO level [284, 285].

In this chapter of the thesis, we derive an all order resummed result in two-dimensional Mellin space for rapidity distribution of a colorless final state F that can be produced in hadron colliders and present the numerical impact only for the production of the scalar Higgs boson at the LHC. We work with double Mellin variables N_1 and N_2 corresponding to z_1 and z_2 in z space and demonstrate the resummation of large logarithms proportional to $\ln N_i$ (in z space, these correspond to plus distributions in both the variables z_1 and z_2) in the limit $N_i \to \infty$ ($z_i \to 1$). Our approach, while it follows Ref. [93], differs from Refs. [275,277–280] in the way the threshold limits are defined. In the latter, resummation is done in Mellin-Fourier space spanned by (N, M), which corresponds to the scaling variable z and the partonic rapidity y_p. By taking the limit $N \to \infty$ and keeping M fixed, the resummed result turns out to be identical to the inclusive one.

We begin this chapter by presenting theoretical framework in Sec. 5.2 where we have demonstrated the theory as well as computational procedure to obtain the results we are aiming for. Then in Sec. 5.3 we derived the numerical implications of our result at the LHC before summarising in Sec. 5.4.

5.2 Theoretical framework

The rapidity distribution of the state F can be written as

$$\frac{d\sigma^I}{dy} = \sigma^I_{\rm B} \sum_{ab=q,\bar{q},g} \int_{x_1^0}^1 \frac{dz_1}{z_1} \int_{x_2^0}^1 \frac{dz_2}{z_2} \mathcal{H}^I_{ab}\left(\frac{x_1^0}{z_1}, \frac{x_2^0}{z_2}, \mu_F^2\right) \Delta^I_{d,ab}(z_1, z_2, q^2, \mu_F^2, \mu_R^2) . \quad (5.1)$$

In the above, μ_R is the ultraviolet renormalization scale, the hadron level rapidity $y = \frac{1}{2}\ln(p_2.q/p_1.q) = \frac{1}{2}\ln\left(x_1^0/x_2^0\right)$ and $\tau = q^2/S = x_1^0 x_2^0$, q being the momentum of the final state F, $S = (p_1 + p_2)^2$, where p_i are the momenta of incoming hadrons P_i $(i = 1, 2)$. For the Drell-Yan process $(I = q)$, the state F is a pair of leptons with invariant mass q^2, $\sigma^I = d\sigma^q(\tau, q^2, y)/dq^2$ whereas for the Higgs boson production through gluon (bottom-antibottom) fusion $[I = g(b)]$, $\sigma^I = \sigma^{g(b)}(\tau, q^2, y)$. The function $\mathcal{H}^I_{ab}$ in Eq.(5.1) is given by

$$\mathcal{H}^I_{ab}(x_1, x_2, \mu_F^2) = f_a^{P_1}(x_1, \mu_F^2)\, f_b^{P_2}(x_2, \mu_F^2) , \quad (5.2)$$

where $f_a^{P_1}(x_1, \mu_F^2)$ and $f_b^{P_2}(x_2, \mu_F^2)$ are the PDFs with momentum fractions x_i $(i = 1, 2)$, renormalized at the factorization scale μ_F. The partonic coefficient functions, $\Delta^I_{d,ab}$, depend on the parton-level scaling variables $z_i = \frac{x_i^0}{x_i}, i = 1, 2$.

Using factorization properties of the cross sections and renormalization group invariance, in Ref. [282], the threshold-enhanced contribution to the $\Delta^I_{d,ab}$ denoted by $\Delta^{\rm SV}_{d,I}$ was shown to exponentiate as

$$\Delta^{\rm SV}_{d,I} = C \exp\left(\Psi^I_d(q^2, \mu_R^2, \mu_F^2, \bar{z}_1, \bar{z}_2, \epsilon)\right)\Big|_{\epsilon=0} , \quad (5.3)$$

where the exponent Ψ^I_d is both UV and IR finite to all orders in perturbation theory. It contains finite distributions computed in $4+\epsilon$ space-time dimensions expressed in terms of two shifted scaling variables $\bar{z}_1 = 1 - z_1$ and $\bar{z}_2 = 1 - z_2$,

$$\Psi^I_d = \left[\ln\left(Z^I(\hat{a}_s, \mu_R^2, \mu^2, \epsilon)\right)^2 + \ln\left|\hat{F}^I(\hat{a}_s, Q^2, \mu^2, \epsilon)\right|^2\right]\delta(\bar{z}_1)\delta(\bar{z}_2)$$
$$- \mathcal{C}\Big(\ln \Gamma_{II}(\hat{a}_s, \mu^2, \mu_F^2, \bar{z}_1, \epsilon)\,\delta(\bar{z}_2) + (\bar{z}_1 \leftrightarrow \bar{z}_2)\Big) + 2\,\Phi^I_d(\hat{a}_s, q^2, \mu^2, \bar{z}_1, \bar{z}_2, \epsilon), \tag{5.4}$$

where $Q^2 = -q^2$ and the scale μ is introduced to define the dimensionless strong coupling constant $\hat{a}_s = \hat{g}_s^2/16\pi^2$ in dimensional regularization, which is related to the renormalized one, a_s through the renormalization constant $Z(a_s(\mu_R^2))$. The definition of double Mellin convolution $\mathcal{C}$ is given in Ref. [282]. The overall operator renormalization constant Z^I renormalizes the bare form factor $\hat{F}^I$; the corresponding anomalous dimension is denoted by γ_I and the diagonal mass factorization kernels Γ_{II} remove the collinear singularities. We have factored out $\hat{F}^I$ and Γ_{II} in $\Delta^{\mathrm{SV}}_{d,I}$ in such a way that the remaining soft distribution function, Φ^I_d, contains only soft gluon contributions. Both $\hat{F}^I$ and Φ^I_d satisfy Sudakov-type differential equations (suppressing the arguments $\hat{a}_s, \mu^2, \bar{z}_1, \bar{z}_2$ for brevity),

$$\chi^2 \frac{d}{d\chi^2}\Pi^I_d = \frac{1}{2}\left[K^I_{d,\Pi}\left(\mu_R^2, \epsilon\right) + G^I_{d,\Pi}\left(\chi^2, \mu_R^2, \epsilon\right)\right], \tag{5.5}$$

where $\chi^2 = Q^2$ for $\Pi^I_d = \ln \hat{F}^I$ and $\chi^2 = q^2$ for $\Pi^I_d = \Phi^I_d$. The constants $K^I_{d,\Pi}(\mu_R^2, \epsilon)$ contain singular terms in ϵ and the $G^I_{d,\Pi}(\chi^2, \mu_R^2, \epsilon)$ are finite in ϵ. It is straightforward to solve the above differential equations in powers of a_s and they can be found in Refs. [84, 85, 282, 284]. Substituting these solutions in Eq. (5.4) and setting $\mu_R^2 = \mu_F^2$, we find

$$\Psi^I_d = \delta(\bar{z}_2)\left(\frac{1}{\bar{z}_1}\left\{\int_{\mu_F^2}^{q^2\,\bar{z}_1}\frac{d\lambda^2}{\lambda^2}\,A_I\left(a_s(\lambda^2)\right) + D^I_d\left(a_s(q^2\,\bar{z}_1)\right)\right\}\right)_+ + \frac{1}{2}\left(\frac{1}{\bar{z}_1\bar{z}_2}\left\{A^I(a_s(z_{12}))\right.\right.$$
$$\left.\left. + \frac{dD^I_d(a_s(z_{12}))}{d\ln z_{12}}\right\}\right)_+ + \frac{1}{2}\delta(\bar{z}_1)\delta(\bar{z}_2)\ln\left(g^I_{d,0}(a_s(\mu_F^2))\right) + \bar{z}_1 \leftrightarrow \bar{z}_2, \tag{5.6}$$

where the subscript $+$ indicates the standard plus distribution, A^I are cusp anomalous dimensions and the constants $z_{12} = q^2\bar{z}_1\bar{z}_2$. The finite function D_d^I is defined through $G_{d,\Phi}^I\left(q^2, z_i, \epsilon\right)$ in the limit $\epsilon \to 0$ expanded in a_s as

$$D_d^I(a_s(q^2 z_i)) = \sum_{j=1}^{\infty} a_s^j\left(q^2 z_i\right) G_{d,\Phi}^{I,(j)}\left(q^2, z_i, \epsilon\right)\Big|_{\epsilon=0} = \sum_{j=1}^{\infty} a_s^j\left(q^2 z_i\right)\left(C_{d,j}^I - f_j^I + \sum_{k=1}^{\infty} \epsilon^k \overline{\mathcal{G}}_{d,j}^{I,k}\right)\Big|_{\epsilon=0}$$

The constants $C_{d,j}^I$ can be expressed in terms of lower order $\overline{\mathcal{G}}_{d,j}^{I,k}$ (see Eq. (32) of Ref. [282]), and the soft anomalous dimensions f_j^I are known up to three loops (see Refs. [145, 286]). The constants $\overline{\mathcal{G}}_{d,j}^{I,k}$ and hence D_d^I in Eq. (5.7) can be determined using

$$\int_0^1 dx_1^0 \int_0^1 dx_2^0 \left(x_1^0 x_2^0\right)^{N-1} \frac{d\sigma^I}{dy} = \int_0^1 d\tau\, \tau^{N-1}\, \sigma^I\,, \tag{5.7}$$

where the σ^I is the inclusive cross section. Since we are interested in the threshold limit, we consider the limit $N \to \infty$ on both sides and use the well-known threshold resummed inclusive cross section, $\sigma^{I,\text{res}}$, in N space to obtain the unknown constants $\overline{\mathcal{G}}_{d,i}^{I,k}$ and hence the unknown D_d^I. Alternatively, we can use the z-space approach to determine these constants in terms of the corresponding ones from the inclusive cross section as they are independent of scaling variables z_i and z. Hence, using the z-space formalism for the inclusive cross section described in Refs. [84, 85] and for rapidity distribution in Ref. [282], we can express $\overline{\mathcal{G}}_{d,i}^{I,k}$ in terms $\overline{\mathcal{G}}_{i}^{I,k}$. Substituting these constants in Eq. (5.7), expanding D_d^I in powers a_s as $D_d^I = \sum_{j=1}^{\infty} a_s^j D_{d,j}^I$ and comparing against D^I from the inclusive cross section, we obtain

$$\begin{aligned}
D_{d,1}^I &= D_1^I,\\
D_{d,2}^I &= D_2^I - \zeta_2\beta_0 A_1^I,\\
D_{d,3}^I &= D_3^I - \zeta_2\left(\beta_1 A_1^I + 2\beta_0 A_2^I + 2\beta_0^2 f_1^I\right) - 4\zeta_3\beta_0^2 A_1^I.
\end{aligned} \tag{5.8}$$

From the above equations it is clear that $D_{d,j}^g = D_{d,j}^q C_A/C_F, j = 1, 2, 3$, i.e., maximally non-Abelian. Following Ref. [287] and defining $\omega = a_s\beta_0 \ln(\overline{N}_1\overline{N}_2)$ where $\overline{N}_i = e^{\gamma_E} N_i, i =$

1, 2, we find

$$\tilde{\Delta}^{\rm SV}_{d,I}(\omega) = \int_0^1 dz_1 z_1^{N_1-1} \int_0^1 dz_2 z_2^{N_2-1} \Delta^{\rm SV}_{d,I} = g^I_{d,0}(a_s) \exp\Big(g^I_d(a_s,\omega)\Big), \tag{5.9}$$

where $\gamma_E = 0.57721566\cdots$ is the Euler-Mascheroni constant. The exponent $g^I_d(a_s,\omega)$ takes the canonical form:

$$g^I_d(a_s,\omega) = g^I_{d,1}(\omega)\ln(\overline{N}_1\overline{N}_2) + \sum_{i=0}^{\infty} a_s^i g^I_{d,i+2}(\omega)\,. \tag{5.10}$$

Rescaling the constants by β_0 as $\overline{g}^I_{d,1} = g^I_{d,1}$, $\overline{g}^I_{d,i+2} = g^I_{d,i+2}/\beta_0^i$, $\overline{A}^I_i = A^I_i/\beta_0^i$, $\overline{D}^I_{d,i} = D^I_{d,i}/\beta_0^i$ and $\overline{\beta}_i = \beta_i/\beta_0^{i+1}$, we find

$$\begin{aligned}
\overline{g}^I_{d,1} &= \overline{A}^I_1\frac{1}{\omega}\left[\omega + (1-\omega)\ln(1-\omega)\right],\\
\overline{g}^I_{d,2} &= \omega\left[\overline{A}^I_1\overline{\beta}_1 - \overline{A}^I_2\right] + \ln(1-\omega)\left[\overline{A}^I_1\overline{\beta}_1 + \overline{D}^I_{d,1} - \overline{A}^I_2\right] + \frac{1}{2}\ln^2(1-\omega)\overline{A}^I_1\overline{\beta}_1\\
&\quad + L_{qr}\ln(1-\omega)\overline{A}^I_1 + L_{fr}\omega\overline{A}^I_1,\\
\overline{g}^I_{d,3} &= -\frac{\omega}{2}\overline{A}^I_3 - \frac{\omega}{2(1-\omega)}\Bigg[-\overline{A}^I_3 + (2+\omega)\overline{\beta}_1\overline{A}^I_2 + \left[(\omega-2)\overline{\beta}_2 - \omega\overline{\beta}_1^2 - 2\zeta_2\right]\overline{A}^I_1 + 2\overline{D}^I_{d,2}\\
&\quad - 2\overline{\beta}_1\overline{D}^I_{d,1}\Bigg] - \ln(1-\omega)\left[\frac{\overline{\beta}_1}{(1-\omega)}\Big(\overline{A}^I_2 - \overline{D}^I_{d,1} - \overline{A}^I_1\overline{\beta}_1\omega\Big) - \overline{A}^I_1\overline{\beta}_2\right] + \frac{\ln^2(1-\omega)}{2(1-\omega)}\overline{A}^I_1\overline{\beta}_1^2\\
&\quad + L_{fr}\overline{A}^I_2\omega - \frac{1}{2}L_{fr}^2\overline{A}^I_1\omega - L_{qr}\frac{1}{(1-\omega)}\left[\Big(\overline{A}^I_2 - \overline{D}^I_{d,1}\Big)\omega - \overline{A}^I_1\overline{\beta}_1\left(\omega + \ln(1-\omega)\right)\right]\\
&\quad + \frac{1}{2}L_{qr}^2\frac{\omega}{(1-\omega)}\overline{A}^I_1,\\
\overline{g}^I_{d,4} &= -\frac{\omega}{3}\overline{A}^I_4 + \frac{1}{6}\frac{\omega(2-\omega)}{(1-\omega)^2}\left[\overline{A}^I_4 - 3\overline{D}^I_{d,3} + 6\zeta_2(\overline{A}^I_2 - \overline{D}^I_{d,1}) + 4\overline{A}^I_1\zeta_3\right]\\
&\quad + \frac{1}{12}\frac{1}{(1-\omega)^2}\Bigg[\omega\Big(4\omega^2 - 3(\omega+2)\Big)\overline{A}^I_3\overline{\beta}_1 + \omega\Big(4\omega^2(\overline{\beta}_2 - \overline{\beta}_1^2) + 3(2-\omega)\overline{\beta}_1^2\Big)\overline{A}^I_2\\
&\quad + \omega\Big(4\omega^2(\overline{\beta}_1^3 - 2\overline{\beta}_1\overline{\beta}_2 + \overline{\beta}_3) - 3(2-3\omega)(\overline{\beta}_1\overline{\beta}_2 - \overline{\beta}_3)\Big)\overline{A}^I_1 + 6\omega(2-\omega)\overline{\beta}_1\overline{D}^I_{d,2}\\
&\quad + 6\omega^2(\overline{\beta}_1^2 - \overline{\beta}_2)\overline{D}^I_{d,1}\Bigg] + \frac{1}{6}\frac{1}{(1-\omega)^2}\Bigg[-\ln^3(1-\omega)\overline{A}^I_1\overline{\beta}_1^3 + 3\ln^2(1-\omega)\overline{\beta}_1^2(\overline{A}^I_2 - \overline{D}^I_{d,1})\\
&\quad + 3\ln(1-\omega)\Big[\overline{\beta}_1\left[\overline{A}^I_2\overline{\beta}_1 - \overline{A}^I_3\right] + \left[(1-\omega)^2\overline{\beta}_3 + \omega^2\overline{\beta}_1\Big(\overline{\beta}_1^2 - 2\overline{\beta}_2\Big) - \overline{\beta}_1\Big(\overline{\beta}_2(1-2\omega)\right.
\end{aligned}$$

$$
\begin{aligned}
&+2\zeta_2\Big)\Big]\overline{A}^I_1 + 2\overline{\beta}_1\overline{D}^I_{d,2}\Big]\Big] + L_{fr}\omega\overline{A}^I_3 - L^2_{fr}\frac{\omega}{2}\Big(2\overline{A}^I_2 + \overline{A}^I_1\overline{\beta}_1\Big) + L^3_{fr}\frac{\omega}{3}\overline{A}^I_1 \\
&+L_{qr}\frac{1}{2(1-\omega)^2}\Big[- \ln^2(1-\omega)\overline{A}^I_1\overline{\beta}^2_1 + 2\ln(1-\omega)\overline{\beta}_1(\overline{A}^I_2 - \overline{D}^I_{d,1}) \\
&+\omega(2-\omega)\left[-\overline{A}^I_3 + 2\overline{D}^I_{d,2} + \overline{A}^I_2\overline{\beta}_1 - 2\overline{A}^I_1\zeta_2\right] + \omega^2\overline{A}^I_1\left(\overline{\beta}^2_1 - \overline{\beta}_2\right)\Big] \\
&-L^2_{qr}\frac{1}{2(1-\omega)^2}\left[\overline{A}^I_1\overline{\beta}_1\ln(1-\omega) - \omega(2-\omega)\left[\overline{A}^I_2 - \overline{D}^I_{d,1}\right]\right] \\
&-L^3_{qr}\frac{1}{6}\frac{(2-\omega)\omega}{(1-\omega)^2}\overline{A}^I_1.
\end{aligned}
\tag{5.11}
$$

where $L_{fr} = \ln(\mu_F^2/\mu_R^2), L_{qr} = \ln(q^2/\mu_R^2)$. Expanding $\ln(g^I_{d,0})$ as $\ln(g^I_{d,0}) = \sum_{i=1}^{\infty} a_s^i l^{I,(i)}_{g_0}$, we find

$$
\begin{aligned}
l^{I,(1)}_{g_0} &= 2G^{I,1}_1 + 2\overline{\mathcal{G}}^{I,1}_{d,1} + 4A^I_1\zeta_2 - 2L_{fr}B^I_1 + 2L_{qr}\left(B^I_1 - \gamma^I_0\right), \\
l^{I,(2)}_{g_0} &= G^{I,1}_2 + \overline{\mathcal{G}}^{I,1}_{d,2} + 2\beta_0\left(G^{I,2}_1 + \overline{\mathcal{G}}^{I,2}_{d,1}\right) + 2\zeta_2\left(2A^I_2 + \beta_0\left(3B^I_1 + 2f^I_1 - 3\gamma^I_0\right)\right) + \frac{2}{3}A^I_1\beta_0\zeta_3 \\
&\quad -2L_{fr}B^I_2 + L^2_{fr}B^I_1\beta_0 + L_{qr}\Big(2B^I_2 - 2\gamma^I_1 - \beta_0\Big(2G^{I,1}_1 + 2\overline{\mathcal{G}}^{I,1}_{d,1} + 4A^I_1\zeta_2\Big)\Big) \\
&\quad +L^2_{qr}\beta_0\Big(- B^I_1 + \gamma^I_0\Big), \\
l^{I,(3)}_{g_0} &= \frac{1}{3}\Big[2G^{I,1}_3 + 2\overline{\mathcal{G}}^{I,1}_{d,3} + 12A^I_3\zeta_2 + \beta_1\Big[4G^{I,2}_1 + 4\overline{\mathcal{G}}^{I,2}_{d,1} + [18B^I_1 + 12f^I_1 - 18\gamma^I_0]\zeta_2 + 2A^I_1\zeta_3\Big] \\
&\quad +4\beta_0[A^I_2 + \beta_0 f^I_1]\zeta_3 + 2\beta_0\Big[2G^{I,2}_2 + 2\overline{\mathcal{G}}^{I,2}_{d,2} + \left(18B^I_2 + 12f^I_2 - 18\gamma^I_1\right)\zeta_2\Big] + \beta^2_0\Big\{8G^{I,3}_1 \\
&\quad +8\overline{\mathcal{G}}^{I,3}_{d,1} - 3\zeta_2\Big(12G^{I,1}_1 - 4\overline{\mathcal{G}}^{I,1}_{d,1} + \frac{8}{5}A^I_1\zeta_2\Big)\Big\}\Big] - 2L_{fr}B^I_3 + L^2_{fr}\left(2B^I_2\beta_0 + B^I_1\beta_1\right) \\
&\quad -\frac{2}{3}L^3_{fr}B^I_1\beta^2_0 + L_{qr}\Big[2B^I_3 - \beta_1[2G^{I,1}_1 + 2\overline{\mathcal{G}}^{I,1}_{d,1} + 4A^I_1\zeta_2] - 2\Big\{\gamma^I_2 + \beta_0\Big(G^{I,1}_2 + \overline{\mathcal{G}}^{I,1}_{d,2} \\
&\quad +4A^I_2\zeta_2\Big) + \beta^2_0\Big[2G^{I,2}_1 + 2\overline{\mathcal{G}}^{I,2}_{d,1} + \left(6B^I_1 + 4f^I_1 - 6\gamma^I_0\right)\zeta_2 + \frac{2}{3}A^I_1\zeta_3\Big]\Big\}\Big] \\
&\quad +L^2_{qr}\left(2\beta_0\left(\gamma^I_1 - B^I_2\right) + \beta_1\left(\gamma^I_0 - B^I_1\right) + 2\beta^2_0\left(G^{I,1}_1 + \overline{\mathcal{G}}^{I,1}_{d,1}\right) + 4A^I_1\beta^2_0\zeta_2\right) \\
&\quad +\frac{2}{3}L^3_{qr}\beta^2_0\left(B^I_1 - \gamma^I_0\right).
\end{aligned}
\tag{5.12}
$$

In the above equation, $G^{I,k}_j$s are obtained from the ϵ-dependent part of $G^I_{d,F}$. The all-order resummed result given in Eq. (5.9) is the main result of this work. Exponentiation of the functions $g^I_{d,i}$ resums the terms $a_s\beta_0\ln(\overline{N}_1\overline{N}_2)$ systematically to all orders in perturbation theory analogous to the inclusive one (see Ref. [287]). The resummed result can be used to study the rapidity distribution of any colorless particle F produced in hadron-hadron collision. In this thesis, we restrict ourselves to the production of a scalar Higgs boson at the LHC and present the numerical impact of the resummed result over the fixed-order result known to NNLO level [102]. This is obtained using

$$\frac{d\sigma^{g,\text{res}}}{dy} = \frac{d\sigma^{g,\text{f.o}}}{dy} + \sigma_B^g \int_{c_1-i\infty}^{c_1+i\infty} \frac{dN_1}{2\pi i} \int_{c_2-i\infty}^{c_2+i\infty} \frac{dN_2}{2\pi i} e^{y(N_2'-N_1')} \left(\sqrt{\tau}\right)^{-2-N_1'-N_2'} \tilde{f}_g(N_1')\tilde{f}_g(N_2') \\ \times \left[\tilde{\Delta}_{d,g}^{\text{SV},N_1',N_2'} - \left(\tilde{\Delta}_{d,g}^{\text{SV},N_1',N_2'}\right)_{\text{trunc}}\right] \tag{5.13}$$

where $N_i' = N_i + 1, i = 1, 2$. In the above equation, the superscript "f.o" refers to the fixed-order result in a_s and "res" refers to the resummed result. The subscript "trunc" refers to the result obtained from Eq. (5.9) by truncating at desired accuracy in a_s. The constants $g_{d,0}^g$ and $g_{d,i}^g$ that appear in $\tilde{\Delta}_{d,g}^{\text{SV}}$ are functions of cusp (A_i^g), collinear (B_i^g), soft (f_i^g), UV (γ_i^g) anomalous dimensions and universal soft terms $\overline{\mathcal{G}}_{d,j}^{g,i}$, and process-dependent constants $G_j^{g,i}$ of virtual corrections, and they are known to NNLL accuracy. We performed double Mellin inversions to obtain the final result in terms of τ and y and used minimal prescription advocated in Ref. [288]. For the resummed result to N^{m}LO+ N^{n}LL we need f.o to N^{m}LO accuracy and $\tilde{\Delta}_{d,g}^{\text{SV}}$ to N^{n}LL accuracy. For the latter, we need $g_{d,0}^g$ up to order a_s^n, and for the exponent, we need all the terms up to $g_{d,n+1}^g$.

5.3 Phenomenology

In the following we study the numerical impact of resummed contributions up to NNLL accuracy for the rapidity distribution of a scalar Higgs boson of mass $M_H = 125$ GeV at the LHC with $\sqrt{S} = 13$ TeV. We have set the number of flavors $n_f = 5$ and the top mass at 173 GeV and use MMHT 2014 [237] PDFs along with the corresponding values of a_s for LO, NLO, and NNLO through the LHAPDF [289] interface, unless otherwise stated. We use the publicly available code FEHIP [102] to obtain $d\sigma^{g,\text{f.o}}/dy$ up to NNLO level.

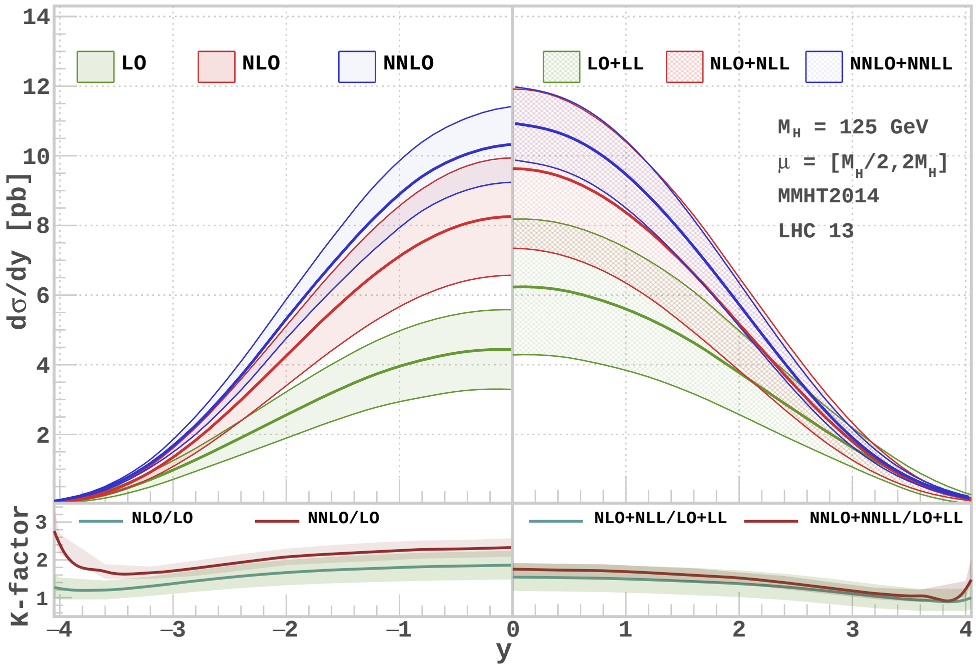

Figure 5.1: Higgs rapidity distributions for fixed-order (left panel) and resummed contributions (right panel) are presented with corresponding K factors on lower panels around the central scale $\mu_R = \mu_F = M_H$.

We have developed an in-house Fortran code to perform double Mellin inversion for the resummed contributions computed in this thesis. In Fig. 5.1, using Eq. (5.13), we present the production cross section for the scalar Higgs boson as a function of its rapidity y up to NNLO in the left panel and to NNLO+NNLL in the right panel along with the respective K factors. The K factor at a given order, say, at N^{n}LO (N^{n}LO + N^{n}LL), is defined by the cross section at that order normalized by the same at LO (LO+LL) at $\mu_R = \mu_F = M_H$. The symmetric band at each order is generated by varying μ_R and μ_F between $[M_H/2, 2M_H]$ around the central scale $\mu_R = \mu_F = M_H$ with the constraint $1/2 \leq \mu_R/\mu_F \leq 2$, adding and subtracting the highest possible errors from all the scale combinations to the central scale. We find that the magnitude and sign of the resummed contribution do vary depending on the order in a_s as well the exact values of y and the scales μ_R, μ_F.

In particular, at the central scale $\mu = \mu_R = \mu_F = M_H$, the percentage correction from the leading-logarithmic (LL) contribution goes from 40% to 50% whereas for next-to-leading-logarithmic (NLL), we find that it varies from 17% to 24% and for NNLL it varies from 6% to 10% in the region $0 \leq y \leq 2.4$, which is evident from Table 5.1.

y	LO	LO+LL	NLO	NLO+NLL	NNLO	NNLO+NNLL	NNLO+NNNLL
0.0	4.435± 1.145	6.231± 1.950	8.255± 1.684	9.632 ± 2.286	10.329± 1.088	10.938 ± 1.050	10.517 ± 0.820
0.8	4.134± 1.067	5.833± 1.831	7.517± 1.530	8.820 ± 2.124	9.407 ± 0.988	9.992 ± 1.025	9.641 ± 0.718
1.6	3.189± 0.819	4.630± 1.468	5.522± 1.117	6.611 ± 1.676	6.877 ± 0.744	7.380 ± 0.849	7.045 ± 0.563
2.4	1.904± 0.492	2.887± 0.942	2.985± 0.597	3.715 ± .998	3.683 ± 0.410	4.040 ± 0.501	3.821 ± 0.305

Table 5.1: Fixed-order and resummed results for Higgs rapidity distribution with corresponding absolute error for different benchmark values of y.

Interestingly, at $\mu = M_H/2$, we find that the cross section at NNLO+NNLL is very close to NNLO for a wider range of y indicating that $\mu = M_H/2$ is a good choice for the fixed-order predictions. A similar conclusion was arrived at in Ref. [253] for the inclusive production of the Higgs boson. From the upper-left panel of Fig. 5.1, we also observe that LO and NLO predictions do not overlap around the central rapidity region. However, at NNLO, partial overlap indicates that the inclusion of higher-order corrections has increased the convergence of perturbation series. The upper-right panel shows the effect of resummation over the fixed order result. We observe that LO+LL has overlap with NLO+NLL for all values of rapidity. In addition, the distribution at NNLO+NNLL falls completely within NLO+NLL band. In fact, NNLO+NNLL increases approximately by 13% with respect to NLO+NLL; the corresponding number for NNLO over NLO is approximately 25%. This implies that the perturbative convergence at the resummed level is better compared to the fixed order result. We have also chosen $M_H/2$ as the central scale and found out that the choice of central scale has a minimum effect on the resummed result at NNLO+NNLL; i.e., the resum result at this order stabilizes irrespective of the above-mentioned choices, whereas at fixed order, this does not happen. Based on the above observations, we can predict that the N^{3}LO will be very close to NNLO+NNLL and the N^{3}LO + N^{3}LL result will lie within the NNLO+NNLL uncertainty band. In the Table 5.1, the impact of N^{3}LL on the NNLO result is also presented.

To understand the impact of unphysical scales μ_R and μ_F on our resummed results, we first varied one while fixing the other to M_H and then varied both simultaneously for various values of rapidity y, the results are presented in Fig. 5.2. As expected, the running

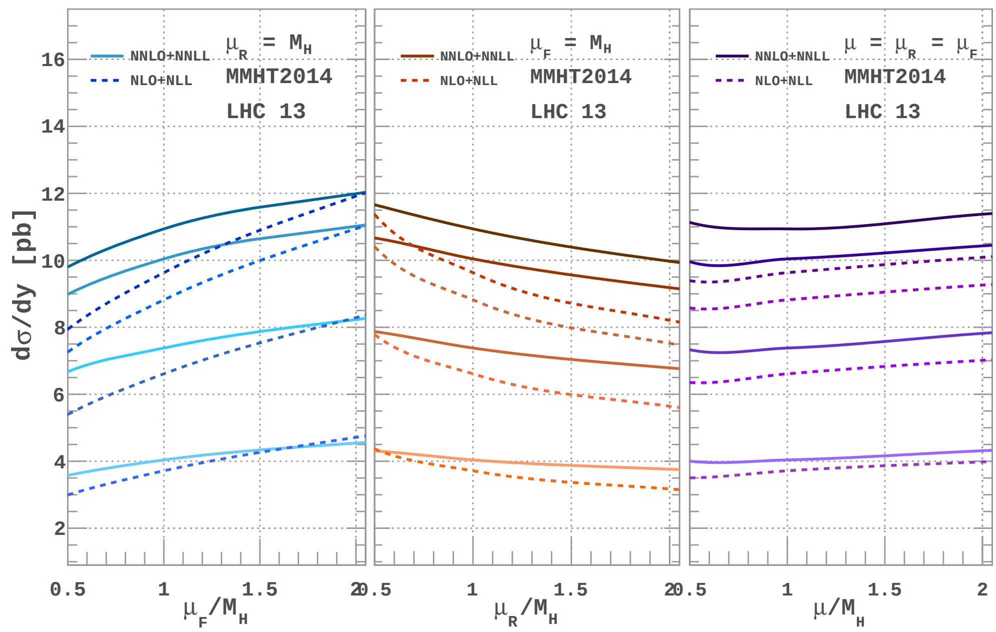

Figure 5.2: μ_F, μ_R scale variations for the NLO+NLL (dashed) and NNLO+NNLL (solid) cases for different benchmark y values (starting from the top, $y = 0, 0.8, 1.6, 2.4$).

coupling constant decreased the cross section as we increased μ_R, while the opposite behaviour was observed for μ_F both in fixed-order and in resummed results. Varying these two scales simultaneously led to a cancellation of the two different behaviors, and the amount of cancellation depended on order of perturbation n and value of y. Finally, to study the impact of choice of PDFs, in Table 5.2, we have presented the results at NNLO+NNLL using the central PDF of each PDF group.

y	MMHT	ABMP	CT10	NNPDF	PDF4LHC
0.0	10.938	10.654	10.709	11.302	10.850
0.8	9.992	9.713	9.820	10.378	9.977
1.6	7.380	7.043	7.362	7.758	7.456
2.4	4.040	3.727	4.105	4.111	4.075

Table 5.2: Using different PDFs, NNLO+NNLL contributions to rapidity distribution for $y = 0, 0.8, 1.6, 2.4$.

5.4 Summary

In this chapter, we have developed a formalism to resum threshold logarithms in double Mellin space for the rapidity distribution of a colorless final state F produced in the hadron collider. We have derived for the first time compact and most general expressions for resummed exponents g_d^I up to NNLO+NNLL accuracy. We find that the resummed result not only changes the fixed order predictions but also remarkably improves the perturbative convergence. We observe that the resummed result at NNLO+NNLL stabilizes over fixed order irrespective of the choices of the central scale between $[M_H/2, 2M_H]$. We have also studied the impact of PDFs on the predictions. The present study can easily be extended to Drell-Yan [290], pseudo-scalar, and $W^\pm$ and Z productions as well as the production of the Higgs boson in $b\bar{b}$ annihilation at hadron colliders.

6 Conclusion

No doubt, the whole particle physics community is standing on the verge of a crucial era, where the main task is to confirm the SM to an unprecedented level of accuracy and then search for the physics beyond SM, if any, through deviations. To set bounds on the parameters of the BSM, unambiguous predictions taking into account QCD radiative corrections has become indispensable. In this context, we have systematically computed higher order QCD corrections to few important field theory quantities in BSM and performed threshold resummation to one of the very important observables called rapidity distribution associated with the SM Higgs boson production.

In Chapter 2 we have computed two-loop virtual corrections to the decay of a pseudo-scalar to three gluons or quark, anti-quark and gluon. The motivation to perform this calculation is of two fold. Firstly, with larger data set that are available at the LHC, constraining BSM scalar sector has become feasible and hence precise theoretical predictions for the production of a pseudo-scalar and its subsequent decays to jets needs to be achieved. Secondly such a computation of NNLO level for the differential rates is technically challenging not only because of the involvement of a large number of Feynman diagrams but also due to the presence of the axial vector coupling. We work in dimensional regularisation and use the 't Hooft-Veltman prescription for the axial vector current. The state-of-the-art techniques including IBP and LI identities have been employed to accomplish this task. The UV renormalisation is quite involved since the two operators, present in the effective Lagrangian, mix under renormalisation due to the axial anomaly.

Moreover, a finite renormalisation constant needs to be introduced in order to fulfil the chiral Ward identities. We confirm the correctness of our results up to finite terms using Catani's factorisation formula which predict all the poles resulting from soft and collinear configurations up to two loops. It is well known in the context of scalar Higgs boson that the leading transcendental terms of finite part of $H \to ggg$ amplitude up to two loop level are related to the corresponding ones for the three particle amplitude with an insertion of the half-BPS operator. This insertion is valid provided that the colour factors in QCD are adjusted in a specific way. We find that this is indeed the case for $A \to ggg$, $q\bar{q}g$ amplitudes presented in this thesis. Finally, with appropriate analytical continuation, our results for $A \to ggg$ and $A \to q\bar{q}g$ up to two loop level in QCD can be readily used for the study of production of a pseudo-scalar in association with a jet up to same level of accuracy at the hadron colliders.

In Chapter 3, we have presented for the first time the complete third order and partial fourth order corrections to the on-shell form factor of the Konishi operator employing state-of-the-art techniques. We have also demonstrated the superiority of the Feynman diagrammatic approach over unitarity method in the context of space-time dimension dependent composite operator such as the Konishi operator. One of the main issues in computing the higher order corrections in $\mathcal{N} = 4$ SYM theory is related to the necessity of preserving the supersymmetry throughout the computation. In order to achieve that, one generally follows either of the two regularization schemes: $\overline{DR}$ and FDH. By performing the computation explicitly in both the schemes, we have shown that the form factor in $\overline{DR}$ automatically provides the correct results, whereas, the results obtained in the FDH needs to be suitably modified. In addition, the modification in FDH is operator dependent and non-trivial. Hence, performing a computation in $\overline{DR}$ is much more preferable for unprotected operators like Konishi. We have clearly demonstrated that in our approach it is much more elegant as well as easier to execute the calculation in $\overline{DR}$ scheme. Hence, as a consequence of our work, the standard Feynman diagrammatic approach is very elegant and advantageous over unitarity method in the context of $\mathcal{N} = 4$ SYM theory, if employed in a systematic way. In the end, the principle of leading transcendentality in the context of non-BPS operator at three loops level is studied for the first time. This has the potential to unravel the underlying deeper connections between the amplitudes in $\mathcal{N} = 4$ SYM theory and QCD.

Next, in Chapter 4 we have computed the three point on-shell form factors for the half-BPS and the Konishi operators for two sets of final states, consisting of $g\phi\phi$ and $\phi\lambda\lambda$, up to two-loop order in pQCD following Feynman diagrammatic methods. We have regularised all the divergences using the $\overline{DR}$ scheme. We have also repeated the computation by regularising in the FDH scheme and compared against the one computed in the $\overline{DR}$ after properly modifying the results in FDH scheme for space-time dimension dependent operators. We found complete agreement between the two approaches. The UV and IR finite three point FFs, $\mathcal{F}^{\mathcal{K},(2),\mathrm{fin}}$ show some interesting features. For the half-BPS operator the FF results at one and two loop orders in perturbative expansion for both external states contain only highest transcendental terms (two and four respectively), expressed fully in terms of HPLs and ζ. The coefficients of these HPLs and ζ's are not functions of any kinematical invariants. In contrast to the half-BPS operator, the three point FF result for the Konishi operator contains both highest as well as lower transcendental terms. When computed between $g\phi\phi$ external state the FF result for the Konishi operator has the same highest transcendental contribution as that of the half-BPS operator. But for the same operator with $\phi\lambda\lambda$ external state, there is no resemblance of highest transcendental terms with the BPS counterpart.

It is well known that the IR divergences of MHV amplitudes have an exponential structure (BDS ansatz). Such a behaviour is reminiscent of the factorisation properties of gauge theory amplitudes. By exponentiating the one loop IR singularities following BDS like exponentiation, we compute the finite remainder functions $\mathcal{R}_f^{\rho,(2)}$. We have presented the finite remainder functions of the three point FFs for both the operators up to second order in perturbative expansion for both choices of f. The leading transcendental terms of the remainder function for the Konishi operator computed between $g\phi\phi$ external state coincide with the corresponding one of the half-BPS. However, for the $\phi\lambda\lambda$ external state we find that the expressions for the Konishi and the half-BPS operators do not have anything common. The reason for the agreement for $g\phi\phi$ state could be due to the fact that both the Konishi operator and the external states have two scalar fields in common. To explore this further, we need more results on other unprotected operators.

Finally in Chapter 5 we have developed a formalism to resum threshold logarithms in double Mellin space for the rapidity distribution of the SM Higgs boson produced in the hadron collider. We achieve this by exploiting the factorisation properties and K+G equations satisfied by the soft and virtual parts of the cross section. We have derived for the first time compact and most general expressions for resummed exponents g_d^I up to NNLO+NNLL accuracy. We find that the resummed result not only changes the fixed-order predictions but also remarkably improves the perturbative convergence. We observe that the resummed result at NNLO+NNLL stabilizes over fixed order irrespective of the choices of the central scale between $[M_H/2, 2M_H]$. Coincidentally, we found that our results on the rapidity distribution of the Higgs boson is the most accurate till date and it is expected to play an important role in coming days at the LHC.

In conclusion, the state-of-the-art techniques, which mostly use our in-house codes, have been employed extensively to carry out all the computations presented in this thesis. It has been a while the Higgs-like particle has been discovered at the LHC and finally, we are very close to having enough statistics for precision measurements of the Higgs quantum numbers and coupling constants to fermions and gauge bosons. This, along with the precise results from theoreticians like us, hopefully, would help to explore the underlying nature of the electroweak symmetry breaking and possibly open the door of new physics.

A Harmonic Polylogarithms

We briefly describe the definition and properties of HPL and 2dHPL that we have used in our paper. The Harmonic Polylogarithm of weight w and comprising of w-dimensional vector $\vec{m}_w$ of parameters is represented by $H(\vec{m}_w; y)$, where y is the argument of the function. The elements of $\vec{m}_w \in \{-1, 0, 1\}$ through which the following rational functions are expressed

$$f(-1; y) \equiv \frac{1}{1+y}, \qquad f(0; y) \equiv \frac{1}{y}, \qquad f(1; y) \equiv \frac{1}{1-y}. \tag{A.1}$$

These functions are related to $H(\vec{m}_w; y)$ via

$$\frac{d}{dy} H(\vec{m}_w; y) = f(\vec{m}_w; y). \tag{A.2}$$

HPLs of weight 1 ($w = 1$) follow from (A.1) and (A.2)

$$H(-1; y) = \log(1+y), \qquad H(0; y) = \log(y), \qquad H(1; y) = -\log(1-y). \tag{A.3}$$

For $w > 1$ $H(m, \vec{m}_w; y)$ is given by

$$H(m, \vec{m}_w; y) \equiv \int_0^y f(m; x) H(\vec{m}_w; y), \qquad m \in \{-1, 0, 1\} \tag{A.4}$$

Moreover the higher dimensional HPLs are defined following the eq. (A.4) for the new elements 2,3 in $\vec{m}_w$, representing a new class of rational functions

$$f(2;y) \;\equiv\; f(1-z;y) \;\equiv\; \frac{1}{1-y-z}, \qquad f(3;y) \;\equiv\; f(z;y) \;\equiv\; \frac{1}{y+z}; \tag{A.5}$$

correspondingly the weight-1 ($w = 1$) two-dimensional HPLs are given by

$$H(2,y) \;\equiv\; -\ln\Big(1-\frac{y}{1-z}\Big), \qquad H(3,y) \;\equiv\; \ln\Big(\frac{y+z}{z}\Big). \tag{A.6}$$

The Shuffle algebra that the HPLs follow is defined as follows: a product of two HPL with weights w_1 and w_2 of the same argument y is a combination of HPLs with weight $(w_1 + w_2)$ and argument y, such that all possible permutations of the elements of $\vec{m}_{w_1}$ and $\vec{m}_{w_2}$ are considered preserving the relative orders of the elements of $\vec{m}_{w_1}$ and $\vec{m}_{w_2}$, that is

$$H(\vec{m}_{w_1};y)\, H(\vec{m}_{w_2};y) \;=\; \sum_{\vec{m}_w = \vec{m}_{w_1} \uplus \vec{m}_{w_2}} H(\vec{m}_w;y) \tag{A.7}$$

B Pseudo-scalar matrix elements

Here, we present finite part of matrix element $\mathcal{S}_f$ for $f = ggg, q\bar{q}g$, namely $\mathcal{S}_{ggg,fin}$ and $\mathcal{S}_{q\bar{q}g,fin}$, by setting $-Q^2 = \mu_R^2$ and taking out Born color factor $N(N^2-1)$, $\frac{N^2-1}{2}$ for the final state ggg, $q\bar{q}g$ respectively. One loop finite result for $f = ggg$ external state is given by

$$
\begin{aligned}
S_g^{G,(0)} &= -128\,C_{1,g}\,\Big(y^4 + 2y^3(-1+z) + 3y^2(-1+z)^2 + 2y(-1+z)^3 + (1-z+z^2)^2\Big)\,,\\
S_g^{G,(1)} &= N\Bigg[\,256\,C_{1,g}\,\Big\{y^4 + 2y^3(-1+z) + 3y^2(-1+z)^2 + 2y(-1+z)^3 + (1-z+z^2)^2\Big\}\\
&\quad\times\Big\{\zeta_2 + H(0;y)\Big\{H(0;z) - H(1;z) - H(2;y)\Big\} + H(0;z)\Big\{H(1;z) - H(2;y)\Big\}\\
&\quad + 2H(1;z)H(3;y) + 2H(1,0;y) + 2H(3,2;y)\Big\} + \frac{1408}{3}C_{1,g}\Big\{y^4 + 2y^3(-1+z)\\
&\quad + 3y^2(-1+z)^2 - 2y(1-z)^3 + (1-z+z^2)^2\Big\}\Big\{H(0;y) + H(0;z) - H(1;z) - H(2;y)\Big\}\\
&\quad - \frac{128}{3}C_{1,g}\Big\{24 + 24y^4 + 48y^3(-1+z) - 47z + 71z^2 - 48z^3 + 24z^4 + y(-1+z)^2(-47\\
&\quad + 48z) + y^2(71 - 143z + 72z^2)\Big\}\Bigg] + n_f\Bigg[\frac{-256\,C_{1,g}}{3}\Big\{y^4 + 2y^3(-1+z) + 3y^2(-1+z)^2\\
&\quad + 2y(-1+z)^3 + (1-z+z^2)^2\Big\}\Big\{H(0;y) + H(0;z) - H(1;z) - H(2;y)\Big\}\\
&\quad + \frac{128\,C_{1,g}}{3}(-1+y)(-1+z)(y+z)\Bigg],\\
S_g^{GJ,(1)} &= \mathbf{n_f}\Bigg[-64\,C_{1,g}\,\Big\{y^4 + 2y^3(-1+z) + 3y^2(-1+z)^2 + 2y(-1+z)^3 + (1-z+z^2)^2\Big\}\Bigg].
\end{aligned}
\tag{B.1}
$$

At two loops, for $f = ggg$ external state, we decompose $S_g^{G,(2)}$ in terms of the color factors as follows

$$S_g^{G,(2)} = S_g^{(2),N^2} + S_g^{(2),n_f/N} + S_g^{(2),n_fN} + S_g^{(2),n_f^2} \tag{B.2}$$

where each color term is given below

$$\begin{aligned}
S_g^{(2),N^2} = N^2\Bigg[\Bigg\{ & 59\zeta_2^2/10 + 2\zeta_3 H(1;z) + 2\zeta_3 H(2;y) - 16\zeta_2 H(1;z)H(2;y) \\
& + 16H(1;z)H(2;y)H(0,0;y) - 8H(1;z)H(3;y)H(0,0;y) + 8H(0,0;y)H(0,0;z) \\
& + 16\zeta_2 H(0,1;y) - 4H(0,0;z)H(0,1;z) + 16\zeta_2 H(1,0;y) \\
& + 8H(1;z)H(3;y)H(1,0;y) + 8H(2;y)H(3;y)H(1,0;y) - 8H(0,0;y)H(1,0;y) \\
& - 16H(2;y)H(3;y)H(1,0;z) + 16\zeta_2 H(1,1;y) + 8H(0,0;y)H(1,1;z) \\
& - 8H(0,0;z)H(1,1;z) - 4H(0,0;y)H(2,0;y) - 16\zeta_2 H(2,2;y) \\
& + 8H(0,0;y)H(2,2;y) + 8H(0,0;z)H(2,2;y) - 16H(1,0;z)H(2,2;y) \\
& + 24H(1;z)H(3;y)H(2,3;y) - 8H(1,0;y)H(2,3;y) + 24H(2;y)H(3;y)H(3,2;y) \\
& - 16H(0,0;y)H(3,2;y) - 16H(1,0;z)H(3,3;y) + 32H(1,1;z)H(3,3;y) \\
& + 12H(2;y)H(0,0,0;y) + 4H(1;z)H(0,0,1;z) + 16H(2;y)H(0,0,1;z) \\
& + 16H(3;y)H(0,0,1;z) - 8H(1;z)H(0,0,2;y) - 24H(1;y)H(0,1,0;y) \\
& - 8H(2;y)H(0,1,0;y) + 16H(2;y)H(0,1,1;z) + 16H(3;y)H(0,1,1;z) \\
& - 48H(1;y)H(1,0,0;y) - 16H(2;y)H(1,0,0;y) + 16H(2;y)H(1,0,1;z) \\
& + 16H(3;y)H(1,0,1;z) + 8H(1;z)H(2,0,0;y) - 8H(1;z)H(2,1,0;y) \\
& - 8H(2;y)H(2,1,0;y) + 8H(1;z)H(2,2,3;y) - 24H(3;y)H(2,3,2;y) \\
& - 32H(1;z)H(2,3,3;y) + 8H(1;z)H(3,0,0;y) - 2H(0;z)\Big\{\zeta_3 + 4H(3;y)H(2,2;y) \\
& + 2H(2;y)\Big\{2\zeta_2 - H(0,0;y) + H(0,1;z) + H(1,0;z) + 4H(1,1;z) - H(2,3;y) \\
& + H(3,2;y)\Big\} - 4H(1;z)\Big\{\zeta_2 + H(2;y)H(3;y) - H(0,0;y) + H(1,0;y) - H(2,0;y) \\
& + H(2,2;y) - H(3,0;y) + 2H(3,3;y)\Big\} - 3H(0,0,1;z) + 2H(0,0,2;y) \\
& - 2H(0,1,1;z) - 4H(0,2,2;y) + H(1,0,0;z) - 2H(1,0,1;z) - H(1,1,1;z) \\
& + 2H(2,0,0;y) + 4H(2,1,0;y) + 4H(3,0,2;y) + 4H(3,2,0;y)\Big\}
\end{aligned}$$

$$- 48H(3;y)H(3,2,2;y) - 2H(0;y)\Big\{\zeta_3 + 4\zeta_2 H(2;y) + 4H(2;y)H(0,0;z)$$
$$- 12H(1;y)H(1,0;y) + 8H(3;y)H(1,1;z) + H(1;z)\Big\{8H(2;y)H(3;y) - 2H(0,0;z)$$
$$+ 4(\zeta_2 + H(1,0;y) + H(2,0;y) - H(2,3;y))\Big\} - 2H(2;y)H(3,2;y) - 2H(0;z)\Big\{2\zeta_2$$
$$+ 2H(1;z)H(3;y) + H(0,1;z) + 2H(1,0;y) - 2H(1,1;z) - H(2,0;y)$$
$$+ 2H(3,2;y)\Big\} + 2H(0,0,1;z) + H(0,0,2;y) - 2H(1,0,0;y) - 2H(1,0,0;z)$$
$$- H(2,0,0;y) - H(2,2,2;y) + 6H(2,3,2;y) - 4H(3,0,2;y) - 4H(3,2,0;y)$$
$$+ 12H(3,2,2;y)\Big\} + 32H(1;z)H(3,3,2;y) + 16H(1;z)H(3,3,3;y)$$
$$- 6H(0,0,0,1;z) - 6H(0,0,0,2;y) + 16H(0,0,1,0;y) + 2H(0,0,1,0;z)$$
$$- 6H(0,0,2,0;y) + 8H(0,0,3,2;y) + 12H(0,1,0,0;y) + 6H(0,1,0,0;z)$$
$$+ 4H(0,1,0,1;z) + 16H(0,1,1,0;y) + 12H(0,1,1,0;z) - 2H(0,1,1,1;z)$$
$$- 6H(0,2,0,0;y) - 2H(0,2,2,2;y) + 12H(1,0,0,0;y) + 6H(1,0,0,0;z)$$
$$+ 4H(1,0,0,1;z) + 24H(1,0,1,0;y) + 12H(1,0,1,0;z) - 2H(1,0,1,1;z)$$
$$+ 32H(1,1,0,0;y) + 16H(1,1,0,0;z) - 2H(1,1,0,1;z) + 16H(1,1,1,0;y)$$
$$- 2H(1,1,1,0;z) - 6H(2,0,0,0;y) - 2H(2,0,2,2;y) - 2H(2,2,0,2;y)$$
$$+ 8H(2,2,1,0;y) - 2H(2,2,2,0;y) + 8H(2,2,3,2;y) + 16H(2,3,3,2;y)$$
$$+ 24H(3,2,3,2;y) + 32H(3,3,2,2;y) + 16H(3,3,3,2;y)\Big\} + C_{1,g}\Big\{\frac{64}{3}\zeta_3\Big\{33$$
$$+ 121y^4 - 114z + 231z^2 - 194z^3 + 121z^4 + 2y^3(-97 + 121z) + 3y^2(77 - 202z$$
$$+ 121z^2) + 2y(-57 + 243z - 303z^2 + 121z^3)\Big\} - \frac{64}{3}\zeta_2 H(0;y)\Big\{121y^4$$
$$+ 218y^3(-1+z) + 297y^2(-1+z)^2 + 178y(-1+z)^3 + 77(1 - z + z^2)^2\Big\}$$
$$- \frac{64}{3}\zeta_2 H(0;z)\Big\{77 + 77y^4 - 178z + 297z^2 - 218z^3 + 121z^4 + 2y^3(-77 + 89z)$$
$$+ 3y^2(77 - 178z + 99z^2) + 2y(-77 + 267z - 297z^2 + 109z^3)\Big\} - \frac{64}{3}\zeta_2 H(1;z)\Big\{11$$
$$+ 99y^4 + 74z - 111z^2 + 114z^3 - 33z^4 + y^3(-62 + 54z) + 3y^2(11 - 14z + 7z^2)$$
$$+ y(18 - 78z + 78z^2 - 66z^3)\Big\} - \frac{64}{3}\zeta_2 H(2;y)\Big\{55 + 11y^4 + 74z - 111z^2 + 114z^3$$
$$+ 11z^4 - 2y^3(-57 + 61z) - 3y^2(37 - 82z + 41z^2) + y(74 - 246z + 246z^2 - 122z^3)\Big\}$$

$$
\begin{aligned}
&- \frac{128}{3} H(0;z)H(1;z)H(2;y)\Big\{22y^4 + 32y^3(-1+z) + 63y^2(-1+z)^2 + 42y(-1+z)^3 \\
&+ 11(3 - 4z + 6z^2 - 4z^3 + 3z^4)\Big\} + \frac{128}{3} H(1;z)H(3;y)^2\Big\{55y^4 + y^3(-88+74z) \\
&+ 6y^2(22 - 44z + 21z^2) + y(-88 + 264z - 264z^2 + 74z^3) + 11(4 - 8z + 12z^2 - 8z^3 \\
&+ 5z^4)\Big\} + \frac{128}{3} H(2;y)H(0,1;z)\Big\{77 + 55y^4 - 86z + 129z^2 - 76z^3 + 66z^4 + y^3(-64 \\
&+ 62z) + 3y^2(42 - 82z + 41z^2) + 6y(-14 + 41z - 41z^2 + 12z^3)\Big\} - \frac{128}{3} y\Big\{22y^3 \\
&+ 32y^2(-1+z) + 33y(-1+z)^2 + 12(-1+z)^3\Big\}\Big\{H(0;y)H(0;z)H(1;z) \\
&- H(0;y)H(0,1;z)\Big\} - \frac{128z}{3} H(0;z)H(1,0;y)\Big\{ - 12 + 12y^3 + 33z - 32z^2 + 22z^3 \\
&+ y^2(-36 + 33z) + y(36 - 66z + 32z^2)\Big\} + \frac{128}{3}\Big\{H(1;z)H(1,0;y) \\
&+ H(2;y)H(1,0;y)\Big\}\Big\{33 + 33y^4 - 90z + 135z^2 - 100z^3 + 44z^4 + y^3(-88 + 90z) \\
&+ 3y^2(44 - 90z + 45z^2) + 2y(-44 + 135z - 135z^2 + 50z^3)\Big\} + \frac{128}{3} H(1;z)H(3,2;y) \\
&\times \Big\{22 + 33y^4 - 90z + 135z^2 - 100z^3 + 33z^4 + 2y^3(-50 + 51z) + 3y^2(45 - 92z \\
&+ 46z^2) + 6y(-15 + 46z - 46z^2 + 17z^3)\Big\} + \frac{128}{3} z\Big\{12y^3 + 3y^2 z + 2yz^2 - 11z^3\Big\} \\
&\times \Big\{H(0;z)H(1;z)H(3;y) + H(0;z)H(3,2;y)\Big\} - \frac{128y}{3}\Big\{11y^3 - 2y^2 z - 3yz^2 - 12z^3\Big\} \\
&\times \Big\{H(0;y)H(1;z)H(3;y) + H(0;y)H(0,1;z) + H(0;y)H(3,2;y) - 2H(0,0,1;z)\Big\} \\
&- \frac{128}{3} H(0,1,0;y)\Big\{99y^4 + y^3(-232 + 234z) + 132(1 - z + z^2)^2 + y^2(363 - 726z \\
&+ 366z^2) + 12y(-21 + 63z - 63z^2 + 22z^3)\Big\} - \frac{128}{3} H(0,1,0;z)\Big\{88 + 88y^4 - 164z \\
&+ 231z^2 - 144z^3 + 66z^4 + 4y^3(-44 + 41z) + 3y^2(88 - 164z + 77z^2) + 2y(-88 \\
&+ 246z - 231z^2 + 72z^3)\Big\} + \frac{128}{3} H(1,0,1;z)\Big\{77 + 77y^4 - 130z + 195z^2 - 120z^3 \\
&+ 66z^4 + 2y^3(-66 + 65z) + 3y^2(66 - 130z + 65z^2) + 6y(-22 + 65z - 65z^2 \\
&+ 20z^3)\Big\} + \frac{256}{3}\Big\{11 + 11y^4 + 14z - 14y^3 z - 36z^2 + 44z^3 - 22z^4 - 6y^2 z(-7 + 6z) \\
&- 2yz(21 - 36z + 22z^2)\Big\}\Big\{\zeta_2 H(1;y) + H(1,1,0;y)\Big\} - \frac{256}{3} H(1,1,0;z)\Big\{11y^4 \\
&+ 10y^3(-1+z) - 10y(-1+z)^3 - 11(1 - z + z^2)^2\Big\} + \frac{128}{3}\Big\{110 + 99y^4 - 174z
\end{aligned}
$$

$$+ 261z^2 - 164z^3 + 99z^4 + 2y^3(-82 + 81z) + 3y^2(87 - 172z + 86z^2) + 6y(-29$$

$$+ 86z - 86z^2 + 27z^3)\Big\}\Big\{H(1;z)H(2;y)H(3;y) + H(2,3,2;y)\Big\} - 2816\Big\{y^4$$

$$+ 2y^3(-1 + z) + 3y^2(-1 + z)^2 + 2y(-1 + z)^3 + (1 - z + z^2)^2\Big\}$$

$$\times\Big\{ - (H(0;y)H(0;z)H(2;y))/3 + H(0;y)H(1;z)H(2;y) + (H(0;y)^2H(0;z)$$

$$+ H(0;y)H(0;z)^2 - H(0;y)^2H(1;z) + H(0;y)H(1;z)^2 - H(0;z)^2H(2;y)$$

$$+ H(0;z)H(2;y)^2)/2 + (H(0;y)H(1;z)H(3;y))/3 + (H(0;z)H(1;z)H(3;y))/3$$

$$- H(1;z)^2H(3;y) + H(1;z)H(3;y)^2 - H(0;y)H(0,2;y) + (H(0;z)H(1,0;y))/3$$

$$+ H(0;y)H(2,2;y) + (H(0;y)H(3,2;y))/3 + \frac{1}{3}H(0;z)H(3,2;y) + \frac{1}{3}H(0,0,1;z)$$

$$+ H(0,0,2;y) - H(0,1,1;z) + 2H(1,0,0;y) + H(1,0,0;z) - H(2,0,0;y)$$

$$- 2H(3,2,2;y)\Big\} - \frac{256}{3}\Big\{11y^4 + y^3(-44 + 58z) + 6y^2(11 - 22z + 12z^2) + 2y(-22$$

$$+ 66z - 66z^2 + 29z^3) + 11(2 - 4z + 6z^2 - 4z^3 + z^4)\Big\}\Big\{H(3;y)H(0,1;z)$$

$$+ H(3,3,2;y)\Big\}\Big\} + C_{3,g}\Big\{ - \frac{128}{9}y^2z^2\zeta_2\Big\{64y^6 + 2y^5(-125 + 62z) + y^4(506 - 691z$$

$$+ 149z^2) + 2y^3(-329 + 771z - 498z^2 + 59z^3) + 2(-1 + z)^2(32 - 70z + 99z^2$$

$$- 61z^3 + 32z^4) + y^2(542 - 1797z + 2076z^2 - 996z^3 + 149z^4) + y(-268 + 1090z$$

$$- 1797z^2 + 1542z^3 - 691z^4 + 124z^5)\Big\} + \frac{128}{9}y^2z^2H(0;y)H(0;z)\Big\{157y^6 + y^5(-628$$

$$+ 760z) + y^4(1250 - 2851z + 1619z^2) + 2y^3(-776 + 2574z - 2841z^2 + 1046z^3)$$

$$+ (-1 + z)^2(157 - 308z + 465z^2 - 314z^3 + 157z^4) + y^2(1238 - 4941z + 8013z^2$$

$$- 5682z^3 + 1619z^4) + y(-622 + 2506z - 4941z^2 + 5148z^3 - 2851z^4 + 760z^5)\Big\}$$

$$+ \frac{128}{3}y^2z^2H(0;z)H(1;z)\Big\{133y^6 + y^5(-532 + 576z) + y^4(1060 - 2243z + 1185z^2)$$

$$+ 2y^3(-659 + 2068z - 2160z^2 + 752z^3) + (-1 + z)^2(133 - 266z + 401z^2 - 268z^3$$

$$+ 133z^4) + y^2(1052 - 4063z + 6311z^2 - 4322z^3 + 1185z^4) + y(-528 + 2126z$$

$$- 4079z^2 + 4152z^3 - 2247z^4 + 576z^5)\Big\} + \frac{128}{9}z^2H(0;z)H(2;y)(-1 + y + z)^2$$

$$\times\Big\{ - 157y^6 + y^5(314 - 182z) + 60(-1 + z)^2z^2(1 - z + z^2) - 3y^4(155 - 207z$$

$$
\begin{aligned}
&+ 58z^2) + 2y^3(154 - 258z + 69z^2 + 38z^3) + 15yz(10 - 37z + 58z^2 - 43z^3 + 12z^4) \\
&+ y^2(-157 - 73z + 561z^2 - 766z^3 + 188z^4)\Big\} + \frac{128}{9}y^2(-1 + y + z)^2\Big\{H(0;y)H(1;z) \\
&+ H(0;y)H(2;y)\Big\}\Big\{60y^6 + 180y^5(-1 + z) + y^4(240 - 645z + 188z^2) + 2y^3(-90 \\
&+ 435z - 383z^2 + 38z^3) + yz(150 - 73z - 516z^2 + 621z^3 - 182z^4) + y^2(60 - 555z \\
&+ 561z^2 + 138z^3 - 174z^4) + z^2(-157 + 308z - 465z^2 + 314z^3 - 157z^4)\Big\} \\
&- \frac{15488}{9}y^2z^2(-1 + y + z)^2\Big\{y^4 + 2y^3(-1 + z) + 3y^2(-1 + z)^2 + 2y(-1 + z)^3 \\
&+ (1 - z + z^2)^2\Big\}\Big\{H(0;y)^2 + H(0;z)^2 + H(1;z)^2 + 2H(1;z)H(2;y) + H(2;y)^2\Big\} \\
&- \frac{128}{3}y^2H(0,1;z)\Big\{20y^8 + 100y^7(-1 + z) - 2(-1 + z)^3z^3(-1 + 2z) + 5y^6(44 - 99z \\
&+ 51z^2) + 2y^5(-140 + 530z - 601z^2 + 232z^3) + y^4(220 - 1260z + 2271z^2 \\
&- 1816z^3 + 595z^4) + y^3(-100 + 870z - 2181z^2 + 2668z^3 - 1805z^4 + 546z^5) \\
&+ yz(50 - 225z + 452z^2 - 625z^3 + 582z^4 - 322z^5 + 88z^6) + y^2(20 - 325z \\
&+ 1082z^2 - 1766z^3 + 1825z^4 - 1114z^5 + 308z^6)\Big\} - \frac{128}{9}y^2H(1,0;y)\Big\{60y^8 \\
&+ 300y^7(-1 + z) + 11y^6(60 - 135z + 19z^2) - 2y^5(420 - 1590z + 685z^2 + 548z^3) \\
&+ y^4(660 - 3780z + 2341z^2 + 4174z^3 - 3389z^4) - 2(-1 + z)^2z^2(278 - 547z \\
&+ 825z^2 - 556z^3 + 278z^4) - y^3(300 - 2610z + 983z^2 + 9648z^3 - 13293z^4 \\
&+ 4966z^5) + y^2(60 - 975z - 1178z^2 + 11892z^3 - 21561z^4 + 15366z^5 - 4250z^6) \\
&+ yz(150 + 1537z - 7528z^2 + 15315z^3 - 15906z^4 + 8656z^5 - 2224z^6)\Big\} \\
&- \frac{128}{9}(-1 + y + z)^2\Big\{60y^8 + 180y^7(-1 + z) + y^6(240 - 645z - 211z^2) \\
&+ 60(-1 + z)^2z^4(1 - z + z^2) + y^5(-180 + 870z + 26z^2 - 590z^3) + y^3z(150 + 719z \\
&- 2484z^2 + 2199z^3 - 590z^4) + y^2z^2(-556 + 719z - 624z^2 + 26z^3 - 211z^4) \\
&+ 15yz^3(10 - 37z + 58z^2 - 43z^3 + 12z^4) - 3y^4(-20 + 185z + 208z^2 - 733z^3 \\
&+ 358z^4)\Big\}\Big\{H(1;z)H(3;y) + H(3,2;y)\Big\}\Bigg\} + C_{2,g}\Bigg\{\frac{128}{9}H(0;y)(-1 + y)y(-1 + z)^2 \\
&\times (y + z)^2\Big\{60y^7 + 15y^6(-16 + 39z) + 2y^5(210 - 1209z + 841z^2) + y^4(-420 \\
&+ 4639z - 7039z^2 + 2851z^3) + y^3(240 - 5265z + 12582z^2 - 10570z^3 + 3068z^4)
\end{aligned}
$$

$$+ z(381 - 1121z + 1861z^2 - 1883z^3 + 1143z^4 - 381z^5) + yz(-1663 + 5417z$$
$$- 8590z^2 + 6912z^3 - 3114z^4 + 657z^5) + y^2(-60 + 3741z - 11521z^2 + 14448z^3$$
$$- 8097z^4 + 1971z^5)\Big\} + \frac{128}{9}H(0;z)(-1+y)^2(-1+z)z(y+z)^2\Big\{y^6(-381 + 657z)$$
$$+ 60(-1+z)^3z^2(1 - z + z^2) + 9y^5(127 - 346z + 219z^2) + y^3(-1+z)^2(1861$$
$$- 4868z + 2851z^2) + y^4(-1883 + 6912z - 8097z^2 + 3068z^3) + y(-1+z)^2(381$$
$$- 901z + 1558z^2 - 1248z^3 + 585z^4) + y^2(-1121 + 5417z - 11521z^2 + 12582z^3$$
$$- 7039z^4 + 1682z^5)\Big\} + \frac{128}{9}(-1+y)^2(-1+z)^2\Big\{H(1;z) + H(2;y)\Big\}\Big\{60y^9$$
$$- 15y^8(16 + 3z) + y^7(420 - 243z - 838z^2) + 60(-1+z)^3z^4(1 - z + z^2)$$
$$+ y^6(-420 + 524z + 1966z^2 - 2417z^3) + y^5(240 - 385z - 3059z^2 + 7144z^3$$
$$- 3916z^4) + y^4(-60 + 14z + 2318z^2 - 9133z^3 + 10350z^4 - 3916z^5) + y^3z(135$$
$$- 1158z + 4566z^2 - 9133z^3 + 7144z^4 - 2417z^5) + y^2z^2(390 - 1158z + 2318z^2$$
$$- 3059z^3 + 1966z^4 - 838z^5) + yz^3(135 + 14z - 385z^2 + 524z^3 - 243z^4 - 45z^5)\Big\}\Big\}$$
$$- \frac{128\,C_{1,g}}{27}\Big\{3256 + 3169y^4 + 6338y^3(-1+z) - 6148z + 9317z^2 - 6338z^3$$
$$+ 3169z^4 + y^2(9317 - 18731z + 9507z^2) + y(-6148 + 18541z - 18731z^2$$
$$+ 6338z^3)\Big\}\Big]. \tag{B.3}$$

$$S_g^{(2),n_f/N} = \frac{n_f}{N}\Big[1024\,C_{1,g}\Big\{y^4 + 2y^3(-1+z) + 3y^2(-1+z)^2 + 2y(-1+z)^3 + (1 - z + z^2)^2\Big\}\zeta_3$$
$$+ \frac{128}{3}\,C_{3,g}\Big\{y^3z^3\Big\{6 + 7y^4 - 25z + 35z^2 - 23z^3 + 7z^4 + y^3(-23 + 20z)$$
$$+ y^2(35 - 57z + 24z^2) + y(-25 + 68z - 57z^2 + 20z^3)\Big\}\Big\{\zeta_2 + H(0;y)H(0;z)$$
$$+ H(0;z)H(1;z)\Big\} + z^3(-1 + y + z)^3\Big\{7y^4 + y^3(-5 + 8z) + 2y^2(4 - 6z + 3z^2)$$
$$+ y(-4 + 2z - 4z^3) - 2z(-1 + 2z - 2z^2 + z^3)\Big\}H(0;z)H(2;y) - y^3(-1 + y + z)^3\Big\{2y^4$$
$$+ 4y^3(-1+z) + y^2(4 - 6z^2) + z(4 - 8z + 5z^2 - 7z^3) - 2y(1 + z - 6z^2 + 4z^3)\Big\}$$
$$\times\Big\{H(0;y)H(1;z) + H(0;y)H(2;y)\Big\} + y^3\Big\{2y^7 + 10y^6(-1+z) + 2y^5(11 - 18z$$
$$+ 6z^2) - y^4(28 - 52z + 12z^2 + 19z^3) + y^3(22 - 36z - 32z^2 + 108z^3 - 65z^4)$$

$$
\begin{aligned}
&+ y^2(-10 + 6z + 72z^2 - 190z^3 + 195z^4 - 75z^5) + y(2 + 8z - 60z^2 + 148z^3 - 205z^4 \\
&+ 150z^5 - 49z^6) + z(-4 + 20z - 47z^2 + 75z^3 - 79z^4 + 49z^5 - 14z^6)\Big\}H(0,1;z) \\
&+ y^3(2y^7 + 10y^6(-1 + z) + 2y^5(11 - 18z + 6z^2) - y^4(28 - 52z + 12z^2 + 5z^3) \\
&+ y^3(22 - 36z - 32z^2 + 62z^3 - 25z^4) + y^2(-10 + 6z + 72z^2 - 120z^3 + 81z^4 - 27z^5) \\
&+ z(-4 + 20z - 35z^2 + 25z^3 - 9z^4 + 3z^5) + y(2 + 8z - 60z^2 + 98z^3 - 69z^4 + 36z^5 \\
&- 9z^6))H(1,0;y) + (-1 + y + z)^3(2y^7 + 4y^6(-1 + z) + y^5(4 - 6z^2) - 2y^2z^3(4 - 6z \\
&+ 3z^2) + y^3z(4 - 8z + 10z^2 - 15z^3) + 2z^4(-1 + 2z - 2z^2 + z^3) + 2yz^3(2 - z + 2z^3) \\
&- y^4(2 + 2z - 12z^2 + 15z^3))(H(1;z)H(3;y) + H(3,2;y))\Big\} + C_{2,g}\Big\{\frac{128}{3}y^2(1 - z) \\
&\times H(0;y)\Big\{2y^7 + y^6(-8 + 9z) + y^5(14 - 25z - 2z^2) + y^4(-14 + 28z + 37z^2 - 59z^3) \\
&+ y^3(8 - 15z - 78z^2 + 204z^3 - 120z^4) + y^2(-2 + z + 66z^2 - 242z^3 + 290z^4 \\
&- 124z^5) + yz(2 - 27z + 117z^2 - 220z^3 + 194z^4 - 72z^5) + 2z^2(2 - 10z + 25z^2 \\
&- 35z^3 + 27z^4 - 9z^5)\Big\} + \frac{128}{3}(-1 + y)z^2H(0;z)\Big\{18y^7 + 18y^6(-3 + 4z) \\
&+ 10y^4(-1 + z)^2(-5 + 12z) - 2(-1 + z)^3z^2(1 - z + z^2) + 2y^5(35 - 97z + 62z^2) \\
&- y(-1 + z)^2z(2 + 5z - 7z^2 + 9z^3) + y^3(20 - 117z + 242z^2 - 204z^3 + 59z^4) \\
&+ y^2(-4 + 27z - 66z^2 + 78z^3 - 37z^4 + 2z^5)\Big\} - \frac{128}{3}(-1 + y)(-1 + z)(-1 + y + z)^2 \\
&\times \Big\{2y^6 + y^5(-4 + 5z) - 2y^4(-2 + z + 7z^2) + y^2z(3 - 8z + 14z^2 - 14z^3) \\
&+ 2z^3(-1 + 2z - 2z^2 + z^3) + yz^2(3 - 2z^2 + 5z^3) - 2y^3(1 - 7z^2 + 8z^3)\Big\} \\
&\times \Big\{H(1;z) + H(2;y)\Big\}\Big\} - \frac{64}{3}C_{1,g}\Big\{142 + 144y^4 + 288y^3(-1 + z) - 289z + 433z^2 \\
&- 288z^3 + 144z^4 + y^2(433 - 867z + 432z^2) + y(-289 + 868z - 867z^2 + 288z^3)\Big\}\Big].
\end{aligned}
\tag{B.4}
$$

$$
\begin{aligned}
S_g^{(2),n_fN} = n_fN\Big[&C_{1,g}\Big\{\frac{128}{3}\zeta_3\Big\{21 + 13y^4 - 36z + 51z^2 - 32z^3 + 13z^4 + y^3(-32 + 26z) \\
&+ y^2(51 - 84z + 39z^2) + y(-36 + 90z - 84z^2 + 26z^3)\Big\} + \frac{128}{3}\zeta_2H(0;y)\Big\{11y^4 \\
&+ 19y^3(-1 + z) + 27y^2(-1 + z)^2 + 17y(-1 + z)^3 + 7(1 - z + z^2)^2\Big\} + \frac{128}{3}\zeta_2H(0;z)
\end{aligned}
$$

$$\times\Big\{7 + 7y^4 - 17z + 27z^2 - 19z^3 + 11z^4 + y^3(-14 + 17z) + 3y^2(7 - 17z + 9z^2)$$
$$+ y(-14 + 51z - 54z^2 + 19z^3)\Big\} + \frac{128}{3}\zeta_2 H(1;z)\Big\{1 - 4y^3 + 9y^4 + 10z - 15z^2 + 12z^3$$
$$- 3z^4 + y^2(3 + 6z - 3z^2) - 6yz(2 - 2z + z^2)\Big\} + \frac{128}{3}\zeta_2 H(2;y)\Big\{5 + y^4 + 10z - 15z^2$$
$$+ 12z^3 + z^4 - 4y^3(-3 + 4z) - 3y^2(5 - 14z + 7z^2) - 2y(-5 + 21z - 21z^2 + 8z^3)\Big\}$$
$$+ \frac{128}{3}H(0;z)H(1;z)H(2;y)\Big\{6 + 4y^4 + 5y^3(-1 + z) + 9y^2(-1 + z)^2 + 6y(-1 + z)^3$$
$$- 8z + 12z^2 - 8z^3 + 6z^4\Big\} + \frac{128}{3}H(1;z)H(3;y)^2\Big\{2y^4 + y^3(-8 + 13z) + 6y^2(2 - 4z$$
$$+ 3z^2) + y(-8 + 24z - 24z^2 + 13z^3) + 2(2 - 4z + 6z^2 - 4z^3 + z^4)\Big\} + \frac{128}{3}y\Big\{2y^3$$
$$- 2y^2z - 3yz^2 - 3z^3\Big\}H(0;y)H(0,1;z) - \frac{128}{3}H(2;y)H(0,1;z)\Big\{14 + 10y^4 - 14z$$
$$+ 21z^2 - 13z^3 + 12z^4 + 2y^3(-5 + 4z) + 3y^2(6 - 10z + 5z^2) + 3y(-4 + 10z - 10z^2$$
$$+ 3z^3)\Big\} + \frac{128}{3}y\Big\{4y^3 + 5y^2(-1 + z) + 6y(-1 + z)^2 + 3(-1 + z)^3\Big\}$$
$$\times\Big\{H(0;y)H(0;z)H(1;z) - H(0;y)H(0,1;z)\Big\} + \frac{128}{3}H(0;z)H(1,0;y)\Big\{4 + 4y^4$$
$$- 11z + 18z^2 - 13z^3 + 8z^4 + y^3(-8 + 11z) + 3y^2(4 - 11z + 6z^2) + y(-8 + 33z$$
$$- 36z^2 + 13z^3)\Big\} - \frac{128}{3}\Big\{6 + 6y^4 - 18z + 27z^2 - 19z^3 + 8z^4 + 2y^3(-8 + 9z)$$
$$+ 3y^2(8 - 18z + 9z^2) + y(-16 + 54z - 54z^2 + 19z^3)\Big\}\Big\{H(1;z)H(1,0;y)$$
$$+ H(2;y)H(1,0;y)\Big\} - \frac{128}{3}H(1;z)H(3,2;y)\Big\{4 + 6y^4 - 18z + 27z^2 - 19z^3$$
$$+ 6z^4 + y^3(-19 + 21z) + 3y^2(9 - 20z + 10z^2) + 3y(-6 + 20z - 20z^2 + 7z^3)\Big\}$$
$$+ \frac{128}{3}\Big\{6y^4 + y^3(-8 + 6z) + 4(1 - z + z^2)^2 + 3y^2(4 - 8z + 3z^2) + y(-8 + 24z$$
$$- 24z^2 + 5z^3)\Big\}\Big\{H(0;y)H(1;z)H(3;y) + H(0;y)H(3,2;y)\Big\} + \frac{128}{3}\Big\{4 + 4y^4 - 8z$$
$$+ 12z^2 - 8z^3 + 6z^4 + y^3(-8 + 5z) + 3y^2(4 - 8z + 3z^2) + y(-8 + 24z - 24z^2 + 6z^3)\Big\}$$
$$\times\Big\{H(0;z)H(1;z)H(3;y) + H(0;z)H(3,2;y)\Big\} + \frac{256}{3}\Big\{y^3(-4 + 6z) + 2(1 - z + z^2)^2$$
$$+ 3y^2(2 - 4z + 3z^2) + y(-4 + 12z - 12z^2 + 7z^3)\Big\}H(0,0,1;z) + \frac{128}{3}\Big\{18y^4$$
$$+ y^3(-43 + 45z) + 24(1 - z + z^2)^2 + 3y^2(22 - 44z + 23z^2) + 3y(-15 + 45z - 45z^2$$
$$+ 16z^3)\Big\}H(0,1,0;y) + \frac{128}{3}\Big\{16 + 16y^4 - 29z$$

$$
\begin{aligned}
&+ 42z^2 - 27z^3 + 12z^4 + y^3(-32 + 29z) + y^2(48 - 87z + 42z^2) + y(-32 + 87z \\
&- 84z^2 + 27z^3)\Big\}H(0,1,0;z) - \frac{128}{3}H(1,0,1;z)\Big\{14 + 14y^4 - 22z + 33z^2 - 21z^3 \\
&+ 12z^4 + y^3(-24 + 22z) + y^2(36 - 66z + 33z^2) + 3y(-8 + 22z - 22z^2 + 7z^3)\Big\} \\
&- \frac{256}{3}\Big\{2 + 2y^4 + 5z - 5y^3z + 3y^2(5 - 3z)z - 9z^2 + 8z^3 - 4z^4 + yz(-15 + 18z \\
&- 8z^2)\Big\}\Big\{\zeta_2 H(1;y) + H(1,1,0;y)\Big\} + \frac{256}{3}\Big\{2y^4 + y^3(-1 + z) - y(-1 + z)^3 \\
&- 2(1 - z + z^2)^2\Big\}H(1,1,0;z) - \frac{128}{3}\Big\{20 + 18y^4 - 30z + 45z^2 - 29z^3 + 18z^4 \\
&+ y^3(-29 + 27z) + y^2(45 - 84z + 42z^2) + 3y(-10 + 28z - 28z^2 + 9z^3)\Big\} \\
&\Big\{H(1;z)H(2;y)H(3;y) + H(2,3,2;y)\Big\} + 512\Big\{y^4 + 2y^3(-1 + z) + 3y^2(-1 + z)^2 \\
&+ 2y(-1 + z)^3 + (1 - z + z^2)^2\Big\} \times \Big\{\frac{1}{2}H(0;y)^2H(0;z) + \frac{1}{2}H(0;y)H(0;z)^2 \\
&- \frac{1}{2}H(0;y)^2H(1;z) + \frac{1}{2}H(0;y)H(1;z)^2 - \frac{1}{3}H(0;y)H(0;z)H(2;y) \\
&- \frac{1}{2}H(0;z)^2H(2;y) + H(0;y)H(1;z)H(2;y) + \frac{1}{2}H(0;z)H(2;y)^2 \\
&- H(1;z)^2H(3;y) - H(0;y)H(0,2;y) + H(0;y)H(2,2;y) + H(0,0,2;y) \\
&- H(0,1,1;z) + 2H(1,0,0;y) + H(1,0,0;z) - H(2,0,0;y) - 2H(3,2,2;y)\Big\} \\
&+ \frac{256}{3}\Big\{2y^4 + y^3(-8 + 13z) + 6y^2(2 - 4z + 3z^2) + y(-8 + 24z \\
&- 24z^2 + 13z^3) + 2(2 - 4z + 6z^2 - 4z^3 + z^4)\Big\}\Big\{H(3;y)H(0,1;z) + H(3,3,2;y)\Big\}\Big\} \\
&+ C_{3,g}\Big\{\frac{64}{9}y^2z^2\zeta_2\Big\{101y^6 + y^5(-392 + 290z) + 2y^4(398 - 679z + 236z^2) \\
&+ 2y^3(-523 + 1404z - 1086z^2 + 217z^3) + (-1 + z)^2(101 - 226z + 315z^2 - 190z^3 \\
&+ 101z^4) + y^2(868 - 3096z + 3993z^2 - 2172z^3 + 472z^4) + 2y(-214 + 892z \\
&- 1548z^2 + 1404z^3 - 679z^4 + 145z^5)\Big\} + \frac{128}{3}H(0;y)H(0;z)y^2z^2\Big\{8y^6 + y^5(-32 \\
&+ 13z) + y^4(66 - 83z + 8z^2) - y^3(86 - 183z + 81z^2 + 16z^3) + 2(-1 + z)^2(4 - 9z \\
&+ 13z^2 - 8z^3 + 4z^4) + y^2(70 - 215z + 220z^2 - 81z^3 + 8z^4) + y(-34 + 136z \\
&- 215z^2 + 183z^3 - 83z^4 + 13z^5)\Big\} - \frac{128}{9}H(0;z)H(1;z)y^2z^2\Big\{64y^6 + y^5(-256 \\
&+ 313z) + 5y^4(100 - 233z + 136z^2) + y^3(-604 + 2091z - 2415z^2 + 928z^3)
\end{aligned}
$$

$$+ 2(-1+z)^2(32-64z+99z^2-67z^3+32z^4)+y^2(476-1983z+3330z^2$$

$$-2421z^3+680z^4)+y(-244+1000z-2031z^2+2139z^3-1177z^4+313z^5)\Big\}$$

$$-\frac{128}{3}H(0;z)H(2;y)z^2(-1+y+z)^2\Big\{8y^6+y^5(-16+35z)+22(-1+z)^2z^2(1-z$$

$$+z^2)+y^4(26-98z+63z^2)+3y^3(-6+41z-61z^2+26z^3)+2yz(14-68z$$

$$+119z^2-98z^3+33z^4)+y^2(8-88z+238z^2-250z^3+94z^4)\Big\}$$

$$-\frac{128}{3}y^2(-1+y+z)^2\Big\{22y^6+66y^5(-1+z)+2y^4(44-98z+47z^2)+y^3(-66$$

$$+238z-250z^2+78z^3)+2z^2(4-9z+13z^2-8z^3+4z^4)+yz(28-88z+123z^2$$

$$-98z^3+35z^4)+y^2(22-136z+238z^2-183z^3+63z^4)\Big\}\Big\{H(0;y)H(1;z)$$

$$+H(0;y)H(2;y)\Big\}+\frac{5632}{9}y^2z^2(-1+y+z)^2\Big\{y^4+2y^3(-1+z)+3y^2(-1+z)^2$$

$$+2y(-1+z)^3+(1-z+z^2)^2\Big\}\Big\{H(0;y)^2+H(0;z)^2+H(1;z)^2+2H(1;z)H(2;y)$$

$$+H(2;y)^2\Big\}+\frac{128}{3}H(0,1;z)y^2\Big\{22y^8+110y^7(-1+z)-2(-1+z)^3z^3(-1+2z)$$

$$+y^6(242-504z+240z^2)+y^5(-308+1004z-998z^2+319z^3)+y^4(242$$

$$-1116z+1726z^2-1150z^3+305z^4)+y^3(-110+714z-1542z^2+1614z^3$$

$$-935z^4+255z^5)+yz(28-124z+243z^2-325z^3+287z^4-147z^5+38z^6)$$

$$+y^2(22-236z+698z^2-1024z^3+945z^4-532z^5+133z^6)\Big\}+\frac{128}{9}H(1,0;y)y^2$$

$$\times\Big\{66y^8+330y^7(-1+z)+2y^6(363-756z+340z^2)+y^5(-924+3012z$$

$$-2822z^2+683z^3)-2(-1+z)^2z^2(20-31z+51z^2-40z^3+20z^4)+y^4(726$$

$$-3348z+4834z^2-2492z^3+259z^4)-y^3(330-2142z+4226z^2-3204z^3$$

$$+567z^4+211z^5)+y^2(66-708z+1798z^2-1674z^3+75z^4+642z^5-257z^6)$$

$$+yz(84-224z+137z^2+423z^3-777z^4+517z^5-160z^6)\Big\}+\frac{128}{9}(-1+y+z)^2$$

$$\Big\{66y^8+198y^7(-1+z)+66(-1+z)^2z^4(1-z+z^2)+y^6(264-588z+218z^2)$$

$$+y^5(-198+714z-628z^2+163z^3)+6yz^3(14-68z+119z^2-98z^3+33z^4)$$

$$+3y^4(22-136z+178z^2-109z^3+38z^4)+2y^2z^2(-20-71z+267z^2-314z^3$$

$$
\begin{aligned}
&+ 109z^4) + y^3z(84 - 142z + 210z^2 - 327z^3 + 163z^4)\Big\}\Big\{H(1;z)H(3;y) + H(3,2;y)\Big\}\Bigg\} \\
&+ C_{2,g}\Bigg\{ - \frac{128}{27}H(0;y)(-1+y)y(-1+z)^2(y+z)^2\Big\{198y^7 + y^6(-792 + 1025z) \\
&+ y^5(1386 - 3992z + 2187z^2) + y^4(-1386 + 6964z - 8471z^2 + 3016z^3) \\
&+ y^3(792 - 6965z + 14159z^2 - 11110z^3 + 3238z^4) + 2z(175 - 486z + 797z^2 \\
&- 836z^3 + 525z^4 - 175z^5) + yz(-1613 + 5147z - 8266z^2 + 6816z^3 - 3126z^4 \\
&+ 692z^5) + y^2(-198 + 4231z - 12050z^2 + 14766z^3 - 8382z^4 + 2076z^5)\Big\} \\
&- \frac{128}{27}H(0;z)(-1+y)^2(-1+z)z(y+z)^2\Big\{y^6(-350 + 692z) + 198(-1+z)^3z^2(1 - z \\
&+ z^2) + 6y^5(175 - 521z + 346z^2) + 2y^3(-1+z)^2(797 - 2539z + 1508z^2) \\
&+ 2y^4(-836 + 3408z - 4191z^2 + 1619z^3) + y(-1+z)^2(350 - 913z + 2055z^2 \\
&- 1942z^3 + 1025z^4) + y^2(-972 + 5147z - 12050z^2 + 14159z^3 - 8471z^4 \\
&+ 2187z^5)\Big\} - \frac{128}{27}(-1+y)^2(-1+z)^2\Big\{198y^9 + y^8(-792 + 757z) + 198(-1+z)^3 \\
&\times z^4(1 - z + z^2) + y^7(1386 - 3153z + 1115z^2) + y^6(-1386 + 5165z - 4546z^2 \\
&+ 225z^3) + y^5(792 - 4466z + 6493z^2 - 1445z^3 - 1383z^4) + y^4(-198 + 1914z \\
&- 5156z^2 + 3014z^3 + 1480z^4 - 1383z^5) + y^3z(-217 + 1782z - 4152z^2 + 3014z^3 \\
&- 1445z^4 + 225z^5) + yz^3(-217 + 1914z - 4466z^2 + 5165z^3 - 3153z^4 + 757z^5) \\
&+ y^2z^2(-38 + 1782z - 5156z^2 + 6493z^3 - 4546z^4 + 1115z^5)\Big\}(H(1;z) + H(2;y))\Bigg\} \\
&+ \frac{64\,C_{1,g}}{27}\Big\{2492 + 2306y^4 + 4612y^3(-1+z) - 4191z + 6497z^2 - 4612z^3 + 2306z^4 \\
&+ y^2(6497 - 13205z + 6918z^2) + y(-4191 + 12784z - 13205z^2 + 4612z^3)\Big\}\Bigg].
\end{aligned}
\tag{B.5}
$$

$$
\begin{aligned}
S_g^{(2),n_f^2} &= n_f^2\Bigg[\frac{128}{9}C_{1,g}\Big\{y^4 + 2y^3(-1+z) + 3y^2(-1+z)^2 + 2y(-1+z)^3 + (1 - z + z^2)^2\Big\} \\
&\times\Big\{ - 3\zeta_2 - 4H(0;y)^2 - 4H(0;z)^2 - 4H(1;z)^2 - 4H(0;y)(H(0;z) - H(1;z) \\
&- H(2;y)) - 8H(1;z)H(2;y) - 4H(2;y)^2 + 4H(0;z)(H(1;z) + H(2;y))\Big\} \\
&+ \frac{256}{27}C_{1,g}\Big\{\Big\{10y^4 + y^3(-20 + 23z) + 3y^2(9 - 20z + 11z^2) + y(-17 + 51z - 57z^2
\end{aligned}
$$

$$
\begin{aligned}
&+ 20z^3) + 2(5 - 7z + 12z^2 - 10z^3 + 5z^4)\Big\}H(0;y) + \Big\{10 + 10y^4 + 20y^3(-1+z) \\
&- 17z + 27z^2 - 20z^3 + 10z^4 + y(-1+z)^2(-14+23z) + 3y^2(8 - 19z + 11z^2)\Big\} \\
&\times H(0;z) - \Big\{10 + 10y^4 - 17z + 27z^2 - 20z^3 + 10z^4 + y^3(-20+17z) \\
&+ 3y^2(9 - 17z + 8z^2) + y(-17 + 54z - 51z^2 + 17z^3)\Big\}\Big\{H(1;z) + H(2;y)\Big\}\Big\} \\
&- \frac{128}{27}C_{1,g}\Big\{3y^4 + 6y^3(-1+z) + y^2(-7 + z + 9z^2) + z(10 - 7z - 6z^2 + 3z^3) \\
&+ y(10 - 17z + z^2 + 6z^3)\Big\}\Big]. \qquad \text{(B.6)}
\end{aligned}
$$

where the constants $C_{i,g}$ are

$$
\begin{aligned}
C_{1,g} &= \frac{Q^2}{yz(-1+y+z)}, C_{2,g} = \frac{Q^2}{y^2z^2(-1+y)^2(-1+z)^2(y+z)^2(-1+y+z)^2}, \\
C_{3,g} &= \frac{Q^2}{y^3z^3(-1+y+z)^3}. \qquad \text{(B.7)}
\end{aligned}
$$

One loop finite result for $f = q\bar{q}g$ external state is given by

$$S_q^{G,(0)} = -64\, C_{1,q}, \qquad \text{(B.8)}$$

$$S_q^{J,(0)} = 0, \qquad \text{(B.9)}$$

$$S_q^{JG,(0)} = 0, \qquad \text{(B.10)}$$

$$S_q^{JG,(1)} = -64\mathbf{n_f}\, C_{1,q}, \qquad \text{(B.11)}$$

$$
\begin{aligned}
S_q^{G,(1)} = N\Big[&- 128\, C_{1,q}\Big\{H(0;y)H(1;z) + H(0;z)H(2;y) - 2H(1;z)H(3;y) - H(0,1;z) \\
&+ H(0,2;y) - H(1,0;y) + H(2,0;y) - 2H(3,2;y)\Big\} + \frac{64\, C_{1,q}}{3}\Big\{10H(0;y) \\
&+ 10H(0;z) - 13H(1;z) - 13H(2;y)\Big\} - \frac{64\, C_{6,q}}{9}\Big\{143y^2 + y(9 - 18z) + z(9 + 143z)\Big\}\Big] \\
&+ n_f\Big[\frac{-64\, C_{1,q}}{3}\Big\{H(0;y) + H(0;z) - 4H(1;z) - 4H(2;y)\Big\} + \frac{1280\, C_{1,q}}{9}\Big] \\
&+ \frac{1}{N}\Big[- 128\, C_{1,q}\Big\{\zeta_2 + H(0;y)H(0;z) + H(1,0;y) + H(1,0;z)\Big\} \\
&- 64\, C_{6,q}\Big\{y + 7y^2 + z - 2yz + 7z^2\Big\}\Big]. \qquad \text{(B.12)}
\end{aligned}
$$

.

At two loops, for $f = q\bar{q}g$ external state, we decompose $S_q^{G,(2)}$ in terms of the color factors as follows

$$S_q^{G,(2)} = S_q^{(2),N^2} + S_q^{(2),N^0} + S_q^{(2),1/N^2} + S_q^{(2),n_f/N} + S_q^{(2),n_fN} + S_q^{(2),n_f^2} \tag{B.13}$$

where each color term is given below

$$\begin{aligned}
S_q^{(2),N^2} = N^2\Bigg[\frac{64\,C_{1,q}}{5}\Bigg\{&27\zeta_2^2 - 80\zeta_3 H(2;y) + 40\zeta_2 H(0;z)H(2;y) - 10H(0;y)^2(H(0;z)\\
&+ 4H(1;z))H(2;y) + 10\zeta_2(H(0,0;y) + H(0,0;z)) + 10H(0,0;y)H(0,0;z)\\
&- 20\zeta_2 H(0,1;y) - 80H(2;y)H(3;y)H(0,1;z) - 10H(0,0;y)H(0,1;z)\\
&- 10\zeta_2 H(1,0;y) - 20\zeta_2 H(1,1;y) + 70\zeta_2 H(1,1;z) - 40H(0,0;y)H(1,1;z)\\
&- 10H(0,1;z)H(1,2;y) + 10\zeta_2 H(2,0;y) + 10H(0,0;z)H(2,0;y)\\
&- 10H(0,1;z)H(2,0;y) + 10\zeta_2 H(2,1;y) + 80\zeta_2 H(2,2;y) - 40H(0,0;z)H(2,2;y)\\
&- 80H(0,1;z)H(2,2;y) + 20\zeta_2 H(3,2;y) - 20H(0,1;z)H(3,2;y)\\
&- 10H(1,0;y)H(3,2;y) - 80H(0,1;z)H(3,3;y) - 160H(1,1;z)H(3,3;y)\\
&- 10H(1;y)H(0,0,1;z) - 40H(2;y)H(0,0,1;z) - 80H(3;y)H(0,0,1;z)\\
&+ 20H(0;z)H(0,0,2;y) - 10H(0;z)H(0,1,0;y) - 20H(1;y)H(0,1,0;y)\\
&+ 30H(2;y)H(0,1,0;z) - 80H(3;y)H(0,1,1;z) - 20H(0;z)H(0,2,2;y)\\
&- 30H(0;z)H(0,3,2;y) + 10H(2;y)H(1,0,0;z) - 10H(1;y)H(1,0,1;z)\\
&- 20H(2;y)H(1,0,1;z) - 60H(3;y)H(1,0,1;z) + 70H(2;y)H(1,1,0;z)\\
&+ 40H(3;y)H(1,1,0;z) + 10H(0;y)\Big\{3\zeta_2 H(2;y) + H(2;y)H(0,1;z)\\
&+ 8H(3;y)H(1,1;z) + 4H(1;z)(\zeta_2 + H(2,0;y) + 2H(3,2;y))\\
&+ H(0;z)\Big\{ - H(1;z)(2H(2;y) + H(3;y)) + H(2,0;y) + 2(\zeta_2 - H(2,2;y)\\
&+ H(3,2;y))\Big\} + H(0,0,1;z) + 4H(0,1,1;z) + 3H(0,3,2;y) + H(1,0,0;z)
\end{aligned}$$

$$
\begin{aligned}
&+ 2H(1,0,1;z) + 2H(1,1,0;z)\Big\} + 10H(0;z)H(2,0,0;y) + 20H(0;z)H(2,1,0;y) \\
&+ 20H(2;y)H(2,1,0;y) + 20H(0;z)H(2,2,0;y) + 40H(0;z)H(2,3,2;y) \\
&- 120H(3;y)H(2,3,2;y) + 80H(0;z)H(3,2,2;y) - 10H(1;z)\Big\{8\zeta_3 - 2\zeta_2 H(3;y) \\
&+ H(2;y)(-9\zeta_2 + 12H(3;y)^2) + H(3;y)H(1,0;y) - 12H(3;y)H(3,2;y) \\
&- H(0;z)\Big\{3\zeta_2 + 4H(2;y)H(3;y) + H(0,0;y) - H(1,0;y) + 4H(2,0;y) \\
&+ 4H(2,2;y) + 3H(3,0;y) + 2H(3,2;y)\Big\} - 4H(0,0,2;y) - H(0,1,0;y) \\
&- 3H(0,2,3;y) - 3H(0,3,0;y) - 4H(1,0,0;y) + H(1,2,3;y) + H(1,3,0;y) \\
&+ 4H(2,0,0;y) - 4H(2,0,3;y) - 2H(2,1,0;y) + 4H(2,2,3;y) \\
&- 4H(2,3,0;y) - 16H(2,3,3;y) + H(3,1,0;y) + 16H(3,3,2;y) \\
&+ 8H(3,3,3;y)\Big\} - 50H(0,0,0,1;z) + 30H(0,0,1,0;z) - 40H(0,0,1,1;z) \\
&- 40H(0,0,2,2;y) - 60H(0,0,3,2;y) + 20H(0,1,0,1;y) - 60H(0,1,0,1;z) \\
&+ 10H(0,1,0,2;y) + 20H(0,1,1,0;y) + 20H(0,1,1,0;z) + 10H(0,1,2,0;y) \\
&- 40H(0,2,0,2;y) + 30H(0,2,1,0;y) - 40H(0,2,2,0;y) + 30H(0,2,3,2;y) \\
&+ 80H(0,3,2,2;y) - 30H(1,0,0,1;z) + 40H(1,0,0,2;y) + 30H(1,0,1,0;z) \\
&+ 40H(1,0,2,0;y) - 40H(1,1,0,0;y) + 10H(1,1,0,0;z) - 30H(1,1,0,1;z) \\
&- 20H(1,1,1,0;y) + 40H(1,1,1,0;z) + 40H(1,2,0,0;y) - 10H(1,2,1,0;y) \\
&- 10H(1,2,3,2;y) - 10H(1,3,0,2;y) - 10H(1,3,2,0;y) - 40H(2,0,0,2;y) \\
&+ 30H(2,0,1,0;y) - 40H(2,0,2,0;y) + 40H(2,0,3,2;y) + 50H(2,1,0,0;y) \\
&+ 10H(2,1,1,0;y) - 40H(2,2,0,0;y) - 40H(2,2,3,2;y) + 40H(2,3,0,2;y) \\
&+ 40H(2,3,2,0;y) + 120H(2,3,2,3;y) + 160H(2,3,3,2;y) + 80H(3,0,2,2;y) \\
&- 10H(3,1,0,2;y) - 10H(3,1,2,0;y) + 80H(3,2,0,2;y) - 10H(3,2,1,0;y) \\
&+ 80H(3,2,2,0;y) - 160H(3,3,2,2;y) - 80H(3,3,3,2;y)\Big\} \\
&+ C_{4,q}\Big\{ - 96yz^3 H(0;y)^2 H(0;z) - \frac{64}{3}yz(3 + 17y^2 + 6z - 4z^2 - 6y(1+z))\zeta_2 H(1;z) \\
&+ \frac{32}{3}yz\Big\{3 + 73y^2 + 6z + 61z^2 - 6y(1+z)\Big\}H(0;z)H(1;z)^2 - 64yz(2 + 7y^2 - 4yz
\end{aligned}
$$

$$+ 7z^2)\zeta_2 H(2;y) + \frac{32}{3}yz\Big\{3 + 53y^2 - 6y(-1+z) - 6z + 65z^2\Big\}H(0;z)^2H(2;y)$$
$$+ \frac{128}{3}yz(3 + 67y^2 - 6yz + 67z^2)H(1;z)H(2;y)H(3;y) - \frac{64}{3}yz\Big\{3 + 61y^2 + 6z$$
$$+ 37z^2 - 6y(1+2z)\Big\}H(0;y)H(0,1;z) + \frac{64}{3}yz\Big\{6 + 95y^2 - 12yz + 95z^2\Big\}H(2;y)$$
$$\times H(0,1;z) + \frac{64}{3}yz\Big\{-3 + 5y^2 + 6y(-1+z) + 6z - 7z^2\Big\}H(0;z)H(0,2;y)$$
$$- \frac{64}{3}yz\Big\{55y^2 - 6y(2+z) + z(12+19z)\Big\}H(1;z)H(0,3;y) + \frac{64}{3}yz\Big\{-3 + y^2 - 6z$$
$$+ 13z^2 + 6y(1+z)\Big\}\Big\{H(1;z)H(1,0;y) + H(2;y)H(1,0;y)\Big\} + \frac{128}{3}yz\Big\{-3 + 7y^2$$
$$+ 6yz + 7z^2\Big\}H(1;z)H(3,2;y) - \frac{64}{3}yz\Big\{43y^2 - 6yz + 31z^2\Big\}\Big\{H(1;z)H(3,0;y)$$
$$+ H(0;y)H(3,2;y)\Big\} - \frac{64}{3}yz\Big\{31y^2 - 6yz + 43z^2\Big\}\Big\{H(0;z)H(1;z)H(3;y)$$
$$+ H(0;z)H(3,2;y)\Big\} + \frac{64}{3}yz\Big\{3 + 35y^2 + 6z - z^2 - 6y(1+3z)\Big\}H(0,0,1;z)$$
$$- 64yz(1 - 2y + 14y^2 + 2z + 17z^2)H(0,1,0;y) - \frac{64}{3}(29y^3z + 20yz^3)H(0,1,0;z)$$
$$+ \frac{64}{3}yz\Big\{-3 + y^2 - 6z + 13z^2 + 6y(1+z)\Big\}H(0,1,1;z) - 256yz(-y + y^2 + z - z^2)$$
$$\times H(0,3,2;y) - \frac{64}{3}yz\Big\{3 + 65y^2 + 6z + 62z^2 - 6y(1+z)\Big\}H(1,0,0;y)$$
$$- 96y^3z\Big\{H(0;y)H(0;z)^2 + 2H(1,0,0;z)\Big\} + \frac{64}{3}yz\Big\{3 + 25y^2 + 6z + 4z^2 - 6y(1+z)\Big\}$$
$$\Big\{\zeta_2 H(1;y) + H(1,1,0;y)\Big\} - \frac{64}{3}yz\Big\{3 + 91y^2 + 6z + 70z^2 - 6y(1+z)\Big\}H(1,1,0;z)$$
$$+ \frac{64}{3}yz\Big\{3 + 65y^2 + 6z + 53z^2 - 6y(1+z)\Big\}\Big\{(H(0;y)^2H(1;z))/2 + H(0;y)H(0,2;y)$$
$$- H(0,0,2;y) + H(2,0,0;y)\Big\} + \frac{64}{3}yz\Big\{3 + 38y^2 + 6z + 26z^2 - 6y(1+z)\Big\}$$
$$\times H(2,1,0;y) + \frac{128}{3}yz(3 + 67y^2 - 6yz + 67z^2)H(2,3,2;y) - 32yz(y^2 + z^2)$$
$$\times \Big\{-\frac{638}{9}\zeta_3 + \zeta_2 H(0;y) + \zeta_2 H(0;z) - \frac{22}{3}H(0;y)H(0;z)H(1;z)$$
$$+ \frac{74}{3}H(0;y)H(1;z)^2 + \frac{70}{3}H(0;z)H(1;z)H(2;y) + \frac{74}{3}H(0;y)H(2;y)^2)$$
$$+ \frac{74}{3}H(0;z)H(2;y)^2 - \frac{148}{3}H(1;z)^2H(3;y) + \frac{148}{3}H(1;z)H(0,2;y)$$
$$+ \frac{40}{3}H(0;z)H(1,0;y) - \frac{62}{3}H(0;z)H(2,0;y) + \frac{148}{3}H(1;z)H(2,0;y)$$
$$- \frac{296}{3}H(3,2,2;y)\Big\} + \frac{512}{3}yz(4y^2 - 3yz + 4z^2)\Big\{\frac{1}{2}H(1;z)H(3;y)^2$$
$$+ H(3;y)H(0,1;z) + H(3,3,2;y)\Big\}\Bigg\} + C_{5,q}\Bigg\{-\frac{32}{3}y^2z^2\Big\{71y^2 + 12y(-1+z)$$

$$
\begin{aligned}
&+ z(-12+71z)\Big\}\zeta_2 - \frac{32}{3}y^2z^2\Big\{70y^2 - 3yz + z(3+67z)\Big\}H(0;y)^2 + \frac{32}{9}y^2z^2\Big\{18y \\
&- 263y^2 + (18-263z)z\Big\}H(0;y)H(0;z) - \frac{32}{3}y^2z^2\Big\{67y^2 - 3y(-1+z) + 70z^2\Big\} \\
&\times H(0;z)^2 + \frac{32}{9}y^2z^2\Big\{215y^2 + 18y(1+z) + z(18+197z)\Big\}H(0;z)H(1;z) \\
&+ \frac{64}{9}z^2\Big\{-380y^4 + 45(-1+z)^2z^2 + 24y^3(1+3z) + y^2(48-291z-164z^2) \\
&+ 9yz(11-16z+5z^2)\Big\}H(0;z)H(2;y) - \frac{3328}{3}y^2z^2(y^2+z^2)\Big\{H(1;z)^2 \\
&+ 2H(1;z)H(2;y) + H(2;y)^2\Big\} - \frac{32}{3}y^2\Big\{30y^4 + 30y^3(-2+z) + z^2(32+28z \\
&- 361z^2) + y^2(30-96z-211z^2) + 2yz(33-91z+27z^2)\Big\}H(0,1;z) \\
&- \frac{32}{3}y^2\Big\{30y^4 + 30y^3(-2+z) + z^2(32+10z-325z^2) + y^2(30-96z-175z^2) \\
&+ 2yz(33-100z+21z^2)\Big\}H(1,0;y) + \frac{64}{9}y^2\Big\{45y^4 + 45y^3(-2+z) + y^2(45-144z \\
&- 164z^2) + 4z^2(12+6z-95z^2) + 3yz(33-97z+24z^2)\Big\}\Big\{H(0;y)H(1;z) \\
&+ H(0,2;y) + H(2,0;y)\Big\} - \frac{64}{3}\Big\{15y^6 + 15y^5(-2+z) + 15(-1+z)^2z^4 \\
&+ y^4(15-48z-268z^2) + 3yz^3(11-16z+5z^2) + y^3z(33-86z+48z^2) \\
&- 2y^2z^2(-16+43z+134z^2)\Big\}\Big\{H(1;z)H(3;y) + H(3,2;y)\Big\}\Big\} + \frac{16}{27}C_{8,q}\Big\{2y(-1+z) \\
&\times \Big\{270y^5 + 2(27-1813z)z^3 + y^4(-540+4274z) + yz^2(216-4175z+3905z^2) \\
&+ y^2z(432-4715z+4400z^2) + y^3(270-4706z+4499z^2)\Big\}H(0;y) + (-1+y) \\
&\times \Big\{2z\Big\{270(-1+z)^2z^3 + y^4(-3626+3905z) + 2yz^2(216-2353z+2137z^2) \\
&+ y^3(54-4175z+4400z^2) + y^2z(216-4715z+4499z^2)\Big\}H(0;z) + 3(-1+z) \\
&\times \Big\{180y^5 + 180(-1+z)^2z^3 - y^4(360+4357z) + yz^2(852-966z-4357z^2) \\
&+ y^2z(852-3420z-2821z^2) + y^3(180-966z-2821z^2)\Big\}\Big\{H(1;z) + H(2;y)\Big\}\Big\}\Big\} \\
&- \frac{4}{81}C_{6,q}\Big\{648 + 393245y^2 + 52272z + 393245z^2 - 432y(-121+245z)\Big\}\Bigg]. \qquad \text{(B.14)}
\end{aligned}
$$

$$
S_q^{(2),N^0} = \Bigg[-32\,C_{1,q}\Big\{7\zeta_2^2 - 12\zeta_3H(1;y) - 16\zeta_3H(1;z) + 4\zeta_2H(1;y)H(1;z) - 4\zeta_3H(2;y)
$$

$$
\begin{aligned}
&+ 4H(0;y)^2H(0;z)H(2;y) - 8\zeta_2H(1;z)H(3;y) + 8H(1;z)H(3;y)H(0,0;y)\\
&- 16H(0,0;y)H(0,0;z) - 16\zeta_2H(0,1;y) - 4\zeta_2H(0,1;z) - 16\zeta_2H(1,0;y)\\
&- 4H(1;z)H(3;y)H(1,0;y) - 16\zeta_2H(1,1;y) - 12\zeta_2H(1,1;z) + 4\zeta_2H(1,2;y)\\
&- 8H(0,1;z)H(1,2;y) - 4\zeta_2H(2,0;y) + 4H(0,1;z)H(2,0;y) - 8\zeta_2H(3,2;y)\\
&+ 8H(0,1;z)H(3,2;y) - 4H(1,0;y)H(3,2;y) - 4H(1;y)H(0,0,1;z)\\
&- 24H(1;y)H(0,1,0;y) + 8H(1;z)H(0,1,0;y) + 4H(1;y)H(0,1,0;z)\\
&+ 4H(2;y)H(0,1,0;z) - 4H(1;z)H(0,2,3;y) - 4H(1;z)H(0,3,0;y)\\
&+ 8H(1;z)H(1,0,0;y) + 8H(2;y)H(1,0,0;z) - 4H(1;y)H(1,0,1;z)\\
&- 8H(3;y)H(1,0,1;z) - 4H(0;y)\Big\{3\zeta_3 - 2\zeta_2H(1;z) - 2\zeta_2H(2;y)\\
&- 2H(2;y)H(0,0;z) + 2H(2;y)H(0,1;z) + H(0;z)\Big\{ - (H(1;z)(H(2;y)\\
&- 3H(3;y))) + H(2,0;y) + 2(\zeta_2 + H(3,2;y))\Big\} + 5H(0,0,1;z) + 3H(0,1,0;z)\\
&- H(0,3,2;y) + 4H(1,0,0;z) + H(1,0,1;z) - H(1,1,0;z)\Big\} + 4H(1;y)H(1,1,0;z)\\
&- 16H(3;y)H(1,1,0;z) - 4H(1;z)H(1,2,3;y) - 4H(1;z)H(1,3,0;y)\\
&- 4H(0;z)\Big\{3\zeta_3 - \zeta_2H(1;y) - \zeta_2H(2;y) + H(2;y)H(1,0;y) + H(1;z)(3\zeta_2\\
&- 2H(0,0;y) + 2H(1,0;y) - H(1,2;y) - H(3,0;y) + 2H(3,2;y)) + 2H(0,0,2;y)\\
&+ 2H(0,1,0;y) + H(0,3,2;y) + 6H(1,0,0;y) - H(1,2,0;y) - 2H(2,0,0;y)\\
&- 2H(2,1,0;y)\Big\} - 8H(1;z)H(3,0,0;y) - 4H(1;z)H(3,1,0;y) + 12H(0,0,0,1;z)\\
&- 8H(0,0,1,0;y) - 4H(0,0,1,0;z) + 24H(0,1,0,1;y) - 4H(0,1,0,1;z)\\
&+ 8H(0,1,0,2;y) + 32H(0,1,1,0;y) - 16H(0,1,1,0;z) + 8H(0,1,2,0;y)\\
&+ 8H(0,2,1,0;y) - 4H(0,2,3,2;y) - 4H(1,0,0,1;z) + 8H(1,0,0,2;y)\\
&- 20H(1,0,1,0;z) + 8H(1,0,2,0;y) - 32H(1,1,0,0;y) - 16H(1,1,0,0;z)\\
&- 4H(1,1,0,1;z) - 16H(1,1,1,0;y) - 16H(1,1,1,0;z) + 8H(1,2,0,0;y)\\
&- 4H(1,2,3,2;y) - 4H(1,3,0,2;y) - 4H(1,3,2,0;y) + 4H(2,0,1,0;y)\\
&+ 8H(2,1,0,0;y) - 4H(3,1,0,2;y) - 4H(3,1,2,0;y) - 4H(3,2,1,0;y)\Big\}
\end{aligned}
$$

$$
\begin{aligned}
&+ C_{2,q}\Bigg\{\frac{32}{9}\Big\{761(-1+z)^2z^2 - 2yz^2(869 - 1630z + 761z^2) + y^4(761 - 1522z \\
&+ 815z^2) + 2y^3(-761 + 1630z - 1139z^2 + 216z^3) + y^2(761 - 1738z + 2494z^2 \\
&- 2278z^3 + 815z^4)\Big\}\zeta_3 + \frac{64}{3}(-1+y)^2\Big\{-12y(-1+z)z^2 + 11(-1+z)^2z^2 \\
&+ y^2(38 - 76z + 35z^2)\Big\}\zeta_2 H(0;y) + \frac{64}{3}(-1+z)^2\Big\{11y^4 + 38z^2 - 76yz^2 - 2y^3(11+6z) \\
&+ y^2(11 + 12z + 35z^2)\Big\}\zeta_2 H(0;z) + \frac{64}{3}(-1+y)^2(-1+z)^2(31y^2 + 22z^2)H(0;y)^2 \\
&\times H(0;z) - \frac{32}{3}\Big\{(-1+z)^2z(-36+103z) + y^4(31 - 62z + 37z^2) + 2yz(54 - 223z \\
&+ 272z^2 - 103z^3) + 2y^3(-31 + 92z - 109z^2 + 42z^3) + y^2(31 - 194z + 458z^2 \\
&- 398z^3 + 109z^4)\Big\}\zeta_2 H(1;z) + \frac{128}{3}(-1+y)^2(-1+z)^2(8y^2 - z^2)H(0;y)H(0;z) \\
&\times H(1;z) - \frac{32}{3}\Big\{13(-1+z)^2z^2 + y^4(13 - 26z + 10z^2) - 2yz^2(7 - 20z + 13z^2) \\
&+ y^3(-26 + 40z + 16z^2 - 24z^3) + y^2(13 - 14z - 28z^2 + 16z^3 + 10z^4)\Big\}H(0;z) \\
&\times H(1;z)^2 - \frac{32}{3}\Big\{(-1+z)^2z(-36+59z) + y^4(59 - 118z + 65z^2) + 2y^3(-77 + 202z \\
&- 191z^2 + 60z^3) - 2y(18 - 108z + 233z^2 - 202z^3 + 59z^4) + y^2(131 - 466z + 658z^2 \\
&- 382z^3 + 65z^4)\Big\}\zeta_2 H(2;y) - 192(-1+y)^2y(-1+z)^2(-1+y+z)H(0;z)^2H(2;y) \\
&- \frac{64}{3}(-1+z)^2\Big\{31y^4 + 4z^2 + 10y^3(-8+3z) - 2y(9 - 9z + 4z^2) + y^2(67 - 48z + 7z^2)\Big\} \\
&\times H(0;z)H(1;z)H(2;y) - \frac{64}{3}(-1+y)^2\Big\{2(-1+z)^2z(9+z) - 6yz(1 - 4z + 3z^2) \\
&+ y^2(41 - 82z + 38z^2)\Big\}H(0;y)H(0,1;z) + \frac{64}{3}\Big\{13(-1+z)^2z^2 + y^4(40 - 80z + 43z^2) \\
&+ y^3(-98 + 238z - 200z^2 + 54z^3) - 2y(9 - 27z + 46z^2 - 41z^3 + 13z^4) + y^2(76 \\
&- 212z + 242z^2 - 122z^3 + 19z^4)\Big\}H(2;y)H(0,1;z) + \frac{64}{3}(-1+z)^2\Big\{5y^4 - 22z^2 \\
&+ y^3(-28 + 30z) + y^2(41 - 48z - 19z^2) + 2y(-9 + 9z + 22z^2)\Big\}H(0;z)H(0,2;y) \\
&- 64\Big\{-6(-1+z)^3z + y^4(10 - 20z + 9z^2) + y^3(-26 + 60z - 36z^2 + 4z^3) \\
&+ y^2(22 - 50z + 20z^2 + 12z^3 - 5z^4) + 2y(-3 + 2z + 13z^2 - 18z^3 + 6z^4)\Big\}H(1;z) \\
&\times H(0,3;y) + \frac{128}{3}(-1+y)^2(-1+z)^2(y^2 + 10z^2)H(0;z)H(1,0;y) - \frac{1408}{3}(-1+y)^2 \\
&\times(-1+z)^2(y^2+z^2)\Big\{H(1;z)H(1,0;y) + H(2;y)H(1,0;y) + (2H(0;z)H(2,0;y))/11\Big\}
\end{aligned}
$$

$$
\begin{aligned}
&- 64(-1+y)^2(-1+z)^2(y^2+4yz+3z^2)(H(1;z)H(3,0;y)+H(0;y)H(3,2;y))\\
&- 64(-1+y)^2(-1+z)^2(3y^2+4yz+z^2)\Big\{H(0;z)H(1;z)H(3;y)+H(0;z)H(3,2;y)\Big\}\\
&+ 64\Big\{-3(-2+z)(-1+z)^2z+y^4(5-10z+4z^2)+2y^3(-5+13z-8z^2+z^3)\\
&+ 2yz(-5+15z-13z^2+3z^3)+y^2(5-12z-2z^2+10z^3-2z^4)\Big\}H(0,0,1;z)\\
&+ 64(-1+y)^2\Big\{2(-1+z)^2z(-3+10z)+2yz(5-8z+3z^2)+y^2(15-30z+14z^2)\Big\}\\
&\times H(0,1,0;y)+64(-1+z)^2\Big\{11y^4+14z^2-28yz^2-2y^3(11+2z)+y^2(11+4z\\
&+ 13z^2)\Big\}H(0,1,0;z)+\frac{64}{3}\Big\{13(-1+z)^2z^2+y^4(13-26z+10z^2)-2yz^2(7-20z\\
&+ 13z^2)+y^3(-26+40z+16z^2-24z^3)+y^2(13-14z-28z^2+16z^3+10z^4)\Big\}\\
&\times H(0,1,1;z)-64\Big\{-3(-1+z)^2z(-2+3z)+y^3(-24+52z-26z^2)+y^4(9-18z\\
&+ 8z^2)+y^2(21-40z+26z^3-8z^4)+2y(-3+20z^2-26z^3+9z^4)\Big\}H(0,3,2;y)\\
&+ \frac{128}{3}(-1+y)^2(-1+z)^2(31y^2+9yz+z(-9+31z))H(1,0,0;y)+\frac{64}{3}(-1+y)^2\\
&\times(-1+z)^2(22y^2+31z^2)\Big\{H(0;y)H(0;z)^2+2H(1,0,0;z)\Big\}-\frac{128}{3}(-1+y)^2(-1+z)^2\\
&\times(11y^2-9yz+(9-7z)z)(\zeta_2H(1;y)+H(1,1,0;y))-\frac{64}{3}\Big\{35(-1+z)^2z^2\\
&+ y^4(26-52z+29z^2)-2yz^2(41-76z+35z^2)+2y^3(-26+64z-59z^2+18z^3)\\
&+ y^2(26-76z+142z^2-130z^3+41z^4)\Big\}H(1,1,0;z)-384(-1+y)^2(-1+z)^2z\\
&\times(-1+y+z)\Big\{(H(0;y)^2H(1;z))/2+H(0;y)H(0,2;y)-H(0,0,2;y)\\
&+ H(2,0,0;y)\Big\}+64(-1+y)^2\Big\{-3(-2+z)(-1+z)^2z+y^2(6-12z+5z^2)\\
&- 2yz(3-8z+5z^2)\Big\}H(2,1,0;y)+64\Big\{3(-1+z)^2z^2-2yz^2(5-8z+3z^2)\\
&+ y^4(3-6z+4z^2)+2y^3(-3+8z-10z^2+4z^3)+y^2(3-10z+24z^2-20z^3+4z^4)\Big\}\\
&\times(H(1;z)H(2;y)H(3;y)-H(1;z)H(3,2;y)+H(2,3,2;y))+512(-1+y)^2\\
&\times(-1+z)^2(y+z)^2((H(1;z)H(3;y)^2)/2+H(3;y)H(0,1;z)+H(3,3,2;y))\Big\}\\
&+ C_{3,q}\Big\{-64y^2z^2\Big\{43y^4(-1+z)-43(-1+z)^2z^2+yz^2(90-133z+43z^2)\\
&+ y^3(86-133z+48z^2)+y^2(-43+90z-96z^2+48z^3)\Big\}\zeta_2-\frac{32}{3}(-1+y)y^2
\end{aligned}
$$

$$\times(-1+z)z^2(307y^3+325yz^2+307(-1+z)z^2+y^2(-307+325z))H(0;y)H(0;z)$$
$$-\frac{32}{3}y^2(-1+z)z^2\Big\{307y^4-307(-1+z)z^2+y^3(-614+325z)+yz(-6-626z$$
$$+307z^2)+y^2(307-319z+325z^2)\Big\}H(0;z)H(1;z)-32(-1+z)z^2\Big\{33y^6$$
$$+(-1+z)^3z^2+y^5(-64+39z)-y(-1+z)^2z(2-10z+z^2)+y^4(26-41z+36z^2)$$
$$+y^3(8-5z-52z^2+22z^3)+y^2(-3+9z+3z^2-9z^4)\Big\}H(0;z)H(2;y)$$
$$-\frac{32}{3}y^2\Big\{3y^6(-1+z)+3y^5(4-13z+9z^2)+(-1+z)^2z^2(-9+6z+406z^2)$$
$$+y^4(-18+105z+280z^2-373z^3)+y^3(12-111z-623z^2+1155z^3-433z^4)$$
$$+y^2(-3+48z+289z^2-749z^3+863z^4-442z^5)-yz(6-36z+57z^2+803z^3$$
$$-1236z^4+406z^5)\Big\}H(0,1;z)-\frac{32}{3}y^2\Big\{3y^6(-1+z)+3y^5(4-13z+9z^2)$$
$$-(-1+z)^2z^2(9-6z+208z^2)+y^4(-18+105z-334z^2+241z^3)+y^3(12$$
$$-111z+605z^2-711z^3+217z^4)+yz(-6+36z-33z^2+425z^3-630z^4+208z^5)$$
$$+y^2(-3+48z-325z^2+479z^3-413z^4+208z^5)\Big\}H(1,0;y)+32y^2\Big\{y^6(-1+z)$$
$$+y^5(4-13z+9z^2)+(-1+z)^2z^2(-3+2z+33z^2)-y^4(6-35z+9z^2+22z^3)$$
$$+y^3(4-37z-3z^2+74z^3-36z^4)-yz(2-12z+13z^2+67z^3-103z^4+33z^5)$$
$$-y^2(1-16z+6z^2+47z^3-77z^4+39z^5)\Big\}\Big\{H(0;y)H(1;z)+H(0,2;y)+H(2,0;y)\Big\}$$
$$-32\Big\{y^8(-1+z)-(-1+z)^4z^4+y(-1+z)^3z^3(2-10z+z^2)+y^7(4-13z+9z^2)$$
$$+y^6(-6+35z+24z^2-55z^3)+y^2(-1+z)^2z^2(-6+8z+42z^2+9z^3)+y^5(4-37z$$
$$-67z^2+175z^3-75z^4)+y^4(-1+16z+20z^2-108z^3+150z^4-75z^5)$$
$$-y^3z(2-20z+30z^2+108z^3-175z^4+55z^5)\Big\}\Big\{H(1;z)H(3;y)+H(3,2;y)\Big\}\Big\}$$
$$+\frac{32}{27}C_{7,q}\Big\{9y(-1+z)(3y^4+y^3(-6+145z)-z^2(11+149z)+y^2(3-109z-69z^2)$$
$$+yz(-36+80z+109z^2))H(0;y)+(-1+y)\Big\{9z\Big\{3(-1+z)^2z^2+y^3(-149+109z)$$
$$+y^2(-11+80z-69z^2)+yz(-36-109z+145z^2)\Big\}H(0;z)+(-1+z)\Big\{27y^4$$
$$+27(-1+z)^2z^2-2y^3(27+1547z)+9y^2(3-46z+38z^2)-2yz(-108+207z$$

$$+ 1547z^2)\Big\}(H(1;z) + H(2;y))\Big\}\Big\} - \frac{16}{81}C_{6,q}\Big(324 + 56327y^2 + 14040z + 56327z^2$$
$$- 216y(-65 + 133z)\Big)\Big]. \tag{B.15}$$

$$\begin{aligned}
S_q^{(2),1/N^2} = \frac{1}{N^2}\Bigg[\frac{-128\,C_{1,q}}{5}\Big\{&37\zeta_2^2 - 15\zeta_3 H(1;y) - 55\zeta_3 H(1;z) + 5\zeta_2 H(1;y)H(1;z)\\
&- 40\zeta_3 H(2;y) + 5\zeta_2 H(1;z)H(2;y) + 5\zeta_2 H(0,0;y) - 10H(1;z)H(3;y)H(0,0;y)\\
&+ 5\zeta_2 H(0,0;z) + 5H(0,0;y)H(0,0;z) + 10\zeta_2 H(0,1;y) - 5\zeta_2 H(0,1;z)\\
&- 5H(0,0;y)H(0,1;z) + 15\zeta_2 H(1,0;y) + 10H(1;z)H(3;y)H(1,0;y)\\
&+ 10\zeta_2 H(1,1;y) + 20\zeta_2 H(1,1;z) + 5\zeta_2 H(1,2;y) - 15H(0,1;z)H(1,2;y)\\
&+ 5H(0,0;z)H(2,0;y) + 5\zeta_2 H(2,1;y) + 10H(1,0;y)H(3,2;y)\\
&- 10H(1;y)H(0,0,1;z) + 20H(1;y)H(0,1,0;y) - 5H(1;z)H(0,1,0;y)\\
&+ 5H(1;y)H(0,1,0;z) - 10H(1;z)H(0,2,3;y) + 10H(1;z)H(0,3,0;y)\\
&- 10H(1;z)H(1,0,0;y) - 5H(2;y)H(1,0,0;z) - 10H(1;y)H(1,0,1;z)\\
&- 10H(2;y)H(1,0,1;z) + 5H(1;y)H(1,1,0;z) - 5H(2;y)H(1,1,0;z)\\
&- 5H(0;y)(4\zeta_3 - 2\zeta_2 H(1;z) - \zeta_2 H(2;y) + 2H(2;y)H(0,0;z) + H(2;y)H(0,1;z)\\
&+ H(0;z)(-4\zeta_2 + H(1;z)H(2;y) + 2H(2,2;y)) - H(0,1,0;z) - H(1,0,0;z)\\
&+ 3H(1,0,1;z) + H(1,1,0;z)) - 10H(1;z)H(1,2,3;y) - 10H(1;z)H(1,3,0;y)\\
&- 10H(1;z)H(2,1,0;y) - 10H(2;y)H(2,1,0;y) - 5H(0;z)\Big\{4\zeta_3 - \zeta_2 H(1;y)\\
&- \zeta_2 H(2;y) + H(2;y)H(1,0;y) - H(1;z)\Big\{4\zeta_2 - H(0,0;y) + H(1,0;y)\\
&+ H(1,2;y)\Big\} - H(0,1,0;y) - 2H(0,2,2;y) - 2H(1,0,0;y) - H(1,2,0;y)\\
&+ H(2,0,0;y) - 2H(2,2,0;y)\Big\{ + 10H(1;z)H(3,0,0;y) - 10H(1;z)H(3,1,0;y)\\
&- 10H(0,0,0,1;z) + 10H(0,0,1,0;y) + 10H(0,0,1,0;z) - 10H(0,0,3,2;y)\\
&- 20H(0,1,0,1;y) - 15H(0,1,0,1;z) - 5H(0,1,0,2;y) - 30H(0,1,1,0;y)\\
&+ 10H(0,1,1,0;z) - 5H(0,1,2,0;y) + 5H(0,2,1,0;y) - 10H(0,2,3,2;y)
\end{aligned}$$

$$
\begin{aligned}
&- 10H(1,0,0,2;y) + 10H(1,0,1,0;z) - 10H(1,0,2,0;y) + 20H(1,1,0,0;y)\\
&+ 5H(1,1,0,0;z) - 20H(1,1,0,1;z) + 10H(1,1,1,0;y) - 10H(1,2,0,0;y)\\
&- 5H(1,2,1,0;y) - 10H(1,2,3,2;y) - 10H(1,3,0,2;y) - 10H(1,3,2,0;y)\\
&- 5H(2,1,0,0;y) + 5H(2,1,1,0;y) + 20H(2,2,1,0;y) - 10H(3,1,0,2;y)\\
&- 10H(3,1,2,0;y) - 10H(3,2,1,0;y)\Big\} + C_{2,q}\Big\{192\Big\{9(-1+z)^2z^2 - 2yz^2(11-20z\\
&+ 9z^2) + y^4(9-18z+10z^2) + 2y^3(-9+20z-16z^2+4z^3) + y^2(9-22z+36z^2\\
&- 32z^3+10z^4)\Big\}\zeta_3 - 64(-1+y)^2\big\{4y(-1+z)z^2 + 6(-1+z)^2z^2 + y^2(3-6z+4z^2)\big\}\\
&\times \zeta_2H(0;y) - 96(-1+y)^2(-1+z)^2z^2H(0;y)^2H(0;z) - 64\Big\{(-1+z)^2(-1+4z\\
&+ 9z^2) + y^4(14-28z+15z^2) + y^3(-26+52z-32z^2+4z^3) + y(4-20z+6z^2\\
&+ 28z^3-18z^4) + y^2(9-10z+12z^2-20z^3+10z^4)\Big\}\zeta_2H(1;z) + 32((-1+z)^2\\
&\times (-1+4z) + y^4(2-4z+3z^2) - 4y(-1+5z-6z^2+2z^3) + y^3(-2+4z-8z^2\\
&+ 4z^3) + y^2(-3+14z-9z^2-2z^3+z^4))H(0;z)H(1;z)^2 - 64\Big\{-2y^3(5-8z+4z^2)\\
&+ 2(-1+z)^2(-1+3z+4z^2) + y^4(8-16z+9z^2) - 2y(-5+20z-15z^2-8z^3\\
&+ 8z^4) + y^2(-6+30z-24z^2-8z^3+9z^4)\Big\}\zeta_2H(2;y) - 32(-1+y)^2(3y^2\\
&+ 4y(-1+z) + (-1+z)^2)(-1+z)^2H(0;z)^2H(2;y) - 64(-1+z)^2\big\{6y^4\\
&+ 4y^3(-3+z) + 3z^2 - 6yz^2 + y^2(6-4z+4z^2)\big\}\big\{\zeta_2H(0;z) + H(0;z)H(1;z)H(2;y)\big\}\\
&+ 64(-1+y)^2\big\{y^2(4-8z+5z^2) + (-1+z)^2(1-4z+9z^2) + 2y(-1+4z-7z^2\\
&+ 4z^3)\big\}H(0;y)H(0,1;z) + 64\Big\{2(-1+z)^2(-1+3z+z^2) + y^4(5-10z+6z^2)\\
&+ 2y^3(-2+4z-5z^2+2z^3) - 2y(-5+20z-21z^2+4z^3+2z^4) + y^2(-9+32z\\
&- 24z^2-2z^3+4z^4)\Big\}H(2;y)H(0,1;z) - 64(-1+y)^2(-1+z)^2\big\{1+y^2-4z+3z^2\\
&+ y(-2+4z)\big\}H(0;y)H(0,2;y) + 64(-1+z)^2(6y^4+8y^3(-2+z) + (-1+z)^2\\
&- 2y(3-4z+z^2) + y^2(15-14z+2z^2))H(0;z)H(0,2;y) - 192(-1+y)^2(-1+z)^2\\
&\times (y^2+z^2)(H(0;y)H(0;z)H(1;z) + H(0;z)H(2,0;y)) + 64\Big\{y^4(2-4z+z^2)\\
&- (-1+z)^2(1-4z+6z^2) + y^3(-2+4z+4z^2-4z^3) + y^2(-3+14z-33z^2+26z^3
\end{aligned}
$$

$$- 5z^4) + 4y(1 - 5z + 11z^2 - 10z^3 + 3z^4)\Big\}H(0,0,1;z) - 32(-1+y)^2(-1+z)^2$$
$$\times (1 + y^2 - 4z + 3z^2 + y(-2+4z))\Big\{H(0;y)^2 H(1;z) - 2H(1;z)H(1,0;y)$$
$$- 2H(2;y)H(1,0;y) - 2H(0,0,2;y)\Big\} - 64(-1+y)^2\Big\{y^2(-1+2z) + (-1+z)^2$$
$$\times (-1 + 4z + 3z^2) + y(2 - 8z + 6z^2)\Big\}H(0,1,0;y) - 64y^2(-1+z)^2(6 + 6y^2$$
$$+ 4y(-3+z) - 4z + z^2)H(0,1,0;z) - 64\Big\{(-1+z)^2(-1+4z) + y^4(2 - 4z + 3z^2)$$
$$- 4y(-1 + 5z - 6z^2 + 2z^3) + y^3(-2 + 4z - 8z^2 + 4z^3) + y^2(-3 + 14z - 9z^2$$
$$- 2z^3 + z^4)\Big\}H(0,1,1;z) - 64\Big\{ - ((-1+z)^2 z(-2+5z)) + y^4(5 - 10z + 4z^2)$$
$$- 2y^3(6 - 14z + 7z^2) + y^2(9 - 20z + 14z^3 - 4z^4) + 2y(-1 + 10z^2 - 14z^3 + 5z^4)\Big\}$$
$$\times \Big\{H(1;z)H(0,3;y) + H(0,3,2;y)\Big\} + 64(-1+y)^3(-1+z)^2(-1+y+4z)$$
$$\times H(1,0,0;y) - 96(-1+y)^2 y^2(-1+z)^2\Big\{H(0;y)H(0;z)^2 + 2H(1,0,0;z)\Big\}$$
$$- 64(-1+y)^2(-1+z)^2(1 + y^2 - 4z + 6z^2 + y(-2+4z))\Big\{\zeta_2 H(1;y) + H(1,1,0;y)\Big\}$$
$$- 64\Big\{(-1+z)^2(-1 + 4z + 3z^2) + y^4(11 - 22z + 12z^2) + y^3(-20 + 44z - 34z^2$$
$$+ 8z^3) + y(4 - 20z + 18z^2 + 4z^3 - 6z^4) + y^2(6 - 8z + 12z^2 - 14z^3 + 5z^4)\Big\}$$
$$\times H(1,1,0;z) - 64(-1+y)^2(-1+z)^2(1 + y^2 - 4z + 3z^2 + y(-2+4z))H(2,0,0;y)$$
$$- 64(-1+y)^2\Big\{y^2(4 - 8z + 5z^2) + (-1+z)^2(1 - 4z + 9z^2) + 2y(-1 + 4z - 7z^2$$
$$+ 4z^3)\Big\}H(2,1,0;y) + 64\Big\{y^4(-1+2z) - (-1+z)^2(2 - 6z + z^2) + 2y^3(4 - 10z$$
$$+ 5z^2) + y^2(-15 + 48z - 42z^2 + 10z^3) + 2y(5 - 20z + 24z^2 - 10z^3 + z^4)\Big\}$$
$$\times \Big\{H(1;z)H(2;y)H(3;y) - H(1;z)H(3,2;y) + H(2,3,2;y)\Big\}\Big\} + C_{3,q}\Big\{ - 32y^2 z^2$$
$$\times \Big\{55y^4(-1+z) - (-1+z)^2 z(4 + 55z) + y^3(106 - 153z + 49z^2) + y^2(-47 + 82z$$
$$- 86z^2 + 49z^3) + y(-4 + 20z + 82z^2 - 153z^3 + 55z^4)\Big\}\zeta_2 - 32(-1+y)y^2(-1+z)z^3$$
$$\times (-1+y+z)^2 H(0;y)^2 - 64(-1+y)y^2(-1+z)z^2(13y^3 + 2y^2(-6+5z)$$
$$+ y(-1 + 2z + 10z^2) + z(-1 - 12z + 13z^2))H(0;y)H(0;z) - 32(-1+y)y^3(-1+z)$$
$$\times z^2(-1+y+z)^2 H(0;z)^2 - 64y^2(-1+z)z^2\Big\{14y^4 + z + 12z^2 - 13z^3$$

$$
\begin{aligned}
&+ 3y^3(-9 + 4z) + y^2(12 - 10z + 11z^2) + y(1 - 3z - 22z^2 + 13z^3)\Big\}H(0;z)H(1;z) \\
&- 32(-1 + z)z^2(-1 + y + z)^2(-11y^4 - 5(-1 + z)z^2 + y^3(6 + 17z) + y^2(5 - 27z + z^2) \\
&+ yz(12 - 6z + 5z^2))H(0;z)H(2;y) - 32z^2(-1 + y + z)^2\Big\{11y^4(-1 + z) \\
&+ 5(-1 + z)^2z^2 + y^3(8 + 7z - 17z^2) + yz(12 - 18z + 11z^2 - 5z^3) - y^2(-5 + 30z \\
&- 28z^2 + z^3)\Big\}H(1;z)H(3;y) + 32y^2\Big\{5y^6(-1 + z) + y^5(20 - 31z + 11z^2) + y^4(-30 \\
&+ 75z - 95z^2 + 52z^3) + y^3(20 - 89z + 209z^2 - 188z^3 + 48z^4) + yz(-12 + 62z \\
&- 65z^2 + 33z^3 - 33z^4 + 15z^5) + y^2(-5 + 52z - 182z^2 + 201z^3 - 85z^4 + 17z^5) \\
&- 5(z^2 - 4z^5 + 3z^6)\Big\}H(0,1;z) - 32y^2(-1 + y + z)^2(5y^4(-1 + z) + y^3(10 - 11z \\
&+ z^2) + z^2(-5 - 6z + 11z^2) - yz(12 - 32z + 11z^2 + 11z^3) + y^2(-5 + 18z - 28z^2 \\
&+ 17z^3))H(0,2;y) + 32y^2(5y^6(-1 + z) + y^5(20 - 31z + 11z^2) + (-1 + z)^2z^2 \\
&\times(-5 - 4z + 39z^2) - y^4(30 - 75z + 41z^2 + 2z^3) + y^3(20 - 89z + 107z^2 - 44z^3 \\
&+ 2z^4) - y^2(5 - 52z + 140z^2 - 133z^3 + 9z^4 + 29z^5) - yz(12 - 68z + 93z^2 + 35z^3 \\
&- 111z^4 + 39z^5))H(1,0;y) - 32y^2(-1 + y + z)^2\Big\{5y^4(-1 + z) + y^3(10 - 11z + z^2) \\
&+ z^2(-5 - 6z + 11z^2) - yz(12 - 32z + 11z^2 + 11z^3) + y^2(-5 + 18z - 28z^2 + 17z^3)\Big\} \\
&\times\Big\{H(0;y)H(1;z) - H(1;z)H(3;y) + H(2,0;y)\Big\} + 32(-1 + y + z)^2(5y^6(-1 + z) \\
&- 5(-1 + z)^2z^4 + y^5(10 - 11z + z^2) + y^2z^2(-10 + 24z - 17z^2 + z^3) + 6y^3z(-2 + 4z \\
&- 3z^2 + z^3) + yz^3(-12 + 18z - 11z^2 + 5z^3) + y^4(-5 + 18z - 17z^2 + 6z^3))H(3,2;y)\Big\} \\
&- 16\,C_{7,q}\Big\{2y(-1 + z)\Big\{5y^4 + y(10 - 19z)z - 3(-1 + z)z^2 + y^3(-10 + 21z) + y^2(5 \\
&- 31z + 16z^2)\Big\}H(0;y) + (-1 + y)(2z(-3y^3 + 5(-1 + z)^2z^2 + y^2(3 - 19z + 16z^2) \\
&+ yz(10 - 31z + 21z^2))H(0;z) + (-1 + z)\Big\{10y^4 + 10(-1 + z)^2z^2 + y^3(-20 + 39z) \\
&+ 2y^2(5 - 37z + 32z^2) + yz(32 - 74z + 39z^2)\Big\}(H(1;z) + H(2;y)))\Big\} \\
&- 4\,C_{6,q}\Big\{8 + 391y^2 + 112z + 391z^2 - 16y(-7 + 15z)\Big\}\Big]. \qquad \text{(B.16)}
\end{aligned}
$$

$$
\begin{aligned}
S_q^{(2),n_f/N} = \frac{n_f}{N}\Bigg[&\frac{64\,C_{1,q}}{9}\Big\{119\zeta_3 - 12H(0;y)^2H(0;z) + 12\zeta_2H(1;y) + 33\zeta_2H(1;z)\\
&+ 21\zeta_2H(2;y) - 12H(2;y)H(0,1;z) + 12H(1;z)H(1,0;y) + 12H(2;y)H(1,0;y)\\
&- 18H(0,1,0;y) - 18H(0,1,0;z) - 12H(0,1,1;z) - 24H(1,0,0;y)\\
&- 24H(1,0,0;z) + 12H(1,1,0;y) + 24H(1,1,0;z) - 6H(0;y)(\zeta_2 + 2H(0;z)^2\\
&- H(0,1;z) - H(0;z)H(1;z)) - 6H(0;z)(\zeta_2 - H(1;z)^2 - 2H(0,2;y) + H(1,0;y)\\
&- 2H(2,0;y) - 2H(1;z)H(2;y))\Big\} + \frac{64\,C_{1,q}}{3}\Big\{33\zeta_2 + 26H(0;y)H(0;z)\\
&+ 26H(0;z)H(1;z) - 26H(0,1;z) + 26H(1,0;y)\Big\} - \frac{64}{27}C_{9,q}\Big\{9(-1+z)\big\{5y^4\\
&- y^3(2+z) - z^2(1+7z) - y^2(3-5z+z^2) + yz(-4+5z^2)\big\}H(0;y) + (-1+y)\\
&\times\Big\{9(y^3(-7+5z) - y^2(1+z^2) - yz(4-5z+z^2) + z^2(-3-2z+5z^2))H(0;z)\\
&- (-1+z)(173y^3 + yz(36+137z) + y^2(180+137z) + z^2(180+173z))(H(1;z)\\
&+ H(2;y))\Big\}\Big\} - \frac{16}{81}C_{6,q}\big\{2521y^2 + 1728y(-1+2z) + z(-1728+2521z)\big\}\Bigg].
\end{aligned}
\tag{B.17}
$$

$$
\begin{aligned}
S_q^{(2),n_fN} = \mathbf{N}\,\mathbf{n_f}\Bigg[&\frac{-64\,C_{1,q}}{9}\Big\{12H(0;y)^2H(1;z) + 12H(0;z)^2H(2;y) + 3H(0;y)\big\{3\zeta_2\\
&+ 2H(0;z)H(1;z) - 10H(1;z)^2 - 10H(2;y)^2 - 10H(0,1;z) + 8H(0,2;y)\\
&- 4H(3,2;y)\big\} + 3H(0;z)\big\{3\zeta_2 + 8H(1;z)^2 - 10H(2;y)^2 - 4H(1;z)(2H(2;y)\\
&+ H(3;y)) - 4H(0,2;y) - 2H(1,0;y) + 4H(2,0;y) - 4H(3,2;y)\big\} + 2\Big\{-43\zeta_3\\
&+ 6\zeta_2H(1;y) + 30H(1;z)^2H(3;y) + 30H(2;y)H(0,1;z) + 12H(3;y)H(0,1;z)\\
&+ 6H(2;y)H(1,0;y) + 12H(0,0,1;z) - 12H(0,0,2;y) - 9H(0,1,0;y)\\
&- 3H(0,1,0;z) + 6H(0,1,1;z) - 12H(1,0,0;y) + 6H(1,1,0;y) - 24H(1,1,0;z)\\
&+ 12H(2,0,0;y) + 12H(2,1,0;y) + 48H(2,3,2;y) + 60H(3,2,2;y)\\
&+ 12H(3,3,2;y) + 6H(1;z)(\zeta_2 + 8H(2;y)H(3;y) + H(3;y)^2 - 5H(0,2;y)\\
&- H(0,3;y) + H(1,0;y) - 5H(2,0;y) - H(3,0;y) + 2H(3,2;y))\Big\}\Big\}
\end{aligned}
$$

$$
\begin{aligned}
&+ C_{5,q}\bigg\{ - \frac{64}{9}z^2\Big\{ - 25y^4 + 36y(-1+z)^2z + 18(-1+z)^2z^2 + 6y^3(1+3z) + y^2(12 \\
&- 84z + 47z^2)\Big\}H(0;z)H(2;y) + \frac{160}{9}y^2z^2(y^2+z^2)\Big\{\zeta_2 + \frac{51}{5}H(0;y)^2 \\
&+ 8H(0;y)H(0;z) + \frac{51}{5}H(0;z)^2 - \frac{106}{5}H(0;z)H(1;z) + \frac{174}{5}H(1;z)^2 \\
&+ \frac{348}{5}H(1;z)H(2;y) + \frac{174}{5}H(2;y)^2\Big\} + \frac{128}{3}y^2\Big\{3y^4 + 6y^3(-1+z) + z^2(2+z \\
&- 13z^2) - y^2(-3+12z+z^2) + yz(6-14z+3z^2)\Big\}\Big\{H(0,1;z) + H(1,0;y)\Big\} \\
&- \frac{64}{9}y^2\Big\{18y^4 + 36y^3(-1+z) + z^2(12+6z-25z^2) + 6yz(6-14z+3z^2) \\
&+ y^2(18-72z+47z^2)\Big\}(H(0;y)H(1;z) + H(0,2;y) + H(2,0;y)) + \frac{128}{3}\Big\{3y^6 \\
&+ 6y^5(-1+z) + 6y(-1+z)^2z^3 + 3(-1+z)^2z^4 + y^2z^2(4-13z-14z^2) \\
&+ y^4(3-12z-14z^2) + y^3z(6-13z+6z^2)\Big\}\Big\{H(1;z)H(3;y) + H(3,2;y)\Big\}\bigg\} \\
&- \frac{64}{27}C_{8,q}\bigg\{y(-1+z)\Big\{54y^5 + (27-490z)z^3 + 4y^4(-27+163z) + yz^2(108-643z \\
&+ 508z^2) + y^2z(135-832z+634z^2) + y^3(54-787z+724z^2)\Big\}H(0;y) \\
&+ (-1+y)(z(54(-1+z)^2z^3 + y^4(-490+508z) + 4y^2z(27-208z+181z^2) \\
&+ y^3(27-643z+634z^2) + yz^2(135-787z+652z^2))H(0;z) + 3(-1+z)(18y^5 \\
&+ 18(-1+z)^2z^3 - y^4(36+497z) + yz^2(78-66z-497z^2) + y^2z(78-288z \\
&- 383z^2) + y^3(18-66z-383z^2))(H(1;z) + H(2;y)))\bigg\} \\
&+ \frac{16}{81}C_{6,q}\Big(36557y^2 - 3024y(-1+2z) + z(3024+36557z)\Big)\bigg]. \qquad \text{(B.18)}
\end{aligned}
$$

$$
\begin{aligned}
S_q^{(2),n_f^2} &= n_f^2\bigg[\frac{-32\,C_{1,q}}{9}\Big\{3H(0;y)^2 + 3H(0;z)^2 + 2H(0;y)(H(0;z) - 4H(1;z)) \\
&- 8H(0;z)(H(1;z) + H(2;y)) + 2(\zeta_2 + 12H(1;z)^2 + 24H(1;z)H(2;y) + 12H(2;y)^2 \\
&- 4H(0,2;y) - 4H(2,0;y))\Big\} + \frac{640\,C_{1,q}}{9}\Big\{H(0;y) + H(0;z) - 4(H(1;z) + H(2;y))\Big\} \\
&- \frac{6400\,C_{1,q}}{27}\bigg]. \qquad \text{(B.19)}
\end{aligned}
$$

where the constants $C_{i,q}$ are

$$
\begin{aligned}
C_{1,q} &= \frac{Q^2(y^2+z^2)}{(-1+y+z)}\,, C_{2,q} = \frac{Q^2}{(-1+y)^2(-1+z)^2(-1+y+z)}\,,\\
C_{3,q} &= \frac{Q^2}{y^2z^2(-1+y+z)^2(-1+y)(-1+z)}\,, C_{4,q} = \frac{Q^2}{yz(-1+y+z)}\,,\\
C_{5,q} &= \frac{Q^2}{y^2z^2(-1+y+z)}\,, C_{6,q} = \frac{Q^2}{(-1+y+z)}\,, C_{7,q} = \frac{Q^2}{yz(-1+y)(-1+z)(-1+y+z)}\\
C_{8,q} &= \frac{Q^2}{yz(-1+y)(-1+z)(-1+y+z)(y+z)}\,,\\
C_{9,q} &= \frac{Q^2}{(-1+y)(-1+z)(-1+y+z)(y+z)}\,. \qquad \text{(B.20)}
\end{aligned}
$$

C 3-point FFs of the half-BPS and Konishi operator up to two-loops

For the half-BPS, and the Konishi operators at one loop, we find

$$
\begin{aligned}
\mathcal{F}_f^{\mathrm{BPS},(1),\mathrm{fin}} &= -\zeta_2 - H(0;y)\Big(H(0;z) - H(1;z)\Big) + H(2;y)\Big(H(0;z) + H(0;y)\Big) \\
&\quad -H(1;z)\Big(2H(3;y) + H(0;z)\Big) - 2H(1,0;y) - 2H(3,2;y)\,, \\
\mathcal{F}_{g\phi\phi}^{\mathcal{K},(1),\mathrm{fin}} &= \mathcal{F}_f^{\mathrm{BPS},(1),\mathrm{fin}} + \frac{6y(1-y-z)}{(1-z)^2}H(0;z) - \frac{2}{z(1-z)}\Big(3y^2 - (3y-7z)(1-z)\Big)\,, \\
\mathcal{F}_{\phi\lambda\lambda}^{\mathcal{K},(1),\mathrm{fin}} &= \mathcal{F}_f^{\mathrm{BPS},(1),\mathrm{fin}} - 3H(0;y)H(1;z) + 3H(0,1;z) - 3H(0;y)H(2;y) \\
&\quad +3H(1,0;y) + 3H(1;z)H(3;y) + 3H(3,2;y) + \frac{6z}{1-y}H(0;y) \\
&\quad -\frac{6z}{y+z}\Big(H(1;z) + H(2;y)\Big) - 14. \qquad \text{(C.1)}
\end{aligned}
$$

The two loop finite result for FF for the half-BPS operator is presented below

$$
\begin{aligned}
\mathcal{F}_f^{\mathrm{BPS},(2),\mathrm{fin}} =& \frac{49}{20}\zeta_2^2 + \zeta_3\Big(H(1;z) + H(2;y) - H(0;y) - H(0;z)\Big) + \zeta_2\Big[3H(0;z) \\
&\times\Big(H(1;z) + H(0;y) - H(2;y)\Big) + 4\Big(H(1;y)^2 - H(2;y)^2\Big) - H(1;z) \\
&\times\Big(3H(0;y) + 8H(2;y) + 2H(3;y)\Big) - 2H(3,2;y) - 3H(0;y)H(2;y) \\
&+ 6H(1,0;y) + 8H(0,1;y)\Big] + H(0;z)\Big[- H(0;y)^2H(1;z) - H(0;y) \\
&\times\Big(H(2;y)^2 - 2H(0,2;y) + 2H(3,2;y)\Big) - 2\Big(H(1;z)\Big(H(2;y)^2 - H(0,3;y)
\end{aligned}
$$

$$
\begin{aligned}
&+ H(2;y)H(3;y) - H(1,0;y) + 2H(2,0;y) + H(3,0;y) + H(3,2;y)\Big) \\
&- H(2;y)H(1,0;y) + H(0,0,2;y) - H(0,1,0;y) - 2H(0,2,2;y) \\
&- 2H(0,3,2;y) - 2H(1,0,0;y) + H(2,0,0;y) + 2H(2,1,0;y) + H(2,3,2;y) \\
&+ 2H(3,2,2;y)\Big)\Big] + \frac{1}{2}H(0,z)^2\Big(H(0;y)^2 + H(2;y)^2 - 2H(0;y)H(2;y)\Big) \\
&+ H(1;z)\Big[- 2H(0;y)^2H(3;y) + 8H(2;y)H(3;y)^2 + \frac{4}{3}H(3;y)^3 \\
&+ 2H(0;y)\Big(H(0,2;y) - 2H(3,2;y)\Big) - 8H(3;y)H(3,2;y) - 2H(0,0,2;y) \\
&- 2H(0,1,0;y) - 2H(0,2,3;y) - 4H(1,0,0;y) + 2H(2,0,0;y) \\
&- 2H(2,0,3;y) - 4H(2,1,0;y) + 4H(2,2,3;y) - 2H(2,3,0;y) \\
&- 8H(2,3,3;y) + 4H(3,0,0;y) + 8H(3,3,2;y)\Big] + \frac{1}{2}H(1;z)^2\Big(H(0;y)^2 \\
&+ 4H(3;y)^2 - 4H(0;y)H(3;y)\Big) + 2H(0;y)\Big(H(0,0,1;z) + H(0,1,0;z) \\
&- H(0,1,1;z) - 2H(0,3,2;y) + H(1,0,0;z) - H(1,0,1;z) - H(1,1,0;z) \\
&- H(2,3,2;y) - 2H(3,2,2;y)\Big) + 8H(1;y)H(0,1,0;y) + H(2;y) \\
&\times \Big[8H(3;y)H(0,1;z) + 6H(0,0,1;z) - 2\Big(H(0,1,0;z) + H(1,0,0;z) \\
&+ 4H(1,1,0;z) + 2H(2,1,0;y) + H(0,1,0;y) + 2H(1,0,0;y)\Big)\Big] \\
&+ 4H(2;y)^2H(0,1;z) + 4H(3;y)\Big(2H(0,0,1;z) + H(0,1,1;z) - H(1,1,0;z) \\
&+ H(1,0,1;z) + 2H(2,3,2;y)\Big) + 4H(3;y)^2H(0,1;z) \\
&+ 2\Big(H(0,0;z)H(1,1;z) + H(0,0;y)H(2,2;y) + 2H(0,0,1,0;y) \\
&+ 2H(0,0,3,2;y) - 4H(0,1,0,1;y) - 4H(0,1,1,0;y) + 4H(1,1,0,0;y)
\end{aligned}
$$

$$+ 4H(1,1,1,0;y) + 2H(2,2,1,0;y) + 2H(2,2,3,2;y)$$

$$- 4H(2,3,2,3;y) - 4H(2,3,3,2;y) + 4H(3,3,2,2;y) + 4H(3,3,3,2;y)\Big). \tag{C.2}$$

The expression above contains only HPLs (see appendix **??**) and zeta functions. We have used several identities among HPLs to simplify the expressions. The FF expression for the Konishi operator sandwiched between $g\phi\phi$ states reads as

$$\begin{aligned}
\mathcal{F}^{\mathcal{K},(2),\mathrm{fin}}_{g\phi\phi} = &\mathcal{F}^{\mathrm{BPS},(2),\mathrm{fin}}_{f} - \zeta_3\Big(\frac{6y(-1+y+z)}{(1-z)^2}\Big) + 3\zeta_2\Big[\frac{2y(-1+y+z)}{(1-z)^2}\Big(H(0;y) \\
&+ 4H(0;z)\Big) - \frac{H(1;y)}{z^2}(-1+y)(-1+y+2z) + \frac{yH(1;z)}{z^2(1-z)^2}\Big(10z^2(-1+z) \\
&+ y(-1+2z+9z^2)\Big) + \frac{H(2;y)}{z^2(1-z)^2}\Big((-1+z)^4 + y^2(1-2z+3z^2) + y(-2 \\
&+ 6z - 8z^2 + 4z^3)\Big)\Big] + \frac{3H(0;z)}{z^2(1-z)^2}\Big[yH(0,2;y)\Big(2z^2(-1+z) + y(-1+2z \\
&+ z^2)\Big) + H(1,0;y)(-1+y)(-1+z)^2(-1+y+2z) - H(2,0;y)\Big((-1+z)^4 \\
&+ y(-2+6z-4z^2) - y^2(-1+2z+z^2)\Big) + H(3,2;y)(-1+z)^2(y^2-z^2)\Big] \\
&+ \frac{3yH(0;y)}{z^2(1-z)^2}\Big[2z^2(-3+2y+3z)H(0,0;z) - y(-1+z)^2H(0,1;z) + H(1,0;z) \\
&\times\Big(2(-1+z)z^2 + y(-1+2z+z^2)\Big)\Big] + H(1,z)\Big[\frac{-6yH(0,3,y)}{(1-z)^2}(-1+y+z) \\
&+ \frac{3H(1,0;y)}{z^2}(-1+y)(-1+y+2z) - \frac{3H(2,3;y)}{z^2(1-z)^2}\Big((-1+z)^4 + y^2(1-2z \\
&+ 3z^2) + y(-2+6z-8z^2+4z^3)\Big) - \frac{3(y^2-z^2)}{z^2}\Big(H(3,0;y) - H(3,3;y)\Big)\Big] \\
&- \frac{3H(2;y)(-1+y+z)}{z^2(1-z)^2}\Big[H(0,1;z)\Big((-1+z)^3 + y(1-2z+3z^2)\Big) \\
&+ 2H(0,0;z)z^2(1+2y-z)\Big] + \frac{3H(3,y)}{z^2}(y^2-z^2)\Big(2H(0,1;z) + H(1,0;z)\Big)
\end{aligned}$$

$$
\begin{aligned}
&+\Big(3-\frac{3y^2}{z^2}\Big)\Big(H(3,0,2;y)+H(3,2,0;y)-H(3,3,2;y)\Big)-\frac{3H(2,3,2;y)}{z^2(1-z)^2}\\
&\times\Big((-1+z)^4+y^2(1-2z+3z^2)+y(-2+6z-8z^2+4z^3)\Big)+\frac{6yH(2,1,0;y)}{(1-z)^2}\\
&\times(-1+y+z)+\frac{3(-1+y)(-1+y+2z)}{z^2}\Big(H(1,2,0;y)+H(1,0,2;y)\Big)\\
&+\frac{6yH(1,1,0;z)}{z^2(1-z)^2}\Big(y(-1+2z+3z^2)+4(-1+z)z^2\Big)-\frac{3H(1,1,0;y)}{z^2}\\
&\times(-1+y)(-1+y+2z)+\frac{3}{z^2(1-z)^2}\Big(H(0,1,0;y)-H(1,0,1;z)\Big)\Big(y^2(1-2z\\
&+3z^2)+2yz^2(-1+z)\Big)+\frac{6H(0,0,1;z)y^2(1-2z)}{z^2(-1+z)^2}+\frac{3yH(0,1,0;z)}{z^2(-1+z)^2}\\
&\times\Big(8z^2(-1+z)+y(1-2z+7z^2)\Big)-\frac{6y(-1+y+z)}{(1-z)^2}H(0,3,2;y)\\
&+\frac{6y(-3+2y+3z)}{(1-z)^2}H(1,0,0;z)+\frac{\zeta_2}{z(1-z)^2}\Big(-10z(-1+z)^2+12y^2(1+z)\\
&+3y(-3-4z+7z^2)\Big)-\frac{H(0;y)H(0;z)}{z(1-z)}\Big(-6y^2+14z(-1+z)+3y(1+9z)\Big)\\
&+\frac{H(1;z)H(0;y)}{z^2}\Big(3y^2+3y(-1+z)-14z^2\Big)-\frac{H(0;z)H(2;y)}{z(1-z)}\Big(3+6y^2-22z\\
&+19z^2+y(-9+39z)\Big)-\frac{H(1;z)H(3;y)}{z^2(1-z)}\Big(y^2(3-9z)+z(-3+8z-5z^2)\\
&-3y(1-5z+6z^2)\Big)+\frac{6yH(0,0;z)}{(1-z)^2}(-1+y+z)-\frac{H(0,1;z)}{z^2(1-z)}\Big(-3y^2(-1+z)\\
&+14z^2(-1+z)+3y(-1+2z+7z^2)\Big)+\frac{H(0,2;y)}{z^2}\Big(3y^2+3y(-1+z)\\
&-14z^2)\Big)-\frac{H(1,0;y)}{z^2(1-z)}\Big(y^2(3-9z)+4z^2(-1+z)+y(-3+9z)\Big)+\frac{H(1,0;z)}{z(1-z)^2}\\
&\times\Big(14z(-1+z)^2+12y^2(1+z)+9y(-1-4z+5z^2)\Big)+\frac{H(2,0;y)}{z^2}\Big(3y^2\\
&+3y(-1+z)-14z^2\Big)-\frac{H(3,2;y)}{z^2(1-z)}\Big(y^2(3-9z)+z(-3+8z-5z^2)
\end{aligned}
$$

$$
- 3y(1-5z+6z^2)\Big) + \frac{144yH(0;z)}{(1-z)^2}(-1+y+z) + \frac{12}{z(1-z)}\Big(12y^2
$$

$$
- 12y(1-z) + 17z(1-z)\Big). \tag{C.3}
$$

The FF for the Konishi operator between $\phi\lambda\lambda$ state is found to be

$$
\begin{aligned}
\mathcal{F}^{\mathcal{K},(2),\text{fin}}_{\phi\lambda\lambda} = \mathcal{F}^{\text{BPS},(2),\text{fin}}_{f} &+ \zeta_2\Big[- 6H(1;y)^2 + 3H(1;z)\Big(3H(0;y) + H(3;y)\Big) \\
&+ \frac{9}{2}\Big(H(1;z) + H(2;y)\Big)^2 - 12H(0,1;y) - 9H(1,0;y) + 9H(0;y)H(2;y) \\
&+ 3H(2,1;y) + 3H(3,2;y)\Big] + 3\Big(- 3H(0,0,0,1;z) - 2H(0,0,1,0;y) \\
&+ 2H(0,0,1,0;z) - 3H(0,0,3,2;y) + 4H(0,1,0,1;y) - H(0,1,0,1;z) \\
&- H(0,1,0,2;y) + 4H(0,1,1,0;y) + 3H(0,1,1,0;z) - H(0,1,2,0;y) \\
&- H(0,3,2,2;y) + H(0,3,3,2;y) + H(1,0,0,2;y) + 4H(1,0,1,0;z) \\
&+ H(1,0,2,0;y) - 4H(1,1,0,0;y) + 3H(1,1,0,0;z) - 2H(1,1,0,1;z) \\
&- 4H(1,1,1,0;y) + H(1,2,0,0;y) + H(2,1,1,0;y) - 3H(2,2,1,0;y) \\
&- 2H(2,2,3,2;y) - H(2,3,0,2;y) - H(2,3,2,0;y) + 4H(2,3,2,3;y) \\
&+ 4H(2,3,3,2;y) - 4H(3,3,2,2;y) - 4H(3,3,3,2;y)\Big) - 3H(0,1;z)\Big(H(2;y)^2 \\
&+ 4H(2;y)H(3;y) + 2H(3;y)^2\Big) + \frac{3}{2}H(0;y)^2\Big(- \frac{3}{2}H(1;z)^2 + H(1;z)H(3;y) \\
&+ H(0,1;z)\Big) - \frac{9}{4}H(0;z)^2H(1;z)^2 + 3H(0,1;z)\Big(H(0,3;y) + 2H(0;y)H(2;y)\Big) \\
&- 9H(0,0;y)H(2,2;y) + 3H(1;z)^2\Big(- H(3;y)^2 + \frac{3}{2}H(0,3;y) + 2H(3,0;y)\Big) \\
&- 3H(0,0,1;z)\Big(3H(2;y) + 4H(3;y)\Big) - 6H(0,1,0;y)\Big(2H(1;y) - H(2;y)\Big)
\end{aligned}
$$

$$
\begin{aligned}
&+ 3H(2;y)H(0,1,0;z) - 12H(3;y)H(0,1,1;z) + 9H(2;y)H(1,0,0;y) \\
&- 6H(2;y)H(1,0,1;z) - 12H(3;y)H(1,0,1;z) + 6H(2;y)H(2,1,0;y) \\
&- 12H(3;y)H(2,3,2;y) + H(0;z)\Big[- 3H(2;y)H(1,0;y) \\
&+ H(1;z)\Big(3H(2;y)H(3;y) - 3H(0,3;y) - 3H(1,0;y) + 3H(3,0;y) \\
&- 3H(3,2;y)\Big) + 3H(0;y)H(3,2;y) - 3H(0,1,0;y) - 6H(0,3,2;y) \\
&+ 6H(2,1,0;y) + 3H(2,3,2;y)\Big] + H(0;y)\Big[3H(1;z)\Big(4H(3,2;y) \\
&- 3H(0,2;y)\Big) - 3H(0,1,0;z) + 9H(0,1,1;z) + 6H(0,3,2;y) + 6H(1,0,1;z) \\
&+ 6H(2,3,2;y) + 12H(3,2,2;y)\Big] + H(1;z)\Big(- 2H(3;y)^3 \\
&- 12H(3;y)H(2,3;y) + 9H(0,0,2;y) + 3H(0,1,0;y) + 6H(0,2,3;y) \\
&+ 3H(0,3,0;y) - 3H(0,3,2;y) + 3H(0,3,3;y) + 12H(1,0,0;y) \\
&- 9H(2,0,0;y) + 6H(2,0,3;y) + 6H(2,1,0;y) - 6H(2,2,3;y) \\
&+ 3H(2,3,0;y) + 12H(2,3,3;y) - 3H(3,0,0;y) - 12H(3,3,2;y)\Big) + \frac{6z}{1-y}\zeta_3 \\
&- \frac{\zeta_2}{1-y}\Big[24zH(0;y) + 6zH(0,z) - \frac{3H(1;y)}{y(1-y-z)}\Big(1 - 3z + 2z^2 + y^2(1+7z) \\
&+ y(-2-4z+6z^2)\Big) - \frac{H(1;z)}{1-y-z}\Big(3 - 9z + 6z^2 + y(-3+9z)\Big) \\
&+ \frac{H(2;y)}{y}\Big(3 - 3z + y(-3+9z)\Big)\Big] + \frac{6H(0,0;y)}{1-y}\Big(- 2zH(0;z) \\
&+ (-1+y+2z)H(1;z)\Big) + \frac{3H(0,1;z)}{y+z}\Big[\frac{H(0;y)}{(1-y)(1-y-z)}\Big(2y^3 + 5y^2(-1+z) \\
&+ z(1-3z+2z^2) + y(3-6z+5z^2)\Big) + \frac{H(2;y)}{y(1-y)}\Big(6y^3 + (1-z)z + y^2(3z-7)
\end{aligned}
$$

$$+ y(1-2z+3z^2)\Big) - \frac{2H(3;y)}{1-y-z}\Big(2y^2+5(-1+z)z+y(-1+7z)\Big)\Big]$$

$$+ \frac{3H(0,2;y)}{y+z}\Big[\frac{H(0;z)}{1-y-z}\Big(4y^2+5(-1+z)z+y(-3+9z)\Big)+2(y-z)H(1;z)\Big]$$

$$- \frac{3H(1,0;y)}{y(1-y-z)}\Big[\Big(1+4y^2+5y(-1+z)-z\Big)\Big(H(0;z)+H(1;z)\Big)\Big]$$

$$+ H(1,0;z)\Big[-\frac{3H(0;y)}{(1-y)(1-y-z)}\Big(3+4y^2+y(-7+z)-z-2z^2\Big)$$

$$- \frac{6z(1+z)}{(1-y)(y+z)}H(2;y) - \frac{3H(3;y)}{y(1-y-z)}\Big(4y^2+3y(-1+z)-(-1+z)z\Big)\Big]$$

$$+ \frac{6H(1,1;z)}{y+z}\Big((y-z)H(0,y)-(y-3z)H(3;y)\Big)+H(2,0;y)\Big[-\frac{3H(0;z)}{y(1-y)}$$

$$\times\Big(-1-4y^2+z+y(5+z)\Big)+\frac{6(y-z)}{y+z}H(1;z)\Big]-\frac{12z}{y+z}H(0;z)H(2,2;y)$$

$$+ H(1;z)\Big[-\frac{6(-3+3y+z)}{1-y}H(0,3;y)+\frac{3H(3,0;y)}{y(1-y-z)}$$

$$\times\Big(4y^2+(-1+z)(3y-z)\Big)\Big]-\frac{3H(0;z)H(3,2;y)}{y(1-y-z)}\Big(4y^2+(3y-z)(-1+z)\Big)$$

$$+ \frac{3H(1;z)}{y(1-y)(y+z)}\Big[\Big(6y^3-(-1+z)z-y^2(7+z)+y(1+2z+3z^2)\Big)H(2,3;y)$$

$$+ 2(-1+y)y(y-3z)H(3,2;y)\Big]-\frac{3H(1;z)H(3,3;y)}{y(y+z)(1-y-z)}\Big((8y+z)(-1+z)z$$

$$+ y^2(1+7z)\Big)-\frac{6H(0,0,1;z)}{(1-y)(y+z)(1-y-z)}\Big(y^3-3y^2+2y(1+z)+z(z^2+z$$

$$- 2)\Big)+\frac{6H(0,0,2;y)}{1-y}(-1+y+2z)+\frac{3}{(1-y)(y+z)(1-y-z)}\Big[\Big(6y^3$$

$$+ y^2(-11+19z)+z(3-13z+10z^2)+y(5-22z+23z^2)\Big)H(0,1,0;y)$$

$$+ \Big(4y^3+7y^2(-1+z)+z(1-3z+2z^2)+y(3-8z+5z^2)\Big)H(0,1,0;z)\Big]$$

$$- \frac{6(y-z)}{y+z}\Big(H(0,1,1;z)-H(0,2,2;y)\Big)+\frac{6}{1-y}\Big[(-1+y+2z)H(0,2,0;y)$$

$$- (-3+3y+z)H(0,3,2;y)-(-1+y+4z)H(1,0,0;y)\Big]$$

$$
\begin{aligned}
&- \frac{3H(1,0,1;z)}{(1-y)(y+z)(1-y-z)}\Big(6y^3 + y^2(-11+7z) + z(-1-z+2z^2) + y(5\\
&- 6z + 3z^2)\Big) - \frac{3H(1,0,2;y)}{y(1-y-z)}\Big(1 + 4y^2 - 5y(1-z) - z\Big) + \frac{3H(1,1,0;y)}{y(1-y)(1-y-z)}\\
&\times \Big(1 - 3z + 2z^2 + y^2(1+7z) + y(-2-4z+6z^2)\Big) + \frac{6H(1,1,0;z)}{(1-y)(y+z)(1-y-z)}\\
&\times \Big((y^2+z^2)(-1+z) + y(1-z+2z^2)\Big) - \frac{3H(1,2,0;y)}{y(1-y-z)}\Big(1 + 4y^2 + 5y(-1+z)\\
&- z\Big) + \frac{6(-1+y+2z)}{1-y}H(2,0,0;y) + \frac{6(y-z)}{y+z}\Big(H(2,0,2;y) + H(2,2,0;y)\Big)\\
&- \frac{6(3y+2z)}{y+z}H(2,1,0;y) + \frac{3H(2,3,2;y)}{y(1-y)(y+z)}\Big(6y^3 - (-1+z)z - y^2(7+z)\\
&+ y(1+2z+3z^2)\Big) + \frac{3}{y(1-y-z)}\Big(4y^2 + (3y-z)(-1+z)\Big)\Big(H(3,0,2;y)\\
&+ H(3,2,0;y)\Big) - \frac{6(y-3z)}{y+z}H(3,2,2;y) - \frac{3H(3,3,2;y)}{y(y+z)(1-y-z)}\Big((-1+z)(8yz\\
&+ z^2) + y^2(1+7z)\Big) - \frac{1}{1-y}\Big(2\zeta_2(5-5y+6z) + (8-8y+12z)H(1,0;y)\Big)\\
&+ 14H(0;y)H(0;z) + 22H(0;y)H(1;z) - 14H(0;z)H(2;y)\\
&- \frac{1}{y+z}\Big[4(2y+5z)\Big(H(1;z)H(3;y) + H(3,2;y)\Big) + (22y+34z)H(0,1;z)\Big]\\
&+ 22H(0;y)H(2;y) - 10H(1,0;z) - \frac{108z}{1-y}H(0;y) + \frac{108z}{y+z}\Big(H(1;z) + H(2;y)\Big)\\
&+ 204\,.
\end{aligned}
\tag{C.4}
$$

Bibliography

[1] **ATLAS** Collaboration, G. Aad *et al.*, *Observation of a new particle in the search for the Standard Model Higgs boson with the ATLAS detector at the LHC*, *Phys. Lett.* **B716** (2012) 1–29, arXiv:1207.7214 [hep-ex].

[2] **CMS** Collaboration, S. Chatrchyan *et al.*, *Observation of a new boson at a mass of 125 GeV with the CMS experiment at the LHC*, *Phys. Lett.* **B716** (2012) 30–61, arXiv:1207.7235 [hep-ex].

[3] P. Banerjee, P. K. Dhani, and V. Ravindran, *Two loop QCD corrections for the process Pseudo-scalar Higgs $\rightarrow 3$ partons*, *JHEP* **10** (2017) 067, arXiv:1708.02387 [hep-ph].

[4] S. Catani, *The Singular behavior of QCD amplitudes at two loop order*, *Phys. Lett.* **B427** (1998) 161–171, arXiv:hep-ph/9802439 [hep-ph].

[5] T. Ahmed, P. Banerjee, P. K. Dhani, N. Rana, V. Ravindran, and S. Seth, *Konishi form factor at three loops in $\mathcal{N} = 4$ supersymmetric Yang-Mills theory*, *Phys. Rev.* **D95** no. 8, (2017) 085019, arXiv:1610.05317 [hep-th].

[6] Z. Bern, L. J. Dixon, and V. A. Smirnov, *Iteration of planar amplitudes in maximally supersymmetric Yang-Mills theory at three loops and beyond*, *Phys. Rev.* **D72** (2005) 085001, arXiv:hep-th/0505205 [hep-th].

[7] A. Brandhuber, G. Travaglini, and G. Yang, *Analytic two-loop form factors in N=4 SYM*, *JHEP* **05** (2012) 082, arXiv:1201.4170 [hep-th].

[8] P. Banerjee, P. K. Dhani, M. Mahakhud, V. Ravindran, and S. Seth, *Finite remainders of the Konishi at two loops in $\mathcal{N} = 4$ SYM*, *JHEP* **05** (2017) 085, arXiv:1612.00885 [hep-th].

[9] P. Banerjee, G. Das, P. K. Dhani, and V. Ravindran, *Threshold resummation of the rapidity distribution for Higgs production at NNLO+NNLL*, *Phys. Rev.* **D97** no. 5, (2018) 054024, arXiv:1708.05706 [hep-ph].

[10] P. W. Higgs, *Broken symmetries, massless particles and gauge fields*, *Phys. Lett.* **12** (1964) 132–133.

[11] P. W. Higgs, *Broken Symmetries and the Masses of Gauge Bosons*, *Phys. Rev. Lett.* **13** (1964) 508–509. [,160(1964)].

[12] P. W. Higgs, *Spontaneous Symmetry Breakdown without Massless Bosons*, *Phys. Rev.* **145** (1966) 1156–1163.

[13] F. Englert and R. Brout, *Broken Symmetry and the Mass of Gauge Vector Mesons*, *Phys. Rev. Lett.* **13** (1964) 321–323. [,157(1964)].

[14] G. S. Guralnik, C. R. Hagen, and T. W. B. Kibble, *Global Conservation Laws and Massless Particles*, *Phys. Rev. Lett.* **13** (1964) 585–587. [,162(1964)].

[15] L. Brink, J. H. Schwarz, and J. Scherk, *Supersymmetric Yang-Mills Theories*, *Nucl. Phys.* **B121** (1977) 77–92.

[16] F. Gliozzi, J. Scherk, and D. I. Olive, *Supersymmetry, Supergravity Theories and the Dual Spinor Model*, *Nucl. Phys.* **B122** (1977) 253–290.

[17] D. R. T. Jones, *Charge Renormalization in a Supersymmetric Yang-Mills Theory*, *Phys. Lett.* **B72** (1977) 199–199.

[18] E. C. Poggio and H. N. Pendleton, *Vanishing of Charge Renormalization and Anomalies in a Supersymmetric Gauge Theory*, *Phys. Lett.* **B72** (1977) 200.

[19] G. 't Hooft and M. J. G. Veltman, *Regularization and Renormalization of Gauge Fields*, Nucl. Phys. **B44** (1972) 189–213.

[20] G. M. Cicuta and E. Montaldi, *Analytic renormalization via continuous space dimension*, Lett. Nuovo Cim. **4** (1972) 329–332.

[21] C. G. Bollini and J. J. Giambiagi, *Dimensional Renormalization: The Number of Dimensions as a Regularizing Parameter*, Nuovo Cim. **B12** (1972) 20–26.

[22] T. Kinoshita, *Mass singularities of Feynman amplitudes*, J. Math. Phys. **3** (1962) 650–677.

[23] T. D. Lee and M. Nauenberg, *Degenerate Systems and Mass Singularities*, Phys. Rev. **133** (1964) B1549–B1562.

[24] F. Bloch and A. Nordsieck, *Note on the radiation field of the electron*, Phys. Rev. **52** (Jul, 1937) 54–59.

[25] P. Fayet, *Supergauge Invariant Extension of the Higgs Mechanism and a Model for the electron and Its Neutrino*, Nucl. Phys. **B90** (1975) 104–124.

[26] P. Fayet, *Supersymmetry and Weak, Electromagnetic and Strong Interactions*, Phys. Lett. **B64** (1976) 159.

[27] P. Fayet, *Spontaneously Broken Supersymmetric Theories of Weak, Electromagnetic and Strong Interactions*, Phys. Lett. **B69** (1977) 489.

[28] S. Dimopoulos and H. Georgi, *Softly Broken Supersymmetry and SU(5)*, Nucl. Phys. **B193** (1981) 150–162.

[29] N. Sakai, *Naturalness in Supersymmetric Guts*, Z. Phys. **C11** (1981) 153.

[30] K. Inoue, A. Kakuto, H. Komatsu, and S. Takeshita, *Aspects of Grand Unified Models with Softly Broken Supersymmetry*, Prog. Theor. Phys. **68** (1982) 927. [Erratum: Prog. Theor. Phys.70,330(1983)].

[31] K. Inoue, A. Kakuto, H. Komatsu, and S. Takeshita, *Low-Energy Parameters and Particle Masses in a Supersymmetric Grand Unified Model*, *Prog. Theor. Phys.* **67** (1982) 1889.

[32] K. Inoue, A. Kakuto, H. Komatsu, and S. Takeshita, *Renormalization of supersymmetry breaking parameters revisited*, *Progress of Theoretical Physics* **71** no. 2, (1984) 413–416, `http://ptp.oxfordjournals.org/content/71/2/413.full.pdf+html`. `http://ptp.oxfordjournals.org/content/71/2/413.abstract`.

[33] R. P. Kauffman and W. Schaffer, *QCD corrections to production of Higgs pseudoscalars*, *Phys. Rev.* **D49** (1994) 551–554, `arXiv:hep-ph/9305279 [hep-ph]`.

[34] A. Djouadi, M. Spira, and P. M. Zerwas, *Two photon decay widths of Higgs particles*, *Phys. Lett.* **B311** (1993) 255–260, `arXiv:hep-ph/9305335 [hep-ph]`.

[35] M. Spira, A. Djouadi, D. Graudenz, and P. M. Zerwas, *SUSY Higgs production at proton colliders*, *Phys. Lett.* **B318** (1993) 347–353.

[36] M. Spira, A. Djouadi, D. Graudenz, and P. M. Zerwas, *Higgs boson production at the LHC*, *Nucl. Phys.* **B453** (1995) 17–82, `arXiv:hep-ph/9504378 [hep-ph]`.

[37] R. V. Harlander and W. B. Kilgore, *Production of a pseudoscalar Higgs boson at hadron colliders at next-to-next-to leading order*, *JHEP* **10** (2002) 017, `arXiv:hep-ph/0208096 [hep-ph]`.

[38] C. Anastasiou and K. Melnikov, *Pseudoscalar Higgs boson production at hadron colliders in NNLO QCD*, *Phys. Rev.* **D67** (2003) 037501, `arXiv:hep-ph/0208115 [hep-ph]`.

[39] V. Ravindran, J. Smith, and W. L. van Neerven, *NNLO corrections to the total cross-section for Higgs boson production in hadron hadron collisions*, *Nucl. Phys.* **B665** (2003) 325–366, arXiv:hep-ph/0302135 [hep-ph].

[40] S. Catani, D. de Florian, and M. Grazzini, *Direct Higgs production and jet veto at the Tevatron and the LHC in NNLO QCD*, *JHEP* **01** (2002) 015, arXiv:hep-ph/0111164 [hep-ph].

[41] C. F. Berger, C. Marcantonini, I. W. Stewart, F. J. Tackmann, and W. J. Waalewijn, *Higgs Production with a Central Jet Veto at NNLL+NNLO*, *JHEP* **04** (2011) 092, arXiv:1012.4480 [hep-ph].

[42] X. Chen, J. Cruz-Martinez, T. Gehrmann, E. W. N. Glover, and M. Jaquier, *NNLO QCD corrections to Higgs boson production at large transverse momentum*, *JHEP* **10** (2016) 066, arXiv:1607.08817 [hep-ph].

[43] R. Boughezal, F. Caola, K. Melnikov, F. Petriello, and M. Schulze, *Higgs boson production in association with a jet at next-to-next-to-leading order in perturbative QCD*, *JHEP* **06** (2013) 072, arXiv:1302.6216 [hep-ph].

[44] X. Chen, T. Gehrmann, E. W. N. Glover, and M. Jaquier, *Precise QCD predictions for the production of Higgs + jet final states*, *Phys. Lett.* **B740** (2015) 147–150, arXiv:1408.5325 [hep-ph].

[45] R. Boughezal, F. Caola, K. Melnikov, F. Petriello, and M. Schulze, *Higgs boson production in association with a jet at next-to-next-to-leading order*, *Phys. Rev. Lett.* **115** no. 8, (2015) 082003, arXiv:1504.07922 [hep-ph].

[46] R. Boughezal, C. Focke, W. Giele, X. Liu, and F. Petriello, *Higgs boson production in association with a jet at NNLO using jettiness subtraction*, *Phys. Lett.* **B748** (2015) 5–8, arXiv:1505.03893 [hep-ph].

[47] F. Caola, K. Melnikov, and M. Schulze, *Fiducial cross sections for Higgs boson production in association with a jet at next-to-next-to-leading order in QCD*, *Phys. Rev.* **D92** no. 7, (2015) 074032, `arXiv:1508.02684 [hep-ph]`.

[48] L. J. Dixon, E. W. N. Glover, and V. V. Khoze, *MHV rules for Higgs plus multi-gluon amplitudes*, *JHEP* **12** (2004) 015, `arXiv:hep-th/0411092 [hep-th]`.

[49] S. D. Badger, E. W. N. Glover, and V. V. Khoze, *MHV rules for Higgs plus multi-parton amplitudes*, *JHEP* **03** (2005) 023, `arXiv:hep-th/0412275 [hep-th]`.

[50] S. D. Badger and E. W. N. Glover, *One-loop helicity amplitudes for H —> gluons: The All-minus configuration*, *Nucl. Phys. Proc. Suppl.* **160** (2006) 71–75, `arXiv:hep-ph/0607139 [hep-ph]`. [,71(2006)].

[51] L. J. Dixon and Y. Sofianatos, *Analytic one-loop amplitudes for a Higgs boson plus four partons*, *JHEP* **08** (2009) 058, `arXiv:0906.0008 [hep-ph]`.

[52] S. Badger, E. W. Nigel Glover, P. Mastrolia, and C. Williams, *One-loop Higgs plus four gluon amplitudes: Full analytic results*, *JHEP* **01** (2010) 036, `arXiv:0909.4475 [hep-ph]`.

[53] S. Badger, J. M. Campbell, R. K. Ellis, and C. Williams, *Analytic results for the one-loop NMHV Hqqgg amplitude*, *JHEP* **12** (2009) 035, `arXiv:0910.4481 [hep-ph]`.

[54] T. Gehrmann, M. Jaquier, E. W. N. Glover, and A. Koukoutsakis, *Two-Loop QCD Corrections to the Helicity Amplitudes for* $H \to 3$ *partons*, *JHEP* **02** (2012) 056, `arXiv:1112.3554 [hep-ph]`.

[55] B. Field, J. Smith, M. E. Tejeda-Yeomans, and W. L. van Neerven, *NLO corrections to differential cross-sections for pseudoscalar Higgs boson*

production, Phys. Lett. **B551** (2003) 137–145, arXiv:hep-ph/0210369 [hep-ph].

[56] W. Bernreuther, P. Gonzalez, and M. Wiebusch, *Pseudoscalar Higgs Bosons at the LHC: Production and Decays into Electroweak Gauge Bosons Revisited*, Eur. Phys. J. **C69** (2010) 31–43, arXiv:1003.5585 [hep-ph].

[57] F. V. Tkachov, *A Theorem on Analytical Calculability of Four Loop Renormalization Group Functions*, Phys. Lett. **B100** (1981) 65–68.

[58] K. G. Chetyrkin and F. V. Tkachov, *Integration by Parts: The Algorithm to Calculate beta Functions in 4 Loops*, Nucl. Phys. **B192** (1981) 159–204.

[59] T. Gehrmann and E. Remiddi, *Differential equations for two loop four point functions*, Nucl. Phys. **B580** (2000) 485–518, arXiv:hep-ph/9912329 [hep-ph].

[60] S. L. Adler, *Axial vector vertex in spinor electrodynamics*, Phys. Rev. **177** (1969) 2426–2438.

[61] J. Kodaira, *QCD Higher Order Effects in Polarized Electroproduction: Flavor Singlet Coefficient Functions*, Nucl. Phys. **B165** (1980) 129–140.

[62] W. L. van Neerven, *Infrared Behavior of On-shell Form-factors in a $N = 4$ Supersymmetric Yang-Mills Field Theory*, Z. Phys. **C30** (1986) 595.

[63] T. Gehrmann, J. M. Henn, and T. Huber, *The three-loop form factor in N=4 super Yang-Mills*, JHEP **03** (2012) 101.

[64] D. Nandan, C. Sieg, M. Wilhelm, and G. Yang, *Cutting through form factors and cross sections of non-protected operators in $\mathcal{N} = 4$ SYM*, JHEP **06** (2015) 156.

[65] W. Siegel, *Supersymmetric Dimensional Regularization via Dimensional Reduction*, Phys. Lett. **B84** (1979) 193–196.

[66] D. M. Capper, D. R. T. Jones, and P. van Nieuwenhuizen, *Regularization by Dimensional Reduction of Supersymmetric and Nonsupersymmetric Gauge Theories*, *Nucl. Phys.* **B167** (1980) 479–499.

[67] Z. Bern and D. A. Kosower, *The Computation of loop amplitudes in gauge theories*, *Nucl. Phys.* **B379** (1992) 451–561.

[68] Z. Bern, A. De Freitas, L. J. Dixon, and H. L. Wong, *Supersymmetric regularization, two loop QCD amplitudes and coupling shifts*, *Phys. Rev.* **D66** (2002) 085002.

[69] M. Wilhelm, *Amplitudes, Form Factors and the Dilatation Operator in $\mathcal{N} = 4$ SYM Theory*, *JHEP* **02** (2015) 149, arXiv:1410.6309 [hep-th].

[70] F. Loebbert, D. Nandan, C. Sieg, M. Wilhelm, and G. Yang, *On-Shell Methods for the Two-Loop Dilatation Operator and Finite Remainders*, *JHEP* **10** (2015) 012, arXiv:1504.06323 [hep-th].

[71] A. Brandhuber, M. Kostacinska, B. Penante, G. Travaglini, and D. Young, *The SU(2|3) dynamic two-loop form factors*, *JHEP* **08** (2016) 134, arXiv:1606.08682 [hep-th].

[72] F. Loebbert, C. Sieg, M. Wilhelm, and G. Yang, *Two-Loop SL(2) Form Factors and Maximal Transcendentality*, *JHEP* **12** (2016) 090, arXiv:1610.06567 [hep-th].

[73] Z. Bern, L. J. Dixon, D. C. Dunbar, and D. A. Kosower, *One loop n point gauge theory amplitudes, unitarity and collinear limits*, *Nucl. Phys.* **B425** (1994) 217–260, arXiv:hep-ph/9403226 [hep-ph].

[74] R. Britto, F. Cachazo, B. Feng, and E. Witten, *Direct proof of tree-level recursion relation in Yang-Mills theory*, *Phys. Rev. Lett.* **94** (2005) 181602, arXiv:hep-th/0501052 [hep-th].

[75] Z. Bern, L. J. Dixon, D. C. Dunbar, and D. A. Kosower, *Fusing gauge theory tree amplitudes into loop amplitudes*, *Nucl. Phys.* **B435** (1995) 59–101, arXiv:hep-ph/9409265 [hep-ph].

[76] Z. Bern, L. J. Dixon, and D. A. Kosower, *On-Shell Methods in Perturbative QCD*, *Annals Phys.* **322** (2007) 1587–1634, arXiv:0704.2798 [hep-ph].

[77] **CMS** Collaboration, V. Khachatryan *et al.*, *Measurements of differential and double-differential Drell-Yan cross sections in proton-proton collisions at 8 TeV*, *Eur. Phys. J.* **C75** no. 4, (2015) 147, arXiv:1412.1115 [hep-ex].

[78] **CDF** Collaboration, T. Affolder *et al.*, *Measurement of $d(\sigma)/dy$ for high mass Drell-Yan e^+e^- pairs from $p\bar{p}$ collisions at $\sqrt{s} = 1.8$ TeV*, *Phys. Rev.* **D63** (2001) 011101, arXiv:hep-ex/0006025 [hep-ex].

[79] **CDF** Collaboration, F. Abe *et al.*, *Measurement of the Lepton Charge Asymmetry in W Boson Decays Produced in $p\bar{p}$ Collisions*, *Phys. Rev. Lett.* **81** (1998) 5754–5759, arXiv:hep-ex/9809001 [hep-ex].

[80] **CDF** Collaboration, T. Affolder *et al.*, *Measurement of $d(\sigma)/dM$ and forward-backward charge asymmetry for high mass Drell-Yan e^+e^- pairs from $p\bar{p}$ collisions at $\sqrt{s} = 1.8$ TeV*, *Phys. Rev. Lett.* **87** (2001) 131802, arXiv:hep-ex/0106047 [hep-ex].

[81] N. Arkani-Hamed, S. Dimopoulos, and G. R. Dvali, *The Hierarchy problem and new dimensions at a millimeter*, *Phys. Lett.* **B429** (1998) 263–272, arXiv:hep-ph/9803315 [hep-ph].

[82] L. Randall and R. Sundrum, *A Large mass hierarchy from a small extra dimension*, *Phys. Rev. Lett.* **83** (1999) 3370–3373, arXiv:hep-ph/9905221 [hep-ph].

[83] T. Ahmed, T. Gehrmann, P. Mathews, N. Rana, and V. Ravindran, *Pseudo-scalar Form Factors at Three Loops in QCD*, *JHEP* **11** (2015) 169, arXiv:1510.01715 [hep-ph].

[84] V. Ravindran, *On Sudakov and soft resummations in QCD*, *Nucl. Phys.* **B746** (2006) 58–76, arXiv:hep-ph/0512249 [hep-ph].

[85] V. Ravindran, *Higher-order threshold effects to inclusive processes in QCD*, *Nucl. Phys.* **B752** (2006) 173–196, arXiv:hep-ph/0603041 [hep-ph].

[86] S. A. Larin, *The Renormalization of the axial anomaly in dimensional regularization*, *Phys. Lett.* **B303** (1993) 113–118, arXiv:hep-ph/9302240 [hep-ph].

[87] M. F. Zoller, *OPE of the pseudoscalar gluonium correlator in massless QCD to three-loop order*, *JHEP* **07** (2013) 040, arXiv:1304.2232 [hep-ph].

[88] T. Ahmed, M. Mahakhud, N. Rana, and V. Ravindran, *Drell-Yan Production at Threshold to Third Order in QCD*, *Phys. Rev. Lett.* **113** no. 11, (2014) 112002, arXiv:1404.0366 [hep-ph].

[89] A. Vogt, S. Moch, and J. A. M. Vermaseren, *The Three-loop splitting functions in QCD: The Singlet case*, *Nucl. Phys.* **B691** (2004) 129–181, arXiv:hep-ph/0404111 [hep-ph].

[90] S. Moch, J. A. M. Vermaseren, and A. Vogt, *The Three loop splitting functions in QCD: The Nonsinglet case*, *Nucl. Phys.* **B688** (2004) 101–134, arXiv:hep-ph/0403192 [hep-ph].

[91] T. Ahmed, M. C. Kumar, P. Mathews, N. Rana, and V. Ravindran, *Pseudo-scalar Higgs boson production at threshold N^3 LO and N^3 LL QCD*, *Eur. Phys. J.* **C76** no. 6, (2016) 355, arXiv:1510.02235 [hep-ph].

[92] G. F. Sterman, *Summation of Large Corrections to Short Distance Hadronic Cross-Sections*, Nucl. Phys. **B281** (1987) 310–364.

[93] S. Catani and L. Trentadue, *Resummation of the QCD Perturbative Series for Hard Processes*, Nucl. Phys. **B327** (1989) 323–352.

[94] T. Ahmed, M. Bonvini, M. C. Kumar, P. Mathews, N. Rana, V. Ravindran, and L. Rottoli, *Pseudo-scalar Higgs boson production at N^3 LO_A +N^3 LL'*, Eur. Phys. J. **C76** no. 12, (2016) 663, `arXiv:1606.00837 [hep-ph]`.

[95] C. W. Bauer, S. Fleming, and M. E. Luke, *Summing Sudakov logarithms in B —> X(s gamma) in effective field theory*, Phys. Rev. **D63** (2000) 014006, `arXiv:hep-ph/0005275 [hep-ph]`.

[96] C. W. Bauer, S. Fleming, D. Pirjol, and I. W. Stewart, *An Effective field theory for collinear and soft gluons: Heavy to light decays*, Phys. Rev. **D63** (2001) 114020, `arXiv:hep-ph/0011336 [hep-ph]`.

[97] C. W. Bauer and I. W. Stewart, *Invariant operators in collinear effective theory*, Phys. Lett. **B516** (2001) 134–142, `arXiv:hep-ph/0107001 [hep-ph]`.

[98] C. W. Bauer, D. Pirjol, and I. W. Stewart, *Soft collinear factorization in effective field theory*, Phys. Rev. **D65** (2002) 054022, `arXiv:hep-ph/0109045 [hep-ph]`.

[99] M. Beneke, A. P. Chapovsky, M. Diehl, and T. Feldmann, *Soft collinear effective theory and heavy to light currents beyond leading power*, Nucl. Phys. **B643** (2002) 431–476, `arXiv:hep-ph/0206152 [hep-ph]`.

[100] M. Beneke and T. Feldmann, *Multipole expanded soft collinear effective theory with nonAbelian gauge symmetry*, Phys. Lett. **B553** (2003) 267–276, `arXiv:hep-ph/0211358 [hep-ph]`.

[101] C. W. Bauer, S. Fleming, D. Pirjol, I. Z. Rothstein, and I. W. Stewart, *Hard scattering factorization from effective field theory*, *Phys. Rev.* **D66** (2002) 014017, arXiv:hep-ph/0202088 [hep-ph].

[102] C. Anastasiou, K. Melnikov, and F. Petriello, *Fully differential Higgs boson production and the di-photon signal through next-to-next-to-leading order*, *Nucl. Phys.* **B724** (2005) 197–246, arXiv:hep-ph/0501130 [hep-ph].

[103] C. Anastasiou, G. Dissertori, and F. Stöckli, *NNLO QCD predictions for the $H \to WW \to \ell\nu\ell\nu$ signal at the LHC*, *JHEP* **09** (2007) 018, arXiv:0707.2373 [hep-ph].

[104] M. Grazzini, *NNLO predictions for the Higgs boson signal in the H —> WW —> lnu lnu and H —> ZZ —> 4l decay channels*, *JHEP* **02** (2008) 043, arXiv:0801.3232 [hep-ph].

[105] K. G. Chetyrkin, B. A. Kniehl, M. Steinhauser, and W. A. Bardeen, *Effective QCD interactions of CP odd Higgs bosons at three loops*, *Nucl. Phys.* **B535** (1998) 3–18, arXiv:hep-ph/9807241 [hep-ph].

[106] O. V. Tarasov, A. A. Vladimirov, and A. Yu. Zharkov, *The Gell-Mann-Low Function of QCD in the Three Loop Approximation*, *Phys. Lett.* **B93** (1980) 429–432.

[107] E. Remiddi and J. A. M. Vermaseren, *Harmonic polylogarithms*, *Int. J. Mod. Phys.* **A15** (2000) 725–754, arXiv:hep-ph/9905237 [hep-ph].

[108] T. Gehrmann and E. Remiddi, *Two loop master integrals for gamma* —> 3 jets: The Planar topologies*, *Nucl. Phys.* **B601** (2001) 248–286, arXiv:hep-ph/0008287 [hep-ph].

[109] T. Gehrmann and E. Remiddi, *Two loop master integrals for gamma* –> 3 jets: The Nonplanar topologies*, Nucl. Phys. **B601** (2001) 287–317, arXiv:hep-ph/0101124 [hep-ph].

[110] D. A. Akyeampong and R. Delbourgo, *Dimensional regularization, abnormal amplitudes and anomalies*, Nuovo Cim. **A17** (1973) 578–586.

[111] S. L. Adler and W. A. Bardeen, *Absence of higher order corrections in the anomalous axial vector divergence equation*, Phys. Rev. **182** (1969) 1517–1536.

[112] D. de Florian, M. Mahakhud, P. Mathews, J. Mazzitelli, and V. Ravindran, *Quark and gluon spin-2 form factors to two-loops in QCD*, JHEP **02** (2014) 035, arXiv:1312.6528 [hep-ph].

[113] D. de Florian, M. Mahakhud, P. Mathews, J. Mazzitelli, and V. Ravindran, *Next-to-Next-to-Leading Order QCD Corrections in Models of TeV-Scale Gravity*, JHEP **04** (2014) 028, arXiv:1312.7173 [hep-ph].

[114] T. Gehrmann and D. Kara, *The $Hb\bar{b}$ form factor to three loops in QCD*, JHEP **09** (2014) 174, arXiv:1407.8114 [hep-ph].

[115] T. Ahmed, M. Mahakhud, P. Mathews, N. Rana, and V. Ravindran, *Two-Loop QCD Correction to massive spin-2 resonance $\rightarrow$ 3 gluons*, JHEP **05** (2014) 107, arXiv:1404.0028 [hep-ph].

[116] T. Ahmed, M. Mahakhud, P. Mathews, N. Rana, and V. Ravindran, *Two-loop QCD corrections to Higgs $\rightarrow b + \overline{b} + g$ amplitude*, JHEP **08** (2014) 075, arXiv:1405.2324 [hep-ph].

[117] T. Ahmed, G. Das, P. Mathews, N. Rana, and V. Ravindran, *Spin-2 Form Factors at Three Loop in QCD*, JHEP **12** (2015) 084, arXiv:1508.05043 [hep-ph].

[118] T. Ahmed, P. Banerjee, P. K. Dhani, M. C. Kumar, P. Mathews, N. Rana, and V. Ravindran, *NNLO QCD corrections to the Drell?Yan cross section in models of*

TeV-scale gravity, Eur. Phys. J. **C77** no. 1, (2017) 22, arXiv:1606.08454 [hep-ph].

[119] T. Ahmed, G. Das, P. Mathews, N. Rana, and V. Ravindran, *The two-loop QCD correction to massive spin-2 resonance $\to q\bar{q}g$*, Eur. Phys. J. **C76** no. 12, (2016) 667, arXiv:1608.05906 [hep-ph].

[120] P. Nogueira, *Automatic Feynman graph generation*, J. Comput. Phys. **105** (1993) 279–289.

[121] J. A. M. Vermaseren, *New features of FORM*, arXiv:math-ph/0010025 [math-ph].

[122] A. von Manteuffel and C. Studerus, *Reduze 2 - Distributed Feynman Integral Reduction*, arXiv:1201.4330 [hep-ph].

[123] C. Studerus, *Reduze-Feynman Integral Reduction in C++*, Comput. Phys. Commun. **181** (2010) 1293–1300, arXiv:0912.2546 [physics.comp-ph].

[124] R. N. Lee, *Group structure of the integration-by-part identities and its application to the reduction of multiloop integrals*, JHEP **07** (2008) 031, arXiv:0804.3008 [hep-ph].

[125] S. Laporta, *High precision calculation of multiloop Feynman integrals by difference equations*, Int. J. Mod. Phys. **A15** (2000) 5087–5159, arXiv:hep-ph/0102033 [hep-ph].

[126] C. Anastasiou and A. Lazopoulos, *Automatic integral reduction for higher order perturbative calculations*, JHEP **07** (2004) 046, arXiv:hep-ph/0404258 [hep-ph].

[127] A. V. Smirnov, *Algorithm FIRE – Feynman Integral REduction*, JHEP **10** (2008) 107, arXiv:0807.3243 [hep-ph].

[128] R. N. Lee, *LiteRed 1.4: a powerful tool for reduction of multiloop integrals*, *J. Phys. Conf. Ser.* **523** (2014) 012059, arXiv:1310.1145 [hep-ph].

[129] R. N. Lee, *Presenting LiteRed: a tool for the Loop InTEgrals REDuction*, arXiv:1212.2685 [hep-ph].

[130] G. F. Sterman and M. E. Tejeda-Yeomans, *Multiloop amplitudes and resummation*, *Phys. Lett.* **B552** (2003) 48–56, arXiv:hep-ph/0210130 [hep-ph].

[131] T. Becher and M. Neubert, *Infrared singularities of scattering amplitudes in perturbative QCD*, *Phys. Rev. Lett.* **102** (2009) 162001, arXiv:0901.0722 [hep-ph]. [Erratum: Phys. Rev. Lett.111,no.19,199905(2013)].

[132] E. Gardi and L. Magnea, *Factorization constraints for soft anomalous dimensions in QCD scattering amplitudes*, *JHEP* **03** (2009) 079, arXiv:0901.1091 [hep-ph].

[133] A. V. Kotikov and L. N. Lipatov, *NLO corrections to the BFKL equation in QCD and in supersymmetric gauge theories*, *Nucl. Phys.* **B582** (2000) 19–43, arXiv:hep-ph/0004008 [hep-ph].

[134] A. V. Kotikov and L. N. Lipatov, *DGLAP and BFKL equations in the $N = 4$ supersymmetric gauge theory*, *Nucl. Phys.* **B661** (2003) 19–61, arXiv:hep-ph/0208220 [hep-ph]. [Erratum: Nucl. Phys.B685,405(2004)].

[135] A. V. Kotikov, L. N. Lipatov, A. I. Onishchenko, and V. N. Velizhanin, *Three loop universal anomalous dimension of the Wilson operators in $N = 4$ SUSY Yang-Mills model*, *Phys. Lett.* **B595** (2004) 521–529. [Erratum: Phys. Lett.B632,754(2006)].

[136] A. V. Kotikov and L. N. Lipatov, *DGLAP and BFKL evolution equations in the N=4 supersymmetric gauge theory*, . arXiv:hep-ph/0112346 [hep-ph].

[137] A. V. Kotikov and L. N. Lipatov, *On the highest transcendentality in N=4 SUSY*, *Nucl. Phys.* **B769** (2007) 217–255, arXiv:hep-th/0611204 [hep-th].

[138] A. Koukoutsakis, *Higgs bosons and QCD jets at two loops*. PhD thesis, Durham U., 2003.

[139] T. Ahmed, P. Banerjee, P. K. Dhani, P. Mathews, N. Rana, and V. Ravindran, *Three loop form factors of a massive spin-2 particle with nonuniversal coupling*, *Phys. Rev.* **D95** no. 3, (2017) 034035, arXiv:1612.00024 [hep-ph].

[140] T. Gehrmann, E. W. N. Glover, T. Huber, N. Ikizlerli, and C. Studerus, *Calculation of the quark and gluon form factors to three loops in QCD*, *JHEP* **06** (2010) 094, arXiv:1004.3653 [hep-ph].

[141] V. V. Sudakov, *Vertex parts at very high-energies in quantum electrodynamics*, *Sov. Phys. JETP* **3** (1956) 65–71. [Zh. Eksp. Teor. Fiz.30,87(1956)].

[142] A. H. Mueller, *On the Asymptotic Behavior of the Sudakov Form-factor*, *Phys. Rev.* **D20** (1979) 2037.

[143] J. C. Collins, *Algorithm to Compute Corrections to the Sudakov Form-factor*, *Phys. Rev.* **D22** (1980) 1478.

[144] A. Sen, *Asymptotic Behavior of the Sudakov Form-Factor in QCD*, *Phys. Rev.* **D24** (1981) 3281.

[145] V. Ravindran, J. Smith, and W. L. van Neerven, *Two-loop corrections to Higgs boson production*, *Nucl. Phys.* **B704** (2005) 332–348.

[146] S. Moch, J. A. M. Vermaseren, and A. Vogt, *Three-loop results for quark and gluon form-factors*, *Phys. Lett.* **B625** (2005) 245–252.

[147] T. Gehrmann, T. Huber, and D. Maitre, *Two-loop quark and gluon form-factors in dimensional regularisation*, *Phys. Lett.* **B622** (2005) 295–302.

[148] T. Gehrmann, G. Heinrich, T. Huber, and C. Studerus, *Master integrals for massless three-loop form-factors: One-loop and two-loop insertions*, Phys. Lett. **B640** (2006) 252–259.

[149] G. Heinrich, T. Huber, and D. Maitre, *Master integrals for fermionic contributions to massless three-loop form-factors*, Phys. Lett. **B662** (2008) 344–352.

[150] G. Heinrich, T. Huber, D. A. Kosower, and V. A. Smirnov, *Nine-Propagator Master Integrals for Massless Three-Loop Form Factors*, Phys. Lett. **B678** (2009) 359–366.

[151] R. N. Lee, A. V. Smirnov, and V. A. Smirnov, *Analytic Results for Massless Three-Loop Form Factors*, JHEP **04** (2010) 020.

[152] R. N. Lee and V. A. Smirnov, *Analytic Epsilon Expansions of Master Integrals Corresponding to Massless Three-Loop Form Factors and Three-Loop g-2 up to Four-Loop Transcendentality Weight*, JHEP **02** (2011) 102.

[153] R. N. Lee, A. V. Smirnov, and V. A. Smirnov, *Dimensional recurrence relations: an easy way to evaluate higher orders of expansion in ϵ*, Nucl. Phys. Proc. Suppl. **205-206** (2010) 308–313.

[154] G. P. Korchemsky and A. V. Radyushkin, *Renormalization of the Wilson Loops Beyond the Leading Order*, Nucl. Phys. **B283** (1987) 342–364.

[155] D. Correa, J. Henn, J. Maldacena, and A. Sever, *The cusp anomalous dimension at three loops and beyond*, JHEP **05** (2012) 098.

[156] A. Vogt, *Next-to-next-to-leading logarithmic threshold resummation for deep inelastic scattering and the Drell-Yan process*, Phys.Lett. **B497** (2001) 228–234.

[157] D. Anselmi, M. T. Grisaru, and A. Johansen, *A Critical behavior of anomalous currents, electric - magnetic universality and CFT in four-dimensions*, Nucl. Phys. **B491** (1997) 221–248.

[158] B. Eden, C. Schubert, and E. Sokatchev, *Three loop four point correlator in N=4 SYM*, *Phys. Lett.* **B482** (2000) 309–314.

[159] M. Bianchi, S. Kovacs, G. Rossi, and Y. S. Stanev, *Anomalous dimensions in N=4 SYM theory at order g**4*, *Nucl. Phys.* **B584** (2000) 216–232.

[160] B. Eden, C. Jarczak, and E. Sokatchev, *A Three-loop test of the dilatation operator in N = 4 SYM*, *Nucl. Phys.* **B712** (2005) 157–195.

[161] Z. Bern, M. Czakon, L. J. Dixon, D. A. Kosower, and V. A. Smirnov, *The Four-Loop Planar Amplitude and Cusp Anomalous Dimension in Maximally Supersymmetric Yang-Mills Theory*, *Phys. Rev.* **D75** (2007) 085010.

[162] F. Cachazo, M. Spradlin, and A. Volovich, *Four-loop cusp anomalous dimension from obstructions*, *Phys. Rev.* **D75** (2007) 105011.

[163] J. M. Henn, S. G. Naculich, H. J. Schnitzer, and M. Spradlin, *More loops and legs in Higgs-regulated N=4 SYM amplitudes*, *JHEP* **08** (2010) 002.

[164] J. M. Henn and T. Huber, *The four-loop cusp anomalous dimension in $\mathcal{N} = 4$ super Yang-Mills and analytic integration techniques for Wilson line integrals*, *JHEP* **09** (2013) 147.

[165] N. Beisert, B. Eden, and M. Staudacher, *Transcendentality and Crossing*, *J. Stat. Mech.* **0701** (2007) P01021.

[166] F. Cachazo, M. Spradlin, and A. Volovich, *Four-Loop Collinear Anomalous Dimension in N = 4 Yang-Mills Theory*, *Phys. Rev.* **D76** (2007) 106004.

[167] Z. Bern, L. J. Dixon, D. A. Kosower, R. Roiban, M. Spradlin, C. Vergu, and A. Volovich, *The Two-Loop Six-Gluon MHV Amplitude in Maximally Supersymmetric Yang-Mills Theory*, *Phys. Rev.* **D78** (2008) 045007.

[168] F. Fiamberti, A. Santambrogio, C. Sieg, and D. Zanon, *Wrapping at four loops in N=4 SYM*, *Phys. Lett.* **B666** (2008) 100–105.

[169] F. Fiamberti, A. Santambrogio, C. Sieg, and D. Zanon, *Anomalous dimension with wrapping at four loops in N=4 SYM*, *Nucl. Phys.* **B805** (2008) 231–266.

[170] V. N. Velizhanin, *The four-loop anomalous dimension of the Konishi operator in N=4 supersymmetric Yang-Mills theory*, *JETP Lett.* **89** (2009) 6–9.

[171] V. N. Velizhanin, *The Non-planar contribution to the four-loop universal anomalous dimension in N=4 Supersymmetric Yang-Mills theory*, *JETP Lett.* **89** (2009) 593–596.

[172] S. J. Parke and T. R. Taylor, *An Amplitude for n Gluon Scattering*, *Phys. Rev. Lett.* **56** (1986) 2459.

[173] F. A. Berends and W. T. Giele, *Recursive Calculations for Processes with n Gluons*, *Nucl. Phys.* **B306** (1988) 759–808.

[174] D. A. Kosower, *Light Cone Recurrence Relations for QCD Amplitudes*, *Nucl. Phys.* **B335** (1990) 23–44.

[175] Z. Bern and D. A. Kosower, *Efficient calculation of one loop QCD amplitudes*, *Phys. Rev. Lett.* **66** (1991) 1669–1672.

[176] Z. Bern, *A Compact representation of the one loop N gluon amplitude*, *Phys. Lett.* **B296** (1992) 85–94.

[177] G. Cristofano, R. Marotta, and K. Roland, *Unitarity and normalization of string amplitudes*, *Nucl. Phys.* **B392** (1993) 345–368.

[178] K. Roland, *Multiloop gluon amplitudes in pure gauge theories*, *Phys. Lett.* **B289** (1992) 148–152.

[179] Z. Bern, D. C. Dunbar, and T. Shimada, *String based methods in perturbative gravity*, *Phys. Lett.* **B312** (1993) 277–284, `arXiv:hep-th/9307001 [hep-th]`.

[180] G. Mahlon, *One loop multi - photon helicity amplitudes*, *Phys. Rev.* **D49** (1994) 2197–2210, arXiv:hep-ph/9311213 [hep-ph].

[181] G. Mahlon, *Multi - gluon helicity amplitudes involving a quark loop*, *Phys. Rev.* **D49** (1994) 4438–4453, arXiv:hep-ph/9312276 [hep-ph].

[182] R. Britto, F. Cachazo, and B. Feng, *New recursion relations for tree amplitudes of gluons*, *Nucl. Phys.* **B715** (2005) 499–522, arXiv:hep-th/0412308 [hep-th].

[183] A. L. Kataev, *Riemann $\zeta(3)$- terms in perturbative QED series, conformal symmetry and the analogies with structures of multiloop effects in N=4 supersymmetric Yang-Mills theory*, *Phys. Lett.* **B691** (2010) 82–86, arXiv:1005.2058 [hep-th].

[184] A. L. Kataev and S. V. Mikhailov, *New perturbation theory representation of the conformal symmetry breaking effects in gauge quantum field theory models*, *Theor. Math. Phys.* **170** (2012) 139–150, arXiv:1011.5248 [hep-ph]. [Teor. Mat. Fiz.170,174(2012)].

[185] A. L. Kataev, *Conformal symmetry limit of QED and QCD and identities between perturbative contributions to deep-inelastic scattering sum rules*, *JHEP* **02** (2014) 092, arXiv:1305.4605 [hep-th].

[186] M. T. Grisaru, H. N. Pendleton, and P. van Nieuwenhuizen, *Supergravity and the S Matrix*, *Phys. Rev.* **D15** (1977) 996.

[187] J. M. Maldacena, *The Large N limit of superconformal field theories and supergravity*, *Int. J. Theor. Phys.* **38** (1999) 1113–1133, arXiv:hep-th/9711200 [hep-th]. [Adv. Theor. Math. Phys.2,231(1998)].

[188] C. Anastasiou, Z. Bern, L. J. Dixon, and D. A. Kosower, *Planar amplitudes in maximally supersymmetric Yang-Mills theory*, *Phys. Rev. Lett.* **91** (2003) 251602.

[189] B. Eden, P. S. Howe, C. Schubert, E. Sokatchev, and P. C. West, *Simplifications of four point functions in N=4 supersymmetric Yang-Mills theory at two loops*, *Phys. Lett.* **B466** (1999) 20–26, arXiv:hep-th/9906051 [hep-th].

[190] B. Eden, C. Schubert, and E. Sokatchev, *Four point functions of chiral primary operators in N=4 SYM*, in *Quantization, gauge theory, and strings. Proceedings, International Conference dedicated to the memory of Professor Efim Fradkin, Moscow, Russia, June 5-10, 2000. Vol. 1+2*, pp. 178–184. 2000. arXiv:hep-th/0010005 [hep-th]. http://alice.cern.ch/format/showfull?sysnb=2220368.

[191] J. M. Drummond, J. Henn, G. P. Korchemsky, and E. Sokatchev, *On planar gluon amplitudes/Wilson loops duality*, *Nucl. Phys.* **B795** (2008) 52–68, arXiv:0709.2368 [hep-th].

[192] F. Cachazo, M. Spradlin, and A. Volovich, *Iterative structure within the five-particle two-loop amplitude*, *Phys. Rev.* **D74** (2006) 045020, arXiv:hep-th/0602228 [hep-th].

[193] Z. Bern, M. Czakon, D. A. Kosower, R. Roiban, and V. A. Smirnov, *Two-loop iteration of five-point N=4 super-Yang-Mills amplitudes*, *Phys. Rev. Lett.* **97** (2006) 181601, arXiv:hep-th/0604074 [hep-th].

[194] L. F. Alday and J. M. Maldacena, *Gluon scattering amplitudes at strong coupling*, *JHEP* **06** (2007) 064, arXiv:0705.0303 [hep-th].

[195] J. M. Drummond, G. P. Korchemsky, and E. Sokatchev, *Conformal properties of four-gluon planar amplitudes and Wilson loops*, *Nucl. Phys.* **B795** (2008) 385–408, arXiv:0707.0243 [hep-th].

[196] A. Brandhuber, P. Heslop, and G. Travaglini, *MHV amplitudes in N=4 super Yang-Mills and Wilson loops*, *Nucl. Phys.* **B794** (2008) 231–243, arXiv:0707.1153 [hep-th].

[197] L. F. Alday and J. Maldacena, *Comments on gluon scattering amplitudes via AdS/CFT*, *JHEP* **11** (2007) 068, arXiv:0710.1060 [hep-th].

[198] J. Maldacena and A. Zhiboedov, *Form factors at strong coupling via a Y-system*, *JHEP* **11** (2010) 104, arXiv:1009.1139 [hep-th].

[199] Z. Gao and G. Yang, *Y-system for form factors at strong coupling in AdS_5 and with multi-operator insertions in AdS_3*, *JHEP* **06** (2013) 105, arXiv:1303.2668 [hep-th].

[200] J. Bartels, L. N. Lipatov, and A. Sabio Vera, *BFKL Pomeron, Reggeized gluons and Bern-Dixon-Smirnov amplitudes*, *Phys. Rev.* **D80** (2009) 045002, arXiv:0802.2065 [hep-th].

[201] A. Brandhuber, B. Spence, G. Travaglini, and G. Yang, *Form Factors in N=4 Super Yang-Mills and Periodic Wilson Loops*, *JHEP* **01** (2011) 134, arXiv:1011.1899 [hep-th].

[202] R. Boels, B. A. Kniehl, and G. Yang, *Master integrals for the four-loop Sudakov form factor*, *Nucl. Phys.* **B902** (2016) 387–414, arXiv:1508.03717 [hep-th].

[203] A. Brandhuber, O. Gurdogan, R. Mooney, G. Travaglini, and G. Yang, *Harmony of Super Form Factors*, *JHEP* **10** (2011) 046, arXiv:1107.5067 [hep-th].

[204] L. V. Bork, D. I. Kazakov, and G. S. Vartanov, *On MHV Form Factors in Superspace for \ = 4 SYM Theory*, *JHEP* **10** (2011) 133, arXiv:1107.5551 [hep-th].

[205] V. K. Dobrev and V. B. Petkova, *ON THE GROUP THEORETICAL APPROACH TO EXTENDED CONFORMAL SUPERSYMMETRY: CLASSIFICATION OF MULTIPLETS*, *Lett. Math. Phys.* **9** (1985) 287–298.

[206] S. Ferrara and E. Sokatchev, *Short representations of SU(2,2/N) and harmonic superspace analyticity*, *Lett. Math. Phys.* **52** (2000) 247–262.

[207] S. Ferrara, *Superspace representations of SU(2,2 / N) superalgebras and multiplet shortening*, . [PoStmr99,016(1999)].

[208] S. Minwalla, *Restrictions imposed by superconformal invariance on quantum field theories*, *Adv. Theor. Math. Phys.* **2** (1998) 781–846.

[209] J. Rasmussen, *Comments on N=4 superconformal algebras*, *Nucl. Phys.* **B593** (2001) 634–650.

[210] K. Konishi, *Anomalous Supersymmetry Transformation of Some Composite Operators in SQCD*, *Phys. Lett.* **B135** (1984) 439–444.

[211] L. Andrianopoli and S. Ferrara, *K-K excitations on AdS(5) x S**5 as N=4 'primary' superfields*, *Phys. Lett.* **B430** (1998) 248–253, `arXiv:hep-th/9803171 [hep-th]`.

[212] Z. Bajnok and R. A. Janik, *Four-loop perturbative Konishi from strings and finite size effects for multiparticle states*, *Nucl. Phys.* **B807** (2009) 625–650, `arXiv:0807.0399 [hep-th]`.

[213] Z. Bajnok, A. Hegedus, R. A. Janik, and T. Lukowski, *Five loop Konishi from AdS/CFT*, *Nucl. Phys.* **B827** (2010) 426–456, `arXiv:0906.4062 [hep-th]`.

[214] B. Eden, P. Heslop, G. P. Korchemsky, V. A. Smirnov, and E. Sokatchev, *Five-loop Konishi in N=4 SYM*, *Nucl. Phys.* **B862** (2012) 123–166, `arXiv:1202.5733 [hep-th]`.

[215] A. B. Goncharov, M. Spradlin, C. Vergu, and A. Volovich, *Classical Polylogarithms for Amplitudes and Wilson Loops*, *Phys. Rev. Lett.* **105** (2010) 151605, `arXiv:1006.5703 [hep-th]`.

[216] E. Bergshoeff, M. de Roo, and B. de Wit, *Extended Conformal Supergravity*, *Nucl. Phys.* **B182** (1981) 173–204.

[217] L. W. Garland, T. Gehrmann, E. W. N. Glover, A. Koukoutsakis, and E. Remiddi, *Two loop QCD helicity amplitudes for e+ e- —> three jets*, *Nucl. Phys.* **B642** (2002) 227–262, arXiv:hep-ph/0206067 [hep-ph].

[218] T. Gehrmann, L. Tancredi, and E. Weihs, *Two-loop QCD helicity amplitudes for $g\,g \to Z\,g$ and $g\,g \to Z\,\gamma$*, *JHEP* **04** (2013) 101, arXiv:1302.2630 [hep-ph].

[219] P. Banerjee, P. K. Dhani, and V. Ravindran, *Two loop QCD corrections for pseudoscalar + jet production, in preparation*, .

[220] L. V. Bork, D. I. Kazakov, and G. S. Vartanov, *On form factors in N=4 sym*, *JHEP* **02** (2011) 063, arXiv:1011.2440 [hep-th].

[221] B. Penante, B. Spence, G. Travaglini, and C. Wen, *On super form factors of half-BPS operators in N=4 super Yang-Mills*, *JHEP* **04** (2014) 083, arXiv:1402.1300 [hep-th].

[222] A. Brandhuber, B. Penante, G. Travaglini, and C. Wen, *The last of the simple remainders*, *JHEP* **08** (2014) 100, arXiv:1406.1443 [hep-th].

[223] L. V. Bork, *On NMHV form factors in N=4 SYM theory from generalized unitarity*, *JHEP* **01** (2013) 049, arXiv:1203.2596 [hep-th].

[224] O. T. Engelund and R. Roiban, *Correlation functions of local composite operators from generalized unitarity*, *JHEP* **03** (2013) 172, arXiv:1209.0227 [hep-th].

[225] L. V. Bork, *On form factors in $\mathcal{N} = 4$ SYM theory and polytopes*, *JHEP* **12** (2014) 111, arXiv:1407.5568 [hep-th].

[226] G. 't Hooft and M. J. G. Veltman, *Regularization and Renormalization of Gauge Fields*, *Nucl. Phys.* **B44** (1972) 189–213.

[227] R. K. Ellis and J. C. Sexton, *QCD Radiative Corrections to Parton Parton Scattering*, *Nucl. Phys.* **B269** (1986) 445–484.

[228] S. G. Naculich, H. Nastase, and H. J. Schnitzer, *Subleading-color contributions to gluon-gluon scattering in N=4 SYM theory and relations to N=8 supergravity*, *JHEP* **11** (2008) 018, arXiv:0809.0376 [hep-th].

[229] T. Gehrmann and E. Remiddi, *Numerical evaluation of two-dimensional harmonic polylogarithms*, *Comput. Phys. Commun.* **144** (2002) 200–223, arXiv:hep-ph/0111255 [hep-ph].

[230] B. Eden, *Three-loop universal structure constants in N=4 susy Yang-Mills theory*, arXiv:1207.3112 [hep-th].

[231] J. Drummond, C. Duhr, B. Eden, P. Heslop, J. Pennington, and V. A. Smirnov, *Leading singularities and off-shell conformal integrals*, *JHEP* **08** (2013) 133, arXiv:1303.6909 [hep-th].

[232] B. Basso, V. Goncalves, S. Komatsu, and P. Vieira, *Gluing Hexagons at Three Loops*, *Nucl. Phys.* **B907** (2016) 695–716, arXiv:1510.01683 [hep-th].

[233] V. Gonçalves, *Extracting OPE coefficient of Konishi at four loops*, arXiv:1607.02195 [hep-th].

[234] C. Anastasiou, C. Duhr, F. Dulat, F. Herzog, and B. Mistlberger, *Higgs Boson Gluon-Fusion Production in QCD at Three Loops*, *Phys. Rev. Lett.* **114** (2015) 212001, arXiv:1503.06056 [hep-ph].

[235] S. D. Drell and T.-M. Yan, *Massive Lepton Pair Production in Hadron-Hadron Collisions at High-Energies*, *Phys. Rev. Lett.* **25** (1970) 316–320. [Erratum: Phys. Rev. Lett.25,902(1970)].

[236] J. Gao, M. Guzzi, J. Huston, H.-L. Lai, Z. Li, P. Nadolsky, J. Pumplin, D. Stump, and C. P. Yuan, *CT10 next-to-next-to-leading order global analysis of QCD*, *Phys. Rev.* **D89** no. 3, (2014) 033009, arXiv:1302.6246 [hep-ph].

[237] L. A. Harland-Lang, A. D. Martin, P. Motylinski, and R. S. Thorne, *Parton distributions in the LHC era: MMHT 2014 PDFs*, Eur. Phys. J. **C75** no. 5, (2015) 204, arXiv:1412.3989 [hep-ph].

[238] **NNPDF** Collaboration, R. D. Ball *et al.*, *Parton distributions for the LHC Run II*, *JHEP* **04** (2015) 040, arXiv:1410.8849 [hep-ph].

[239] J. Butterworth *et al.*, *PDF4LHC recommendations for LHC Run II*, J. Phys. **G43** (2016) 023001, arXiv:1510.03865 [hep-ph].

[240] S. Alekhin, J. Blümlein, S. Moch, and R. Placakyte, *Parton Distribution Functions, α_s and Heavy-Quark Masses for LHC Run II*, Phys. Rev. **D96** no. 1, (2017) 014011, arXiv:1701.05838 [hep-ph].

[241] S. Dawson, *Radiative corrections to Higgs boson production*, Nucl. Phys. **B359** (1991) 283–300.

[242] A. Djouadi, M. Spira, and P. M. Zerwas, *Production of Higgs bosons in proton colliders: QCD corrections*, Phys. Lett. **B264** (1991) 440–446.

[243] R. V. Harlander and W. B. Kilgore, *Soft and virtual corrections to proton proton —> $H + x$ at NNLO*, Phys. Rev. **D64** (2001) 013015, arXiv:hep-ph/0102241 [hep-ph].

[244] S. Catani, D. de Florian, and M. Grazzini, *Higgs production in hadron collisions: Soft and virtual QCD corrections at NNLO*, *JHEP* **05** (2001) 025, arXiv:hep-ph/0102227 [hep-ph].

[245] R. V. Harlander and W. B. Kilgore, *Next-to-next-to-leading order Higgs production at hadron colliders*, Phys. Rev. Lett. **88** (2002) 201801, arXiv:hep-ph/0201206 [hep-ph].

[246] C. Anastasiou and K. Melnikov, *Higgs boson production at hadron colliders in NNLO QCD*, *Nucl. Phys.* **B646** (2002) 220–256, arXiv:hep-ph/0207004 [hep-ph].

[247] J. Kubar-Andre and F. E. Paige, *Gluon Corrections to the Drell-Yan Model*, *Phys. Rev.* **D19** (1979) 221.

[248] G. Altarelli, R. K. Ellis, and G. Martinelli, *Leptoproduction and Drell-Yan Processes Beyond the Leading Approximation in Chromodynamics*, *Nucl. Phys.* **B143** (1978) 521. [Erratum: Nucl. Phys.B146,544(1978)].

[249] B. Humpert and W. L. van Neerven, *Infrared and Mass Regularization in Af Field Theories 2. QCD*, *Nucl. Phys.* **B184** (1981) 225–268.

[250] T. Matsuura and W. L. van Neerven, *Second Order Logarithmic Corrections to the Drell-Yan Cross-section*, *Z. Phys.* **C38** (1988) 623.

[251] T. Matsuura, S. C. van der Marck, and W. L. van Neerven, *The Calculation of the Second Order Soft and Virtual Contributions to the Drell-Yan Cross-Section*, *Nucl. Phys.* **B319** (1989) 570–622.

[252] R. Hamberg, W. L. van Neerven, and T. Matsuura, *A complete calculation of the order $\alpha - s^2$ correction to the Drell-Yan K factor*, *Nucl. Phys.* **B359** (1991) 343–405. [Erratum: Nucl. Phys.B644,403(2002)].

[253] C. Anastasiou, L. J. Dixon, K. Melnikov, and F. Petriello, *Dilepton rapidity distribution in the Drell-Yan process at NNLO in QCD*, *Phys. Rev. Lett.* **91** (2003) 182002, arXiv:hep-ph/0306192 [hep-ph].

[254] C. Anastasiou, K. Melnikov, and F. Petriello, *Higgs boson production at hadron colliders: Differential cross sections through next-to-next-to-leading order*, *Phys. Rev. Lett.* **93** (2004) 262002, arXiv:hep-ph/0409088 [hep-ph].

[255] C. Anastasiou, C. Duhr, F. Dulat, E. Furlan, T. Gehrmann, F. Herzog, and B. Mistlberger, *Higgs boson gluon?fusion production at threshold in N^3LO QCD*, *Phys. Lett.* **B737** (2014) 325–328, arXiv:1403.4616 [hep-ph].

[256] S. Moch and A. Vogt, *Higher-order soft corrections to lepton pair and Higgs boson production*, *Phys. Lett.* **B631** (2005) 48–57, arXiv:hep-ph/0508265 [hep-ph].

[257] E. Laenen and L. Magnea, *Threshold resummation for electroweak annihilation from DIS data*, *Phys. Lett.* **B632** (2006) 270–276, arXiv:hep-ph/0508284 [hep-ph].

[258] A. Idilbi, X.-d. Ji, J.-P. Ma, and F. Yuan, *Threshold resummation for Higgs production in effective field theory*, *Phys. Rev.* **D73** (2006) 077501, arXiv:hep-ph/0509294 [hep-ph].

[259] M. C. Kumar, M. K. Mandal, and V. Ravindran, *Associated production of Higgs boson with vector boson at threshold N^3LO in QCD*, *JHEP* **03** (2015) 037, arXiv:1412.3357 [hep-ph].

[260] T. Ahmed, N. Rana, and V. Ravindran, *Higgs boson production through $b\bar{b}$ annihilation at threshold in N^3LO QCD*, *JHEP* **10** (2014) 139, arXiv:1408.0787 [hep-ph].

[261] T. Ahmed, G. Das, M. C. Kumar, N. Rana, and V. Ravindran, *RG improved Higgs boson production to N^3LO in QCD*, arXiv:1505.07422 [hep-ph].

[262] Y. Li, A. von Manteuffel, R. M. Schabinger, and H. X. Zhu, *N^3LO Higgs boson and Drell-Yan production at threshold: The one-loop two-emission contribution*, *Phys. Rev.* **D90** no. 5, (2014) 053006, arXiv:1404.5839 [hep-ph].

[263] S. Catani, L. Cieri, D. de Florian, G. Ferrera, and M. Grazzini, *Threshold resummation at N^{3}LL accuracy and soft-virtual cross sections at N^{3}LO*, *Nucl. Phys.* **B888** (2014) 75–91, arXiv:1405.4827 [hep-ph].

[264] S. Catani and L. Trentadue, *Comment on QCD exponentiation at large x*, *Nucl. Phys.* **B353** (1991) 183–186.

[265] G. Bozzi, S. Catani, D. de Florian, and M. Grazzini, *Higgs boson production at the LHC: Transverse-momentum resummation and rapidity dependence*, *Nucl. Phys.* **B791** (2008) 1–19, arXiv:0705.3887 [hep-ph].

[266] G. Bozzi, S. Catani, G. Ferrera, D. de Florian, and M. Grazzini, *Transverse-momentum resummation: A Perturbative study of Z production at the Tevatron*, *Nucl. Phys.* **B815** (2009) 174–197, arXiv:0812.2862 [hep-ph].

[267] G. Bozzi, S. Catani, G. Ferrera, D. de Florian, and M. Grazzini, *Production of Drell-Yan lepton pairs in hadron collisions: Transverse-momentum resummation at next-to-next-to-leading logarithmic accuracy*, *Phys. Lett.* **B696** (2011) 207–213, arXiv:1007.2351 [hep-ph].

[268] S. Catani and M. Grazzini, *QCD transverse-momentum resummation in gluon fusion processes*, *Nucl. Phys.* **B845** (2011) 297–323, arXiv:1011.3918 [hep-ph].

[269] S. Catani, M. Grazzini, and A. Torre, *Soft-gluon resummation for single-particle inclusive hadroproduction at high transverse momentum*, *Nucl. Phys.* **B874** (2013) 720–745, arXiv:1305.3870 [hep-ph].

[270] P. F. Monni, E. Re, and P. Torrielli, *Higgs Transverse-Momentum Resummation in Direct Space*, *Phys. Rev. Lett.* **116** no. 24, (2016) 242001, arXiv:1604.02191 [hep-ph].

[271] M. A. Ebert and F. J. Tackmann, *Resummation of Transverse Momentum Distributions in Distribution Space*, *JHEP* **02** (2017) 110, arXiv:1611.08610 [hep-ph].

[272] M. Grazzini, S. Kallweit, D. Rathlev, and M. Wiesemann, *Transverse-momentum resummation for vector-boson pair production at NNLL+NNLO*, *JHEP* **08** (2015) 154, arXiv:1507.02565 [hep-ph].

[273] G. Ferrera and J. Pires, *Transverse-momentum resummation for Higgs boson pair production at the LHC with top-quark mass effects*, *JHEP* **02** (2017) 139, arXiv:1609.01691 [hep-ph].

[274] E. Laenen and G. F. Sterman, *Resummation for Drell-Yan differential distributions*, in *The Fermilab Meeting DPF 92. Proceedings, 7th Meeting of the American Physical Society, Division of Particles and Fields, Batavia, USA, November 10-14, 1992. Vol. 1, 2*, pp. 987–989. 1992. http://lss.fnal.gov/cgi-bin/find_paper.pl?conf-92-359.

[275] G. F. Sterman and W. Vogelsang, *Threshold resummation and rapidity dependence*, *JHEP* **02** (2001) 016, arXiv:hep-ph/0011289 [hep-ph].

[276] A. Mukherjee and W. Vogelsang, *Threshold resummation for W-boson production at RHIC*, *Phys. Rev.* **D73** (2006) 074005, arXiv:hep-ph/0601162 [hep-ph].

[277] P. Bolzoni, *Threshold resummation of Drell-Yan rapidity distributions*, *Phys. Lett.* **B643** (2006) 325–330, arXiv:hep-ph/0609073 [hep-ph].

[278] T. Becher and M. Neubert, *Threshold resummation in momentum space from effective field theory*, *Phys. Rev. Lett.* **97** (2006) 082001, arXiv:hep-ph/0605050 [hep-ph].

[279] T. Becher, M. Neubert, and G. Xu, *Dynamical Threshold Enhancement and Resummation in Drell-Yan Production*, *JHEP* **07** (2008) 030, arXiv:0710.0680 [hep-ph].

[280] M. Bonvini, S. Forte, G. Ridolfi, and L. Rottoli, *Resummation prescriptions and ambiguities in SCET vs. direct QCD: Higgs production as a case study*, *JHEP* **01** (2015) 046, arXiv:1409.0864 [hep-ph].

[281] M. A. Ebert, J. K. L. Michel, and F. J. Tackmann, *Resummation Improved Rapidity Spectrum for Gluon Fusion Higgs Production*, *JHEP* **05** (2017) 088, arXiv:1702.00794 [hep-ph].

[282] V. Ravindran, J. Smith, and W. L. van Neerven, *QCD threshold corrections to di-lepton and Higgs rapidity distributions beyond N^2 LO*, *Nucl. Phys.* **B767** (2007) 100–129, arXiv:hep-ph/0608308 [hep-ph].

[283] V. Ravindran and J. Smith, *Threshold corrections to rapidity distributions of Z and $W^{\pm}$ bosons beyond N^2 LO at hadron colliders*, *Phys. Rev.* **D76** (2007) 114004, arXiv:0708.1689 [hep-ph].

[284] T. Ahmed, M. K. Mandal, N. Rana, and V. Ravindran, *Rapidity Distributions in Drell-Yan and Higgs Productions at Threshold to Third Order in QCD*, *Phys. Rev. Lett.* **113** (2014) 212003, arXiv:1404.6504 [hep-ph].

[285] T. Ahmed, M. K. Mandal, N. Rana, and V. Ravindran, *Higgs Rapidity Distribution in $b\bar{b}$ Annihilation at Threshold in N^3LO QCD*, *JHEP* **02** (2015) 131, arXiv:1411.5301 [hep-ph].

[286] S. Moch, J. A. M. Vermaseren, and A. Vogt, *The Quark form-factor at higher orders*, *JHEP* **08** (2005) 049.

[287] S. Catani, D. de Florian, M. Grazzini, and P. Nason, *Soft gluon resummation for Higgs boson production at hadron colliders*, *JHEP* **07** (2003) 028, arXiv:hep-ph/0306211 [hep-ph].

[288] S. Catani, M. L. Mangano, P. Nason, and L. Trentadue, *The Resummation of soft gluons in hadronic collisions*, *Nucl. Phys.* **B478** (1996) 273–310, arXiv:hep-ph/9604351 [hep-ph].

[289] A. Buckley, J. Ferrando, S. Lloyd, K. Nordström, B. Page, M. Rüfenacht, M. Schönherr, and G. Watt, *LHAPDF6: parton density access in the LHC precision era*, *Eur. Phys. J.* **C75** (2015) 132, arXiv:1412.7420 [hep-ph].

[290] P. Banerjee, G. Das, P. K. Dhani, and V. Ravindran, *Threshold resummation of the rapidity distribution for Drell-Yan production at NNLO+NNLL*, arXiv:1805.01186 [hep-ph].